Theses and Dissertations

Summer 2014

Development of a highly resolved 3-D computational model for applications in water quality and ecosystems

Oscar Eduardo Hernandez Murcia
University of Iowa

www.manaraa.com

DEVELOPMENT OF A HIGHLY RESOLVED 3-D COMPUTATIONAL MODEL

FOR APPLICATIONS IN WATER QUALITY AND ECOSYSTEMS

by

Oscar Eduardo Hernandez Murcia

A thesis submitted in partial fulfillment
of the requirements for the Doctor of
Philosophy degree in Civil and Environmental Engineering
in the Graduate College of
The University of Iowa

August 2014

Thesis Supervisors: Professor Larry Weber
                         Adj. Assistant Prof. Douglas Schnoebelen

Graduate College
The University of Iowa
Iowa City, Iowa

CERTIFICATE OF APPROVAL

_____

PH.D. THESIS

_____

This is to certify that the Ph.D. thesis of

Oscar Eduardo Hernandez Murcia

has been approved by the Examining Committee
for the thesis requirement for the Doctor of Philosophy
degree in Civil and Environmental Engineering at the August 2014
graduation.

Thesis Committee: _____
                    Larry Weber, Thesis Supervisor

                    _____
                    Douglas Schnoebelen, Thesis Supervisor

                    _____
                    Marcela Politano

                    _____
                    Jerald Schnoor

                    _____
                    Gene F. Parkin

                    _____
                    George Constantinescu

To Talina, Nicolas, Lisa, Marlene, Vianey, Alex and Urias

ACKNOWLEDGMENTS

Quiero agradecer a mi familia por el apoyo incondicional. A mi esposa, Elizabeth y mi hija, Talina. Ellas iluminaron el camino para que fuese posible terminar este trabajo. También quiero agradecer a Urias y Marlen, mis padres, por su apoyo y fueron quienes inculcaron en mí desde temprana edad el deseo a aprender más. Mis hermanas y sobrino, Vianey, Alex y Nicolas, fueron también un a poyo increíble en buenos y malos momentos. También quiero agradecer a toda mi familia: Abuela Lina, Ariel, Mireya, Dora, Nubia, Elizabeth, Lilia, Hector, Camilo, Lina Mendez, Lina Murcia, Cindy, Cristy, Jorge, Oscar, Javier, Liliana, David, Felipe y sus familias. También quiero agradecer a Diana, Gina y Donald por su apoyo.

También quiero agradecer a German Acero, German Santos y Alfonso Rodriguez por su invaluable, amistad, ayuda y consejos.

I would also like to thank all the support and discussions provided by Douglas Schnoebelen. I'm grateful for his help and advice.

Also, I would like to thank, Larry for helping me shape the ideas presented in this research.

I'm also wanted to thank Marcela Politano for the time and discussions provided during this research.

ABSTRACT

This dissertation presents the development and application of a computational model called BioChemFOAM developed using the computation fluid dynamic software OpenFOAM (Open source Field Operation And Manipulation). BioChemFOAM is a three dimensional incompressible unsteady-flow model that is coupled with a water-quality model via the Reynolds Average Navier-Stokes (RANS) equations. BioChemFOAM was developed to model nutrient dynamics in inland riverine aquatic ecosystems. BioChemFOAM solves the RANS equations for the hydrodynamics with an available library in OpenFOAM and implements a new library to include coupled systems of species transport equations with reactions. Simulation of the flow and multicomponent reactive transport are studied in detail for fundamental numerical experiments as well as for a real application in a backwater area of the Mississippi River. BioChemFOAM is a robust model that enables the flexible parameterization of processes for the nitrogen cycle. The processes studied include the following main components: algae, organic carbon, phosphorus, nitrogen, and dissolved oxygen. In particular, the research presented has three phases. The first phase involves the identification of the common processes that influence the nitrogen removal. The second phase covers the development and validation of the model that uses common parameterization to simulate the main features of an aquatic ecosystem. The main processes considered in the model and implemented in BioChemFOAM are: fully resolved hydraulic parameters (velocity and pressure), temperature variation, light's influence on the ecosystem, nutrients dynamics, algae growth and death, advection and diffusion of species, and isotropic turbulence (using a two-equation k-epsilon model). The final phase covers the application and analysis of the model and is divided in two sub stages: 1) a qualitative comparison of the main processes involved in the model (validation with the exact solution of different

iv

components of the model under different degrees of complexity) and 2) the quantification of main processes affecting nitrate removal in a backwater floodplain lake (Round Lake) in Pool 8 of the Mississippi River near La Crosse, WI.

The BioChemFOAM model was able to reproduce different levels of complexity in an aquatic ecosystem and expose several main features that may help understand nutrient dynamics. The validation process with fabricated numerical experiments, discussed in Chapter 4, not only presents a detailed evaluation of the equations and processes but also introduces a step-by-step method of validating the model, given a level of complexity and parameterization when modeling nutrient dynamics in aquatic ecosystems. The study cases maintain fixed coefficients and characteristic values of the concentration in order to compare the influences that increasing or decreasing complexity has on the model, BioChemFOAM. Chapter 4, which focuses on model validation with numerical experiments, demonstrates that, with characteristic concentration and coefficients, some processes do not greatly influence the nutrient dynamics for algae.

Chapters 5 and 6 discuss how BioChemFOAM was subsequently applied to an actual field case in the Mississippi River to show the model's ability to reproduce real world conditions when nitrate samples are available and other concentrations are used from typical monitored values. The model was able to reproduce the main processes affecting nutrient dynamics in the proposed scenarios and for previous studies in the literature. First, the model was adapted to simulate one species, nitrate, and its concentration was comparable to measured data. Second, the model was tested under different initial conditions. The model shows independence on initial conditions when reaching a steady mass flow rate for nitrate. Finally, a sensitivity analysis was performed using all eleven species in the model. The sensitivity takes as its basis the influence of processes on nitrate fate and transport and it defines eight scenarios. It was found in the present parameterization that green algae as modeled does not have a significant influence on improving nitrate spatial distributions and percentage of nitrate removal

(PNR). On the other hand, reaction rates for denitrification at the bed and nitrification in the water shows an important influence on the nitrate spatial distribution and the PNR. One physical solution, from the broad range of scenarios defined in the sensitivity analysis, was selected as most closely reproducing the backwater natural system. The selection was based on published values of the percentage of nitrate removal (PNR), nitrate spatial concentrations, total nitrogen spatial concentrations and mass loading rate balances. The scenario identified as a physically valid solution has a reaction rate of nitrification and denitrification at the bed of 2.37×10^{-5} s^{-1}. The PNR was found to be 39% when reaching a steady solution for the species transport. The denitrification at the bed process was about 6.7% of the input nitrate mass loading rate and the nitrification was about 7.7% of the input nitrate mass loading rate.

The present research and model development highlight the need for additional detailed field measurements to reduce the uncertainty of common processes included in advanced models (see Chapter 2 for a review of models and Chapter 3 for the proposed model). The application presented in Chapter 6 utilizes only spatial variations of nitrate and total nitrogen to validate the model, which limits the validation of the remaining species. Despite the fact that some species are not known a priori, numerical experiments serve as a guide that helps explain how the aquatic ecosystem responds under different initial and boundary conditions. In addition, the PNR curves presented in this research were useful when defining realistic removal rates in a backwater area. BioChemFOAM's ability to formulate scenarios under different driving forces makes the model invaluable in terms of understanding the potential connections between species concentration and flow variables. In general, the case study presents trends in spatial and temporal distributions of non-sampled species that were comparable to measured data.

TABLE OF CONTENTS

LIST OF TABLES

LIST OF FIGURES

CHAPTER 1

INTRODUCTION

1.1 <u>Background</u>

Currently, Computational Fluid Dynamic (CFD) modeling represents an important tool to explore physical, chemical and biological processes. Understanding these processes are vital to preserving the world we live in and to making our environment sustainable.

Nutrient management is an increasingly urgent concern in the Midwest United States and worldwide. Agricultural operations, especially in the Midwest, introduce nutrients such as nitrogen and phosphorus, often at artificially-high levels, into the environment via streams and rivers. Excessive nutrients loads have been observed in the riverine environments of agricultural watersheds, and the impact of these loads is the subject of much uncertainty (Galloway et al., 2004). Excessive nutrient loading in aquatic environments can result in accelerated eutrophication, which is a naturally-ocurring condition characterized by high levels of algae production (Wetzel, 2001). Accelerated eutrophy occurs when algae is produced in excess, forming large blooms and introducing additional organic matter into the environment. As the biological oxygen demand from the decay of additional organic material increases, it can exceed its potential to be balanced within the ecosystem and cause dissolved oxygen levels to diminish. When this occurs, the concentrations of oxygen fall below $2mg/L$, and the environment can no longer sustain a full complement of native biodiversity. This condition, known as hypoxia, impacts aquatic ecosystems worldwide (Diaz, 2001). As the global food demand grows, fertilizer use worldwide also is projected to increase by up to fifty percent by 2050, leading scientists to conclude that hypoxia may continue to increase in frequency and magnitude (Tilman et al., 2001).

Non-point source nutrient loads from Midwestern agricultural fields contribute to hypoxia in the Gulf of Mexico. The tile-drained, row cropped agriculture of Iowa, Minnesota, Illinois, Indiana, and Ohio is considered to be the main Mississippi River System nutrient load

contributors via the Upper Mississippi River (UMR) and Ohio River (Goolsby, Battaglin, Aulenbach, & Hooper, 2001). Illinois and Iowa, comprising approximately nine percent of the entire Mississippi River Basin (MRB), contribute as much as 35% of the total nitrogen to the Mississippi River (Aulenbach, Buxton, Battaglin, & Coupe, 2007; Goolsby et al., 1999). Scientific evidence correlates nutrient loads originating in this region to the size of the northern Gulf of Mexico, which is considered to be second largest coastal hypoxic zone worldwide (Rabalais, Turner, & Scavia, 2002). In 2008, nutrient loads that originated in the UMR basin agricultural fields contributed significantly to a hypoxic zone extending over an area of 20,720 square kilometers. The size and duration of northern Gulf of Mexico hypoxia have been shown to eradicate the benthic habitat, disturb the food web, and disrupt biogeochemical processes (Conley, Carstensen, Vaquer-Sunyer, & Duarte, 2009; Craig & Crowder, 2005).

The recent revelation of the broad impact that anthropogenic nutrients have on aquatic ecosystems has made large river system nutrient management an urgent concern, especially in the UMR. Numerous nutrient management practices at various stages and scales of nutrient fate and processing are currently being proposed to mitigate excessive nutrient loading. The use of restored and created wetlands has demonstrated the ability to remove significant nutrient loads from river systems efficiently and at a relatively low cost. It has been estimated that restoring 21,000 to 52,000 km^2 of riparian wetlands would reduce nutrient loads enough to significantly decrease the size of the northern Gulf of Mexicos's hypoxic zones. Wetlands and possibly small lakes could be strategically situated and designed to receive nutrient-laden water from divided rivers and flood waters or to intercept groundwater and tiled drainage (Mitsch & Day Jr, 2006; Mitsch et al., 2001; Mitsch & Gosselink, 2008).

An enhanced assessment of current scenarios and the maximization of nutrient removal in designed wetlands require careful consideration of project-scale processes (Kadlec & Wallace, 2008). In this context, computer modeling in particular CFD modeling, is a valuable analytical tool used by engineers and scientists to predict system responses to different stresses. Defining of ecosystem models using wetlands or lakes allows designers and managers to simulate scenarios

in order to improve decision-making abilities and optimize benefits to the overall ecosystem. Current models often yield a general overview of the processes involved by simplifying methods that consider hydrodynamics, chemistry, and biological processes. Typically, those elements are at the core of contemporary water quality models. The work shown by (Mooij et al., 2010) offers an overview of the challenges and opportunities inherent in integrating ecosystem modeling approaches. In order to make further progress in floodplain lake or riverine ecosystem modeing it is important to avoid 'reinventing the wheel' or 'having tunnel vision'. The conclusion illustrates that there are already numerous numerical models that were built for a particular ecosystem and even used to study in detail another ecosystem with similar characteristics. However, those models are often "rigid" and difficult to adapt when new processes or further improvements in the physics are required to gain insight into scenarios that could potentially foster a better understanding of a sustainable ecosystem.

This thesis further investigates the hypothesis that CFD modeling tools can be used to accurately simulate nutrient removal at project scale. The work presented in this thesis represent the extension of a preliminary effort in an ongoing initiative to develop a physically-based, comprehensive nutrient dynamics model at The University of Iowa's IIHR-Hydroscience & Engineering. Initial efforts presented by (Schubert, 2009) are taken as a starting point from which to improve the biological, chemical, and physical processes involved in nutrient removal. This thesis shows that the nutrient-processing potential for a riparian wetland can be studied using residence time profiles. The comparison of a first-order denitrification rate and the CFD approach to calculate the outlet concentration are presented. The study also shows that internal flow conditions have significant impact on the residence time in an aquatic ecosystem. Furthermore, the results suggest that the management and design of physical changes to the ecosystem can help maximize residence time and increase the nutrient removal potential and that those changes can not be calculated using conventional methods. Finally, it is concluded that the model illustrates the need further explanation in finite chemistry and fluid in order to better provide support for science-based adaptive ecosystem management.

1.2 <u>Motivation</u>

Restoration of inland riverine zones plays a key role in managing the sustainability of the interaction between human societies and natural habitats. Designers and managers use a variety of decision-making resources to optimize nutrient removal. Numerical models are important resources and provides important hydraulic and geochemical features that impact nitrogen removal processes. These spacial and temporal variations are present in an ecosystem and are key features to consider when building numerical models. The heterogeneity of these systems is likely to affect the cumulative nutrient removal and should be included in a process-based model. In terms of providing our knowledge of physical processes, CFD modeling tools are esssential to understanding the interaction among all of the components in an aquatic ecosystem. Furthermore, CFD modeling's foundations in first physical principles makes it an attractive alternative to use when studying ecosystem dynamics. However, little work has been completed on using CFD modeling tools to model the nutrient removal processes at management scale (around 10 km^2). Further research is needed to develop a comprehensive framework for using CFD to model nutrient processing at the project wetland scale in support of science-based adaptive management on the UMR (Upper Mississippi River), (NESP, 2006). Such research started with a preliminary study made by IIHR-Hydroscience & Engineering in which a FLUENT CFD modeling tool was used to model transpor of nitrate and to model denitrification at the bottom of a backwater area, Round Lake located at Pool 8 in the UMR, (Schubert, 2009). The results were a proof of concept that shows CFD's potential to model nutrient removal at project scale.

The work presented in this thesis introduces an extension of the work presented by (Schubert, 2009) as a preliminary effort in an ongoing initiative to develop a physically-based, comprehensive nutrient dynamics model at The University of Iowa's IIHR-Hydroscience & Engineering. In this modeling framework, Figure 1-1 shows the components that are incorporated. CFD modeling tools are used to implement basic scientific knowledge about nutrient dynamics for ecosystem modeling at various project scales. The present work extends

the hydrodynamic, biological and chemical processes considered in the preliminary application by incorporating: algae, organic carbon, phosphorus, nitrogen and dissolved oxygen (only nitrate sedimen flux is considered in this research). These processes are represented by a series of coupled passive scalar equations and boundary conditions at the water surface, the stream bottom, and banks with a highly resolved hydrodynamic model that considers variations of temperature and the influence of light on algae dynamics. OpenFOAM (public CFD library for mutiphysics modeling) was selected to include such processes due to its robustness, flexibility, and relatively fast implementation of the basic equations that drive the physical processes.
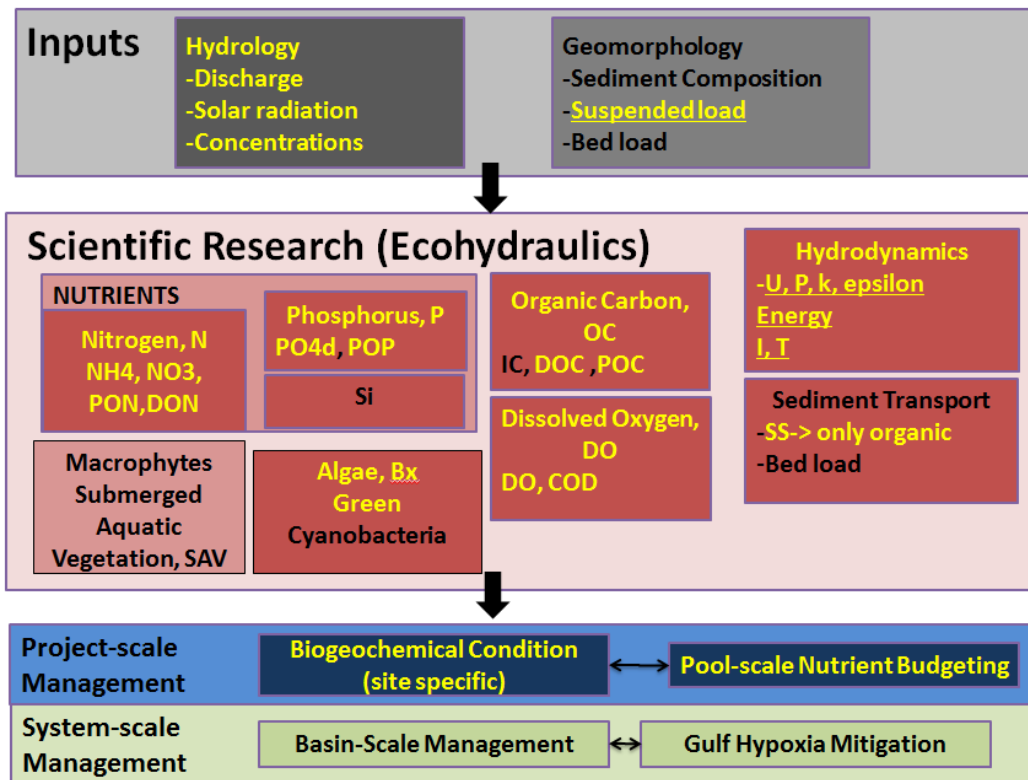
Figure 1-1: Modeling Framework for Nutrient Removal Research Initiative at IIHR, modified from [Schubert, 2009]. Elements highlighted in yellow are addressed in the present research.

1.3 Research Needs, Hypothesis, Research Questions and
Objectives

As discussed earlier, there is a need to undertand nutrient dynamics in environmental systems such as the UMR. Nutrient dynamics' impact highly influences the management of an ecosystem at the river reach or pool scale. Numerous studies related to ecological models have been applied to different ecosystems (Mooij et al., 2010). However, some models mentioned by (Mooij et al., 2010) greatly simplify the first principles or are inaccessible to researchers and managers due to private policies. The main simpifications on complex dynamical models, (Mooij et al., 2010), are: hydrostatic distribution of pressure in the vertical direction and the dilution approximations and simplification on biological cycles. Furthermore, these models can only be applied to a particular set of hydrodynamic, biological, and chemical processes. In order to improve the outcomes of a numerical model, conceptual and technical concepts should be encapsulated in a model environment. As noted by (Mooij et al., 2010), there is a clear need to find ways to integrate models that focus on spatial dynamics, hydrology, and lower trophic levels with models that focus on the whole food web. Furthermore, those models should include an inate ability to increase and decrease the complexity of each process parameterization.

The present study emerges as a response to filling the "gaps" for models to study nutrient removal in ecological systems when simplifying the hydrodynamic, biological and chemical interaction. A review of the state of the art model that exist for modeling hydrodynamic, biology and chemical components in ecosystems (Chapter 2 of this thesis) shows a lack of cohesion among models. This means that the hydrodynamic and the ecological components are decoupled in most of the cases, and their interaction becomes a difficult task when interchanging information. Also, many of the models were developed only for a particular application, and their uses in new environments imply a lot of work confined to a few people who know the models' core components. This makes it difficult for new researchers who want to add or update new processes that drive an aquatic ecosystem. Furthermore, the models presented in the literature often show validations in cases without testing the different components that are

available in the model, so the end user may not be confident enough to apply the model to a new environment and to formulate a new parameterization. In conclusion, the present research emerges as a response to integrate a robust model that focuses on the spatial dynamics of ecological systems based on highly resolved hydrodynamic, biological, chemical, and energy processes.

The implementation of Computational Fluid Dynamics processes provides additional components for theoretical and experimental fluid dynamics. It has been proven to be an invaluable tool to foster understanding of the physical processes that influence the fluid flow, ranging from aircraft design to hydraulic structure design, (Andersson, 2012; Ferziger & Perić, 1996). CFD is the art of transforming the partial derivatives and integrals representing fundamental physical principles (e.g., conservation of mass, conservation of momentum and conservation of energy) into a discretized form (discretized equations converts PDEs to algebraic equations by using numerical methods).Finite Volume Method is utilized in this thesis to solve these fundamental equations to obtain a distribution of flow fields over space and time at discrete points. The distribution of fields over a domain represent a collection of numbers that can be used to interpret its actual state. These fields are a set of numbers distributed in a domain, e.g. velocity vectors over a channel may signal where the water is going.

The main hypothesis is that Computational Fluid Dynamics (CFD) modeling tools can be used to accurately simulate flow and nutrient dynamics at different spatial and temporal scales in an aquatic ecosystem. This statement is used to define the scope of the present research through the following research questions:

• Is it possible to improve the modeling approach of an ecosystem by integrating of hydrodynamics, chemistry, and biological processes in a robust platform?

• What can be learned about the processes that affect ecosystems' nutrient dynamics by applying a robust model that is based on fundamental principles?

• What are the advantages of using a fully 3-D at Pool scale in an ecosystems in the UMR?

The overall objective of this research is to develop and apply a highly resolved CFD model to simulate hydrodynamic, biological, and chemical processes at project scale in aquatic ecosystems. Specifically, the objectives are to:

• Develop a robust model to incorporate any ecological system into a highly resolved hydrodynamic, biological and chemical model.

• Validate the CFD model and evaluate its performance for basic physical and numerical solutions and for simulated scenarios.

• Understand the principal processes that affect nitrogen fate and transport when using a highly resolved CFD model (testing hypothesis).

1.4 Thesis Overview

The objectives presented in previous sections can be achieved via a systematic and dynamic set of steps that present the essential components driving the research. Those steps are outlined in Chapters 2 through 7 and include:

1. Reviews of modeling approaches to different components in ecosystem models and of state of the art of modeling tools (Chapter 2). This chapter introducesthe new contributions coming from the highly resolved hydrodynamic, biological, and chemical ecological model that have beed developed in an open platform and that allow the easy incorporation of any ecological cycle or scale.

2. Development of the modeling tool that incorporates hydrodynamics and transport of species (Chapter 3). The equations implemented in the model take as reference (Ji, 2008), which

is a review of the model presented by (Cerco & Cole, 1994) for Chesapeake Bay, and a core part of the EFDC (Environmental Fluid Dynamics Code, (EPA, 2012)). The software selected to implement the equations is OpenFOAM. The model, BioChemFOAM, utilizes the finite volume method (FVM) to solve partial differential equations. OpenFOAM libraries were used to implement the basic fundamental concepts (e.g., systems of PDEs that descrips the fate and transport of species) on hydrodynamics and environmental modeling. The hydrodynamic concepts implementes the rigid-lid approach (water surface do not change significantly so can be set as a fixed surface) and the environmental modeling implements funamental principles of environmental modeling. The hydrodynamic principles covered here include conservation of mass, conservation of momentum, conservation of energy and the turbulence model when the system requires it. On the other hand, the first principles used in environmental modeling involve the transport of passive scalars which incorporates advection, diffusion, and reactions. Typically, an ecological model contains a hydrodynamic module (HM) and a Species Transport module (ST). The ST module involves the interaction between biological and chemical component as well as its transports. The typical elements of an ST module are algae, organic carbon, phosphorus, nitrogen, dissolved oxygen, sediment fluxes (only nitrate is included), and submerged aquatic vegetation (not included in the present research). In this thesis, commonly used equations are considered to build a series of passive scalar equations that couple all the processes into a ST module (or water quality model). Such a model is fed by the results of a hydrodynamic model that solves velocity, pressure, and temperature field. The hydrodynamic model solves the RANS equations with a k-ε closure model for turbulence plus a transport equation for the temperature field (decoupled from flow field; no density changes are included). The ST module solves a series of couple passive scalar equations in the bulk of the domain that accounts for biological and chemical processes affecting nutrient dynamics, and energy exchange at the free surface (e.g., the mathematical model of light that influences photosynthesis).

3. The Validation of BioChemFOAM - Numerical Experiments (Chapter 4). This chapter presents the validation process using numerical experiments. This section introduces a series of numerical experiments that reproduce fundamental Physical, Chemical, and Biological processes (PCBP) in an aquatic ecosystem. It introduces six (6) cases to test different components of BioChemFOAM and to demostrate its robustness when complexity is added in a systematic manner. In order to validateBioChemFOAM, an additional model was implemented in MATLAB (BioChemMATLAB) that considered only chemical and biological process. BioChemMATLAB was used to compare results obtained from BioChemFOAM and validate the parameterization implemented in both models. The comparison of the two codes is done to ascertain that the equations derived from PCBP are solved correctly. The model, BioChemFOAM, was tested in a well known flow in a cavity and in an ideal channel. Also, a new set of chemical and biological processes was implemented from (Sun, Petersen, & Clement, 1999), that confirms the validity of the proposed method, splitting-operator, applied to the full set of species transport equations introduced in BioChemFOAM (see Chapter 3). This approach, using an additional code, published results, and characteristic coefficients and parameters, was used to fully validate the proposed model and show its robustness.

4. The Validation of the Hydrodynamic Component in BioChemFOAM using sample data from previous studies in a Backwater Area in the Mississippi River (Chapter 5). In this section, a comparison of flow fields between BioChemFOAM and commercial code FLUENT is performed. Both models reproduce the same flow patterns for the summer of 2009. The flow field from this stage on was left constant to accelerate calculation in the ST module.

5. The Validation of Species Transport in BioChemFOAM using sample data from a Backwater Area in the Upper Mississippi River (Chapter 6). This section validates the model BioChemFOAM with previous data and under different degrees of complexity. The first case compares BioChemFOAM results with previous studies when modeling only nitrate transport

that reacts with the bed. The second case shows a characteristic spatial and temporal distribution of species for a summer period in a backwater area. The third case shows the solution independence when different initial conditions are imposed. Finally, BioChemFOAM is utilized to study the removal rate when different conditions are imposed. The results of the last part are compared with typical removal rates encountered in the literature.

6. Finally, Conclusions and Future Work (Chapter 7) summarizes the findings and suggests improvements to the current model.

1.5 <u>Main thesis contributions</u>

This section includes a list of primary contributions highlighted by the present research:

- Development of a robust, highly-resolved nutrient dynamics tool, 3-D BioChemFOAM, that is based on available sample data and common practices used to formulate water quality models. Detailed discussion in Chapters 3, 4, 5, and 6.

- Novel introduction of a framework to add complexity to a species fate and transport tool by including main nutrient dynamic processes through parameterizations. A detailed description is offered in Chapters 4, 5, and 6.

- Implementation of a new method in OpenFOAM to solve sets of species transport equations that include couple reaction terms through PCBP (Chapter 3).

- Application of the model to one real case in the Mississippi River backwater using available data to cauculate percentange of nitrate removal, PNR, (Chapters 5 and 6).

- Implementation of a splitting-operator method in OpenFOAM to solve coupled PDEs with coupled reactive terms (Chapter 3 and 6).

- Review and analysis of current state of the art models that address species transport in aquatic ecosystems. (Chapter 1 and 2).

CHAPTER 2

LITERATURE REVIEW

2.1 Hydrodynamic and Water Quality Modeling

2.1.1 Experimental investigation

The literature reagarding the measurements of ecosystems parameters at the level of detail required for a highly resolved species transport models is often scarce. The experiments described in the following paragraphs covers studies on wetlands, lakes, and pollution control typically recorded as wetland traetment options in urban environments. These studies bring us closer to future applications in riverine environments such as floodplains and backwater lakes of the Mississippi river. The final application points towards future validation of the proposed model.

A recent study (Mitsch et al., 2012) shows the performance of a one hectare flow through two riverine wetlands that were created in 1993 and 1994 at the 20-ha Wilma H. Schiermeier ORWRP, a complex of created and natural freshwater riverine wetlands located on the campus of The Ohio State University in Columbus, Ohio. The inflow water is taken from the Olentangy River, which has nutrient and sediment concentrations sufficient for the investigation of long-term trends in wetland retention without excessive overload or saturation. The wetlands was monitored over 15 years. One of the wetlands was planted and the other was unplanted. The planted wetland had a higher plant community diversity index over 15 years, whereas the unplanted wetland was more productive. Wetland soils turned hydric within a few years; organic carbon in the soil doubled in 10 years and almost tripled in 15 years. Nutrient removal was similar in the two wetlands in most years with a trend of decreasing phosphorus removal over 15 years. Denitrification accounted for a small percentage of the nitrogen reduction in the wetlands. The wetlands were effective carbon sinks with retention rates of 18,002,700 kilograms of carbon per hectare per year, which is higher than in comparable wetlands and more commonly studied boreal peatlands. Methane emission rates were low enough to allay concern that the wetlands are

net sources of climate change radiative forcing. Planting appears to have influenced carbon accumulation, methane emissions, and macrophyte community diversity.

Another study concenrning wetlands on riverine environments (Spieles & Mitsch, 1999) compares the nitrate removal efficiency of two constructed wetlands located in central Ohio, USA. The Licking County Wastewater Treatment Wetland (LCW), located near Kirkersville, OH, USA and two experimental wetlands of the Olentangy River Wetland Research Park (ORW) in Columbus, OH. Both were monitored over 2 years for inflow and outflow rates, average water depths, and precipitation. Nutrient measurements were also performed on nitrate plus nitrite ion concentration inflow and temperature. With an inflow of 12.3 $kgNha^{-1}day^{-1}$ of nitrite and 12.5 $mgNL^{-1}$, the percentage removal was almost 29 % in the wastewater wetland and 37-40% in the riverine wetlands.

The last examples of measurements along a riverine environment shows a general trends of the variables that influence nitrogen removal but lack the level of detail needed to fully validate a CFD code. To improve the level of detail continuous data is being collected by IIHR-LACMRERS in a Mississippi River backwater area, (Schubert, 2009). This information, in combination with characteristic values optained from a water quality study performed in an Upper Mississippi River area called Lake Pepin (LimnoTech, 2007), will be used to validate the model in a Mississippi River backwater area.

2.1.2 Numerical models, review

There are many varieties of environmental water quality modeling. These models vary both in complexity and in terms of the processseses modeled to represent the state of a catchment, river, lake, or wetland based on hydrodynamic, chemical, and biological processes. These inputs are the framework of the software, and understanding them is vital to applying the software accurately. The more processes modeled, the bigger the challenge in building a computational model. Table 2-1 shows the classification of computational models based on fluid mechanics and

following combustion principles (combustion solves fluid, heat, and mass transport equations; the chemical species concentrations calculations provide solutions to a series of stoichiometric reactions that influence the flow field; and environmental applications solves a series of chemical stoichiometric relations plus the biological processesand commontly do not change the fluid flow field). The 3-D models classified earlier fully solve the Navier-Stokes equations and do not simplify in the vertical direction. The quais three dimensional (3qD) classification simplifies the Navier-Stokes equations in the vertical direction and assumes a hydrostatic vertical distribution.

Table 2.1: Classification criteria for Water Quality Models

Condition	Classification Adjectives
Time dependence	Steady (S) or Unsteady (US)
Spatial dependence	One dimension (1D), Two dimensions (2D), Three dimensions (3D) or quasi three dimensions (q3D)
Flow conditions	Laminar flow (LF) or Turbulent flow (TF).
Initial phases of reactants	Single-phase (1P), two-phase (2P), or multiple-phase (MP).
Sites of reactions	Homogeneous (HO), Heterogeneous (HE).
Rate of reactions	Chemical equilibrium (infinite rate, IR) or finite rate (FR).
Degree of compressibility of flow	Incompressible flow (IF) or compressible flow (CF).

The models shown in Tables 2.2 and 2.3 represent the present "state of the art" in water quality modeling. These models have been used to assess the performance of ecological systems in rivers, lakes, and wetlands. The selection of a model depends on the particular physical processes in the system under study. The principal characteristics of each model and some applications are explained in the following paragraphs.

$CE-QUAL-R1$ (RivWQM) is spatially one dimensional and horizontal averaged; temperature and concentration gradients are computed only in the vertical direction. The model simulate vertical profiles of water quality in lakes and reservoirs as well as density- and wind-driven vertical mixing of constituents through a series of horizontal layers. It does not require any surface water flow or routing modeling; inflows and outflows are added directly to or removed directly from the appropriate layers. It is not suitable for domains in which the lateral or longitudinal variations in water quality are important, (Wlosinski, Lessem, Dortch, Schneider, & Martin, 1995). A Monte Carlo option allows easy analysis of sensitivity to input parameters. The water quality parameters modeled are: temperature, zooplankton, algae, fish, silica, dissolved organic matter, phosphorus, nitrogen, dissolved oxygen, metals, sulfur, inorganic suspended sediments, total dissolved solids, alkalinity, pH, detritus and sediment diagenesis, (USACE, 2012). The model was applied to a small eutrophic reservoir near Spring Valley, WI, USA and showed an acceptable agreement between measured and calculated values (Wlosinski & Collins, 1985). This application was one of the first attempts to predict hydrodynamic, biological and chemical variables in an ecosystem and is rarely used today due to its lack of consideration of the spatial variability of the state variables in a ecosystem.

The *TWQM*, Tail Water Quality Model, focuses on dissolved oxygen and other constituents (e.g., reduced iron and manganese, ammonium, and sulfide) that typically cause water quality concerns immediately downstream from deep reservoir releases. The model can be applied relatively quickly in a user-friendly environment on a personal computer. It also can be used to evaluate the effects, such as adding hydropower, of altering reservoir releases, and to

estimate the amount of tailwater required for the natural recovery to better water quality conditions, (USACE, 2012). Extensive coverage of the methods used in this model can be found in the literature (M. S. Dortch, Tillman, & Bunch, 1992). The model was calibrated in four locations: Nimrod Dam, Rough River, Canyon Dam (Guadalupe River, Texas) and Greeson Dam. The Greeson Dam showed acceptable agreement between observed and predicted values for Dissolved Oxygen (DO), Dissolved Manganese (DM) and unacceptable values for Ammonia Nitrogen (AN), Organic Nitrogen (ON), and Nitrate Nitrogen (NN). The application of the model at Nimrod Dam showed an acceptable agreement for DO and DM but not for AN, ON, Dissolved Iron (DI), and Sulfite. The Rough River application showed good agreement between measured and calculated values for: DO and DM but not for ON and DI. Finally, Canyon Dam showed good agreement for DO, DM, AN, and NN but poor agreement for Sulfide (M. S. Dortch et al., 1992). In general, model does not capture the variation of all the species considered and is limited in reproducing the dynamical processes of an ecosystem.

BATHTUB allows users to apply a series of steady-state models in a spatially segmented hydraulic network in order to predict eutrophication responses in lakes and reservoirs. Its supporting programs, *FLUX* and *PROFILE*, facilitate estimation of nutrient loading and water quality conditions, respectively, (USACE, 2012). Applications of *BATHTUB* are typically limited to steady-state evaluations of the relationships between nutrient loading, transparency, and hydrology, and eutrophication responses. Short-term responses and effects related to structural modifications or responses to variables other than nutrients can not be explicitly evaluated.The programs and models have been applied to US Army Corps of Engineer reservoirs (Kennedy, 1995), as well as a number of other lakes and reservoirs. BATHTUB is cited as an effective model for lake and reservoir water quality assessment and management, particularly where data are limited (Ernst, Frossard, & Mancini, 1994).

QUAL2K is a river and stream water quality model. The model is one dimensional; the channel is well-mixed vertically and laterally; and the flow is steady and non-uniform. The model calculates the diurnal heat budget and water-quality kinetics and considers the following

processes: carbonaceous BOD, anoxia, sediment-water interactions, bottom algae, light extinction, pH and pathogens, (EPA, 2011). One recent application (Cho & Ha, 2010), performs a parameter optimization of the *QUAL2K* model for a multiple-reach river using an influence coefficient algorithm in the Gangneung Namdaecheon River. However, this model still lack of spatial variability of the variables involved in an ecosystem.

CE-QUAL-RIV1 is a one-dimensional (cross-sectionally averaged) hydrodynamic and water quality model, meaning that the model resolves longitudinal variations in hydraulic and quality characteristics and is applicable where lateral and vertical variations are small. *CE-QUAL-RIV1* consists of two parts; a hydrodynamic code (*RIV1H*) and a water quality code (*RIV1Q*). The hydrodynamic code is applied first to predict water transport, and its results are written to a file which is then read by the quality model. It can be used to predict one-dimensional hydraulic and water quality variations in streams and rivers with highly unsteady flows, although it can also be used for prediction under steady flow conditions, (M. Dortch, Schneider, Martin, Zimmerman, & Griffin, 1990; EPA, 2011).

CE-QUAL-ICM can be used for two or three dimensional water quality modeling often estuarine/coastal environments, harbors, and embayments and is recommended for deep narrow estuaries. It is based on the finite volume modeling approach. This model evolved from a 3D water quality model that was developed for Chesapeake Bay to evaluate the effectiveness of a nutrient reduction proposal on Bay eutrophication. The model now contains a bottom sediment chemistry submodel that interacts with the water column for simulating sediment oxygen demand and nutrient fluxes. The *CE-QUAL-ICM* modeling approach involves first applying a 2D or 3D hydrodynamic model and then coupling the output to *CE-QUAL-ICM* for driving the transport terms, (Cerco & Cole, 1995). (Sucsy & Hendrickson, 2004) present an application for the Lower St. Johns River to calculate nutrient load reductions. The results of this study provide recommended nutrient Pollution Load Reduction Goals for the Lower St. Johns River and also calculate the assimilative capacity of the river and provide recommendations for Total Maximum Daily Loads (TMDL).

PCE-QUAL-ICM, which is based on *CE-QUAL-ICM*, is a three-dimensional eutrophication model developed at the U.S. Army Corps of Engineers Waterways Experiment Station (CEWES), Vicksburg, MS. This water quality model is semi-explicit in time, and is based on an unstructured cell-centered finite volume numerical method. The Hydrodynamics data such as velocity and turbulent diffusion are read externally, and the model then computes the advection-diffusion-reaction of a number of physical and state variables such as temperature, salinity, sediments, oxygen and algae. The sequential FORTRAN 77 code was parallelized using a data/domain decomposition strategy using a single program multiple data (SPMD) paradigm. WQMPP, a pre / post processor for the PCE-QUAL-ICM water quality model which splits the global domain into a specified number of smaller domains and sets up the local data files and message passing tables, has been developed. WQMPP, when run in post-processor mode, also combines the local subdomain output to produce global output in a format similar to that produced by the original *CE-QUAL-ICM* code. *PCE-QUAL-ICM*, the parallel water quality model, enhances *CE-QUAL-ICM* with message passing. Inter-processor communication is accomplished using MPI communication libraries and the parallel code has been ported onto the CRAY-T3E, IBM-SP2 and SGI O2000(Chippada et al., 1998).

PREWET, a screening-level, can be rapidly aplied with minimal input data to estimate the amount of water quality improvement provided by wetlands. Given basic characteristics about the wetland, pollutant removal efficiency (RE) can be computed for total suspended solids, total coliform bacteria, biochemical oxygen demand, total nitrogen, total phosphorus, and contaminants (e.g., organic chemicals and trace metals). The RE depends on the wetland detention time and the removal rate, K (day^{-1}), for the constituent. The removal rate depends on a number of processes, such as microbial metabolism, adsorption, volatilization, denitrification, settling, etc., and ambient conditions, such as water temperature. The model is focused on dominant long-term removal mechanisms and makes use of literature values or mathematical formulations for those mechanisms when possible. A report documents the analytical model formulations for predicting pollutant RE provided by wetlands. These formulations have been

programmed into an interactive, user-friendly, PC-based computer program. Predicted RE's for total suspended solids, total nitrogen, and total phosphorus are compared to observed RE's at the Cache River Wetland, Arkansas, (USACE, 2012).

ICM, an eutrophication model, and *TOXI*, an organic chemical model, are incorporated into *CE-QUAL-ICM*. The release version of the eutrophication model computes 22 state variables including physical properties; multiple forms of algae, carbon, nitrogen, phosphorus, silica, and dissolved oxygen. Recently, two size classes of zooplankton, two benthos compartments (deposit feeders and filter feeders), submerged aquatic vegetation (roots and shoots biomass), epiphytes, and benthic algae were added, although this version of the code is not generally released to the public. Each state variable may be individually activated or deactivated. One significant feature of ICM, the eutrophication version, is a diagenetic sediment sub-model. The sub-model interactively predicts sediment-water oxygen and nutrient fluxes. Alternatively, these fluxes may be specified based on observations. The eutrophication model has been applied to a variety of sites, including: Chesapeake Bay, Inland Bays of Delaware, New York Bight, Newark Bay, New York - New Jersey Harbors and Estuaries, Lower Green Bay, Los Angeles - Long Beach Harbors, Cache River wetland, San Juan Bay and Estuaries, Florida Bay and Lower St. Johns River (on-going) The ICM/TOXI model incorporates the toxic chemical routines from EPA's WASP (Water Analysis Simulation Program) model into the transport code for ICM, adds a more detailed benthic sediment model, and enhance the linkages to sediment transport models. ICM/TOXI includes: physical processes such as sorption to DOC and three solid classes, volatilization, and sedimentation; and chemical processes such as ionization, hydrolysis, photolysis, oxidation, and biodegradation. ICM/TOXI can simulate temperature, salinity, three solids classes, and three chemicals (total chemical for organic chemicals and trace metals). Each species can exist in five phases (water, DOC-sorbed, and sorbed to three solids types) via local equilibrium partitioning. The WASP toxic chemical model upon which ICM/TOXI is based has been applied to a wide variety of sites. ICM/TOXI will be released when the documentation/user guide report is published, (USACE, 2012).

Delft3D Suite allows to simulate the interaction of water, sediment, ecology and water quality in time and space. The suite is mostly used to model natural environments like coastal, river, and estuarine areas, but it is equally suitable for artificial environments like harbours, and locks. *Delft3D* consists of a number of programs, which are linked to and integrated with one-another. Two models are important for WQM: *D-Flow* and *D-Water Quality*. *D-Flow* simulates non-steady flows in relatively shallow water. It incorporates the effects of tides, winds, air pressure, density differences (due to salinity and temperature), waves, turbulence (from a simple constant to the $k - \varepsilon$ model), and drying and flooding. With the integrated heat and mass transport solver, Deltares (Its an independent institute for applied research in the field of water, subsurface and infrastructure located in The Netherlands, http://www.deltares.nl/en/about-deltares) front running knowledge of stratified hydrodynamics has been built into this program. The output of the program is used in all the other programmes in *Delft3D suite*. The second model, *D-Water Quality*, simulates the far and mid-field water and sediment quality due to a variety of transport and water quality processes. It includes several advection diffusion solvers and an extensive library of standardized process formulations with user-selected substances. Default processes allow the user to simulate the decay of BOD and nitrification, elementary growth of algae and nutrient cycling, exchange of substances with the atmosphere, adsorption and desorption of contaminant substances, and the deposition and re-suspension of particles and adsorbed substances to and from the bed. The D-Water Quality program is also available as add-on for *TELEMAC* (http://www.opentelemac.org/)users, from (DELTARES, 2009).

EcoLab (DHI, 2011) is used for ecological modeling can be applied to water quality and ecological studies related to rivers, wetlands, lakes, reservoirs, estuaries, coastal waters, and the sea, spatial predictions of any ecosystem response, simple and complex water quality studies, impact and remediation studies, planning and permitting studies, and water quality forecast. (Bermúdez, García, Quintela, & Delgado, 2008) applied the model to the Lignitos de Meirama open pit coal mine (Spain) and concluded that the model that the surface water quality would be good enough to satisfy the Spanish water quality standards in two years. The model uses also

Mike 3 HD which is based on RANS using Boussinesq approximation and hydrostatic pressure. This model is an improvement over the last models due to its spacial variability of the ecological variables and improvement in the hydrodynamic model (DHI, 2004). It still lacks a complete resolution of the pressure field when assuming hydrostatic pressure distribution in the vertical direction.

WASP5, (Ambrose, Wool, & Martin, 1993)is a dynamic compartment model that can be used to analyze a variety of water quality problems in such diverse bodies of water as ponds, streams, lakes, reservoirs, rivers, estuaries, and coastal waters. An application of the model is presented by (Tufford & McKellar, 1999). The model was applied to Lake Marion using field data from 1985 to 1990 used to parameterize the models. Phytoplankton kinetic rates and constants were obtained from a related in situ study; others from modeling literature (Tufford & McKellar, 1999). The hydrodynamic model was calibrated to estimates of daily lake volume and the water quality model was calibrated for ammonia, nitrate, ortho-phosphate, dissolved oxygen, chlorophyll-a, biochemical oxygen demand, organic nitrogen, and organic phosphorus. Water quality calibration suggested the model characterized phytoplankton and nutrient dynamics quite well. The model uses a Finite Difference approximation that may not ensure local and global conservation of species transport. This approcimation is based on the information obtained from an external hydrodynamic model which make it difficult to use when trying to couple the two models. In addition, the quality of the external hydrodynamic model used can affect the final results.

CE-QUAL-W2 is a 2D (longitudinal-vertical) water quality and hydrodynamic model for rivers, estuaries, lakes, reservoirs and river basin systems. It models basic eutrophication processes such as temperature, nutrient, algae, dissolved oxygen, organic matter and sediment relationships. The current model release enhancements have been developed under research contracts between the Corps and Portland State University under the supervision of Dr. Scott Wells. The model's capabilities include longitudinal-vertical hydrodynamics and water quality in stratified and non-stratified systems, multiple algae, epiphyton/periphyton, zooplankton,

macrophyte, CBOD, and generic water quality groups, internal dynamic pipe/culvert model, hydraulic structures (weirs, spillways) algorithms, including those for submerged and 2-way flow over submerged hydraulic structures and a dynamic shading algorithm based on topographic and vegetative cover. Its limitation is its assumption of well-mixed conditions in a lateral direction and hydrostatic assumption for vertical momentum equation (PSU, 2012).

CCHE3D is a three dimensional numerical simulation model for simulating free surface turbulent flows with sediment transport, pollutant transport, and water quality analysis capabilities. The full Reynolds equations are solved using the efficient Element Method, which is a collocation approach of the finite element method. Several turbulence closure schemes are available for users to select for different applications. The model can be used for both small scaled near field, detailed flows and sediment transport analyses and large scale engineering applications (NCCHE, 2012). The model uses the Fine Element Method in conjunction with the Finite Volume Method. The free surface is computed with the free surface kinematic equation. Boussinesq assumption is used to formulate turbulence stresses. Several turbulence closure schemes are available including two zero equation models, parabolic and mixing length, and four two equation models, standard k-ε, RNG k-ε, k-ω, and non-linear k-ε model. The simpler models are for efficient studies, while the more complex models resolve more details of the flow distributions. Wall functions can be applied as boundary conditions for vertical walls as well as for irregular bed surfaces. The model can use a hydrostatic pressure assumption. The model has been applied to Deep Hollow Lake in the Mississippi alluvial plain to simulate the concentrations of phosphate and organic phosphorus, the results shows considerable agreement between measurements and calculations (Chao, Jia, Cooper, Shields Jr, & Wang, 2006).

SSIIM is an acronym for a Sediment Simulation In Intakes with Multiblock option. The program is designed for used in teaching and research for hydraulic/river/sedimentation engineering. It solves the Navier-Stokes equations using the control volume method with the SIMPLE algorithm and the k-ε turbulence model. It also solves the convection-diffusion equation for sediment transport using van Rijn's formula for the bed boundary. A water quality

module is also included. The water quality is calculated with the convection-diffusion equation for each given species. The manual (Olsen, 2011) lists the following limitations: the program neglects non-orthogonal diffusive terms; the grid lines in the vertical direction have to be exactly vertical; kinematic viscosity of the fluid is equivalent to water at 20^oC and can not be changed because it is hard coded; and the program is not made for the marine environment so all effects of density gradients due to salinity differences are not taken into account. The manual laso mentions that the program still contains approximately one bug for each 2000 lines of source code, which is a significant problem because *SSIIM* has over 100000 lines of code and several modules has not been tested. The model implements a convection-diffusion equation for the concentration of a particular species, and the program allows all the properties of the species to be inserted in text files that can be processed by the software. The model does not have parallel computational capabilities.

ELCOM (www.cwr.uwa.edu.au), <u>E</u>stuary and <u>L</u>ake <u>CO</u>mputer <u>M</u>odel, is a three-dimensional hydrodynamics model used for predicting the velocity, temperature and salinity distribution in natural water bodies subjected to external environmental forcing such as wind stress, surface heating or cooling, (Brown, 2011). The unsteady Reynolds-averaged, hydrostatic, Boussinesq, Navier-Stokes, and scalar (e.g., potential temperature, salinity, or tracer) transport equations with an eddy-viscosity/diffusivity closure for the horizontal turbulence correlations are used as the basis for the estuary and lake computer model (ELCOM). ELCOM do not assume a relationship between the vertical Reynolds stress terms and the resolved shear, but instead apply a mixing model to directly compute the vertical turbulent transport. Molecular diffusion in the vertical direction is neglected as turbulent transport and numerical diffusion are generally dominant. The free-surface evolution is governed by the vertical integration of the continuity equation for incompressible flow in the water column applied to the kinematic boundary condition, (Hodges, Imberger, Saggio, & Winters, 2000). One recent application is given implements ice formation in the model(Oveisy, Boegman, & Imberger, 2012). The model was validated against observed data from both a large and small Canadian mid-latitude lake (Lake

Ontario and Harmon Lake, respectively), and the results show good agreement between snow thickness and temperature profiles. It is not mentioned in the literature that the model has the ability to be run in parallel computers. The model is one of the most completes ones found in the literature but at this time tha author does not have acces to manuals that would give an in-depth view of the robustness of the model.

HEM-3D, (Park, Jung, Kim, & Ahn, 2005), is a three dimensional <u>H</u>ydrodynamic-<u>E</u>utrophication <u>M</u>odel. It consists of a hydrodynamic model and a water quality model linked internally. The hydrodynamic model is EFDC which is a 3D model based on continuity, momentum, salt balance, and heat balance equations with hydrostatic and Boussinesq approximations. For turbulent closure, the second momentum turbulence model. The WQM models 21 state variables based on the *CE-QUAL-ICM* model. The physical transport and biochemical processes are decoupled.

Table 2.2 Description of Underlined Water Quality Models (WQM), Part A. (RWQM: Reservoir WQM, H: hydrodynamic, RivWQM: River WQM, EsCoWQM: Estuary and Coastal WQM, WWQM: Wetland WQM. Private: the software can be used only by the owner. Public: license not needed. Owner: license needed in order to use the model.)

Model Name	Classification Adjectives	Owner
CE-QUAL-R1 (RWQM)	1D - LF - 1P - HO - FR - IF	USACE. Download currently available for U.S. Army Corps of Engineers use only
CE-QUAL-W2 (RWQM)	2D - LF - 1P - HO - FR - IF	USACE. One version can be found at Portland State University.
TWQM (RWQM)	1D - S	USACE. Public.
Bathtub	0D - S - 1P	USACE. Public.
QUAL2k (RivWQM)	1D(S)	EPA. Public.
CE-QUAL-RIV1	1D - US - H	USACE. Owner.
PREWET (WWQM)	0D - 1P	USACE. Owner.

Table 2.3: Description of Water Quality Models (WQM), Part B. (RWQM: Reservoir WQM, H: hydrodynamic, RivWQM: River WQM, EsCoWQM: Estuary and Coastal WQM, WWQM: Wetland WQM. Private: the software can be used only by the owner. Public: license not needed. Owner: license needed in order to use the model.)

Model Name	Classification Adjectives	Owner
CE-QUAL-ICM (EsCoWQM/WWQM)	1D/2D/q3D-H	USACE. Internal use only.
ICM/TOXI (CoFate)	q3D	USACE. Internal use only.
Delft3D Suite	q3D - US . D-Flow 3D. D-Water	Deltares. Owner.
ECO Lab	1D/2D/3D-S/US-H-WQM-1P	Mike by DHI. Owner.
WASP	1D/2D/3D - S - LF - 1P	EPA. Public.
CCH3D	3D - US - LF/TF - 1P - IF	NCCHE at TUM. Owner.
SSIIM	3D - US -LF/TF - 1P - IF	NTNU at NUST. Owner.
ELCOM	3D - US -LF/TF - 1P - IF	CWR. Owner.
HEM-3D	3D - US -TF - 1P - IF	SMIC. Owner.
OpenFOAM	3D - S/US - LF/TF - MP - IF/CF	OpenFOAM. Public.
FLUENT	3D - S/US - LF/TF - MP- IF/CF	ANSYS, Inc. Owner

2.2 Limitations of actual models

The information collected helped to identify the following limitations of the models presened here:

- Several of the models do not compute hydrodynamics and lack interaction among hydrodynamic, biological, and chemical processes.

- They lack flexibility, and it is diffucult or not available to add new processes that are involved in an ecosystem.

- The models that implement 3D interactions of state variables do not present a systematic validation of all the processes involved for an ecosystem.

- The most complex models (e.g., the ones that solve Navier-Stokes equations with a closure model for turbulence) are not accessible to the general public.

- The majority of the models do not have the ability to run in parallel high performance computers.

2.3 OpenFOAM libraries general description

OpenFOAM is an Open platform for Field Operation and Manipulation C++ class software library for continuum mechanics. The library makes it easy to develop reliable and efficient computational continuum-mechanics codes by retaining as closely as possible, in the programing language, the conventional programing notation of tensors and partial differential equations. C++ object-oriented programing language enable the creation of data types that closely mimic those from continuum mechanics, and the operator overloading allows normal mathematical symbols to be used for basic operations, (Weller, Tabor, Jasak, & Fureby, 1998). The set of programming libraries use three basic principles in Object Oriented Programming: abstraction, inheritance, and polymorphism. Abstraction is the ability to represent conceptual constructs in the program and to hide details behind an interface. This is achieved by allowing the programmer to create classes to represent conceptual objects in the code, classes that

encapsulate (i.e., contain and protect) the data that make up the object. Inheritance enables relationships among the various classes to be expressed, representing commonality among different classes of objects by class extension. Finally, polymorphism is the ability to provide the same interface to objects with different implementations, thus representing a conceptual equivalence among classes that in practical terms have to be coded differently. Examples of this in FOAM include the implementation of boundary conditions (Weller et al., 1998). The implementation of the libraries use the Finite Volume Method (FVM) to solve a continuum mechanics problem.

In general, the overal philosophy of OpenFOAM is to build physical models based on first fundamental principles: conservation of mass, conservation of momentum, conservation of energy and constitutive relations. The implementation works as a toolbox in which it is easy to transform equations such as (momentum equation):

$$\frac{\partial(\rho \mathbf{U})}{\partial t} + \nabla \cdot (\rho \mathbf{U}\mathbf{U}) - \nabla \cdot (\rho \mathbf{R}) = -\nabla p \tag{2.1}$$

into an OpenFOAM formulation like:

$$\begin{aligned}&\text{fvm::ddt(rho,U)}\\&+\text{fvm::div(phi,U)}\\&+\text{turbulence} - \text{divRhoR(U)}\\&== \text{fvc::grad(p)}\end{aligned} \tag{2.2}$$

In general, any equation can be rewritten as equation (2.2). Those equations are present in a C++ file that contains a particular application. For example, they can be encapsulated into a personalized solver that can solve the incompressible laminar Navier-Stokes Equations (NSE). The equation can be recast in one master file (with extension .C) that solves the coupled system of equations by one of the well-known methods SIMPLE or PISO, (Ferziger & Perić, 1996). The structure of the program is similar to a flow chart (Versteeg & Malalasekera, 2007). More information of OpenFOAM can be found in (ESI, 2014) and (OpenFOAMWiki, 2014), and

several forums on the internet, (TheOpenFOAMExtendedProject, 2014), (CFDOnline, 2014).
Finally, the platform OpenFOAM is flexible enough so that almost any parameterization can be
included. This appeals to future work and accesibility for future users in using OpenFOAM to
implement hydrodynamics and species transport processes for a varaiety of aquatic ecosystems.

CHAPTER 3

DESCRIPTION OF PROPOSED MODEL BIOCHEMFOAM

3.1 Introduction

This section presents the mathematical formulation of Physical, Chemical, and Biological Processes (PCBP) included in BioChemFOAM. It is divided into nine sub-sections. Section 3.2 introduce the general module components. Sections 3.3 and 3.4 introduce the mathematical formulation from first principles using fundamental stoichiometric relations. Section 3.5 presents a description and the values of typical coefficients defined during the parameterization of the processes. Section 3.6 introduces an example of how the Boundary Conditions and Initial Conditions (IC) are used in BioChemFOAM. Section 3.7 shows the main numerical methods used to solve the system of equations for the Hydrodynamic and Species Transport Modules. Section 3.8 summarizes the equations to be solved and presents the solution strategy to solve the Species Transport module (ST). Finally, Section 3.9 presents the highlights and description of the implification of the proposed model.

At this point, it is also worthy to mention the importance of the proposed model. The previous chapters exposed the framework for the application of an ecological model at project scale (e.g. the restoration of inland zones to reduce nitrogen loads) and the gaps left by the actual models (lack of cohesion, difficulty accessing parameterizations, and simplification of physical processes). The present model and applications have been created to improve the actual models in order to advance research modeling in environmental systems by incorporating common parameterizations in a robust platform. Its integration of the first principle of physics and it robustness make it an ideal modeling tool to help understand the processes that occur in systems such as pools along the Mississippi River. The features inherit in the modeling tool present an invaluable alternative for managers and environmental agencies to use when they evaluate and plan restoration projects that improve the sustainability of bodies of water. Furthermore, its public platform makes its easy to improves the sustainability of bodies of water and to

incorporate processes through parameterizations that influence a particular ecosystem. The chapter discusses the application of the model to fundamental components in an aquatic ecosystem and to explore the numerics behind the application as well as its implication but also its application to a real case.

3.2 General Description of Physical, Chemical and Biological Processes (PCBP) included in BioChemFOAM

The general idea is the apply fundamental laws of physics to environmental flows, specifically to water quality modeling in inland waters. The laws used to describe the physical processes in this research are: Beer's Law (in this thesis light intensity is modeled with a mathemathical parameterization), Kinetic formulation see, for example (Clair, Perry, & Gene, 2003) or (Schnoor, 1996) page 99 or (Kee, Coltrin, & Glarborg, 2005) page 381, Monod Formulation (Monod, 1949), and conservation laws (mass, momentum and energy). There are additional simplifications to solve the turbulence flow that will be presented in detail later. As a first introduction, the model's simplification comes from using the Reynolds decomposition and Boussinesq approximation for turbulence modeling (Andersson, 2012).

Transport processes are at the core of any physical system that involves the interaction of different transformations. The main processes are: diffusion (molecular and turbulent), convection or advection, dispersion, interfacial transfer, and multiphase transport (Gulliver, 2007). In the present research, the fluid is incompressible with one phase, and the molecular diffusion is several orders of magnitude smaller than turbulent diffussivity (Martin & McCutcheon, 1998). In this research, a constant molecular diffusion is defined for all the dissolved species, $1x10^{-9}$ m^2/s, (Martin & McCutcheon, 1998).

In any CFD application, the following three phases need to be covered to present a final product: pre-processing, solver and post-processing (Stern et al., 2006). The software used in the present research for each phase are: Gridgen (POINTWISE, 2012) and blockMesh(pre-

processing, mesh generation) (see (OpenFOAM, 2012) for further information), Open*FOAM* (solvers and libraries), tecplot ((TECPLOT, 2014)) and PARAVIEW (post-processing, see (Kitware-ParaView, 2014) for further information).

In order to model physical, chemical and biological processes involved in an ecosystem the approach adopted in the present thesis include: numerical modeling and a case study. The first part shows and describes the implementation of necessary physical mathematical equations to represent the main processes in conjunction with fabricated numerical experiments that show the robustness and precision of the model (see Chapter 4).

The first principles that were implemented previously defined, and detailed description of the simplification is presented here. The laws utilized to formulate the model are conservation of mass, conservation of momentum, conservation of energy and transport of passive scalars. The model is based on RANS (Reynold Average Navier-Stokes equations) and a k-ε model for turbulence closure with Boussinesq approximation. The chemical and biological processes are modeled as kinetic equations and external loads. The rates of a scalar growth, e.g., algae and other reactions are implemented as Monod formulation, (Monod, 1949). The influences of different processes in a particular biological cycle (in this work: algae, organic carbon, phosphorus, nitrogen and dissolved oxygen) are assumed to have a multiplicative effect. For example, the algae growth term is driven by the maximum growth rate (a constant), a growth limiting function for nutrients, a growth limiting function for light intensity, and a growth limiting function for temperature.

The modeling of species in BioChemFOAM, is based on the EPA code, EFDC (EPA, 2011). The model takes into account common species that act on an ecosystem like the one shown in Figure 3.1. The compartments shown in Figure 3.1 are presented in detail in Figure 3.2. This box contains all the interactions of physical processes. The idealization presented in Figure 3.2 also shows four major elements that are defined to encapsulate species concentration (e.g., the N element in red is an example of a sub-box). Each of this sub-boxes represents a group of

species characterized by its concentration, e.g., nitrate ($NO3=NO_2^-+NO_3^-$) is contained in the

sub-box called N in red in Figure 3.2.
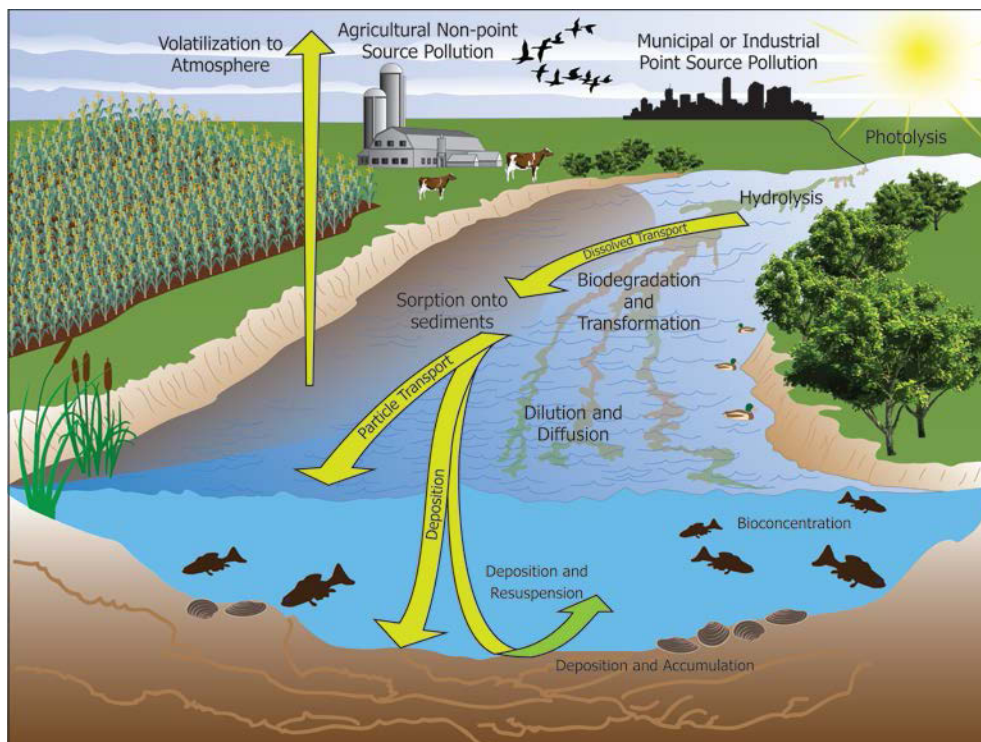
Figure 3-1. Scheme showing a typical aquatic ecosystem. The figure also shows two compartments, which represent cells after the discretization of the domain when building a Computational Fluid Dynamics (CFD) application.
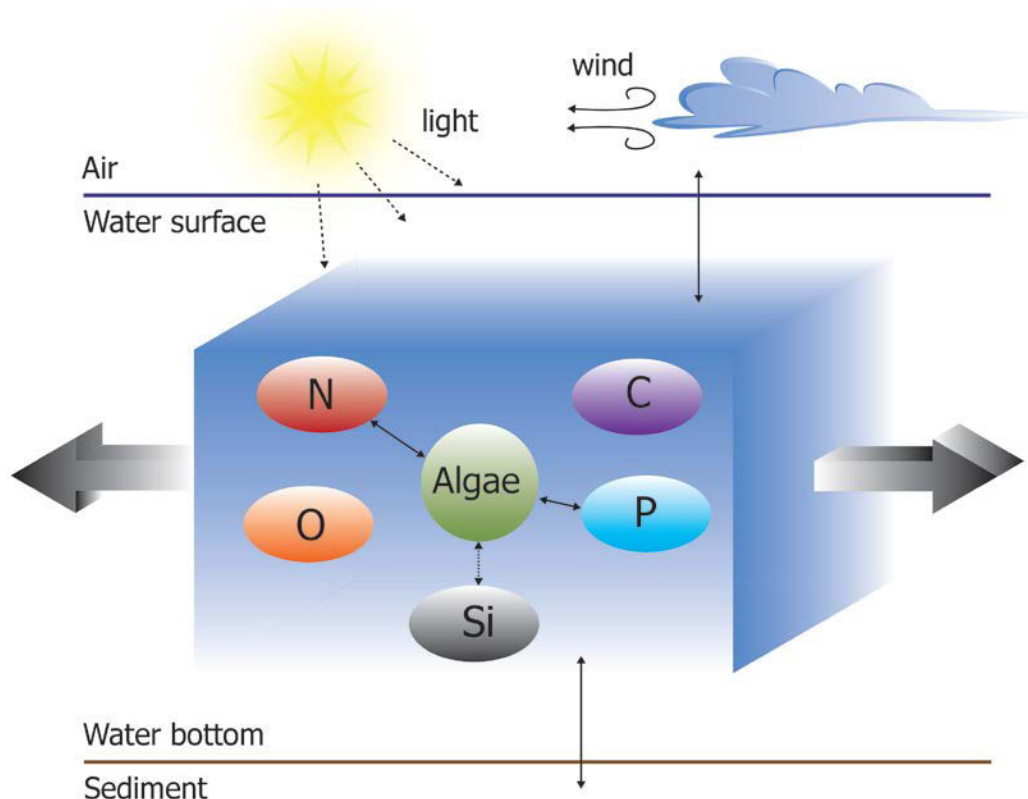
Figure 3-2. Detail of a typical Compartment, representing cells after the discretization of the domain when building a Computational Fluid Dynamics (CFD) application. Extracted from Figure 3.1 . The large black arrows represent the interaction between water compartments. The small back arrows on top and bottom, represent, respectively, the water-air interface and the water-sediment interactions. The ovals or nodes inside the Compartment represent a group of species to model. The node Algae: is a generic name used to describe algae (e.g., green algae) in suspension. The N node represents all species whose major component is nitrogen, e.g., nitrate plus nitrite given as a variable NO3. The C node represents all species that have carbon, e.g., Dissolved Organic Carbon DOC. The P node represents species with major phosphorus components, e.g., dissolved orthophosphate with a variable name, PO4. The Si node represents components that includes silica, and it is not modeled in the present research. The O node represents the dissolved oxygen in the water.

3.3 Stoichiometry for Chemical and Biological Processes

This section introduces the main stoichiometric relations used in the next section to formulate the mathematical model. The present model takes as a central component a living organism called algae, which is denoted by the variable name Bx. Algae interact mainly with three cycles (nitrogen,phosphorus, and carbon), and with oxygen. The applications presented in this thesis asume algae to be green algae. The main stoichiometric relationships that influence each of these components are presented in Table 3.1. These relations are explained and used in the next section when formulating the mathematical model into BioChemFOAM. The relations are used to formulate the interation of the nodes presented in Figure 3.2.

Table 3-1. Stoichiometric relations used to formulate BioChemFOAM chemical and biological parameterization

ID	Stoichiometry	Processes
1	$106CO_2 + 16NO_3^- + HPO_4^{2-} + 122H_2O + 18H^+ +$ Trace elements $\underset{R}{\overset{P}{\rightleftharpoons}} \underbrace{C_{106}H_{263}O_{110}N_{16}P_1}_{\text{Algal protoplasm}} + 138O_2$	Photosynthesis (P) and Respiration (R). [1]
2	$6CO_2 + 6H_2O + 18H^+ + \text{ligh energy} \underset{R}{\overset{P}{\rightleftharpoons}} C_6H_{12}O_6 + 6O_2$	Decomposition of Organic carbon (R). [2]
3	$NH_4^+ + 2O_2 \longrightarrow NO_3^- + H_2O + 2H^+$	Nitrification. [2]
3a	$2NH_4^+ + 3O_2 \xrightarrow{\text{bacteria nitrosomonas}} 2NO_2^- + 2H_2O + 4H^+$	First stage nitrification. [2]
3b	$2NO_2^- + O_2 \xrightarrow{\text{nitrobacter}} 2NO_3^-$	Second stage nitrification. [2]
5	$5CH_2O + 4NO_3^- + 4H^+ \longrightarrow 5CO_2 + 2N_2 + 7H_2O$	Net denitrification [3]
6	$106CO_2 + 16NH_4^+ + H_2PO_4^- + 106H_2O$ $\longrightarrow \underbrace{\text{protoplasm}}_{\substack{\text{living substance} \\ \text{of algae cells}}} + 106O_2 + 15H^+$ $106CO_2 + 16NO_3^- + H_2PO_4^- + 122H_2O$ $\longrightarrow \text{protoplasm} + 138O_2$	Used to define Dissolved Oxygen (DO) processed by algae. DO produced depends on the form of nitrogen utilized for algae to growth. [2]

Source:

(1) Schnoor, J. L. (1996). *Environmental modeling: fate and transport of pollutants in water, air, and soil*: John Wiley and Sons.

(2) Cerco, C. F., & Cole, T. M. (1994). Three-Dimensional Eutrophication Model of Chesapeake Bay. Volume 1: Main Report: DTIC Document.

(3) Stumm, W., & Morgan, J. J. (1981). *Aquatic chemistry: an introduction emphasizing chemical equilibria in natural waters*: John Wiley.

3.4 Mathematical formulation of Physical, Chemical and

Biological Processes (PCBP) in BioChemFOAM

This section first describes the hydrodynamic component and then the species fate and transport component in BioChemFOAM.

The hydrodynamic component solves the Reynolds Average Navier- Stokes Equations (RANS) with the Boussinesq approximation to couple the density variations in an incompressible flow. An standard k-ε model is used for turbulence flows, if necessary. Finally, a set of passive scalar equations are presented for different components of the ecological system.

The mass, momentum, and energy equation in strong conservation form is:

$$\frac{\partial \vec{U}}{\partial t} + \frac{\partial \vec{F}}{\partial x} + \frac{\partial \vec{G}}{\partial y} + \frac{\partial \vec{H}}{\partial z} = \vec{Q} \tag{3.1}$$

The terms in Equation (3.1) are:

$$\vec{U} = \begin{bmatrix} 0 \\ u \\ v \\ w \\ T \end{bmatrix} \tag{3.2}$$

$$\vec{F} = \begin{bmatrix} u \\ u^2 + \hat{p}/\rho_0 - \hat{\tau}_{xx} \\ vu - \hat{\tau}_{xy} \\ wu - \hat{\tau}_{xz} \\ Tu - \alpha \frac{\partial T}{\partial x} \end{bmatrix} \tag{3.3}$$

$$\vec{G} = \begin{bmatrix} v \\ uv - \hat{\tau}_{yx} \\ v^2 + \hat{p}/\rho_0 - \hat{\tau}_{yy} \\ wv - \hat{\tau}_{yz} \\ Tv - \alpha \dfrac{\partial T}{\partial y} \end{bmatrix} \tag{3.4}$$

$$\vec{H} = \begin{bmatrix} w \\ uw - \hat{\tau}_{zx} \\ vw - \hat{\tau}_{zy} \\ w^2 + \hat{p}/\rho_0 - \hat{\tau}_{zz} \\ Tw - \alpha \dfrac{\partial T}{\partial z} \end{bmatrix} \tag{3.5}$$

$$\vec{Q} = \begin{bmatrix} 0 \\ f_x \\ f_y \\ f_z + \beta g(T - T_0) \\ \dot{q}/C_v \end{bmatrix} \tag{3.6}$$

In the previous equations, $\hat{p}$ is the reduced pressure equal to the total pressure minus the hydrostatic pressure. $\hat{\tau}_{ij} = \tau_{ij}/\rho_0$ and thermal diffusivity are given by $\alpha = k/(\rho C_v)$.

Equation 3.1 represents the differential form of the NSE and in order to use the equations in the finite volume method (FVM), we need to put the equation into integral form as follows:

$$\frac{\partial}{\partial t} \iiint_{CV} U_i dV + \iint_{CS} (F_i, G_i, H_i) \cdot \vec{n} dA = \iiint_{CV} Q_i dV \tag{3.7}$$

Furthermore, the RANS model when using a time averaging feature to filter out all the turbulence eddies gives the following two equations after applying the Reynolds averaging for conservation of mass and momentum:

$$\frac{\partial U_i}{\partial x_i} = 0 \tag{3.8}$$

$$\rho \frac{\partial U_i}{\partial t} + \rho \frac{\partial (U_i U_j)}{\partial x_j} = -\frac{\partial P}{\partial x_i} + \frac{\partial}{\partial x_j}\left[\overline{\tau}_{ij} + \rho \overline{u_i' u_j'}\right] \tag{3.9}$$

The last term in the last equation is the sum of viscous stresses and Reynolds stresses. The first term can be expressed as:

$$\overline{\tau}_{ij} = 2\mu\left[\frac{\partial U_i}{\partial x_j} + \frac{\partial U_j}{\partial x_i}\right] \tag{3.10}$$

Using the approximation of Boussinesq 1877 for the Reynolds stresses (Eddy-viscosity model), the stresses might be proportional to the mean rates of deformation as follows:

$$-\rho \overline{u_i' u_j'} = \mu_t\left[\frac{\partial U_i}{\partial x_j} + \frac{\partial U_j}{\partial x_i}\right] - \frac{2}{3}\rho \delta_{ij} k \tag{3.11}$$

Also, a generic transport equation for a passive scalar is included in the system of equations. The scalar ϕ has the following form after using the Eddy-diffusion model:

$$\frac{\partial (\rho \phi)}{\partial t} + \frac{\partial}{\partial x_j}\left[\rho U_j \overline{\phi} + \rho \overline{u_i' \phi'}\right] = \frac{\partial}{\partial x_j}\left(\Gamma_\phi \frac{\partial \overline{\phi}}{\partial x_j}\right) \tag{3.12}$$

Modeling turbulence processes is an important component when an eddy appears in the main flow. The following study use the two-equation model k-ε. The turbulent kinetic energy, k, is given by:

$$k = \frac{1}{2}\left(\overline{u'u'} + \overline{v'v'} + \overline{w'w'}\right) = \frac{1}{2}\overline{u_i'u_i'} \qquad (3.13)$$

The turbulent eddy viscosity in Equation (3.11) uses the approximation that the velocity scale is equal to $q = (k)^{1/2}$ and the length scale is $l = k^{3/2}/\varepsilon$, so we get:

$$\mu_t = \rho C_\mu \frac{k^2}{\varepsilon} \qquad (3.14)$$

Now, the turbulent kinetic energy, k, equation is:

$$\rho\frac{\partial k}{\partial t} + \rho\frac{\partial\left(kU_j\right)}{\partial x_j} = \underbrace{\frac{\partial}{\partial x_j}\left(\mu\frac{\partial k}{\partial x_j}\right)}_{A} - \underbrace{\frac{\partial}{\partial x_j}\left(\frac{\rho}{2}\overline{u_j'u_i'u_i'} + \overline{p'u_j'}\right)}_{B} - \underbrace{\rho\overline{u_i'u_j'}\frac{\partial U_i}{\partial x_j}}_{C} - \underbrace{\mu\overline{\frac{\partial u_i'}{\partial x_k}\frac{\partial u_i'}{\partial x_k}}}_{D}$$

$$\rho\frac{\partial k}{\partial t} + \rho\frac{\partial\left(kU_j\right)}{\partial x_j} = \underbrace{\frac{\partial}{\partial x_j}\left(\mu\frac{\partial k}{\partial x_j}\right)}_{A} - \frac{\mu_t}{Pr_t}\frac{\partial\kappa}{\partial x_j} - \underbrace{\mu_t\left(\frac{\partial U_i}{\partial x_j} + \frac{\partial U_j}{\partial x_i}\right)\frac{\partial U_i}{\partial x_j}}_{P_k} - \varepsilon \qquad (3.15)$$

in which A is the rate of molecular diffusion of k, B is the rare of turbulent transport given by:

$$B = \frac{\mu_t}{Pr_t}\frac{\partial\kappa}{\partial x_j} \qquad (3.16)$$

C is the rate of turbulent production, P_κ, and D is the rate of turbulent dissipation given by:

$$D = \varepsilon = \frac{\kappa^{3/2}}{l} \qquad (3.17)$$

As a default in the present study the turbulent dissipation, ε, is calculated by solving a transport equation as follows:

$$\rho \frac{\partial \varepsilon}{\partial t} + \rho \frac{\partial (\varepsilon U_j)}{\partial x_j} = C_{\varepsilon 1} P_k \frac{\varepsilon}{k} - \rho C_{\varepsilon 2} \frac{\varepsilon^2}{k} + \frac{\partial}{\partial x_j} \left(\frac{\mu_t}{\sigma_\varepsilon} \frac{\partial \varepsilon}{\partial x_j} \right) \qquad (3.18)$$

The last equation closes the system of equations to be solved, (3.8), (3.9), (3.15), and (3.18), when considering turbulent flow. Notice that equations (3.17) and (3.18), represent the well known k-ε model. Typical values for the coefficients inEequation (3.18) are:

$$C_\mu = 0.09; C_{\varepsilon 1} = 1.44; C_{\varepsilon 2} = 1.92; Pr_t = 1.0; \sigma_\varepsilon = 1.3.$$

The species fate and transport component is based on a typical scalar transport equations with a few modifications in place that consider the fate and transport of the species. Equation (3.12) presents the base to model scalar transport in a fluid flowing at a free surface. The equation presented introduce effects of turbulence. It can be restated, when considered more than one species transported in the bulk flow, as follows:

$$\underbrace{\frac{\partial (\rho \phi_i)}{\partial t}}_{\text{temporal variation}, \mathcal{T}} + \underbrace{\nabla \cdot (\rho \mathbf{u} \phi_i)}_{\text{convection}, \mathcal{A}} = \underbrace{\nabla \cdot \mathbf{J}_i}_{\text{diffusion}, \mathcal{D}} + \underbrace{R_i}_{\text{Reactions}, \mathcal{R}} + \underbrace{S_i}_{\text{sources/sinks}, \mathcal{S}} \qquad (3.19)$$

ϕ_i is the local mass fraction of species i; R_i is the net rate of production of species i by chemical reactions; and S_i are sources or sinks from the dispersed phase plus any other sources. The form of this equation can be solved for $N-1$ species where N is the total number of fluid phase chemical species, in our case only one phase is considered. When one of the species is considered to be the predominant (e.g., when there is a larger mass fraction, water in our case), mass conservation is ensured by the difference between the $N-1$ species and with the predominant one. The last equation is also utilized to model energy (ϕ_i=temperature) in BioChemFOAM. The temperature equation only considers temporal variation, convection, and turbulent diffusion. The diffusion term is modeled as in Equation 3.20, but only considers the first term with Schmidt number changed to the Prandtl number and set equal to one (assumed).

The first term on the Right Hand Side (RHS) of Equation 3.19 can be modeled as laminar or turbulent flow. The turbulent flow diffusion flux of species i is given by:

$$\mathbf{J}_i = \left(\underbrace{-\rho D_{i,m}}_{\text{mass diffusion}} + \underbrace{\frac{\mu_t}{Sc_t}}_{\text{turbulent diffusion}} \right) \nabla \phi_i - D_{T,i} \frac{\nabla T}{T} \tag{3.20}$$

$D_{i,m}$ is the mass diffusion (molecular diffusion) coefficient for species i in the mixture; μ_t is turbulent viscosity; Sc_t is the turbulent Schmit number (kinematic viscosity/mass diffusion) and $D_{T,i}$ is the thermal (Soret) diffusion coefficient, which is considered as zero in this research (typically not modeled in water quality models). The last equation uses the Dilute Approximation.

The second term on the RHS of Equation 3.19 can be modeled in three ways: the laminar finite-rate model, the eddy-dissipation model and the eddy-dissipation-concept. In this study, a Laminar finite-rate model is adopted. The effect of turbulent fluctuation is ignored, and reaction rates are determined by Arrhenious kinetic expressions or constant/variable rates of reactions. The net source of chemical species i due to reaction is given by:

$$R_i = M_{w,i} \sum_{r=1}^{N_R} \hat{R}_{i,r} \tag{3.21}$$

$M_{w,i}$ is the molecular weight of species i and $\hat{R}_{i,r}$ is the Arrhenious molar rate of creation/destruction of species i in reaction r.

In the present study, not all the stoichiometric chemical reactions are included at ones. Instead, the main processes are modeled with a Kinetic formulation over the main processes, which are described in subsequent paragraphs. This means that the term, R_i in Equation 3.21 has a different representation.

Fate and transport processes for a passive scalar in an environment can be depicted as in Figure 3.3. Also, Figure 3.4 shows an example of the interaction of all species included in BioChemFOAM when green algae is considered. This algae species is modeled since is assumed

that it was predeted by a small organism, even that measurements in similar ecosystem (LimnoTech, 2007), shows that its concentration is low. The purpose is to test the model when predation of one algae species exists.
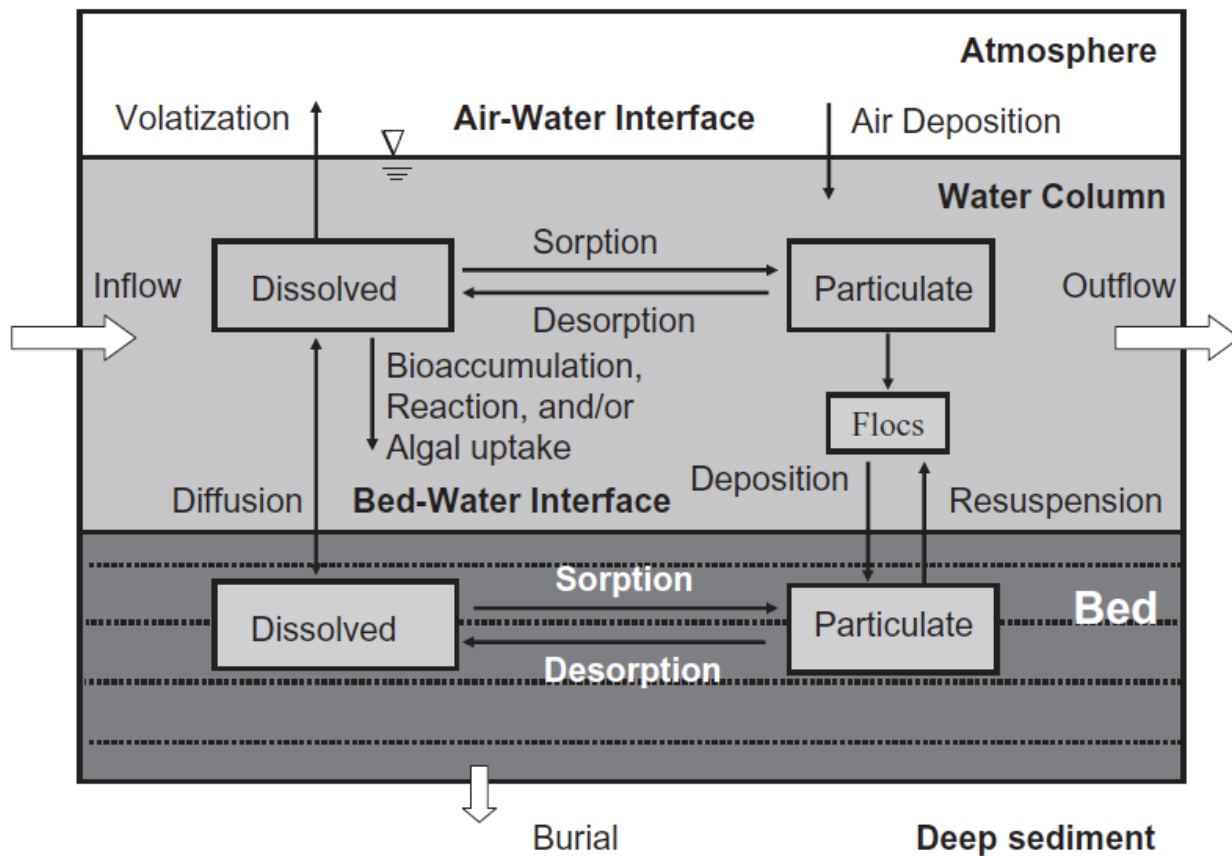
Figure 3-3. Fate and transport processes for a passive scalar (Ji, 2008), Chapter No. 4 Figure 4.3.1). In the figure the particulate component can be converted into a dissolved component by bacteria (not shown in the figure).
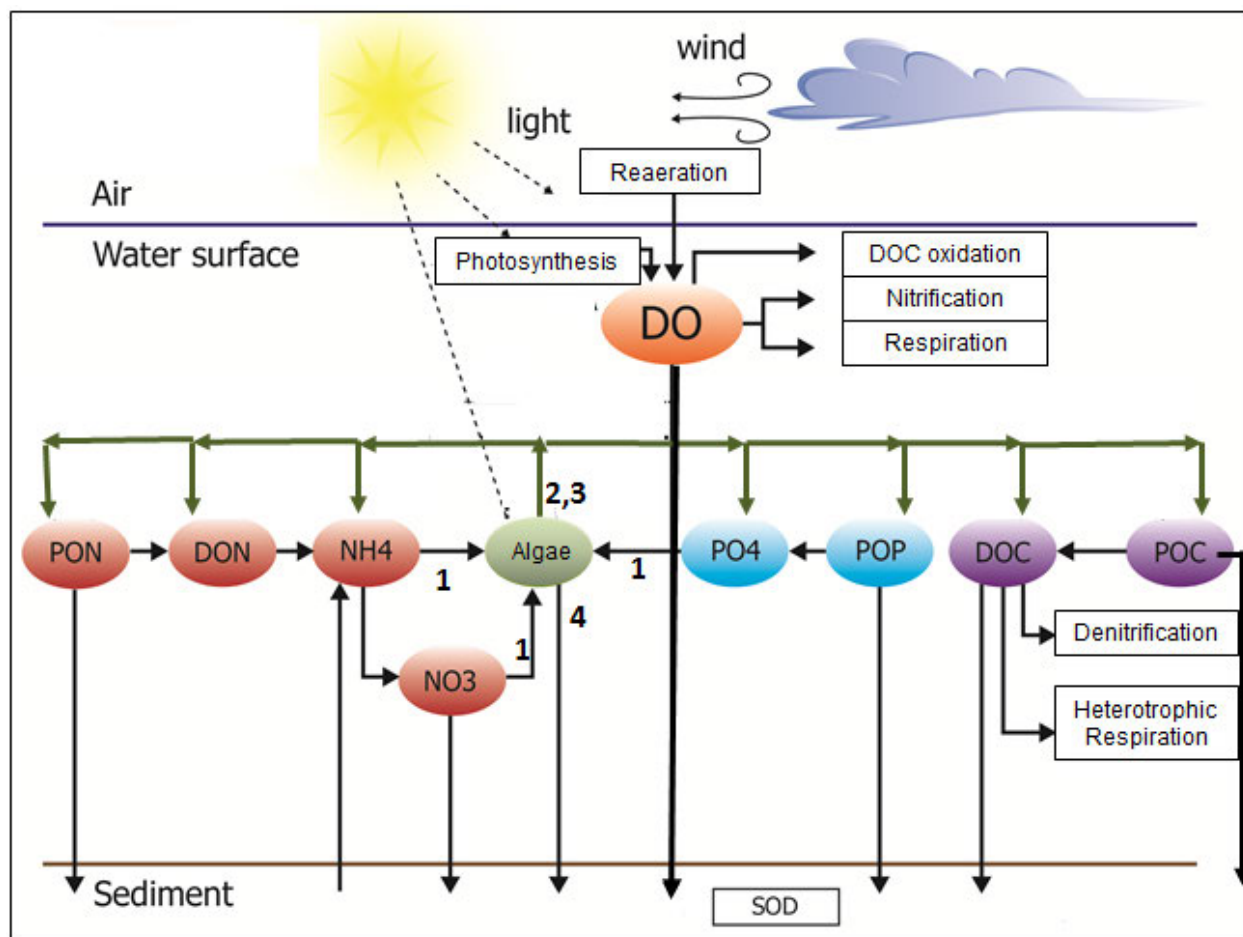
Figure 3-4. Diagram showing the interaction of all species considered in the proposed model BioChemFOAM. This diagram shows an example of the functional relation when green algae is considered. All arrows represent fluxes (processes). The solid line represents main fluxes from one species to another. The green line represents the metabolism and predation of algae, which is commonly very small but considered here for completeness. The green line also shows that some of the end products from algae can be recycled to all other species. The numbers on the figure shows a chemical and biological process affecting algae concentration. The number 1 shows the growth uptake from ammonia and nitrate. The numbers 2 and 3 represents the metabolism and predation of algae. The number 4 indicates settling of algae. Those processes can be recalled from Equation 3.27.

The processes included in the model for species transport at bulk, species interaction with bottom and species interaction at water surface are:

1. Algae, Bx. (In this research only green algae is modeled)
2. Organic Carbon, C.
3. Phosphorus, P.
4. Nitrogen,N
5. Dissolved Oxygen, DO.

In BioChemFOAM bacteria is not modeled because we don't have data at the moment to caculate the fate and transport. The inclusion of bacteria on the model is important and its modeling will be addressed in future research.

The stoichiometric relations (see Section 3.3, Table 3-1) and the dynamics of the ecological model are used to define fundamental variables that were implemented in the model. The following equations describes the functional relation of the included variables in the proposed modeling tool presented in Figure 3-4.

Total Nitrogen includes four master variables. Those variables are grouped in inorganic and organic form as shown in Equation 3.22. It is common practice to further decompose the variable PON in a fast and slow component. Here, we only include the fast component, known as the refractory Particulate Organic Carbon and usually denominated as $RPON$. This idea also applies when deriving the equations for Phosphorus and Carbon. The Total Nitrogen is defined as follows:

$$TN = \overbrace{\underbrace{NO_2^- + NO_3^-}_{NO3=nitrite+nitrate} + \underbrace{NH_3/NH_4^+}_{NH4=ammonia+ammoniumion}}^{\text{Inorganic,TIN}} + \overbrace{PON + DON}^{\text{Organic,TON}} \qquad (3.22)$$

Total Phosphorus is presented in Equation 3.23. In the actual model POP, and PO4d are modeled. Here, only the dissolved orthophosphate is modeled since it is directly available for uptake by algae.

$$TP = \overbrace{\underbrace{PO4p + PO4d}_{\text{orthophosphates}}}^{\text{Inorganic,TIP}} + \overbrace{POP + DOP}^{\text{Organic,TOP}} \qquad (3.23)$$

At this stage PO4p is not considered since we only want to study the dissolved constituent that is uptake directly by algae.

Finally, Total Carbon is defined in Equation 3.24. The present model only includes the organic part and disregards the influence of the inorganic component (e.g. carbonic dioxide). In this research, the term is not included as is common practice (Cerco & Cole, 1994).

$$TC = \overbrace{CO_2 + CO_3^{-2} + HCO_3^- + H_2CO_3}^{\text{Inorganic,TIC}} + \overbrace{POC + DOC}^{\text{Organic,TOC}} \qquad (3.24)$$

The following sectin describes the equations that are implemented in the model based on the research by (Ji, 2008), which is a review of the model presented by (Cerco & Cole, 1994).

1. Algae. Algae is defined as a group of microorganicsm that photosynthesizes and use chlorophyll as the primary pigment for carbon fixation. In this research, the variable *Bx* (see Figure 3-4) encapsulates a generic species (common species are: green, blue-green or cyanobacteria. In the following formulation green algae is assumed). Algal kinetics are governed by the following processes: (1) algal growth; (2) metabolism, including respiration and excretion; (3) predation; (4) settling; and (5) external sources (assumed zero now on). The growth component is represented in Figure 3-4 by three solid dark arrows from NH4, NO3, and PO4 pointing into the node Bx. Metabolism is represented in the same figure by light solid arrows while predation is represented as a dark dashed line. In BioChemFOAM, algae (green) is parameterized as follows:

$$\text{Net algal production} + \text{Convection} = \text{Diffusion} + \text{Reactions}$$

$$-\text{Settling} \pm \text{Sources / Sinks} \qquad (3.25)$$

$$\underbrace{\frac{\partial(\phi_{1x})}{\partial t}}_{\text{net algal production}} + \underbrace{\nabla \cdot (\mathbf{u}\phi_{1x})}_{\text{Convection}} = \underbrace{\nabla \cdot (-D_{1x,m}\nabla\phi_{1x})}_{\text{Diffusion}} + \underbrace{R_{1x}}_{\text{Reactions}} + \underbrace{S_{1x}}_{\text{4.Sources/Sinks}} \qquad (3.26)$$

$$R_{1x} = \underbrace{P_x(NH4,NO3,PO4).B_x}_{\text{1. growth}} - \underbrace{BM_x(T).B_x}_{\text{2. metabolism}} - \underbrace{PR_x(B_x,T).B_x}_{\text{3. algal predation}}$$

$$= \underbrace{PM_x.f_1(N).f_2(I).f_3(T).B_x}_{P_x(NH4,NO3,PO4)}$$

$$- \underbrace{BMR_x.e^{(KTB_x.(T-20))}.B_x}_{BM_x(T)}$$

$$- \underbrace{PRR_x.\left(\frac{B_x}{B_{xp}}\right)^{\alpha_p}.e^{(T-20)}.B_x}_{PR_x(B_x,T)} \qquad (3.27)$$

In which: $\phi_{1x} = B_x$ is the algal biomass of algal group x (gC/m^3, $[M/L^3]$), and $P_x(NH4,NO3,PO4d)$ is the production rate of algal group x ($[d]^{-1}$) that is a function of variables $NH4$, $NO3$, and $PO4$. In the present model, $PO4 = PO4d$ represents the dissolved orthophosphate ready for algae uptake. $BM_x(T)$ represents the basal metabolism rate of algal group x ($[d^{-1}]$), which is a function of temperature (T), modeled as $BMRx * exp(KTBx * (T-20))$. $BMRx$ is the basal metabolism rate at TRx for algal group x (d^{-1}). $KTBx$ is the effect of temperature on metabolism for algal group x ($^oC^{-1}$).

$PR_x(B_x,T)$ is the predation rate of algal group x ($[d^{-1}]$) and is usually a function of B_x and temperature. PRR_x is the reference predation rate for a given algae group x ($[d^{-1}]$). B_{xp} is the reference algal concentration for predation ($mg-C/L$). α_p is the exponential factor. The advantage of this formulation is that when B_x concentrations are larger(smaller)than the reference algal concentration, B_{xp}, the predation rate will be very large(small). PM_x is the

maximum growth rate for algal group x ($[d^{-1}]$). $f_1(N)$ is the growth limiting function for nutrients ($0 <= f_1 <= 1$). $f_2(I)$ is the growth limiting function for light intensity ($0 <= f_2 <= 1$). Finally, $f_3(T)$ is the growth-limiting function for temperature ($0 <= f_3 <= 1$).

The growth function presented in Equation 3.27 includes three fundamental dimensionless parameterizations. The growth limiting function is usually expressed using one of the following methods: multiplicative formulation, minimum formulation, harmonic mean formulation or arithmetic mean formulation (Bowie & Tech, 1985). In BioChemFOAM, a multiplicative approach is implemented as follows:

$$f_1(N) = f(N).f(P)$$

$$f_1(N) = \frac{NH4 + NO3}{KHN_x + NH4 + NO3} \cdot \frac{PO4_d}{KHP_x + PO4_d} \tag{3.28}$$

In which $NH4 + NO3$ are the ammonia and nitrate concentrations ($[mg - N / L^3]$), $PO4_d$ is dissolved orthophosphate ($[mg - P / L^3]$), KHN is the half saturation constant for nitrogen ($[mg / L^3]$) and KHP is the half saturation constant for phosphorus ($[mg / L^3]$).

To get a formulation for growing algae by light, a common parameterization is described and then a mathematicla formulation included in BioChemFOAM is presented. Light intensity parameterization (Cerco & Cole, 1994), is usually modeled as:

$$f_2(I) = \frac{2.718(FD)}{K_{ess}.\Delta z}\left(e^{-\alpha_B} - e^{-\alpha_T}\right) \tag{3.29}$$

In which the constants depend on light (solar energy or radiation), depth and two coefficients that account for the reduction of light traveling though water.

$$\alpha_B = \frac{I_0}{FD \cdot (I_s)_x} e^{(-K_{ess}.(H_T + \Delta z))} \tag{3.30}$$

$$\alpha_T = \frac{I_0}{FD \cdot (I_s)_x} e^{(-K_{ess}.(H_T))} \tag{3.31}$$

FD is the fractional daylenght ($0 <= FD <= 1$), K_{ess} : total light extinction coefficient ($[L^{-1}]$), Δz represents layer thickness ($[L]$), I_0 : daily total light extinction coefficient ($langleys / day$), and H_T is the depth from the free surface to the top of the layer ($[L]$).

$$K_{ess} = Ke_b + Ke_{TSS} + Ke_{Chl} . \sum_{x=c,d,g}^{3} \left(\frac{B_x}{CChl_x} \right) \tag{3.32}$$

Ke_b is the background light extinction ($[L^{-1}]$), Ke_{TSS} is the light extinction coefficient for total suspended solids ($L^{-1} . M / L^3$), TSS is the total suspended solid concentration ($[M / L^3]$), Ke_{Chl} is the light extinction coefficient for chlorophyll a ($[L^{-1} / M . Chl / L^3]$), and $CChl_x$ is the carbon / chlorophyll ratio in algal group x (g C/mg Chl). The optimal light intensity $(I_s)_x$ for photosynthesis is expressed as:

$$(I_s)_x = \text{Min} \left\{ (I_0)_{avg} e^{-K_{ess} . (D_{opt})_x} , (I_s)_{min} \right\} \tag{3.33}$$

$(D_{opt})_x$ is the depth of maximum algal growth for algal group x ($[L]$) and $(I_0)_{avg}$: adjusted surface light intensity (langleys/day).

$$(I_0)_{avg} = CI_a . I_0 + CI_b . I_1 + CI_c . I_2 \tag{3.34}$$

where I_1 : daily light intensity 1 day preceding the model day (langleys/day), I_2 is daily light intensity 2 days preceding the model day (langleys/day) and Cl_a , Cl_b , and Cl_c are weighting factors when added together, must equal one.

The light growing function equations presented in the last paragraph require a considerable number of coefficients to represents the light transport in water and its influence in algae growth. A mathematical parameterization is proposed, as a first approach, based on extintion of light due to algae cocentration. The mathemathical formulation used here is only intended to include attenuation of light due to algae concentration as a diffusion process with a variable diffusion coefficcient. The parameterization does not consider physical processes

(absorbtion, emmition ans scattering) acting in a typica radiative transport equation. The following mathemathical formulation is expresed:

$$-\nabla \cdot \left(\underbrace{\underbrace{exp\left(-\frac{Bx}{Bx_{min} + Bx}\right)}_{\text{extinction coefficient}} \nabla I}_{\text{DiffusionProcess}} \right) = 0 \tag{3.35}$$

Equation 3.35 states that when light reach the water body surface its transport is modeled as a diffusion process. In order to account for the blockage of light due to algae growth an exponential coefficient $exp(...) = e^{..}$ (here "$...$" means all terms inside the parenthesis which are presented on Equation 3.35 as an extinction coefficient) is included to account the reduction of light in zones were algae growth and may block light penetration. In other words, if algae concentration increase, light may be reduced. Bx_{min} is a minimum concentration defined to avoid zero in the denominator when algae are not present, at the moment is assumed to be 0.001 mg-C/L. I represents visible, photosynthetically available light (units of ly/day, ly: langley) as defined by (Chapra, 2008). Having defined the transport of light into the mass of water, the new dimensionless light growing function is expressed as:

$$f_2(I) = \frac{I}{I_s} exp\left(1 - \frac{I}{I_s}\right) \tag{3.36}$$

where I is the light level and I_s is the optimal light level (calculated from Equation 3-37) that ranges from about 100 to 400 lyd^{-1} for a particular algae species (Chapra, 2008).

The final dimensionless function that affects algae growth is temperature. This is modeled as presented by (Cerco & Cole, 1994). Its parameterization is given by:

$$f_3(T) = \begin{cases} e^{-KTG1_x(T-TM1_x)^2}, & \text{if } T < TM1_x; \\ 1.0, & \text{if } TM_x1 \leq x \leq TM2_x; \\ e^{-KTG2_x(T-TM2_x)^2}, & \text{otherwise.} \end{cases} \tag{3.37}$$

$TM1_x$ is the lower end of the optimal temperature range for algal growth for algal group x, $TM2_x$ is the upper end of optimal temperature range for algal growth for algal group x, $KTG1_x$ is the effect of temperature below $TM1_x$ on growth for algal group x, $KTG2_x$ is the effect of temperature above $TM2_x$ on growth for algal group x, and subscript $x = c$ for cyanobacteria, d for diatom, and g for green algae (In this research only green algae is considered).

2. Organic Carbon, OC. The cycle consists of photosynthesis, respiration, and decomposition. Since some organic carbon decay at faster rates than others, organic carbon can be divided into those that decay at a fast rate (labile) and those that decay at a slower rate (refractory) (Cerco & Cole, 1994). BioChemFOAM lumps both variables into one master variable called POC in order to reduce complexity but accounting for processes that may affect the fate and transport of the species. In models that represent nutrient dynamics (see for example Cerco and Cole, 1994), organic carbon can be categorized as: (1) $\phi_2 = RPOC$ (Refractory Particulate Organic Carbon), (2) $\phi_3 = LPOC$ (Labile Particulate Organic Carbon), and (3) $\phi_4 = DOC$ (Dissolved Organic Carbon). In BioChemFOAM, the master variable POC is used instead of $LPOC$ and $RPOC$. The total organic carbon is the sum of all organic carbon compounds and can be expressed as:

$$TOC = \underbrace{RPOC + LPOC}_{POC} + DOC \qquad (3.38)$$

The transformation of organic carbon is represented in a cascade approach : (1) Algal predation and algal excretion contribute to POC, and DOC, (2) Hydrolysis converts POC to DOC and (3) Denitrification and heterotrophic respiration remove DOC. Except for the time scale of decomposition, $LPOC$ and $RPOC$ have similar properties and can be recast as the variable POC. The reaction of POC is primarily controlled by the following processes: (1) algal predation, (2) hydrolysis to DOC, (3) settling, and (4) external loads. Since

BioChemFOAM utilizes POC, the governing equation for particulate organic carbon (POC) should have the following format:

$$\text{Net change of } POC + \text{Convection} = \text{Diffusion} + \text{Reactions}$$

$$-\text{settling} \pm \text{sources}/\text{sinks} \tag{3.39}$$

$$\underbrace{\frac{\partial(\phi_2)}{\partial t}}_{\text{Net change of } POC} + \underbrace{\nabla \cdot (\mathbf{u}\phi_2)}_{\text{Convection}} = \underbrace{\nabla \cdot (-D_{2,m}\nabla\phi_2)}_{\text{Diffusion}} + \underbrace{R_2}_{\text{Reactions}} + \underbrace{S_2}_{\text{sources/sinks}} \tag{3.40}$$

And its corresponding source term is given by:

$$R_2 = \underbrace{\sum_{x=1}^{1} FCLP.PR_x(B_x,T).B_x}_{\text{algal predation}} - \underbrace{K_{POC}(B_x,T).POC}_{\text{hydrolysis}} \tag{3.41}$$

where $POC = \phi_2$ is the concentration of labile particulate organic carbon ($g-C/m^3$), FCLP is the fraction of predated carbon produced as particulate organic carbon, and $K_{POC}(B_x,T)$ is the hydrolysis rate of particulate organic carbon (T^{-1}).

The processes for dissolved organic carbon, $DOC = \phi_3$, are more complicated than the ones for POC. They include: (1) algal excretion, (2) algal predation, (3) hydrolysis from POC, (4) heterotrophic respiration of DOC, (5) denitrification, and (6) external loads. This yields:

$$\text{Net change of } DOC + \text{Convection} = \text{Diffusion} + \text{Reactions}$$

$$\pm \text{sources}/\text{sinks} \tag{3.42}$$

$$\underbrace{\frac{\partial(\phi_3)}{\partial t}}_{\text{Net change of } DOC} + \underbrace{\nabla \cdot (\mathbf{u}\phi_3)}_{\text{Convection}} = \underbrace{\nabla \cdot (-D_{3,m}\nabla\phi_3)}_{\text{Diffusion}} + \underbrace{R_3}_{\text{Reactions}} + \underbrace{S_3}_{\text{sources/sinks}} \quad (3.43)$$

$$R_3 = \underbrace{\sum_{x=1}^{1}\left(FCD_x + (1-FCD_x)\frac{KHR_x}{KHR_x + DO}\right).BM_x(T).B_x}_{\text{algal excretion}}$$

$$+ \underbrace{\sum_{x=1}^{1}\left(FCDP.PR_x(B_x,T).B_x\right)}_{\text{algal predation}}$$

$$+ \underbrace{K_{LPOC}(B_x,T).POC}_{POC\text{ hydrolysis}} - \underbrace{K_{HR}(DO,B_x,T).DOC}_{DOC\text{ heterotropic respiration}}$$

$$- \underbrace{Denit(DO,NO3,B_x,T).DOC}_{\text{Denitrification}} \quad (3.44)$$

where POC is the particulate organic carbon. DOC is the concentration of dissolved organic carbon ($g - C/m^3$), FCD_x is a constant for algal group x ($0 < FCD_x < 1$), KHR_x is the half saturation constant of DO for algal DOC excretion for group x ($g - O_2/m^3$), DO is the dissolved oxygen concentration ($g - O_2/m^3$), $FCDP$ is the fraction of predated carbon produced as dissolved organic carbon(day^{-1}), $K_{HR}(DO,B_x,T)$ is the heterotrophic respiration rate of dissolved organic carbon (day^{-1}) and $Denit$ is the denitrification rate (day^{-1}). Zooplankton (small organisms in water) consume algae and recycle carbon back into the water as POC and DOC. Since zooplankton are not modeled directly, two empirical parameters, $FCLP$, and $FCDP$, are used to distribute algal carbon among POC (Zooplankton consumes algae and recycles back to the water as POC and DOC), and DOC, their sum equal to 1.0, as follows:

$$FCLP + FCDP = 1 \quad (3.45)$$

If the Refractory part of POC is included, the last equation have an extra term $FCRP$. In Equation 3.44, $-K_{HR} \cdot DOC$, represents the heterotrophic respiration that converts DOC into

CO_2 . A Michaelis-Menton function can be used to represent the dependency of heterotrophic respiration rate, K_{HR} , on DO concentration. It has the form:

$$K_{HR}(DO, B_x, T) = \frac{DO}{KHOR_{DO} + DO} . K_{DOC} \qquad (3.46)$$

where $KHOR_{DO}$ is the oxic respiration half saturation constant for DO (gO_2 / m^3) and K_{DOC} is the heterotrophic respiration rate of dissolved organic carbon at infinite dissolved oxygen concentration (day^{-1}).

The dissolution (hydrolysis) rate, $LPOC$,and the heterotrophic respiration rate of DOC , K_{LPOC} , and K_{DOC} , can be specified by the following equations:

$$K_{LPOC}(B_x, T) = \left(K_{LC} + K_{LCalg} . \sum_{x=1}^{1} B_x \right) . e^{KT_{HDR}(T - TR_{HDR})} \qquad (3.47)$$

$$K_{DOC}(B_x, T) = \left(K_{DC} + K_{DCalg} . \sum_{x=1}^{1} B_x \right) . e^{KT_{MNL}(T - TR_{HDR})} \qquad (3.48)$$

where K_{LC} is the minimum dissolution rate of labile particulate organic carbon (day^{-1}), K_{DC} is the minimum respiration rate of DOC (day^{-1}), K_{LCalg} is a constant that relates the dissolution of labile particulate organic carbon to algal biomass ($day^{-1} / gC / m^3$), K_{DCalg} is a constant that relates respiration to algal biomass ($day^{-1} / gC / m^3$), KT_{HDR} is the effect of temperature on hydrolysis of particulate organic matter ($^oC^{-1}$) (bacteria is not considered in the model but in future research its influence may need to be considered), TR_{HDR} is the reference temperature for hydrolysis of particulate organic matter (^oC), KT_{MNL} is the effect of temperature on mineralization of dissolved organic matter ($^oC^{-1}$), and TR_{MNL} is the reference temperature for the mineralization of dissolved organic matter (^oC). The remaining parameters can be found in the Nitrogen section.

3. Phosphorus, P. Phosphorus exists in organic and inorganic forms. Both forms include particulate and dissolved phases. Total phosphorus, TP, is a measure of all forms of phosphorus and is widely used for setting trophic state criteria. TP can be split into the following state

variables in a water quality model: (1) $RPOP = \phi_5$, (2) $LPOP = \phi_6$, (3) $DOP = \phi_7$, and (4) $PO4t = \phi_8$. Phosphorus transformations can be represented in a cascade approach: (1) hydrolysis converts $RPOP$ and $LPOP$ to DOP, (2) mineralization converts DOP to $PO4t$, and (3) algal uptake $PO4d$ for growth occurs.

The POP, Particulate Organic Phosphorus, fate and transport is largely determined by (1) algal metabolism, (2) algal predation, (3) hydrolysis of POP to dissolved organic phosphorus, (4) settling (not included in the following equations), and (5) external loads.

The species dynamics and kinetic equation for POP ($RPOP$ and $LPOP$ are lumped in the present tool) can be described as:

$$\underbrace{\frac{\partial(\phi_4)}{\partial t}}_{\text{Change of } POP} + \underbrace{\nabla \cdot (\mathbf{u}\phi_4)}_{\text{Convection}} = \underbrace{\nabla \cdot (-D_{4,m}\nabla\phi_4)}_{\text{Diffusion}} + \underbrace{R_4}_{\text{Reactions}} + \underbrace{S_4}_{\text{sources/sinks}} \qquad (3.49)$$

$$R_4 = \underbrace{\sum_{x=1}^{1} [FPL_x.BM_x(T)].APC.B_x}_{\text{algal basal metabolism}}$$

$$- \underbrace{\sum_{x=1}^{1} [FPLP.PR_x(B_x,T)].APC.B_x}_{\text{algal predation}}$$

$$- \underbrace{K_{LPOP}.POP}_{POP\,\text{hydrolysis}} \qquad (3.50)$$

where POP is the concentration of particulate organic phosphorus (gP/m^3), FPL_x is the fraction of metabolized phosphorus by algal group x produced as POP, $FPLP$ is the fraction of predated phosphorus produced as POP, APC is the mean phosphorus/carbon ratio in all algal groups (gP/gC), and K_{LPOP} is the hydrolysis rate of POP (day^{-1}).

The major processes of Dissolved Orthophosphate ($PO4 = \phi_5$) are: (1) algal metabolism, (2) algal predation, (3) hydrolysis from POP, (4) algae uptake and (5) external sources. Since DOP is not modeled explicitly, Mineralization (transformation of DOP into total

orthophosphate) is lumped inside hydrolysis in BioChemFOAM. These processes can be incorporated in the following equation:

$$\text{Change of } PO4 + \text{Convection} = \text{Diffusion} + \text{Reactions}$$

$$\pm \text{sources} / \text{sinks} \tag{3.51}$$

$$\underbrace{\frac{\partial(\phi_5)}{\partial t}}_{\text{Change of } PO4} + \underbrace{\nabla \cdot (\mathbf{u}\phi_5)}_{\text{Convection}} = \underbrace{\nabla \cdot (-D_{5,m}\nabla\phi_5)}_{\text{Diffusion}} + \underbrace{R_5}_{\text{Reactions}} + \underbrace{S_5}_{\text{sources/sinks}} \tag{3.52}$$

$$R_5 = \underbrace{\sum_{x=1}^{1}\left[FPD_x.BM_x(T)\right].APC.B_x}_{\text{algal basal metabolism}}$$

$$+ \underbrace{\sum_{x=1}^{1}\left[FPDP.PR_x(B_x,T)\right].APC.B_x}_{\text{algal predation}}$$

$$+ \underbrace{K_{POP}(PO4d, B_x, T).POP}_{POP\text{ hydrolysis}}$$

$$- \underbrace{P_x(NH4, NO3, PO4).APC.B_x}_{\text{algae uptake}} \tag{3.53}$$

where DOP is the concentration of dissolved organic phosphorus (gP/m^3), FPD_x is the fraction of metabolized phosphorus by algal group x produced as DOP, $FPDP$ is the fraction of predated phosphorus produced as DOP and $K_{DOP}(PO4d, B_x, T)$ is the mineralization representing the amount taken by algae. $PO4d$ is dissolved orthophosphates (see Equation 3.23) and is the portion that can be taken directly by algae, although some assimilation of organic phosphorus may occur, especially during periods of P deficiencies. The remaining parameters influencing $PO4$ are define as:

$$K_{POP} = \left(K_P + K_{LPalg}.\sum_{x=1}^{1}B_x\right).e^{KT_{HDR}(T-TR_{HDR})} \tag{3.54}$$

$$K_{DOP} = \left(K_{DP} + K_{DPalg} \cdot \sum_{x=1}^{1} B_x \right) \cdot e^{KT_{MNL}(T-TR_{HDR})} \tag{3.55}$$

K_{LP} is the minimum hydrolysis rate of labile particulate organic phosphorus (day^{-1}), K_{DP} is the minimum mineralization rate of dissolved organic phosphorus (day^{-1}), K_{LPalg} is the constant that relates the hydrolysis of refractory and labile particulate organic phosphorus to algal biomass ($day^{-1} / g - C / m^3$), and K_{DPalg} is the constant that relates mineralization to algal biomass ($day^{-1} / g - C / m^3$). The term $KHP/(KHP + PO4d)$ that multiplies K_{DPalg} presented in (Cerco & Cole, 1994) is not included into BioChemFOAM K_{POP} parameterization since it is lumped into K_{DPalg}. Furthermore, this term is generally zero in real applications (Cerco & Cole, 1994) (LimnoTech, 2007).

The total algae loss by basal metabolism is accounted for in Equation 3.27, second term, is distributed with:

$$FPL_x + FPD_x = 1 \tag{3.56}$$

Finally, algae predation coefficients are distributed as follows:

$$FPLP + FPDP = 1 \tag{3.57}$$

The last two equations include fractions from inorganic phosphorus lumped into FPDx and FPDP.

4. Nitrogen, N. In natural waters, the primary forms of nitrogen include: Nitrate ion (NO_3^-), Nitrite ion (NO_2^-), dissolved nitrogen gas (N_2), dissolved ammonia gas (NH_3), ammonium ion (NH_4^+), and organic nitrogen (ON). Total nitrogen is the sum of all nitrogen forms and can be represented as:

$$TN = NO_2^- + NO_3^- + NH_3 / NH_4^+ + TON \tag{3.58}$$

The total Kjeldahl nitrogen (TKN) test involves digestion and distillation to determine both organic nitrogen and ammonia in a water sample. It has the form:

$$TKN = \underbrace{NH_3 / NH_4}_{NH4} + ON = TN - \underbrace{(NO_2^- + NO_3^-)}_{NO3} \tag{3.59}$$

In water quality models, the forms of nitrogen can be grouped as (Cerco & Cole, 1994): (1) $RPON$ (not included in the present research)and $LPON$ which are lumped into PON in BioChemFOAM, (2) DON, (3) $NH4$, and (4) $NO3$. Nitrogen transformations are represented in a cascade approach: (1) hydrolysis converts PON to DON, (2) mineralization converts DON to $NH4$, (3) nitrification converts $NH4$ to $NO3$, (4) algal uptake $NH4$ and $NO3$ for growth, and (5) denitrification removes $NO3$ out from the aquatic system. Organic nitrogen includes all substances in which nitrogen is bonded to carbon and occurs in both dissolved and particulate forms. Particulate organic nitrogen (PON) includes small organisms (algae, bacteria, etc.), both living and dead, and fragments of organisms. Dissolved organic nitrogen is mostly from waste excreted by organisms or from the hydrolysis of PON. Particulate organic nitrogen, including $RPON$ and $LPON$, has the following sources and sinks: (1) algal basal metabolism, (2) algal predation, (3) hydrolysis to DON, (4) settling (not included in the following equations), and (5) external loads.

$$\text{Change of } PON + \text{convection} = \text{Diffusion} + \text{Reactions}$$

$$\pm\text{sources} / \text{sinks} \tag{3.60}$$

The Labile Particulate Organic Nitrogen, $LPON$:

$$\underbrace{\frac{\partial (\phi_6)}{\partial t}}_{\text{Change of PON}} + \underbrace{\nabla \cdot (\mathbf{u} \phi_6)}_{\text{Convection}} = \underbrace{\nabla \cdot (-D_{6,m} \nabla \phi_6)}_{\text{Diffusion}} + \underbrace{R_6}_{\text{Reactions}} + \underbrace{S_6}_{\text{sources/sinks}} \tag{3.61}$$

$$R_6 = \underbrace{\sum_{x=1}^{1} (FNL_x . BM_x) . ANC_x . B_x}_{\text{algal basal metabolism}} + \underbrace{\sum_{x=1}^{1} (FNLP . PR_x) . ANC_x . B_x}_{\text{algal predation}}$$

$$- \underbrace{K_{LPON} . PON}_{PON \text{ hydrolysis}} \tag{3.62}$$

where $PON = \phi_6$ is the concentration of labile particulate organic nitrogen (gN/m^3), $FNL_x =$ is the fraction of metabolized nitrogen by algal group x produced as particulate organic nitrogen, $FNLP$ is the fraction of predated nitrogen produced as particulate organic nitrogen, ANC_x is the nitrogen/carbon ratio in algal group x (gN/gC), and K_{LPON} is the hydrolysis rate of particulate organic nitrogen (day^{-1}).

Dissolved Organic Nitrogen, $DON = \phi_7$, includes: (1) algal basal metabolism, (2) algal predation, (3) hydrolysis from PON, (4) mineralization to ammonium, and (5) external loads. The equation is given by:

$$\underbrace{\frac{\partial(\phi_7)}{\partial t}}_{\text{Change of DON}} + \underbrace{\nabla \cdot (\mathbf{u}\phi_7)}_{\text{Convection}} = \underbrace{\nabla \cdot (-D_{7,m}\nabla\phi_7)}_{\text{Diffusion}} + \underbrace{R_7}_{\text{Reactions}} + \underbrace{S_7}_{\text{sources/sinks}} \qquad (3.63)$$

$$R_7 = \underbrace{\sum_{x=1}^{1}(FND_x.BM_x).ANC_x.B_x}_{\text{algal basal metabolism}} + \underbrace{\sum_{x=1}^{1}(FNDP.PR_x).ANC_x.B_x}_{\text{algal predation}}$$

$$+ \underbrace{K_{LPON}.PON}_{\text{PON hydrolysis}} - \underbrace{K_{DON}.DON}_{\text{PON hydrolysis}} \qquad (3.64)$$

where DON is the concentration of dissolved organic nitrogen (g-N/m 3), FND_x is the fraction of metabolized nitrogen by algal group x produced as dissolved organic nitrogen, $FNDP$ is the fraction of predated nitrogen produced as dissolved organic nitrogen and K_{DON} is the mineralization rate of dissolved organic nitrogen (day^{-1}).

Ammonium Nitrogen ($NH4 = \phi_8$) accurs in natural waters, and exists in two forms: un - ionized (NH_3) and ionized (NH_4^+). NH_4^+ is the dominant form and usually has much higher concentrations than NH_3. For this reason, only NH_4^+ concentrations are commonly simulated in water quality models. Major sources and sinks for ammonia nitrogen include: (1) algal basal metabolism, predation, and uptake; (2) mineralization from dissolved organic nitrogen; (3) nitrification to nitrate; (4) exchange at the sediment-water column interface, and (5) external loads. The transport equation for $NH4 = NH_3 + NH_4^+$ can be described as:

$$\underbrace{\frac{\partial(\phi_8)}{\partial t}}_{\text{Change of NH4}} + \underbrace{\nabla \cdot (\mathbf{u}\phi_8)}_{\text{Convection}} = \underbrace{\nabla \cdot (-D_{8,m}\nabla \phi_8)}_{\text{Diffusion}} + \underbrace{R_8}_{\text{Reactions}} + \underbrace{S_8}_{\text{sources/sinks}} \qquad (3.65)$$

$$R_8 = \underbrace{\sum_x^1 (FNI_x.BM_x).ANC_x.B_x}_{\text{algal basal metabolism}}$$

$$+ \underbrace{\sum_x^1 (FNIP.PR_x).ANC_x.B_x}_{\text{predation}}$$

$$- \underbrace{\sum_x^1 (PN_x.P_x).ANC_x.B_x}_{\text{uptake by algae}}$$

$$+ \underbrace{K_{DON}.PON}_{\text{DON mineralization}} - \underbrace{Nit(DO,NH4,T).NH4}_{\text{nitrification}} \qquad (3.66)$$

where FNI_x is the fraction of metabolized nitrogen by algal group x produced as inorganic nitrogen, $FNIP$ is the fraction of predated nitrogen produced as inorganic nitrogen, PN_x is the preference for ammonium uptake by algal group x ($0 < PN_x < 1$), and Nit is the nitrification rate (day^{-1}).

Nitrate Nitrogen ($NO3 = NO_2^- + NO_2^- = \phi_9$) interacts with each component of the ecological model. Nitrogen oxides (NO_x) represent inorganic compounds containing both nitrogen and oxygen, and include NO_2^-, NO_3^-, and others. Major sources and sinks for nitrate nitrogen include: (1) algal uptake, (2) nitrification from ammonium, (3) denitrification to nitrogen gas, (4) $NO3$ flux at the sediment bed water column interface, and (5) external sources. The $NO3$ transport equation describing these processes can be expressed as:

$$\underbrace{\frac{\partial(\phi_9)}{\partial t}}_{\text{Change of NO3}} + \underbrace{\nabla \cdot (\mathbf{u}\phi_9)}_{\text{Convection}} = \underbrace{\nabla \cdot (-D_{9,m}\nabla \phi_9)}_{\text{Diffusion}} + \underbrace{R_9}_{\text{Reactions}} + \underbrace{S_9}_{\text{sources/sinks}} \qquad (3.67)$$

Nitrogen processes affecting nitrogen concentrations include: (1) Algal Uptake: Algae consume $NH4$ and $NO3$ for growth via photosynthesis, (2) Mineralization and Hydrolysis:

Particulate organic nitrogen dacays into DON via hydrolysis, and then DON is converted to NH4 via mineralization , (3) Nitrification: Ammonia is oxidized to nitrite (NO_2^-) and then to nitrate (NO_3^-) via nitrification, and (4) Denitrification: Under anaerobic conditions, nitrate is reduced to nitrogen gas (N_2) and then released from the modeling system (This process is assumed to occur in the bulk of the flow and in the sediment water interface. The bulk flow denitrification takes place if there is DOC suspended in the water. Here we assume that the pH does not varies significantly, less than 8), and (5) Nitrogen Fixation: Some blue - green algae can directly fix N_2 from the atmosphere. This process is an important external source to a body of water and can significantly affect the nitrogen dynamics. However, $NH4$ and $NO3$ are preferred forms of nitrogen for algae consumption.

$$R_9 = \underbrace{\sum_x^1 \left[[1 - PN_x(NH4, NO3)].P_x \right].ANC_x.B_x}_{\text{algal uptake}}$$

$$+ \underbrace{Nit(DO, NH4, T).NH4}_{\text{nitrification}}$$

$$- \underbrace{ANDC.Denit(DO, NO3, Bx, T).DOC}_{\text{denitrification}} \qquad (3.68)$$

where $ANDC$ is the mass of nitrate nitrogen reduced per mass of dissolved organic carbon oxidized ($0.933 gN / gC$) (see Table 3-1, ID = 5, Net denitrification) (Stumm & Morgan, 1981).

The effects of algae are present in the terms within summation. These represent the effects of algae on nitrogen. In this research only one term is included since only one species of algae is simulated, green algae. Algae can influence nitrogen processes through: (1) algae death, (2) algal growth, (3) algal preference for ammonia over nitrate, and (4) nitrogen fixation. Through algal metabolism and algal predation, the nitrogen of algal biomass can be recycled into organic nitrogen and inorganic nitrogen, and is represented by the distribution coefficients. For algal basal metabolism:

$$FNL_x + FND_x + FNI_x = 1 \tag{3.69}$$

and for algal predation:

$$FNLP + FNDP + FNIP = 1 \tag{3.70}$$

Two forms of nitrogen, $NH4$ and nitrate $NO3$, are used during algal uptake and growth, and $NH4$ is the preferred form of nitrogen over $NO3$ for algal growth. The prefered form for uptake is parameterized using the ammonia preference factor, PN_x. It is a function of the ammonia (NH4, state variable) and nitrate (NO3, state variable) concentrations, and is expressed as:

$$PN_x = NH4.\frac{NO3}{(KHN_x + NH4)(KHN_x + NO3)}$$

$$+ NH4.\frac{KHN_x}{(NH4 + NO3)(KHN_x + NO3)} \tag{3.71}$$

Equation 3.71 is somewhat similar to the Michaelis-Menton formulation that has been used to describe limiting functions. The half saturation constant, KHN_x, is first introduced in Equation 3.28 (half saturation cosntant for nitrogen) with respect to the growth limiting function for nutrients, $f_1(N)$. The PN_x partitions the nitrogen uptake between ammonia and nitrate, with values ranging from 0 to 1. The preference for ammonium is 1 when nitrate is absent and is 0 when ammonium is absent. At $PN_x = 1$, $NO3$ is zero and algae uptakes nitrogen only in the form of $NH4$. At $PN_x = 0$, $NH4$ is zero and algae uptakes nitrogen only in the form of $NO3$. This approach is commonly used in water quality models (Cerco & Cole, 1995; Cerco & Cole, 1994). At $KHN_x = 10 \mu g / L$, the values of PN_x show that PN_x is most sensitive at low values of $NH4$ and $NO3$. For a given concentration of $NH4$, PN_x is almost a constant when $NO3$ is $> 20 \mu g / L$. More over, mineralization and hydrolysis are represented by:

$$K_{LPON} = \left(K_N + \frac{KHN}{KHN + NH4 + NO3} K_{LNalg}.\sum_{x=1}^{1} B_x \right).e^{KT_{HDR}(T - TR_{HDR})} \tag{3.72}$$

$$K_{DON} = \left(K_{DN} + \frac{KHN}{KHN + NH4 + NO3} K_{DNalg}.\sum_{x=1}^{1} B_x \right).e^{KT_{MNL}(T - TR_{MNL})} \tag{3.73}$$

where K_N = minimum hydrolysis rate of labile particulate organic nitrogen (day^{-1}), K_{DN} = minimum mineralization rate of dissolved organic nitrogen (day^{-1}), K_{RNalg} and K_{LNalg} are the constants that relate hydrolysis of refractory and labile particulate organic nitrogen to algal biomass ($day^{-1}/gC/m3$), K_{DNalg} is the constant that relates mineralization to algal biomass ($day^{-1}/gC/m^3$), and KHN is the mean half-saturation constant for algal nitrogen uptake ($gN/m3$), which has the form:

$$KHN = \frac{1}{3}\sum_{x}^{3} KHN_x \qquad (3.74)$$

Nitrification is the process by which an NH_4^+ is oxidized to NO_2^- and then to NO_3^-. The process of nitrification in natural water is complex, mainly depending upon: (1)dissolved oxygen concentration, (2)nitrogen concentrations, (3)water temperature, (4)nitrifying bacteria, and (5) pH level. The nitrification process is often represented as a first-order kinetics, as in the term of ($-Nit.NH4$) (see Equation 3.68) . The nitrification rate, Nit , can be formulated as a function of $NH4$, DO , and temperature (T):

$$Nit = \left(\frac{DO}{KHNit_{DO} + DO}\right)\left(\frac{NH4}{KHNit_N + NH4}\right).Nit_m.f_{Nit}(T) \qquad (3.75)$$

and

$$f_{Nit}(T) = e^{-KNit1.(T-TNit)^2} \qquad (3.76)$$

where $KHNit_{DO}$ is the nitrification half saturation constant for dissolved oxygen ($gO2/m3$), $KHNit_N$ is the nitrification half saturation constant for ammonium ($gN/m3$), Nit_m is the maximum nitrification rate at TNi t (day^{-1}), $TNit$ is the optimum temperature for nitrification (^oC) and $KNit1$ is the effect of temperature below $TNit$ on nitrification rate ($^oC^{-2}$). Equation (77) shows that the nitrification process can be limited by low concentrations of DO and $NH4$. The $f_{Nit}(T)$ parameterization as presented here is a simplification of the model

presented by (Cerco & Cole, 1994). BioChemFOAM considers only one coefficient in temperature limitations, $KNit1$. This is done to reduce complexity while keeping the effect of temperature on the process.

Denitrification is the process by which nitrate is reduced to nitrite and then to nitrogen gas by bacteria. In BioChemFOAM, a Michaelis-Menton function is used to express the denitrification rate, $Denit$:

$$Denit = \left(\frac{KHOR_{DO}}{KHOR_{DO} + DO} \right) \left(\frac{NO3}{KHDN_N + NO3} \right).AANOX.K_{DOC} \qquad (3.77)$$

where $KHDN_N$ is the denitrification half saturation constant for nitrate ($gN/m3$) and $AANOX$ is the ratio of denitrification rate to oxic dissolved organic carbon respiration rate (that makes the anoxic respiration slower than oxic respiration, with a typical value of 0.5 used by (Cerco & Cole, 1994).

5. *Dissolved Oxygen, DO*. It is one of the most important water quality variables in aquatic systems. Dissolved oxygen is a basic requirement for a healthy aquatic ecosystem and indicates the capability of the body of water to support a balanced ecosystem. The net change of $DO = \phi_{10}$ can be determined by:

$$\underbrace{\frac{\partial (\phi_{10})}{\partial t}}_{\text{Change of DO}} + \underbrace{\nabla \cdot (\mathbf{u}\phi_{10})}_{\text{Convection}} = \underbrace{\nabla \cdot (-D_{10,m}\nabla \phi_{10})}_{\text{Diffusion}} + \underbrace{R_{10}}_{\text{Reactions}} + \underbrace{S_{10}}_{\text{sources/sinks}} \qquad (3.78)$$

The reaction term as presented by (Ji, 2008) is formulated in general as follows:

$$R_{10} = \underbrace{\sum_x^1 ((1.3 - 0.3PN_x).P_x).AOCR.B_x}_{\text{photosynthesis}}$$

$$- \underbrace{\sum_x^1 \left((1 - FCD_x) \frac{DO}{KHR_x + DO}.BM_x \right).AOCR.B_x}_{\text{respiration}}$$

$$\underbrace{- AONT.Nit(DO, NH4, T).NH4}_{\text{Nitrification}} \underbrace{- AOCR.K_{HR}.DOC}_{DOC\,\text{decomposition}}$$

$$\underbrace{- \frac{DO}{KH_{COD} + DO} KCOD.COD}_{COD,\text{oxygen demand from reduced methane}} + \underbrace{K_r.(DO_s - DO)}_{\text{reaeration}}$$

$$+ \underbrace{SOD / \Delta z}_{\text{Sediment Oxygen Demand}} \tag{3.79}$$

where PN_x is the preference for ammonium uptake by algal group x ($0 <= PN_x <= 1$), given by Equation 3.71. $AONT$ is the mass of DO consumed per unit mass of ammonium nitrogen nitrified ($4.33gO2 / gN$) (Cerco & Cole, 1994). $AOCR$ is the dissolved oxygen/carbon ratio in respiration ($2.67g - O_2 / g - C$) (Cerco & Cole, 1994). K_r is the reaeration coefficient (day^{-1}), applied to the surface layer only and DO_s is the saturation concentration of dissolved oxygen ($g - O_2 / m^3$). There is also a contribution from the sediment oxygen demand applied to the bottom layer that is not included in the present research. Usually the term is modeled as a flux and the name of the variable could be SOD. It is the sediment oxygen demand ($g - O_2 / m^2 / day$) that is applied to the bottom layer only; a direction of positive is towards the water column. SOD is not included at the moment in BioCHemFOAM.

The general reaction term presented in Equation 3.79 is utilized in the cases presented in Chapter 4 for 0-D, 2-D and 3-D cases without the SOD term. This is done since it is assumed in those cases that the depth is divided only in one layer, the depth direction. An additional formulation is presented when applying the model in the fully 3-D model to a real case in Chapter 6. The new reaction term is given by:

$$R_{10} = \underbrace{\sum_{x}^{1} \left((1.3 - 0.3 PN_x).P_x \right).AOCR.B_x}_{\text{photosynthesis}}$$

$$\underbrace{- \sum_{x}^{1} \left((1 - FCD_x) \frac{DO}{KHR_x + DO}.BM_x \right).AOCR.B_x}_{\text{respiration}}$$

$$\underbrace{- AONT.Nit(DO, NH4, T).NH4}_{\text{Nitrification}} - \underbrace{AOCR.K_{HR}.DOC}_{DOC \text{ decomposition}}$$

$$\underbrace{- \frac{DO}{KH_{COD} + DO} KCOD.COD}_{COD, \text{oxygen demand from reduced methane}} \tag{3.80}$$

The previous parameterization is necessary in the fully 3-D model (see Chapter 6) since now the reaeration (included in BioChemFOAM) and Sediment Oxygen Demand occurs at the boundary of the domain (not includeed in BiOChemFOAM), the first at the water air interface and the latter at the sediment water interface.

Finally, the Chemical Oxygen Demand, $COD = \phi_{11}$, that accounts for oxygen demand from reduced substances such as methane is parameterized as:

$$\frac{\partial(\phi_{11})}{\partial t} + \nabla \cdot \left(\mathbf{u}\phi_{11} \right) = \nabla \cdot \left(-D_{11,m} \nabla \phi_{11} \right) + R_{11} + S_{11} \tag{3.81}$$

$$R_{11} = \frac{DO}{KH_{COD} + DO} KCOD.COD + \frac{BFCOD}{\Delta z} \tag{3.82}$$

The contribution of this term, dissolved oxygen depletion, is small (Di Toro, 2001). In the present research, parameterization is kept consistent with previous models (Cerco & Cole, 1994), but its reaction is small and does not afect considerably the DO concentration. Applications in Chapters 4 and 6 utilize small reaction coefficients, allowing only the species to be transported, and do not play an inportant role in the chemical and biological discussed in the present research. An additional reason to keep the species is to test the numerical implementation when one of the species is inactive through the reaction coefficient KCOD.

Finally the species transport equations for POC (Equation 3.40), POP (Equation 3.49), and PON (Equation 3.61), haves an extra term that simulates settling as $\nabla \bullet (u_z \phi_i)$ added to the left part of each transport equation. u_z represent a fixed vertical settling velocity for the particulate organic matter and is fixed to be -0.1m/day, (Schnoor, 1996). Resuspention is not modeled in BioChemFOAM.

3.5 Coefficients included in the proposed model

A review of the equations to be solved and the coefficients used in the hydrodynamic module (HM) and Species Transport Module (ST) is presented in the following tables, which present an order of magnitude of the coefficients and may change for a specific application.

The variables and equations solved in BioChemFOAM are summarized in Tables 3-2 and 3-3. Tables 3-2 and 3-3 presents the equations for the species transport module, and Table 3-4 presents the equations solved in the hydrodynamic module in conjunction with the temperature and light that was previously described.

The ST module solves a series of pasive scalar equations, DOC, PO4, DON, NH4, NO3, DO and COD have the following formulation:

$$\underbrace{\frac{\partial (\rho \phi_i)}{\partial t}}_{temporal\,variation,\mathcal{T}} + \underbrace{\nabla \cdot (\rho \mathbf{u} \phi_i)}_{convection,\mathcal{A}} = \underbrace{\nabla \cdot \mathbf{J}_i}_{diffusion,\mathcal{D}} + \underbrace{R_i}_{Reactions,\mathcal{R}} + \underbrace{S_i}_{sources/sinks,\mathcal{S}}$$

For algae(Bx), POC, PON, POP and POC the transport equations is:

$$\underbrace{\frac{\partial (\rho \phi_i)}{\partial t}}_{temporal\,variation,\mathcal{T}} + \underbrace{\nabla \cdot (\rho \mathbf{u} \phi_i) - \nabla \bullet (u_z \phi_i)}_{convection,\mathcal{A}} = \underbrace{\nabla \cdot \mathbf{J}_i}_{diffusion,\mathcal{D}} + \underbrace{R_i}_{Reactions,\mathcal{R}} + \underbrace{S_i}_{sources/sinks,\mathcal{S}}$$

Table 3-2. Equations to be solved in BioChemFOAM for algae, carbon species and phosphorus species.. Column 1 includes the name of the variable. Column 2 presents the parameterization in functional form. Column 3 contains the reference to the passive scalar transport equation, and the last column presents the references to the source term (R_i) for each variable in the model. In the column, the "Parametrization R_i" terms on the right hand side represent functional relations between variables, e.g., $Px(NH4, NO3, PO4)$ means that the growth function for algae depends on the variables $NH4$, $NO3$, and $PO4$. The same applies for the other terms in that column.

Variable	Parameterization Ri	T. Eq. #	S. Eq. #
$B_x = \phi_{1x}$	$R_{1x} = \underbrace{P_x(NH4,NO3,PO4).B_x}_{\text{growth}} - \underbrace{BM_x(T).B_x}_{\text{metabolism}} - \underbrace{PR_x(B_x,T).B_x}_{\text{algalpredation}}$	3.26	3.27
$POC = \phi_2$	$R_2 = \underbrace{\sum_{x=1}^{1} FCLP.PR_x(B_x,T).B_x}_{\text{algal predation}} - \underbrace{K_{POC}(B_x,T).POC}_{\text{hydrolysis}}$	3.40	3.41
$DOC = \phi_3$	$R_3 = \underbrace{\sum_{x=1}^{1}\left(FCD_x + (1-FCD_x)\frac{KHR_x}{KHR_x + DO}\right).BM_x(T).B_x}_{\text{algal excretion}} + \underbrace{\sum_{x=1}^{1}\left(FCDP.PR_x(B_x,T).B_x\right)}_{\text{algalpredation}}$ $+\underbrace{K_{LPOC}(B_x,T).POC}_{POC\,\text{hydrolysis}} - \underbrace{K_{HR}(DO,B_x,T).DOC}_{DOC\,\text{heterotropic respiration}} - \underbrace{Denit(DO,NO3,B_x,T).DOC}_{\text{Denitrification}}$	3.43	3.44
$POP = \phi_4$	$R_4 = \underbrace{\sum_{x=1}^{1}\left[FPL_x.BM_x(T)\right].APC.B_x}_{\text{algal basal metabolism}} - \underbrace{\sum_{x=1}^{1}\left[FPLP.PR_x(B_x,T)\right].APC.B_x}_{\text{algal predation}} - \underbrace{K_{LPOP}.POP}_{POP\,\text{hydrolysis}}$	3.49	3.50
$PO4 = \phi_5$	$R_5 = \underbrace{\sum_{x=1}^{1}\left[FPD.BM_x(T)\right].APC.B_x}_{\text{algal basal metabolism}} + \underbrace{\sum_{x=1}^{1}\left[FPDP.PR_x(B_x,T)\right].APC.B_x}_{\text{algal predation}} + \underbrace{K_{POP}(PO4d,B_x,T).POP}_{POP\,\text{hydrolysis}}$ $-\underbrace{P_x(NH4,NO3,PO4).APC.B_x}_{\text{algae uptake}}$	3.52	3.53

Table 3-3. Equations to be solved in BioChemFOAM nitrogen species, oxygen, and COD. Column 1 lists the names of the variables. Column 2 presents the parameterization in functional form. Column 3 contains the reference to the passive scalar transport equation, and the last column presents the references to the source term (R_i) for each variable in the model. In the column, "Parametrization R_i" terms on the right hand side represent functional relations among variables, e.g., $Px(NH4, NO3, PO4)$ -means that the growth function for algae depends on the variables $NH4$, $NO3$, and $PO4$. The same applies for the other terms in that column.

Variable	Parameterization Ri	T. Eq. #	S. Eq. #
$PON = \phi_6$	$$R_6 = \sum_{x=1}^{1}\left(FNL_x.BM_x\right).ANC_x.B_x + \sum_{x=1}^{1}\left(FNLP.PR_x\right).ANC_x.B_x - \underbrace{K_{LPON}.PON}_{PON\,\text{hydrolysis}}$$ $\underbrace{\qquad}_{\text{algal basal metabolism}}$ $\underbrace{\qquad}_{\text{algal predation}}$	3.61	3.62
$DON = \phi_7$	$$R_7 = \sum_{x=1}^{1}\left(FND_x.BM_x\right).ANC_x.B_x + \sum_{x=1}^{1}\left(FNDP.PR_x\right).ANC_x.B_x + \underbrace{K_{LPON}.PON}_{PON\,\text{hydrolysis}} - \underbrace{K_{DON}.DON}_{PON\,\text{hydrolysis}}$$ $\underbrace{\qquad}_{\text{algal basal metabolism}}$ $\underbrace{\qquad}_{\text{algal predation}}$	3.63	3.64
$NH4 = \phi_8$	$$R_8 = \underbrace{\sum_{x}^{1}\left(FNI_x.BM_x\right).ANC_x.B_x}_{\text{algal basal metabolism}} + \underbrace{\sum_{x}^{1}\left(FNIP.PR_x\right).ANC_x.B_x}_{\text{predation}} - \underbrace{\sum_{x}^{1}\left(PN_x.P_x\right).ANC_x.B_x}_{\text{uptake by algae}}$$ $$+ \underbrace{K_{DON}.PON}_{DON\,\text{mineralization}} + \underbrace{Nit(DO, NH4, T).NH4}_{\text{nitrification}}$$	3.65	3.66
$NO3 = \phi_9$	$$R_9 = \underbrace{\sum_{x}^{1}\left[[1 - PN_x(NH4, NO3)].P_x\right].ANC_x.B_x}_{\text{algal uptake}} + \underbrace{Nit(DO, NH4, T).NH4}_{\text{nitrification}}$$ $$- \underbrace{ANDC.Denit(DO, NO3, B_x, T).DOC}_{\text{denitrification}}$$	3.67	3.68
$DO = \phi_{10}$	When applied to the model in Chapter 4. $$R_{10} = \underbrace{\sum_{x}^{1}\left((1.3 - 0.3PN_x).P_x\right).AOCR.B_x}_{\text{Photosynthesis}} - \underbrace{AONT.Nit(DO, NH4, T).NH4}_{\text{Nitrification}}$$ $$- \underbrace{AOCR.K_{HR}.DOC}_{DOC\,\text{decomposition}} - \underbrace{\frac{DO}{KH_{COD} + DO}KCOD.COD}_{COD,\text{oxygen demand from reduced methane}} + \underbrace{K_r.(DO_s - DO)}_{\text{Reaeration}}$$ When applied the model in Chapter 6 $$R_{10} = \underbrace{\sum_{x}^{1}\left((1.3 - 0.3PN_x).P_x\right).AOCR.B_x}_{\text{Photosynthesis}} - \underbrace{AONT.Nit(DO, NH4, T).NH4}_{\text{Nitrification}}$$ $$- \underbrace{AOCR.K_{HR}.DOC}_{DOC\,\text{decomposition}} - \underbrace{\frac{DO}{KH_{COD} + DO}KCOD.COD}_{COD,\text{oxygen demand from reduced methane}}$$	3.78	3.79 3.80
$COD = \phi_{11}$	$$R_{11} = \frac{DO}{KH_{COD} + DO}KCOD.COD + \frac{BFCOD}{\Delta z}$$	3.81	3.82

Table 3-4. Equations solved for flow field variables: velocity vectors U, pressure P, turbulent kinetic energy k, and dissipation ε. The temperature equation, T, is decoupled from the flow field in this version of BioChemFOAM, and light influence on photosynthesis, I, is modeled with a mathematical expression that only takes into account attenuation due to algae growth by a variable diffusion coefficient.

Variable	Equation	T. Eq. #
U	$$\frac{\partial U_i}{\partial x_i} = 0$$ $$\rho \frac{\partial U_i}{\partial t} + \rho \frac{\partial (U_i U_j)}{\partial x_j} = -\frac{\partial P}{\partial x_i} + \frac{\partial}{\partial x_j}\left[2\mu\left[\frac{\partial U_i}{\partial x_j} + \frac{\partial U_j}{\partial x_i}\right] + \mu_t\left[\frac{\partial U_i}{\partial x_j} + \frac{\partial U_j}{\partial x_i}\right] - \frac{2}{3}\rho\delta_{ij}k \right]$$	3.61
k	$$\rho\frac{\partial k}{\partial t} + \rho\frac{\partial(kU_j)}{\partial x_j} = \underbrace{\frac{\partial}{\partial x_j}\left(\mu\frac{\partial k}{\partial x_j}\right)}_{A} - \frac{\mu_t}{Pr_t}\frac{\partial \kappa}{\partial x_j} \underbrace{- \mu_t\left(\frac{\partial U_i}{\partial x_j} + \frac{\partial U_j}{\partial x_i}\right)\frac{\partial U_i}{\partial x_j}}_{P_k} - \varepsilon$$	3.15
ε	$$\rho\frac{\partial \varepsilon}{\partial t} + \rho\frac{\partial(\varepsilon U_j)}{\partial x_j} = C_{\varepsilon 1}P_k\frac{\varepsilon}{k} - \rho C_{\varepsilon 2}\frac{\varepsilon^2}{k} + \frac{\partial}{\partial x_j}\left(\frac{\mu_t}{\sigma_\varepsilon}\frac{\partial \varepsilon}{\partial x_j}\right)$$	3.18
T	$$\underbrace{\frac{\partial(T)}{\partial t}}_{\text{temporal variation},\,\mathcal{T}} + \underbrace{\nabla\cdot(\mathbf{u}T)}_{\text{convection},\,\mathcal{A}} = \underbrace{\nabla\cdot\upsilon_t\nabla T}_{\text{diffusion},\,\mathcal{D}}$$	3.19
I	$$-\nabla\cdot\underbrace{\left(\underbrace{exp\left(-\frac{Bx}{Bx_{min} + Bx}\right)}_{\text{extinction coefficient}}\nabla I\right)}_{\text{Diffusion Process}} = 0$$	3.35

Table 3-5. Model coefficients for algae. The coefficients can be reviewed from Equation 3.27. The last column shows the value assumed in BioChemFOAM for applications in Chapters 4 and 6.

Coefficient	Units	Values from references	Description	Ref.	BioChemFOAM
PM_x	$[day^{-1}]$	Diatoms 0.55-5.0; Green 0.7-9.2; Blue-green 0.41-11	Maximum growth rate for algal group x.	[1] Table 6-5	Value assumed for Green Algae is 2.5
KHN	$\left[\dfrac{mg-N}{L}\right]$	Diatoms 0.015-0.923; Green 0.001-1.236; Blue-green 0.0-4.34	Half saturation constant for nitrogen	[1] Table 6-10	0.1
$TM1_x$	$[^oC]$	15	Lower end of optimal temperature range for algal growth group x.	[2]	15
$Tm2_x$	$[^oC]$	20	Upper end of optimal temperature range for algal growth group x.	[2]	20
$KTG1_x$	$[1]$	Diatoms 0.004; Greens 0.008	Effect of temperature below $TM1_x$ on growth for algal group x.	[1] Table 9-1	0.008
$KTG2_x$	$[1]$	Diatoms 0.006; Greens 0.01	Effect of temperature below $TM1_x$ on growth for algal group x.	[1] Table 9-1	0.01

Source:

(1) Bowie, G. L., & Tech, T. (1985). Rates, constants, and kinetics formulations in surface water quality modeling.

(2) Cerco, C. F., & Cole, T. M. (1994). Three-Dimensional Eutrophication Model of Chesapeake Bay. Volume 1: Main Report: DTIC Document

Table 3-6. Model coefficients for algae -See Equation 3.27.

Coefficient	Units	Values from references	Description	Ref.	BioChemFOAM
$\left(I_s\right)_x$	$\left[\dfrac{ly}{day}\right]$	Diatoms 88-300; Green 88-160; Blue-Green 43-600	Optimal light intensity for algal group x.	[1] Table 6-8	300
BMR_x	$\left[day^{-1}\right]$	0.02-0.36	Basal metabolism rate at TR_x for algal group x.	[2] Table 9-2	0.02
KTB_x	$\left[{}^o C^{-1}\right]$	0.069	Effects of temperature on metabolism for algal group x.	[2] Table 9-2	0.069
PRR_x	$\left[day^{-1}\right]$	Diatoms 0.065-0.215; Greens 0.215	Predation rate at reference temperature TR_x for algal group x.	[2]	0.215
B_{xp}	[mg-C/L]	-	Reference algal concentration for predation for algal group x.	-	0.01(assumed)
α_p	[1]	-	Exponential dependence factor.	-	0.01 (assumed)

Source:

(1) Bowie, G. L., & Tech, T. (1985). Rates, constants, and kinetics formulations in surface water quality modeling.

(2) Cerco, C. F., & Cole, T. M. (1994). Three-Dimensional Eutrophication Model of Chesapeake Bay. Volume 1: Main Report: DTIC Document

Table 3-7. POC model coefficients. See Equation 3.41.

Coefficient	Units	Values from references	Description	Ref.	BioChemFOAM
FCLP	[1]	0.55	Fraction of predated carbon produced as particulate organic carbon.	*	0.55

Source:

*Cerco, C. F., & Cole, T. M. (1994). Three-Dimensional Eutrophication Model of Chesapeake Bay. Volume 1: Main Report: DTIC Document

Table 3-8. Model coefficients for DOC. -See Equation 3.44.

Coefficient	Units	Values from references	Description	Ref.	BioChemFOAM
FCD_x	[1]	0-1	A constant for algal group x, fraction of basal metabolism exuded as DOC.	-	0.0
KHR_x	[g-O$_2$/m^3]	0.5	Half saturation constant of DO for algal DOC excretion for group x.	[2]	0.5
FCDP	[1]	0.1	Fraction of predated carbon produced as dissolved organic carbon.	[2]	0.45 (assumed)
$K_{Dca\lg}$	[day^{-1}/gC/m3]	0.0	Constant that relates respiration to algal biomass.	[2]	0.0
$KHOR_{DO}$	[gO$_2$/m^3]	0.5	Oxic respiration half saturation constant for DO.	[2]	0.5
K_{DC}	[day^{-1}]	0.01	Minimum respiration rate of DOC	[2]	0.01
KT_{MNL}	[^{o}C^{-1}]	0.069	Effect of temperature for mineralization of dissolved organic matter	[2]	0.069
TR_{MNL}	[^{o}C]	20	Reference temperature for mineralization of dissolved organic matter.	[2]	20
$KHDN_N$	[g-N/m^3]	0.005[3]-0.1[2]	Denitrification half saturation constant for nitrate.	[2] & [3]	0.01
$AANOX$	[1]	0.5	Ratio of denitrification rate to oxic dissolved organic carbon respiration rate.	[2]	0.5
K_C	[day^{-1}]	0.075	Minimum dissolution rate of particulate organic carbon	[2]	0.075
$K_{Ca\lg}$	[d^{-1}/mg-C/L]	0.0	Constant that relates dissolution of POC to algal biomass.	[2]	0.0
KT_{HDR}	[^{o}C^{-1}]	0.069	Effect of temperature on hydrolysis of POC.	[2]	0.069

Source: [2] Cerco, C. F., & Cole, T. M. (1994). Three-Dimensional Eutrophication Model of Chesapeake Bay. Volume 1: Main Report: DTIC Document [3] LimnoTech. (2007). Upper Mississippi River - Lake Pepin Water Quality Model; Development, Provisional Calibration and Preliminary Application: Minnesota Pollution Control Agency (LimnoTech, 2007)

.

Table 3-9. Model coefficients for PO4 (dissolved orthophosphate directly available for algae). See Equation 3.53.

Coefficient	Units	Values from references	Description	Ref.	BioChemFOAM
FPD_x	[1]	1.0	Fraction of metabolized phosphorus by algal group x produced as DOP.	[2]	0.5 (assumed)
$FPDP$	[1]	0.5	Fraction of predated phosphorus by algal group x produced as DOP.	[2]	0.65 (assumed)
APC	[g-P/g-C]	1/42	Mean Phosphorus/Carbon relation in all algae groups.	[2]	1/42=0.024
K_P	[day^{-1}]	0.075	Hydrolysis rate of particulate organic phosphorus.	[2]	0.075
K_{Palg}	[day^{-1}]	0.1	Minimum mineralization rate DOP.	[2]	0.1
K_{Dalg}	[d^{-1}/g-C/m^3]	0.2	Constant that relates mineralization to algal biomass.	[2]	0.2

Source: [2] Cerco, C. F., & Cole, T. M. (1994). Three-Dimensional Eutrophication Model of Chesapeake Bay. Volume 1: Main Report: DTIC Document.

Table 3-10. DON model coefficients. -See Equation 3.64.

Coefficient	Units	Values from references	Description	Ref.	BioChemFOAM
FND_x	[1]	1.0	Fraction of metabolized nitrogen by algal group x produced as DON.	[2]	0.3 (assumed)
$FNDP$	[1]	0.1	Fraction of predated nitrogen by algal group x produced as DON.	[2]	0.3 (assumed)
ANC	[g-N/g-C]	0.167	Nitrogen/Carbon ration in algae group x.	[2]	0.167
K_N	[day^{-1}]	0.005-0.075	Minimum hydrolysis rate of PON.	[2]	0.04
KHN	[mg-N/L]	0.01	Mean half-saturation constant for algae nutrient uptake.	[2]	0.01
K_{Nalg}	[d^{-1}/mg-C/L]	0.0	Constant that relates hydrolysis of PON to algal biomass.	[2]	0.0
K_{DN}	[day^{-1}]	0	Minimum mineralization rate of DON.	[2]	0.015
K_{DNalg}	[d^{-1}/g-C/m^3]	0	Constant that relates mineralization to algal biomass.	[2]	0.0

Source: [2] Cerco, C. F., & Cole, T. M. (1994). Three-Dimensional Eutrophication Model of Chesapeake Bay. Volume 1: Main Report: DTIC Document.

Table 3-11. NH4 and NO3 model coefficients. See Equations 3.66 and 3.68.

Coefficient	Units	Values from references	Description	Ref.	BioChemFOAM
FNI_x	[1]	0.0	Fraction of metabolized nitrogen by algae group x produced as inorganic nitrogen.	[2]	0.1 (assumed)
$FNIP$	[1]	0.0	Fraction of predated nitrogen produced as inorganic nitrogen.	[2]	0.15 (assumed)
$KHNit_{DO}$	[gO$_2$/m^3]	0.6-3	Nitrification half saturation constant for DO.	[2]	1.0
Nit_m	[mg-N.L^{-1}.day^{-1}]	0.006-0.446	Maximum nitrification rate at TNit.	[2]	0.027 (by default)
$TNit$	[^{o}C]	20	Optimum temperature for nitrification.	[2]	20
$KTNit1$	[^{o}C^{-2}]	0.0045-0.06	Effect of temperature below TNit on nitrification rate.	[2]	0.05
$ANDC$	[g-N/g-C]	0.933	Mass of nitrate nitrogen reduced per mass of dissolved organic carbon oxidized.	-	0.933 (from stoichiometric reactions)

Source: [2] Cerco, C. F., & Cole, T. M. (1994). Three-Dimensional Eutrophication Model of Chesapeake Bay. Volume 1: Main Report: DTIC Document.

Table 3-12. DO, dissolved oxygen model coefficients. See Equation 3.79 and 3.80.

Coefficient	Units	Values from references	Description	Ref.	BioChemFOAM
$AOCR$	$[g\text{-}O_2/g\text{-}C]$	2.67	The dissolved oxygen/carbon ratio		2.67 [**]
$AONT$	$[g\text{-}O_2/g\text{-}N]$	4.33	Mass of DO consumed per unit mass of ammonium nitrogen nitrified.		4.33 [*]
KH_{COD}	$[mg\text{-}O2/L]$	0.5	Half saturation constant of DO required for oxidation of COD.	[2]	0.5
$KCOD$	$[day^{-1}]$	1-42(domestic wastewater); 43-144 (Chesapeake bay)	Oxidation rate of COD.	[2]	1e-12[***]. assumed

Source: [2] Cerco, C. F., & Cole, T. M. (1994). Three-Dimensional Eutrophication Model of Chesapeake Bay. Volume 1: Main Report: DTIC Document.

Note: .

(*) The value is lower than the value 4.57g-O2/g-C obtained from stoichiometric relations presented in Table 3-1. (WEZERNAK & GANNON, 1968) reported that with nitrifying bacteria, <2mol oxygen are actually consumed per mol of ammonium nitrified.

(**) From stoichiometric relations, for every gram of algae carbon consumed by respiration 32g/12g of oxygen are also consumed, see Table 3-1.

(***) This is assumed to be small since unreliable values for COD concentrations were found in the literature to contrast results determined with BioChemFOAM for backwater areas. The only purpose served by preserving the variable COD is to check the numerical calculations in Chapters 4, and 6

Table 3-13. POP and PON model coefficients. See Equations 3.50 and 3.62.

Coefficient	Units	Values from references	Description	Ref.	BioChemFOAM
FPL_x	[1]	0.5	Fraction of metabolized phosphorus by algae group produced as POP.	[2]	0.5
$FPLP$	[1]	0.2-0.35	Fraction of predated phosphorus produced as POP.	[2]	0.35
FNL_x	[1]	0.5	Fraction of metabolized nitrogen by algae group x.	[2]	0.5
$FNLP$	[1]	0.55	Fraction of predated nitrogen produced as PON.	[2]	0.55

Source: [2] Cerco, C. F., & Cole, T. M. (1994). Three-Dimensional Eutrophication Model of Chesapeake Bay. Volume 1: Main Report: DTIC Document

3.6 Boundary Conditions (BC) and Initial Conditions (IC)

The boundary conditions present in a typical ecological model can be divided into three categories: Liquid-Liquid(L-L), Liquid-Gas(L-G) and Liquid-Soil(L-S). The L-L represent the boundary conditions defined at the inflow(s) and outflow(s) of the domain. The L-G interface represent the interaction between water and air at the water surface. Finally, the L-S represents the interaction between the water column, the sediment bed, and the banks.

In order to capture realistic physical processes it is important to define the appropriate Boundary Conditions (BC) and Initial Conditions (IC) for all the state variables included in the Hydrodynamic Module (HM), Sediment Transport Module (not included in the present research) and Species Transport Module (ST). One rectangular generic domain that is taken as an example to indicate the appropriate boundary conditions, as shown in Figure 3-5.

The definitions of BC and IC depends on the scenario under consideration and will be discussed later in Chapter 4, 5 and 6. The reason to define two sets of BC for Chapters 4 and 6 is explained next.

In Chapter 4, all boundaries for the species are zero gradient at walls and fixed value at the inputs. This is done in order to compare the solution from a 0-D model with solutions from 2-D and 3-D models. In Chapter 6, a more realistic BC are introduced to account for mass exchange at L-G (oxygen) and L-S (nitrate). interfaces The boundaries are defined for dissolved oxygen and nitrate. Details are provided in Chapter 6.

In general, the splitting operator method is used to solve the system of PDEs. This method splits the PDEs in two steps: one that solves $\mathcal{T} + \mathcal{A} - \mathcal{D} = 0$ (transport step, see Equation 3.19 for the generic transport equation. Hereforth, when the system of transport equations is mentioned, this nomenclature is used to simplify the derivatives included in the general transport equation) and the second that solves $\mathcal{T} = \mathcal{R}$ (reaction step). Since the problem has been divided into two steps, we need to define appropriate BCs for the physical problem. In this thesis, the boundary conditions for dissolved oxygen (DO) and nitrate (NO3) are embedded in the system of ODE that calculates the reaction step in order to speed up the numerical calculations in

BioChemFOAM. A working case is introduced in Chapter 6. To our knowledge, it hasn't been used before. Subsequently, the Boundary conditions for the transport step are set for all species to be zero gradient in order to be consistent when moving the boundaries to the set of ODEs. The proposed approach allows us the freedom of define complex numerical interaction at boundaries such as water-sediment or air-sediment interface in BioChemFOAM when the boundaries does not change (e.g water surface do not change considerably in time).
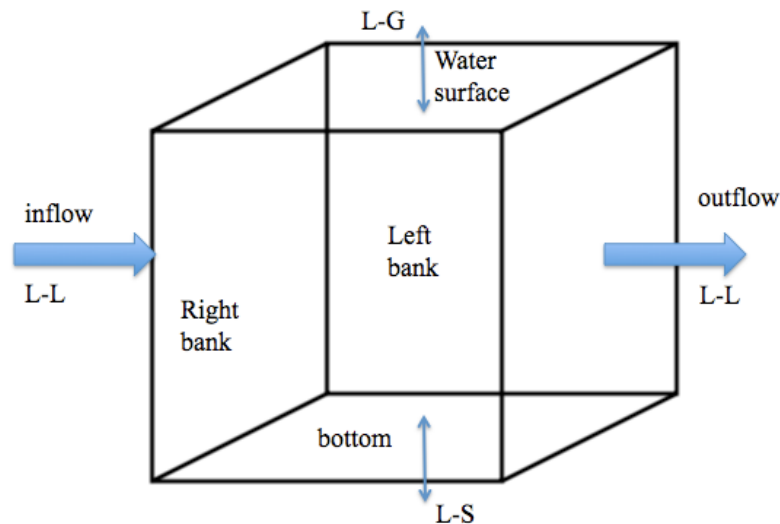
Figure 3-5. The generic domain showing the main BC(Boundary Conditions) and IC(Initial Conditions). The blue arrows in the figure shows the main flow path and location of boundaries in an ideal domain.

3.7 Numerical Methods - BioChemFOAM modules
implementation in OpenFOAM and solution strategy

The fundamental laws implemented in this research involve a set of partial differential equations with reactions and diffusion terms. Those equations can be found in different engineering applications. One of the most complex examples of such flows is the turbulent reacting flows. Another example is the species transport of environmental flows. This kind of problem generally does not influence the flow field when the chemical and biological processes take places inside of the body of water (note: if algae grows and generates conglomerates of algae it may change flow patterns; also macrophytes growth may affect the flow patterns and a new set of equations may be needed to represent such phenomena). The last statement makes all of the species transport equations decouple from the hydrodynamic and energy equations. The set of PDE to be solved (presented in the previous section) is a coupled system of non-linear equations. The challenge here is to apply an appropriate numerical scheme that accurately solves these equations in a reasonable period of time.

There are three methods to solve the system of partial equations for the passive scalars (or non-passive) scalars (Cant & Mastorakos, 2008):

(1) The direct approach in which the source term is included explicitly in the CFD solver. In this case, the equations can be solved by linearization of the source term. In most cases with stiff chemistry, simply using CFD code with a source term added will not work well. This approach was tested in OpenFOAM but it did not work when implemented. The OpenFOAM version used was 2.1.1.

(2) The operator splitting (or fractional step) approach, where CFD techniques are used for the solution of the passive scalar Equation 3.19 without the source term and ordinary differential equation (ODE) solvers for the solution of the source terms for every CFD grid cell or node. This is the norm for multi-dimensional calculations in atmospheric modeling (Chock & Carmichael, 2002), and in many DNS(Direct Numerical Simulations) codes for combustion (Singer, Pope, & Najm, 2006). In our case with environmental flows the influence of the

chemical and biological reactions do not have any influence in the momentum equations so the solution is decouple. This method is therefore implemented in this thesis.

(3) The method of lines, which transforms the governing partial differential equation into a (large) set of ODEs, which is then solved with one solver (explicit or implicit).

The method used to solve the system of passive scalar equation is the operator splitting method since it provides flexibility in temporal scales and utilizes ODE solvers that are generally faster. Figure 3-6 shows the strategy to solve the system of partial differential equations.

The left part of Figure 3-6 shows the general flow chart to solve the system of equations. The process starts by solving the hydrodynamic module, then it solves temperature, and then it solves light and species as a coupled process. This is done since algae may affect the distribution of light if it is abundant in the domain. The right part of Figure 3-6 shows a chart with the splitting operator for the system of passive scalar equations. First it solves light, then it solves T+A-D=0, and finally T=R. The last step is repeated until a desired convergence criterion is reached. Currently, BioChemFOAM utilizes the maximum error differences between iterations for each species in order to give a global residual at the end of each iteration, m (see left part of Figure 3-6). The maximum, m, iterations is set to 25 but, in this thesis the maximum number reached was 10 iterations to reach a converged solution, the residual is at least 1e-5 between successive iterations. This is done to speed computational calculations.

The code implemented in BioChemFOAM was executed in the high performance computing cluster, NEON, available at The University of Iowa, in order to get flow field distribution of the state variables (velocity, pressure, temperature, turbulent fields, light field and species scalar concentrations). The model's applications presented in this thesis in Chapter 4 runs relatively fast but applications presented in Chapter 6 need a considerable number of calculations to reach a converged solution for each time step.160 cores were used for those applications.

Furthermore, the time step defined in all of the applications was 0.5 second for the outer iterations (see left flow chart of Figure 3-6) and an inner iteration was set to 0.05second (see right flow chart of Figure 3-6). These values were defined since they produce stable and accurate

solutions in the cases presented in this thesis. No attempt was made to further investigate the stability of the solution when different time steps are used since those values were optimal for the kind of applications presented in this research.

The numerical integration of time in the T+A-D=0 step was performed with an Euler scheme, and the numerical integration for T=R was performed with a 4th order Runge-Kutta method. Both methods are coupled within a master code called BioChemFOAM. The solution of the ODEs is implemented through a template library generated in C++ and OpenFOAM tools. This template library inherits the ODE functions available in OpenFOAM. Onces the library is ready, an additional library was generated to combine the T+A-D=0 and T=R step. Finally, everything is combined in a master C++ file that performs the calculations, as shown in the left part of Figure 3-6. An example of the implementation is presented in Figure 3-7.

The hydrodynamic module utilizes the pisoFOAM solver available in OpenFOAM. This solves the RANS unsteady equations with a generic turbulence flow (in this research k-epsilon model is utilized) using a pressure implicit method with splitting of operators. The method utilizes a co-located methodology to solve the flow fields by using a Finite Volume Method.

Finally, the different operators appearing in the system of equations to be solved (see previous section) are discretized as shown in Table 3-14. The discretization process can be reviewed in (Rusche, 2003) and (Jasak, 1996); and no further details are provided in this research.

Table 3-14. Numerical schemes for the vector operators acting on the different flow fields. (e.g. see equation 3.19, scalar transport).

Name operator	Symbol/description	Numerical Method
Time first derivative	$\dfrac{\partial}{\partial t}$	Euler for (T+A-D=0) RK4 for (T=R)
Gradient	∇	Gauss linear
Divergence	$\nabla\bullet$	Gauss linear
Laplacian	∇^2	Gauss linear corrected
Interpolation	Point to point	linear
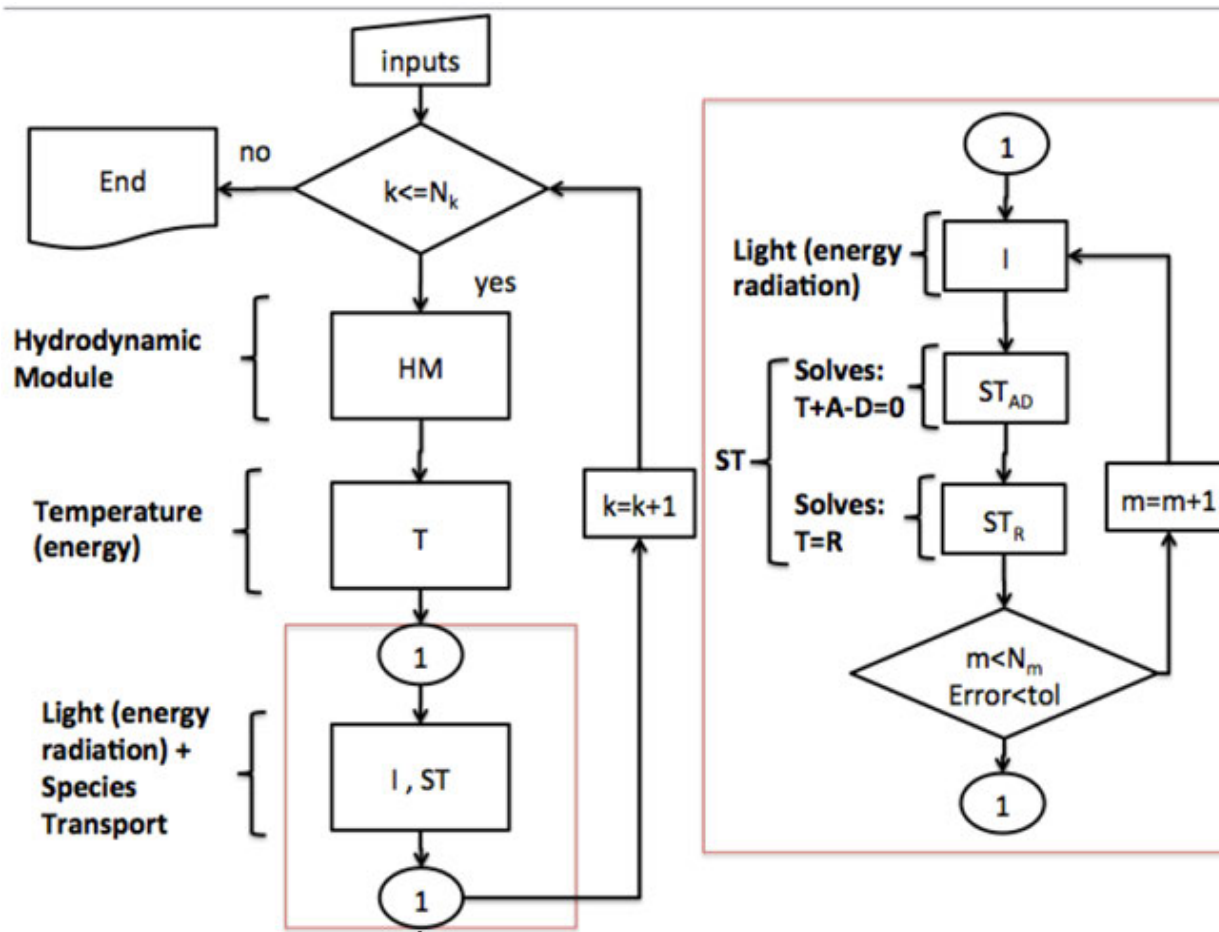
Figure 3-6. Splitting operator method implemented in BioChemFOAM. The left side of the figure shows the general loop when solving the hydrodynamic (HM) and species transport (ST) modules. The right side of the figure (enclosed in a red rectangle) shows the detail when solving the species transport module (ST). "Inputs" represent all coefficients, IC, BC, and mesh. The "k" integer is for the time loop. " N_k " is the total number of time steps. "HM" is the hydrodynamic module. "T" is the temperature module that contains the energy equation, and no coupling with the flow field at this stage is included. "I" is the light module (radiation). "ST=ST_{AD}+ST_R" is the module that solves the system of partial differential equations for the 11 species. " ST_{AD} " is the sub-module to solve system of unsteady advection-diffusion species partial differential equations, in total 11. " ST_R " is the sub-module to solve the system of unsteady reaction species ordinary differential equations. The "m" integer is for the internal iteration in the operator splitting method. " N_m " is the total number of iterations. "Error" calculated is the error between two successive internal iterations. "tol" is the minimum error between the internal iteration for the species and for a time step.

```
while (runTime.loop())
{
    Info<< "Time = " << runTime.timeName() << nl << endl;

#   include "readPISOControls.H"
#   include "CourantNo.H"

    fvVectorMatrix UEqn
    (
        fvm::ddt(U)
      + fvm::div(phi, U)
      - fvm::laplacian(nu, U)
    );

    solve(UEqn == -fvc::grad(p));

    // --- PISO loop

    for (int corr=0; corr<nCorr; corr++)
    {
//  #include "TEC1.H"
#       include "CiEqn.H"

#       include "Ci2Eqn.H"
#       include "Ci3Eqn.H"
#       include "Ci4Eqn.H"
#       include "Ci5Eqn.H"
        volScalarField rUA = 1.0/UEqn.A();

        U = rUA*UEqn.H();
        phi = (fvc::interpolate(U) & mesh.Sf())
            + fvc::ddtPhiCorr(rUA, U, phi);

        adjustPhi(phi, U, p);

        for (int nonOrth=0; nonOrth<=nNonOrthCorr; nonOrth++)
        {
            fvScalarMatrix pEqn
            (
                fvm::laplacian(rUA, p) == fvc::div(phi)
            );

            pEqn.setReference(pRefCell, pRefValue);
            pEqn.solve();

            if (nonOrth == nNonOrthCorr)
            {
                phi -= pEqn.flux();
            }
        }

#       include "continuityErrs.H"

        U -= rUA*fvc::grad(p);
        U.correctBoundaryConditions();
    }

    runTime.write();

    Info<< "ExecutionTime = " << runTime.elapsedCpuTime() << " s"
        << "  ClockTime = " << runTime.elapsedClockTime() << " s"
        << nl << endl;
}
```

Figure 3-7. An example of a C++ file inside BioChemFOAM.

3.8 Highlights and Simplifications of the proposed model

BioChemFOAM is a highly resolved nutrient dynamic model that encapsulate main processes affecting nutrient dynamics in an aquatic ecosystem. This model presents different features and simplification:

The highlights of the proposed model are:

- Unsteady hydrodynamic and species transport of fresh water environments.

- The new parameterization can be easily implemented through the platform available in OpenFOAM.

- It can run in parallel computer clusters.

- Each module of BioChemFOAM (hydrodynamic(HM)+species trasport(ST)) can be executed independently or in conjunction. This can be seen in the applications presented later in this research, Chapter 4, 5, and 6. If coupling is necessary, modification of the numerics must be done to account for the coupling effect of the equations (e.g. adding sediment transport that change the flow field). Although, the model does not have this

ability at the moment the implementation and algorithms are of great value since they stablish a fundamental base from which to model aquatic ecosystems in a holistic way. It is also important to mention that the libraries in OpenFOAM are extensive and can be added to the present framework at any moment to improve the model's parameterization.

- The Hydrodynamics Module (HM) considers an unsteady incompressible turbulent flow.
- Species Transport module (ST) considers unsteady fate and turbulent transport of species. Its solution is performed with a novel library to solve the system of species transport equations.
- The actual parameterization for Algae only allows to model blue and green algae. Since we defined equations for one algae group the parameterization as it is can only include one algae species.
- The fluxes of species through the water-air interface are only considered for oxygen as modeled by (Cerco & Cole, 1994).
- The fluxes of species are only considered for nitrate at the water-sediment interface. This is done since we are modeling a summer flow tough a backwater area that have zero cocnentration of nitrate et the sediment which enhance the mass flow from the sediment to the water.

The simplifications presented here can be extended in future research. In this research, we introduce basic components that can be improved by implementing a new parameterization of PCBP.

The improvemes that can be made on BioChemFOAM are grouped in Hydrodynamic and Species Transport.

For Hydrodynamic component:

- Motion of the water surface is included.
- No sediment transport is included.

and for Species Transport component:

- No radiation affecting temperature is considered in the transport equation for temperature, which menas that light may warm the water and change the temperature distribution.

- No buoyancy is considered in the momentum equation due to density gradients.

- The Schmidt number (kinematic viscosity/mass diffusion) is equal to one in the diffusion term for species transport, see Equation 3.19. Also, the Prandtl number (kinematic viscosity/thermal diffusivity) is taken as one in the transport equation for temperature.

- Usually, $PO4t$ represents the total phosphates and is dependent on sediment transport. Since we do not include sediment transport, we include the dissolved reactive portion in the variable $PO4$.

- Silica is not modeled. This means that Diatoms (Cyanobacteria) are not calculated.

- No sources (e.g. runoff or groudwater flow) are included in the present model's applications.

CHAPTER 4

VALIDATION OF BIOCHEMFOAM – NUMERICAL EXPERIMENTS

4.1 Introduction

This section presents seven numerical experiments used to test the methods and parameterization of BioChemFOAM and systematically validate the code. The goal is to increase the complexity[1] in the proposed model and framework.

Figure 4-1 presents the steps followed to verify and validate BioChemFOAM. The first step defines characteristic coefficients in natural aquatic ecosystems that influence PCBP (Physical, Chemical and Biological Processes presented in Chapter 3). The second step, verification, checks that the set of PDEs introduces the appropriate paremeterization for all PCBP and its presented in Sections 4.2 to 4.6. The third step validates the methods used to solve the set of PDEs, and is explained in Section 4.7. Finally, in Chapters 5 and 6, a real case application is presented that validates the model by applying it to a backwater area located in the Mississippi river. For all the cases presented in this section, the coefficients afecting the parameterization are left constant (see Chapter 3). Furthermore, the light and temperature equations are assumed constant in all the application .

Section 4.2 introduce a 0-D example comparing BioChemFOAM to the code BioChemMATLAB (see Appendix A for details). The case simulates a well-mixed unsteady model of a cavity with 11 species. The cavity case is a bench mark case utilized in computational fluid dynamics to validate CFD codes, (Ghia, Ghia, & Shin, 1982). In the cavity applications presented in this chapter, the geometry remains the same.

---

[1] Here "model complexity" is used to define a change BioChemFOAM due to simplifications such as moving from a fully 3D spatial model to a 2D special mode. An additional example is presented for cases that do or do not include physical processes such as advection or diffusion in the generic transport equation.

In Section 4.2, BioChemFOAM is applied to the cavity. The domain (cavity) has to be discretized in small containers (cells). These cells represent small well-mixed tanks and they reproduce the same results as BioChemMATLAB under the same Initial Conditions (IC). BioChemFOAM and BioChemMATLAB were compared to determine whether the libraries in OpenFOAM and BioChemFOAM are adecualy solving the system of equations defined in Chapter 3. The comparison shows that both models solves the system of equations adequately.

Section 4.3 introduces an unsteady case were species convects and reacts on the cavity. In this case, the flow field is considered zero. Section 4.4 models an unsteady laminar flow where species convect and react in a cavity. Section 4.5 introduces an unsteady laminar flow where species convect, react, and diffuse through the cavity. Section 4.6 introduces an unsteady flow in a channel. The species module considers convection and reactions. The hydrodynamic module considers advection only.

Section 4.7 tests the method (splitting operator) used to solve the system of PDEs by using an exact solution [Sun et~al., 1999]. It shows that BioChemFOAM was able to reproduce the analytical results presented by (Sun et al., 1999).

Throughout this section a special nomenclature is used to simplify the transport equation for an arbitrary chemical or biological component. This is done in order to define a complexity level active in BioChemFOAM. For example, using equation 3.19 for transport and fate of a generic species we can define variables that represent each process as follows:

$$\underbrace{\frac{\partial(\rho\phi_i)}{\partial t}}_{\text{temporal variation},\mathcal{T}} + \underbrace{\nabla\cdot(\rho\mathbf{u}\phi_i)}_{\text{convection},\mathcal{A}} = \underbrace{\nabla\cdot\mathbf{J}_i}_{\text{diffusion},\mathcal{D}} + \underbrace{R_i}_{\text{Reactions},\mathcal{R}} + \underbrace{S_i}_{\text{sources/sinks},\mathcal{S}} \qquad (4.1)$$

so we get a general equation representing all of the process that affects the fate and transport of species as follows:

$$\mathcal{T} + \mathcal{A} - \mathcal{D} = \mathcal{R} + \mathcal{S} \qquad (4.2)$$

The last form of the fate and transport equation is used along with the thesis to define active and inactive processes in a particular scenario. For instance, $\mathcal{T} = \mathcal{R}$ means that we only model temporal and reaction terms for the species defined in Chapter 3 (This is the case for the first example presented in Section 4.2, 0-D model).

```
┌─────────────────────┐
│ Define Characteristic│
│   Coefficients and  │
│   Concentrations    │
└─────────────────────┘
           ↓
┌─────────────────────┐
│ Verification of ODEs│
│ parameterization of │
│        PCBP         │
└─────────────────────┘
           ↓
┌─────────────────────┐
│  Validate methods to│
│    solve PDEs with  │
│ parameterization of │
│        PCBP         │
└─────────────────────┘
           ↓
┌─────────────────────┐
│  Apply model to real│
│   case, Backwater   │
│  area Mississippi   │
│       River         │
└─────────────────────┘
```
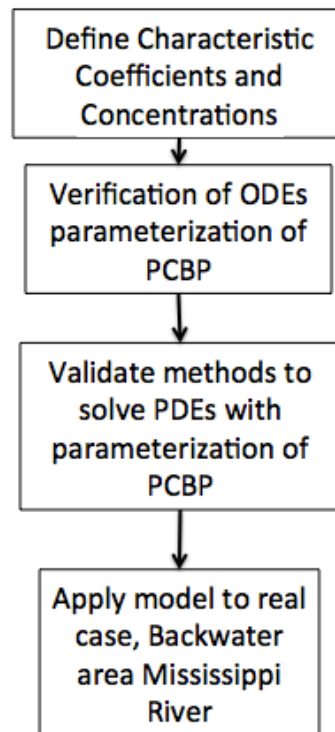
Figure 4-1 Flow chart describing the process of validation in BioChemFOAM. From top to bottom the degree of complexity increases, e.g., 2-D flow to 3-D flow. PCBP represents the Physical, Chemical, and Biological Processes. ODEs are Ordinary Differential Equations. PDEs are Partial Differential Equations.

<u>4.2 Well mixed unsteady model of a cavity, 11 species.</u>

<u>Species module only with reactions.</u>

This model was built to study the transient evolution of basic species in an aquatic ecosystem. It was formulated to help understand complex 3-D models like the one presented in Chapter 3. BioChemFOAM models $\mathcal{T} = \mathcal{R}$ (see previous section for an explanation of this nomenclature). The model solves eleven (11) primary components, defined as characteristics in a water quality model (Cerco & Cole, 1994). The temperature and light intensity was fixed to $20^{o}C$ and 300ly/day approximately $150W/m^{2}$. This is done to ensures optimal algae growth and decay. The values also represent characteristic values in an aquatic ecosystem. Furthermore, the cavity case can be seen as a reactor in which light and temperature are kept constant during a period of time (this is also the situation assumed for the next cases that involve the cavity and a channel).

4.2.1 General configuration- Parameterization, Numerical Mesh, Boundary Conditions (BC), Initial Conditions (IC)

The model utilizes the equations described in Chapter 3. Eleven equations are solved using coefficients presented in Section 3.5. Figure 4-2 presents the mesh and location of boundary conditions. Table 4-1 presents the boundary conditions (BC) and initial conditions (IC).
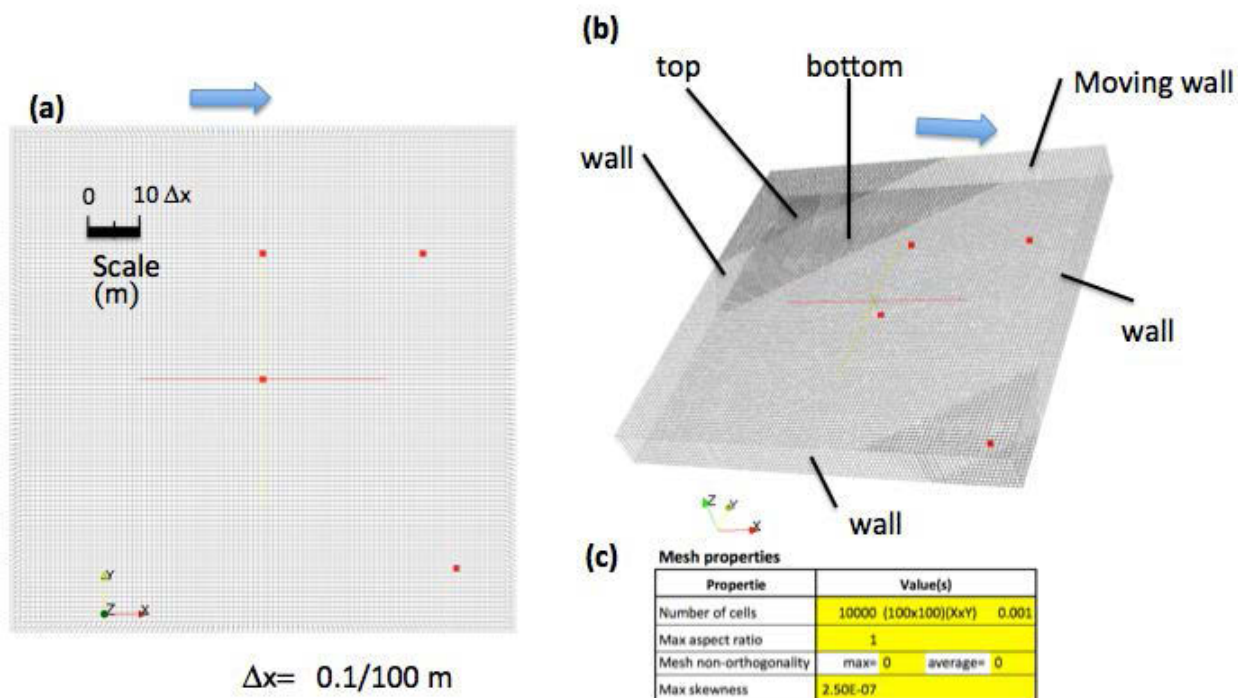
Figure 4-2. Characteristics of the mesh for the cavity case, well-mixed unsteady model of a cavity, 11 species. (a) Mesh detail and scale. (b) Mesh in 3-D with a surface at which boundary conditions are defined. (c) Mesh properties optioned with the function "checkMesh" in OpenFOAM. The blue arrow represents the direction of motion when a velocity (lid velocity) is imposed on the surface. It is called a "Moving wall", see (b).

Table 4-1. Boundary Conditions (BC) and Initial Conditions (IC) case well-mixed unsteady model of a cavity with eleven species. fV= fixed value; zG= zero gradient; N.A= not applicable; and empty= means that it is not included in the model.

		BC name		
	IC value ↓	Moving wall	wall	Top&bottom
U(m/s)	(0,0,0)	fV=0	fV=0	empty
$P/\rho(m^2/s^2)$	0	fV=0	fV=0	empty
Bx (mg-C/L)	0.01	zG	zG	empty
DOC (mg-C/L)	1	zG	zG	empty
PO4 (mg-P/L)	0.06	zG	zG	empty
DON (mg-N/L)	0.4	zG	zG	empty
NH4 (mg-N/L)	0.055	zG	zG	empty
NO3 (mg-N/L)	0.4	zG	zG	empty
DO (mg-O_2/L)	6.8	zG	zG	empty
COD (mg-O_2/L)	9	zG	zG	empty
POC (mg-C/L)	1	zG	zG	empty
POP (mg-P/L)	0.071	zG	zG	empty
PON (mg-N/L)	0.4	zG	zG	empty
I (ly/day)	300	NA	NA	NA
T (^{o}C)	20	NA	NA	NA

4.2.2 Results and Comments

BioChemFOAM was executed successfully for 80 days and compared with a code called BioChemFOAM developed in MATLAB (see details in Appendix A). Figure 4-3 through 4-9 show a comparison of concentration evolution for one cell at the center of the numerical domain compared with the MATLAB solution. BioChemFOAM was able to reproduce the same concentration patterns shown by the MATLAB code. The same patterns are presented in the remaining cells of the domain, since each cell works as a well mixed tank (results not shown for other cells). BioChemFOAM, was able to reproduce an unsteady evolution of species in a well-mixed numerical experiment.

Additionally, the influence of each process was analyzed by showing the weight over time, as presented in Figures 4-10 to 4-15 . Figure 4-10 shows the important processes affecting algae (green algae). The most important process is growth (a gain). Furthermore, metabolism respiration + excretion and predation (both are losses) have a mild influence on the fate of algae. Figures 4-11 to 4-15 show a similar plot as Figure 4-10, but for all species that influence the fate of nutrients in an aquatic ecosystem. It shows that after 7 days of simulation algae (Bx), PO4, DON, NH4, NO3, DO, POC, POP and PON reach and a steady state. The steady state can be reached since we define constant light and temperature in the cavity. DOC is still active after 60 days since its reaction rates are slow as shown in Figure 4-11. Figure 4-11, 4-12, 4-13

Figure 4-3 (top) showst that algae growth the first 7 days since nutrients are available in abundance, see Figures 4-4 (top) and 4-5 . Figures 4-10 to 4-15 are useful in identify potential process that have a lower influence in the model, given characteristic coefficients and initial concentrations. The processes that haves a lower impact on species concentration, e.g., predation of agae, were considered in all applications in this thesis to not only test the numerical model but also to show the model's ability to model additional processes. The error on all species shown in Figures 4-10 to 4-15 is about 0.5% (comparison between MATLAB code and BioChemFOAM). Figure 4-6 shows a

fast DO reaction since the reareation coeffient (K_r) was about $0.4s^{-1}$ and the saturated dissolved oxygen was about 9mg-O2/L. This is implemented to test the model when dissolved oxygen changes fast over time.

The coefficients and parameterization were defined in such a way that there are enough nutrients and light for a small concentration of algae to grow. This is done to test the ability of the model to reproduce different parameterizations in an aquatic ecosystem and to test the numerical method when sharp gradient occurs. This particular case considers green algae since the predation term is present in the set of equations. (Yoshida, Jones, Ellner, Fussmann, & Hairston, 2003), studied green algae that is consumed by rotifers and Brachionus Calyciflorus in small micro-cosmos. The results shows that it is possible for green algae to be predated by those biological components. In the present model, BioChemFOAM includes a predation term in order to be complete when these organism are present.
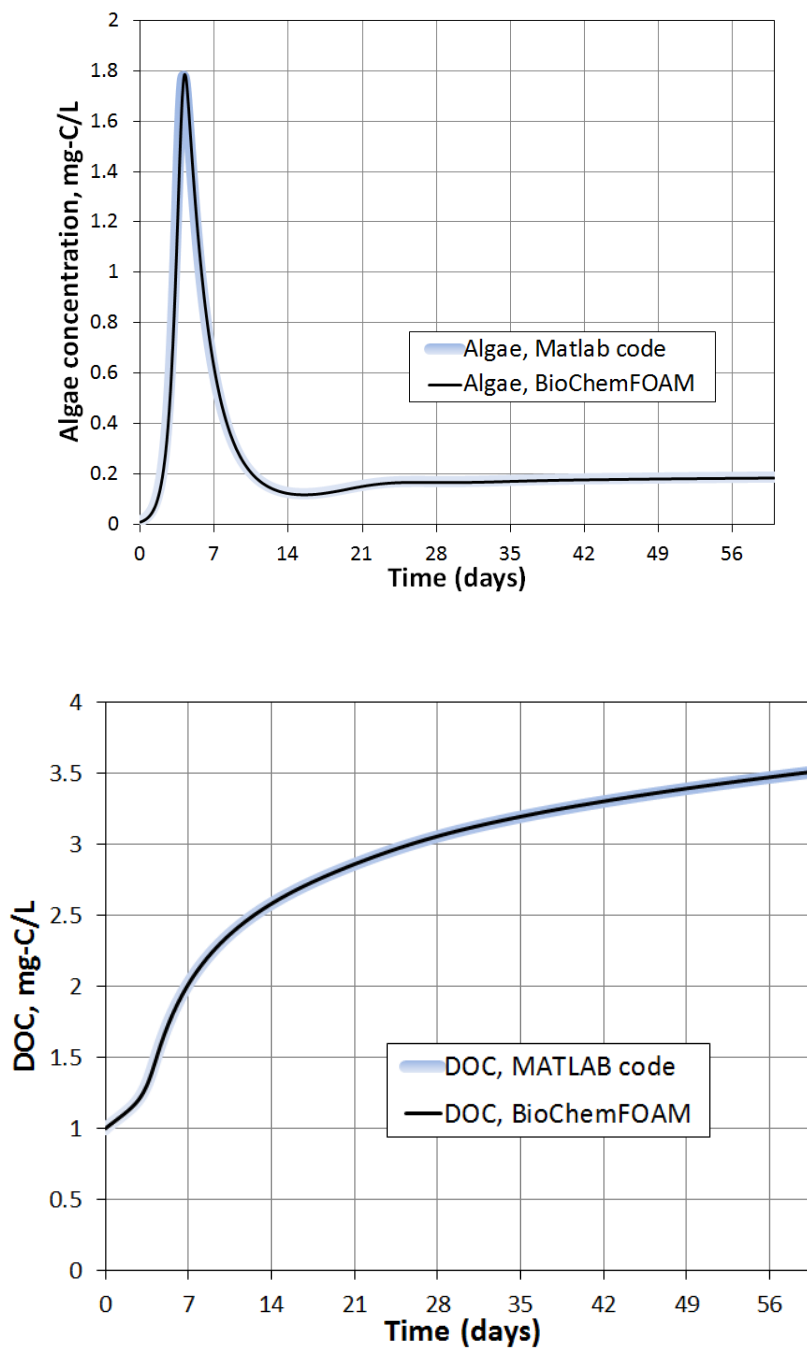
Figure 4-3 Time evolution of species for one cell at the center of the cavity (see Figure 4-2) with BioChemFOAM and MATLAB code. "Batch" system. (top) It's the algae concentration over time. (bottom) It's the Dissolved Organic Carbon concentration over time. Light and temperature are constant during the simulation so algae can growth all the time provided there are enough nutrients.
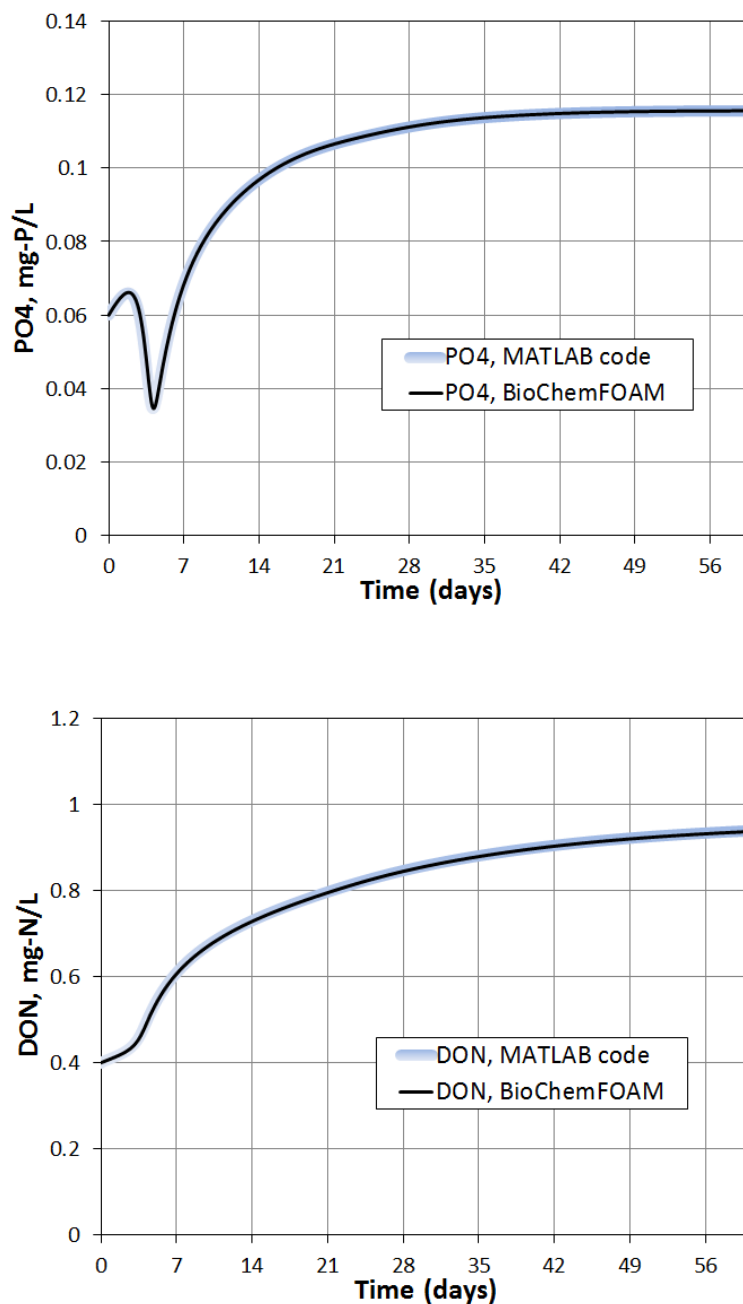
Figure 4-4. Time evolution of species for one cell at the center of the cavity (see Figure 4-2) with BioChemFOAM and MATLAB code. "Batch" system. (top) It's the dissolved orthophosphate concentration over time. (bottom) It's the Dissolved Organic Nitrogen concentration over time. Light and temperature are constant during the simulation so algae can growth all the time provided there are enough nutrients.
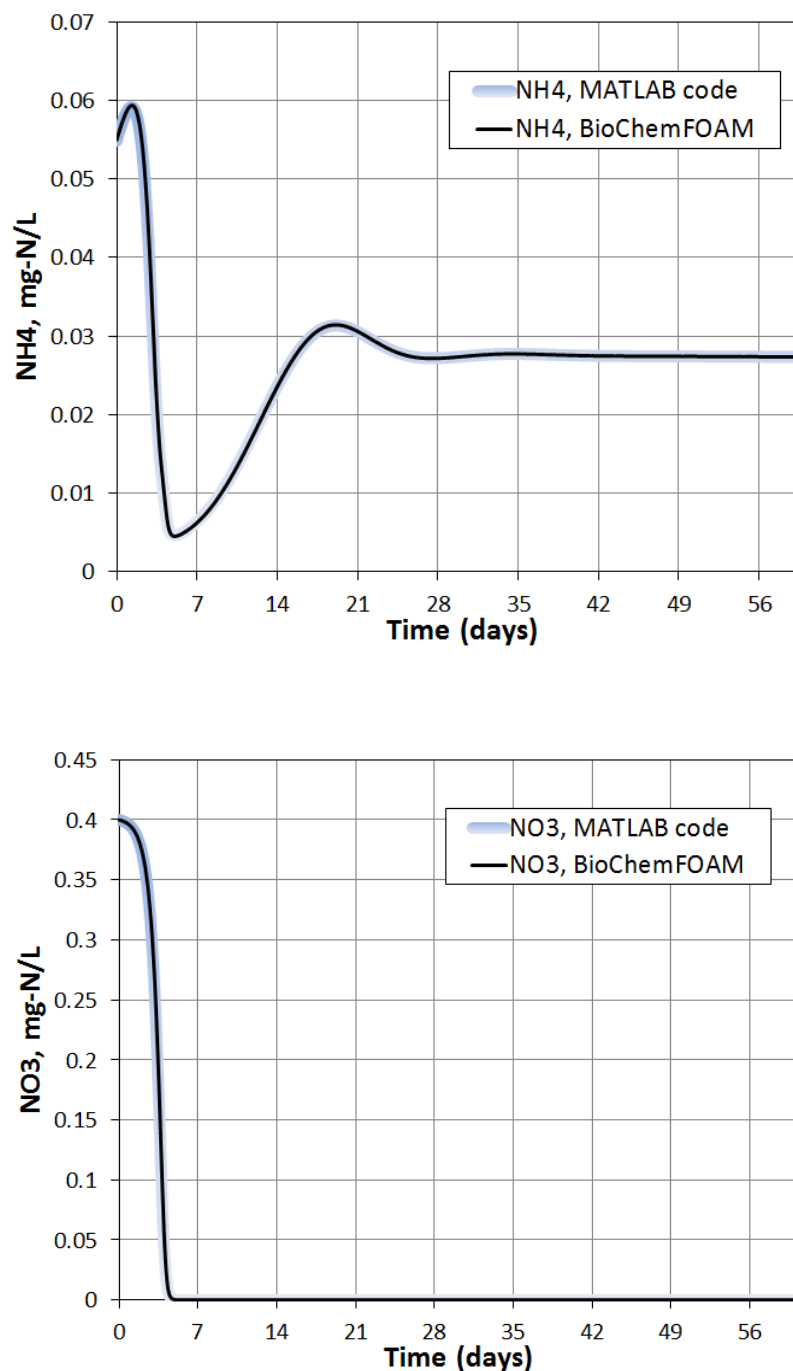
Figure 4-5. Time evolution of species for one cell at the center of the cavity (see Figure 4-2) with BioChemFOAM and MATLAB code. "Batch" system. (top) It's the ammonia ($NH_4^+ + NH_3$) concentration over time. (bottom) It's the ammonia concentration ($NO_3^- + NO_2^-$) over time. Light and temperature are constant during the simulation so algae can growth all the time provided there are enough nutrients.
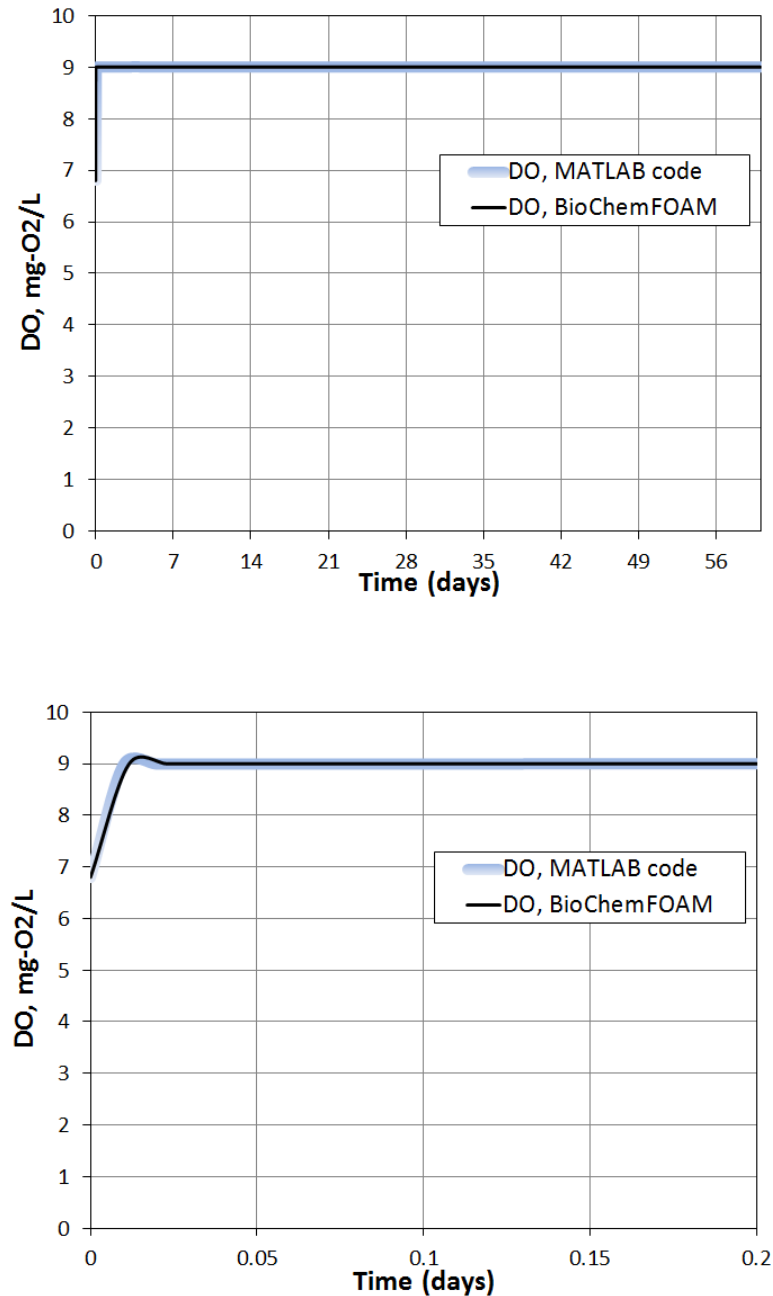
Figure 4-6. Time evolution of species for one cell at the center of the cavity (see Figure 4-2) with BioChemFOAM and MATLAB code. "Batch" system. (top) It's the Dissolved Oxygen concentration over time for 56 days. (bottom) It's the Dissolved Oxygen concentration over time showing the first 0.2 days of the simulation. The DO changes fast at the beginning since the reaereation coefficient is assumed as 0.46s^{-1} and the saturated dissolved oxygen is 9 mg-O2/L. Light and temperature are constant during the simulation so algae can growth all the time provided there are enough nutrients.
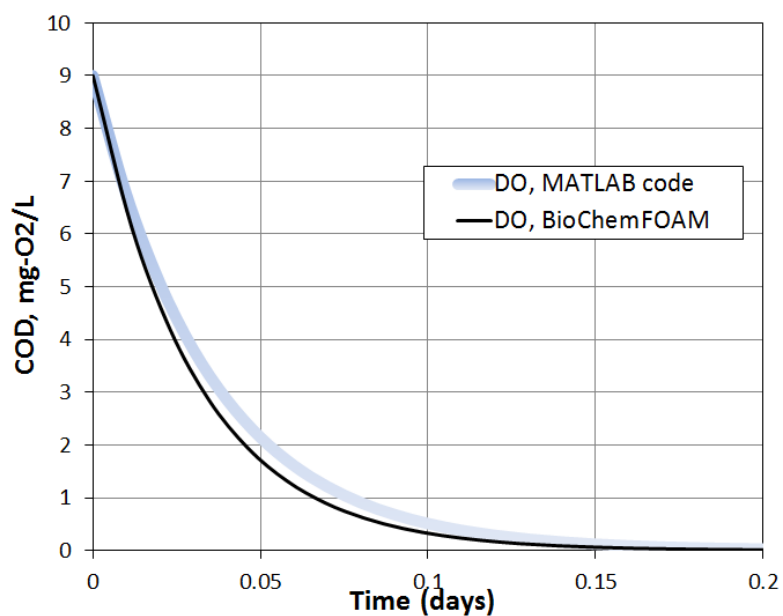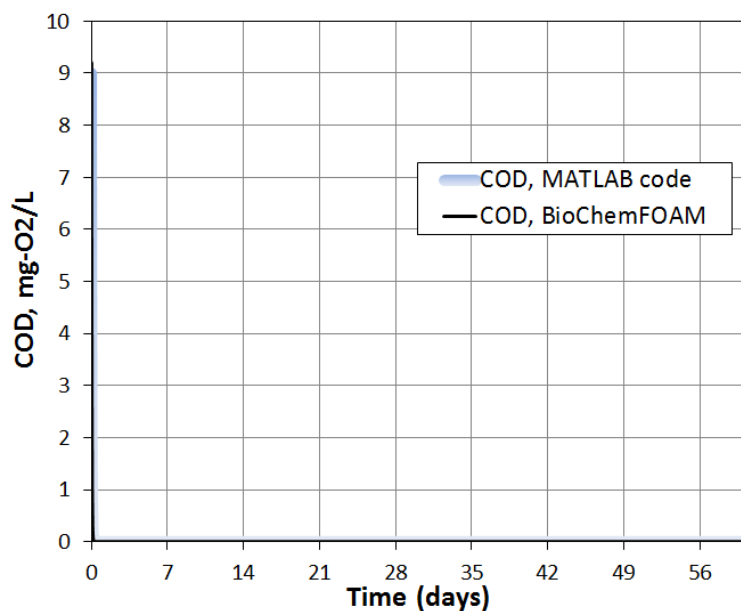
Figure 4-7. Time evolution of species for one cell at the center of the cavity (see Figure 4-2) with BioChemFOAM and MATLAB code. "Batch" system. (top) It's the Chemical Oxygen Demand concentration from reduced substances over time for 56 days. (bottom) It's the Chemical Oxygen Demand concentration over time showing the first 0.2 days of the simulation. The COD changes fast at the beginning since the oxidation rate is 35 day^{-1} (assumed). Light and temperature are constant during the simulation so algae can growth all the time provided there are enough nutrients.
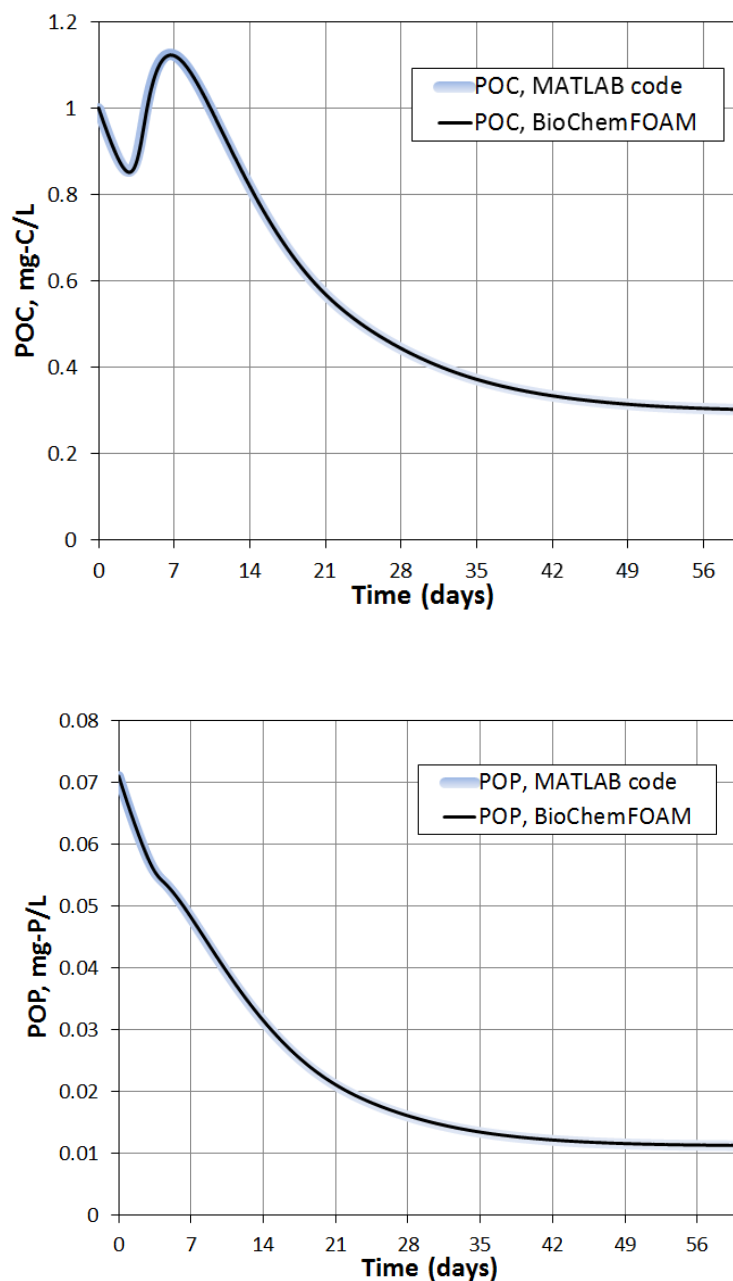
Figure 4-8. Time evolution of species for one cell at the center of the cavity (see Figure 4-2) with BioChemFOAM and MATLAB code. "Batch" system. (top) It's the Particulate Organic Carbon concentration over time showing 56 days of the simulation. (bottom) It's the Particulate Organic Phosphorus concentration over time showing the first 0.2 days of the simulation. Light and temperature are constant during the simulation so algae can growth all the time provided there are enough nutrients.
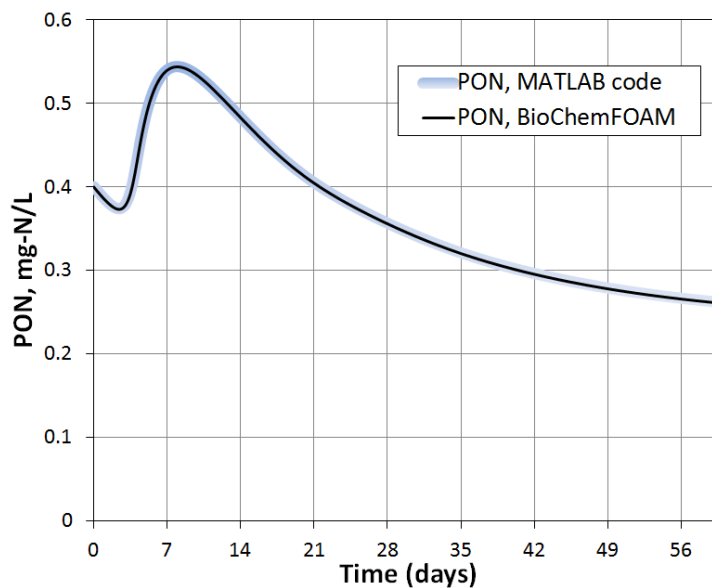
Figure 4-9. Particulate Organic Nitrogen for one cell at the center of the cavity (see Figure 4-2) comparison between BioChemFOAM and MATLAB code. "Batch" system. Light and temperature are constant during the simulation so algae can growth all the time provided there are enough nutrients
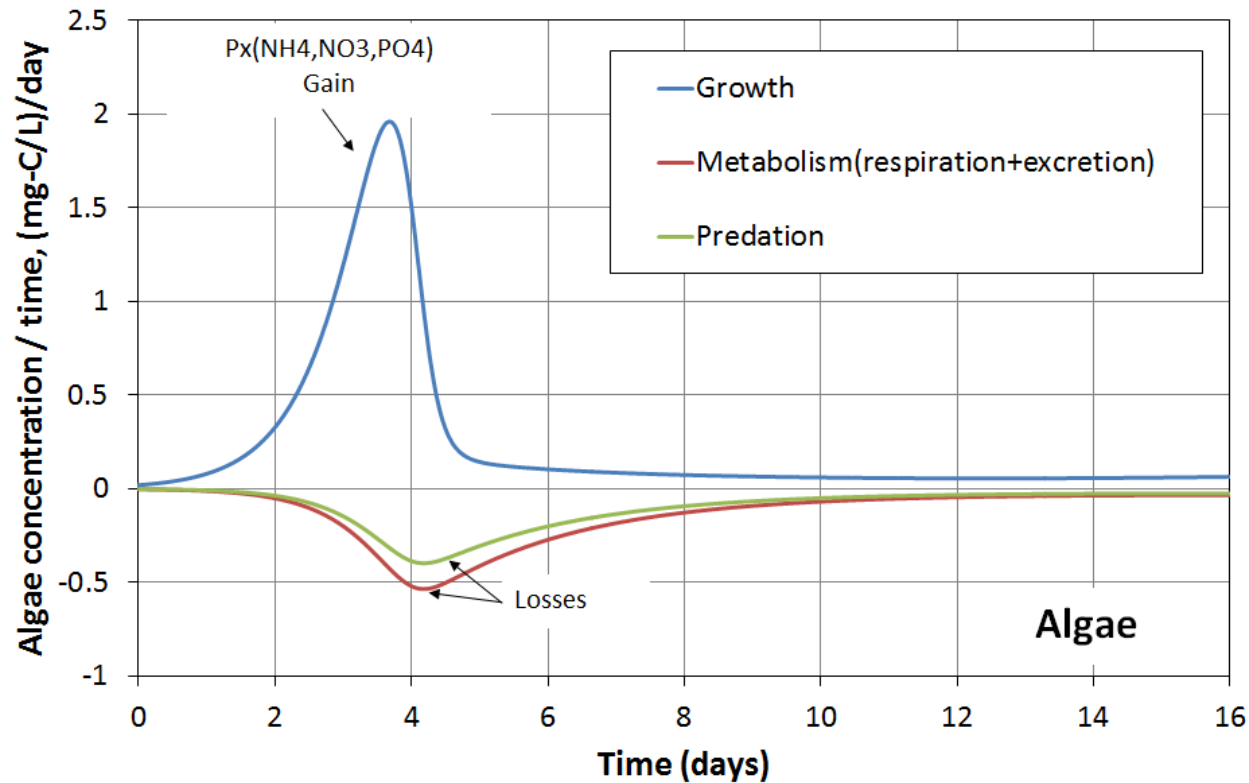
Figure 4-10. Time evolution of processes (horizontal axes) for Algae (green algae) for characteristic concentration and coefficients. Px(NH4,NO3,PO4).Bx is the growth term presented in Equation 3.27. Bx is algae concentration. PO4 is dissolved orthophosphates. NH4 is ammonia. NO3 is nitrate. "Batch" reactor. Light (300 ly/day) and temperature (20°C) are constant.
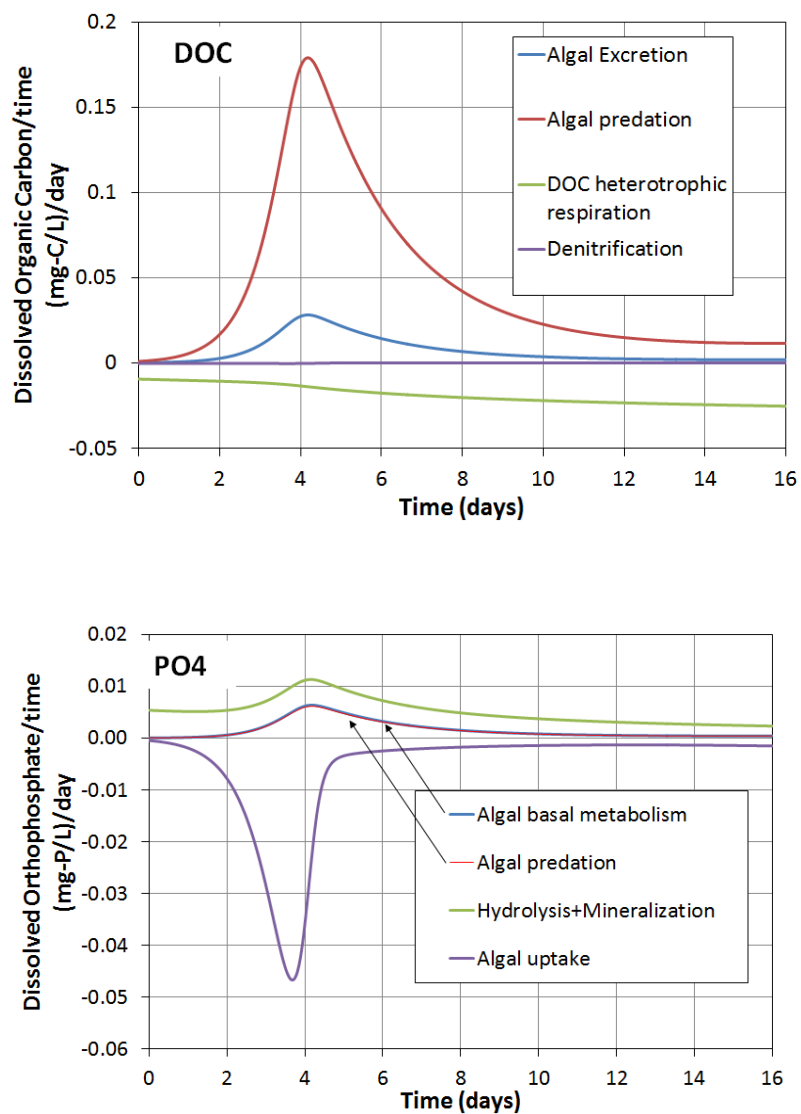
Figure 4-11. Time evolution of processes for Dissolved Organnic Carbon (DOC) and dissolved orthophosphate (PO4). BioChemFOAM results. "Batch" reactor. Light (300 ly/day) and temperature (20°C) are constant.
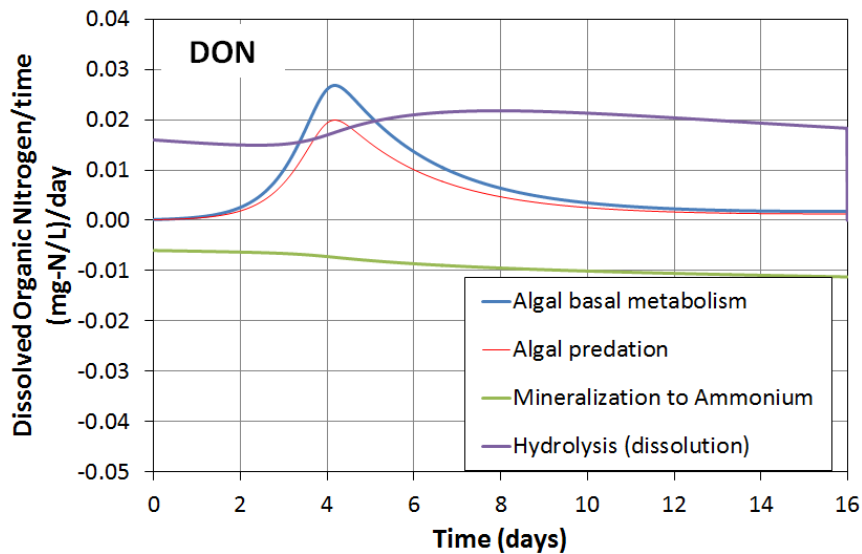
Figure 4-12. Time evolution of processes for Dissolved Organnic Nitrogen (DON). BioChemFOAM results. "Batch" reactor. Light (300 ly/day) and temperature (20°C) are constant.
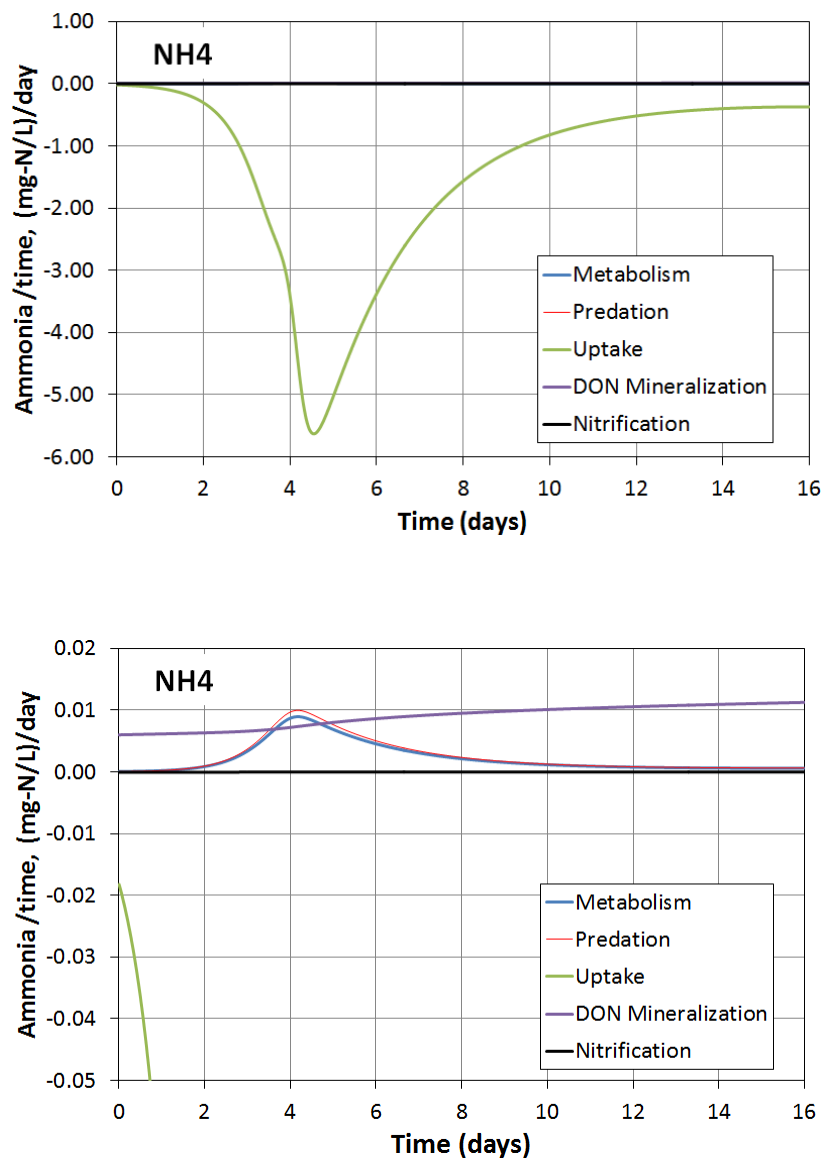
Figure 4-13. Time evolution of processes for Ammonia (NH4= NH_4^++NH_3). (top) All processes. (bottom) Closer look at other processes with minor influence on ammonia. "Batch" reactor. Light (300 ly/day) and temperature (20^oC) are constant.
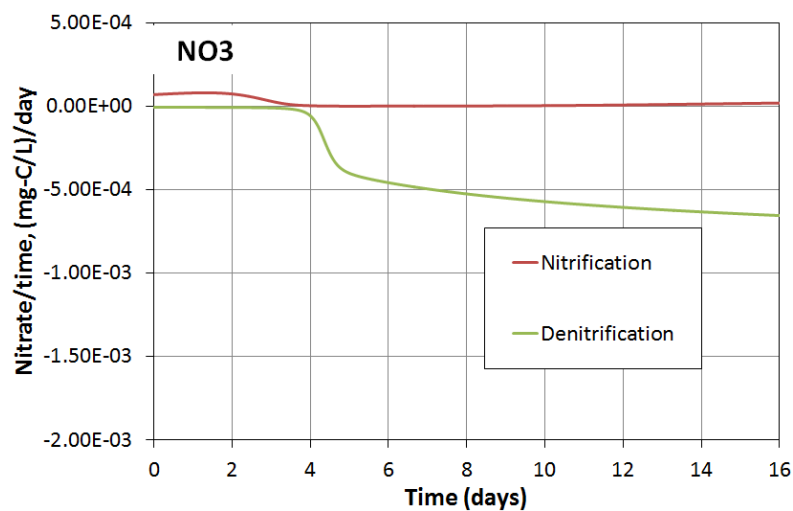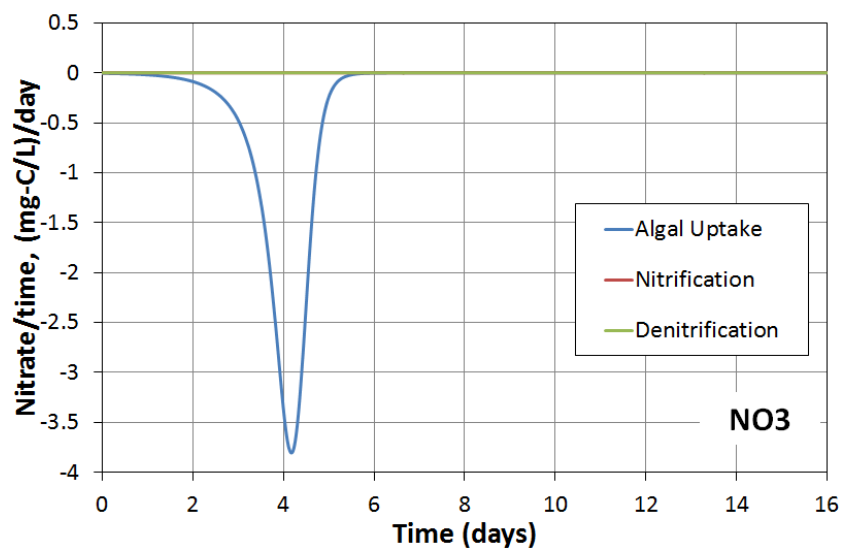
Figure 4-14. Time evolution of processes for Nitrate (NO3= NO_3^-+NO_2^-). (top) All processes. (bottom) Closer look at other processes with minor influence on ammonia. "Batch" reactor. Light (300 ly/day) and temperature (20^oC) are constant.
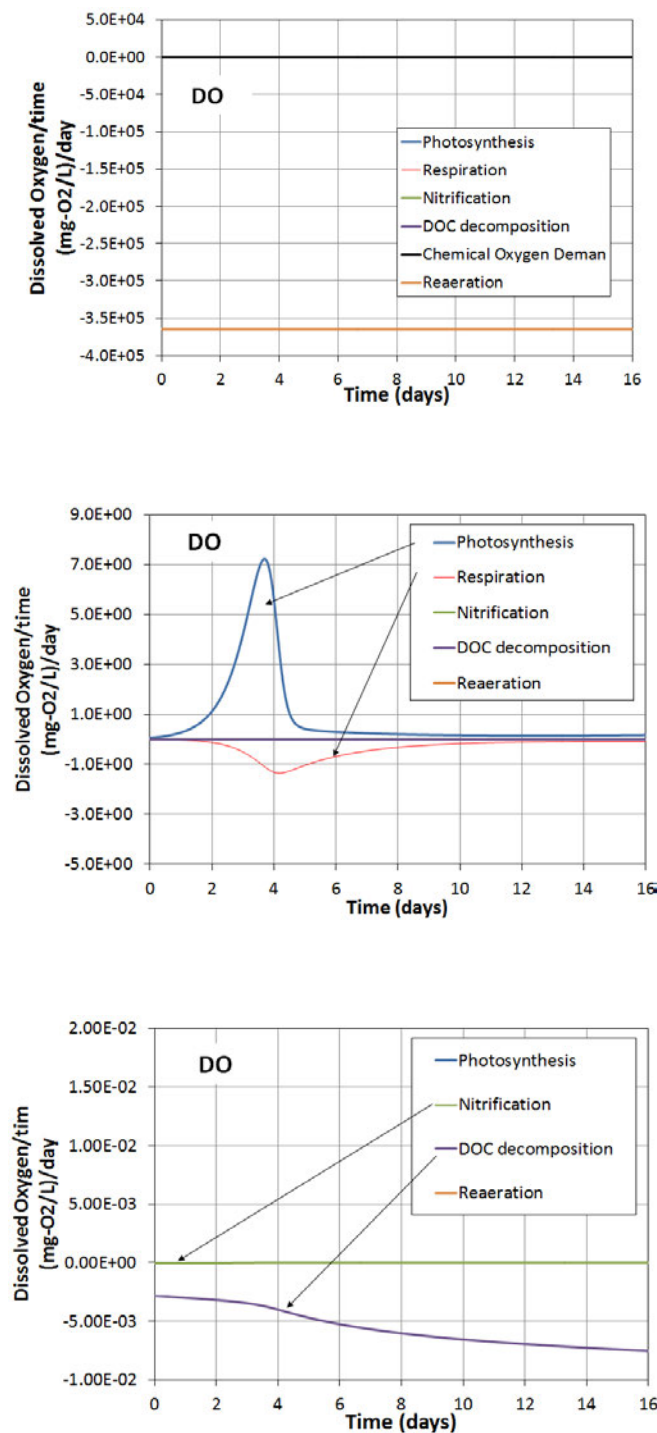
Figure 4-15. Time evolution of processes for Dissolved Oxygen at the center of the cavity. (top) All processes. (middle) Closer look at other processes, photosysnthesis and respiration. (bottom) Closer look other processes, Nitrification and chemical oxygen demand for reduced subtances. "Batch" reactor. Light (300 ly/day) and temperature (20°C) are constant.
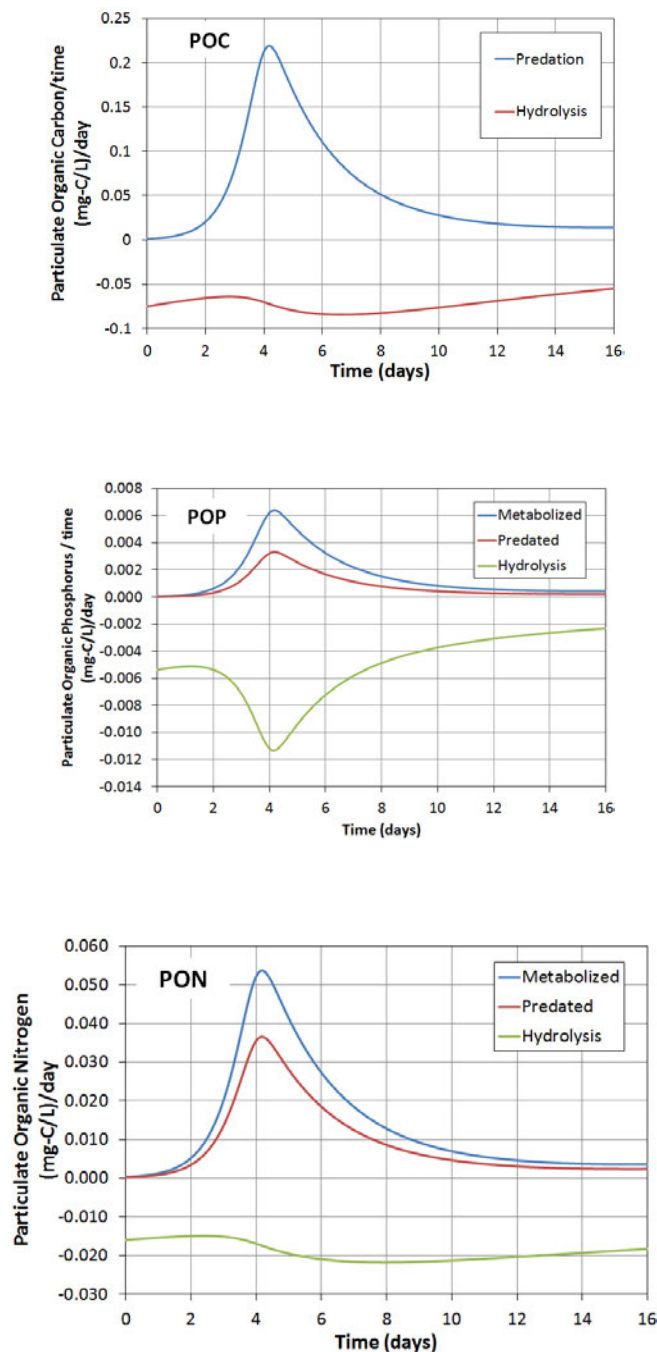
Figure 4-16. Time evolution of processes for Particulate Organic Carbon (POC), Particulate Organic Phosphorus (POP), and Particulate Organic Nitrogen (PON). (top) POC processes. (middle) POP processes. (bottom) PON processes. "Batch" reactor. Light (300 ly/day) and temperature (20°C) are constant.

4.3 2D unsteady model of a cavity. Species module with convection and reactions. Hydrodynamic model equations active with zero flow field.

This test compares the solution of BioChemFOAM implemented in OpenFOAM with a code developed in MATLAB when BioChemFOAM considers advection and reaction in the general species transport equation, $\mathcal{T} + \mathcal{A} = \mathcal{R}$. The MATLAB code implements the same reactions defined in BioChemFOAM and It is classified as a 0-D model since it does not consider the spatial variation of any reaction. The goal is to test BioChemFOAM when a zero flow field is imposed in the domain.

Figure 4-2 shows the boundary conditions. The simulation seeks to resemble completed mixed tanks in each cell of the 2-D cavity domain. Since the advection is zero, $\mathcal{A}$, the expected solution should be the same as the represented in Section 4.2 .

4.3.1 General configuration- Parameterization, Numerical Mesh, Boundary Conditions (BC), Initial Conditions (IC)

In order to be consistent in all cases and to reproduce solutions for which we know what to expect the parameterization, numerical mesh, BC and IC are the same as those defined in the previous section. A rectangular 2-D mesh (cavity) is selected to define a 2-D mesh in OpenFOAM. The number of cells is 10000. In this case, since a zero flow field is considered in the system of equations, we expect that the tool reproduce the same solution as in Section 4.2. We are testing the discretization process of BioChemFOAM to make sure that it does not introduce large numerical errors that may deviate from previously validated results.

4.3.2 Results and Comments

Figure 4-16 throug 4-21 show that BioChemFOAM was able to reproduce the concentration profiles for the 11 species when running the code for 4 days. The short period of time was selected to check the model's ability to capture sharp gradients of concentrations. BioChemFOAM was able to reproduce concentration profiles when a zero flow field is considered in the fate and transport equations. Furthermore, the test shows that the numerical methods utilized to discretize the advection term do not introduce significative errors that deteriorate the final solution.
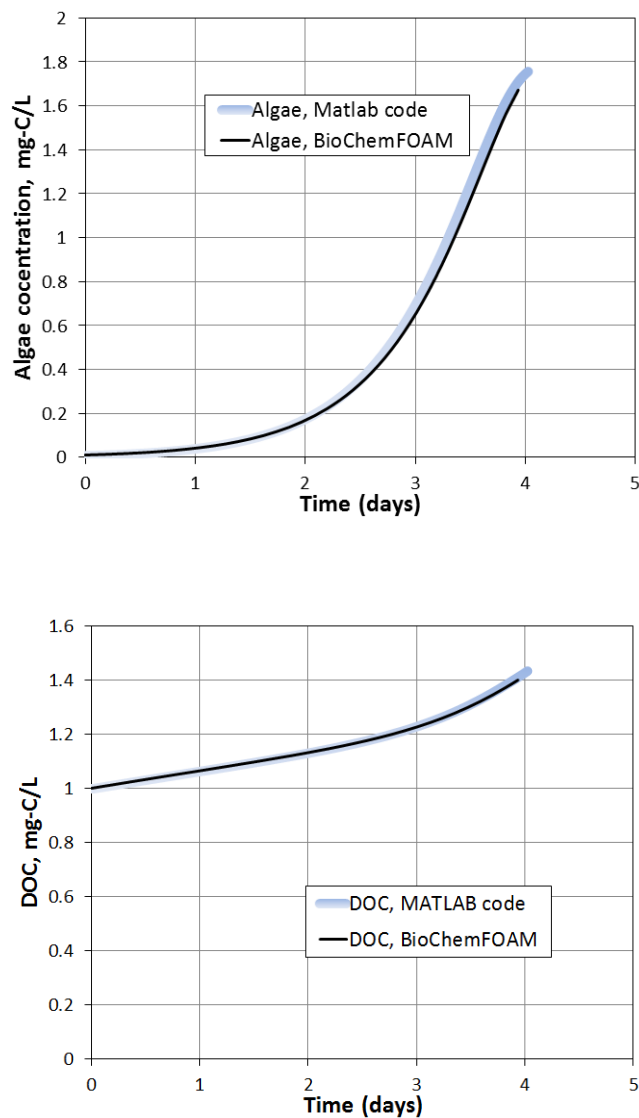
Figure 4-17. Time evolution of algae and Dissolved Organic Carbon (DOC) included in BioChemFOAM when the species transport module has the configuration $\mathcal{T} + \mathcal{A} = \mathcal{R}$ and the flow field is zero (velocity is zero). The sample point is located at the center of the cavity. "Batch" reactor ssytem. Light (300 ly/day) and temperature (20$^{\mathrm{o}}$C) are constant.
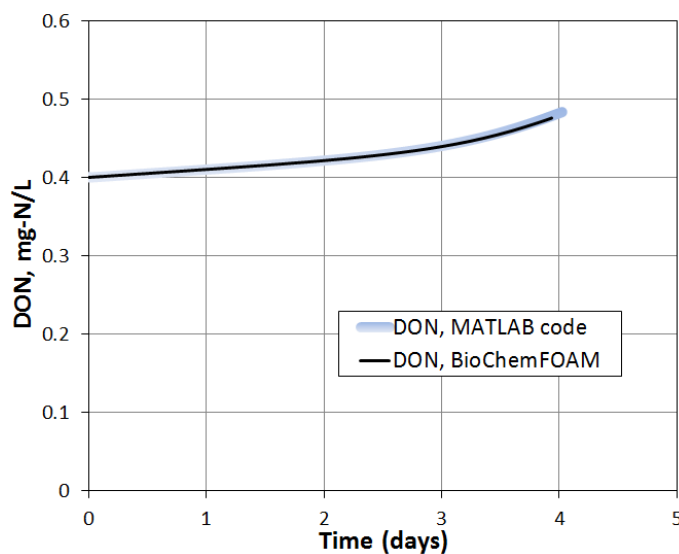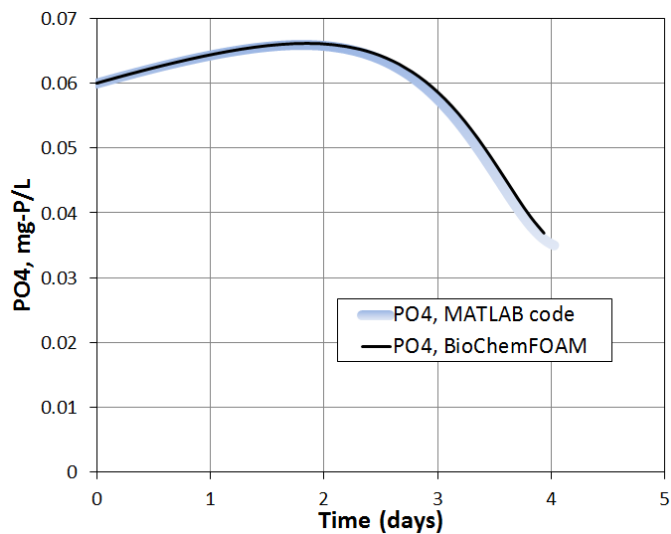
Figure 4-18. Time evolution of dissolved orthophosphate (PO4) and Dissolved oorganic nitrogen (DON) in BioChemFOAM when the species transport module has the configuration $\mathcal{T} + \mathcal{A} = \mathcal{R}$ and the flow field is zero (velocity is zero). The sample point is located at the center of the cavity. "Batch" reactor ssytem. Light (300 ly/day) and temperature (20°C) are constant.
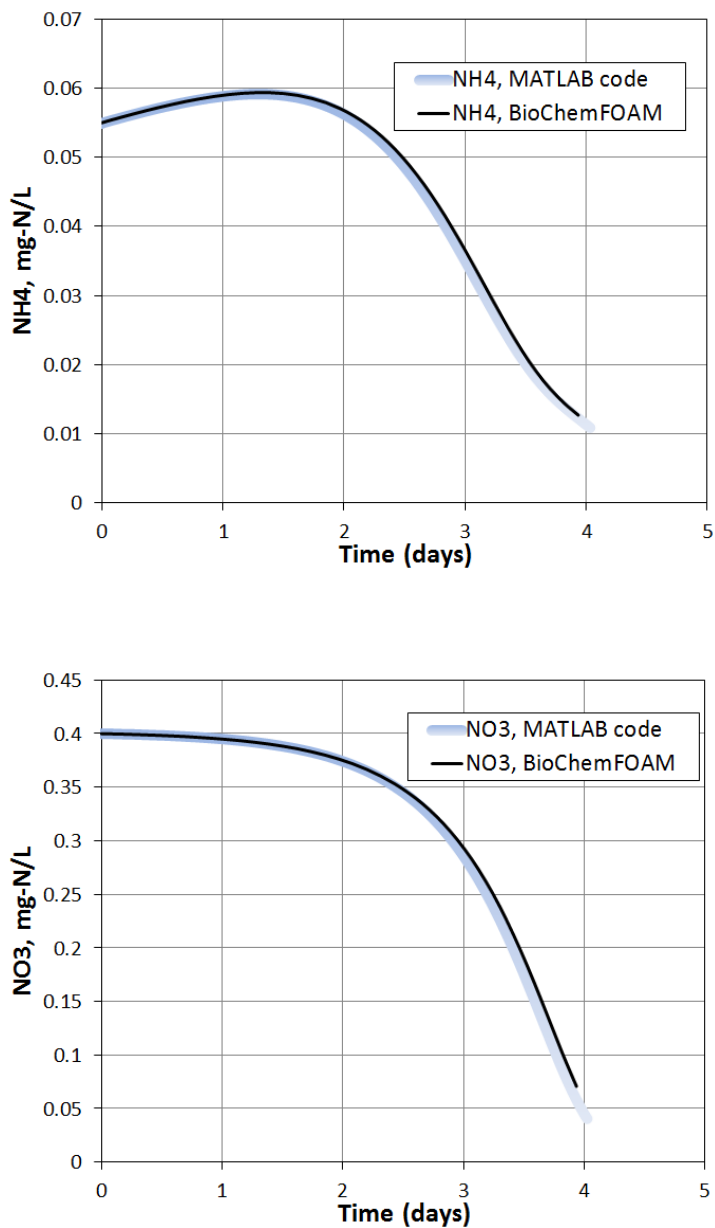
Figure 4-19. Time evolution of ammonia (NH4= NH_4^++NH_3) and nitrate (NO3=$_3^-$+NO_2^-)) in BioChemFOAM when the species transport module has the configuration $\mathcal{T} + \mathcal{A} = \mathcal{R}$ and the flow field is zero (velocity is zero). The sample point is located at the center of the cavity. "Batch" reactor ssytem. Light (300 ly/day) and temperature (20$^\text{o}$C) are constant.
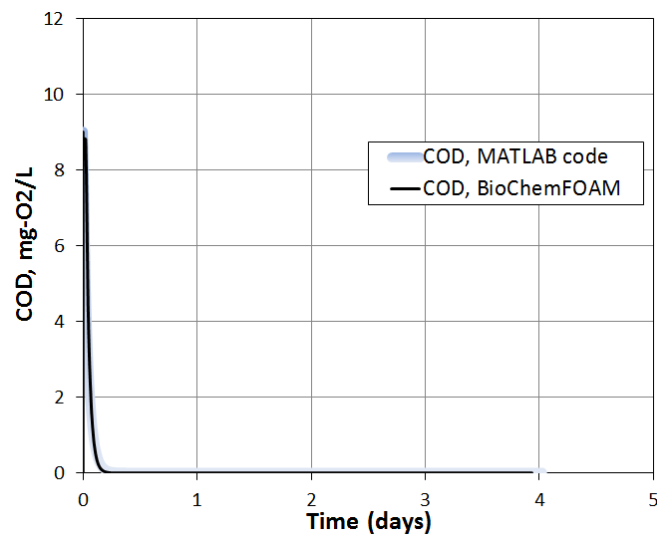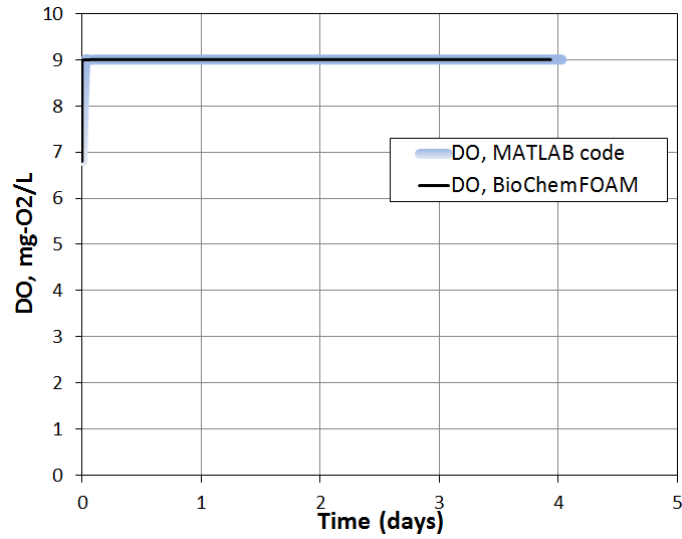
Figure 4-20. Time evolution of dissolved oxygen (DO) and chemcial oxygen deman for reduced substances (COD) in BioChemFOAM when the species transport module has the configuration $\mathcal{T} + \mathcal{A} = \mathcal{R}$ and the flow field is zero (velocity is zero). The sample point is located at the center of the cavity. "Batch" reactor ssytem. Light (300 ly/day) and temperature (20°C) are constant.
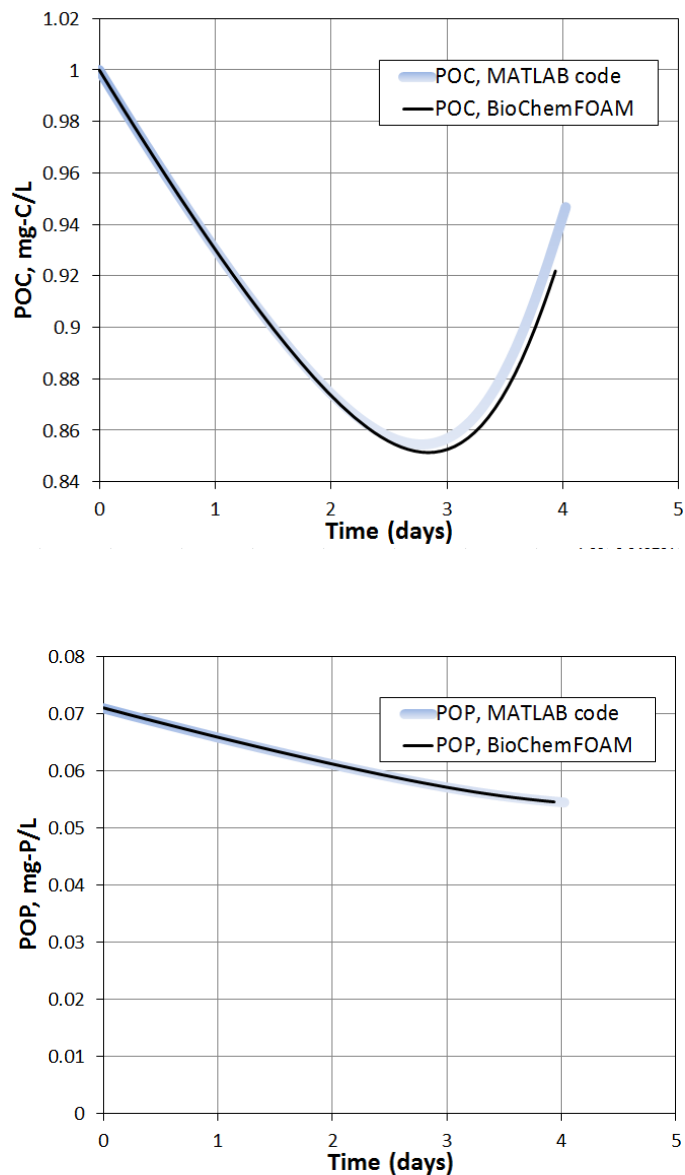
Figure 4-21. Time evolution of particulate organic carbon (POC) and particulate organic phosphorus (POP) in BioChemFOAM when the species transport module has the configuration $\mathcal{T} + \mathcal{A} = \mathcal{R}$ and the flow field is zero (velocity is zero). The sample point is located at the center of the cavity. "Batch" reactor ssytem. Light (300 ly/day) and temperature (20$^{\mathrm{o}}$C) are constant.
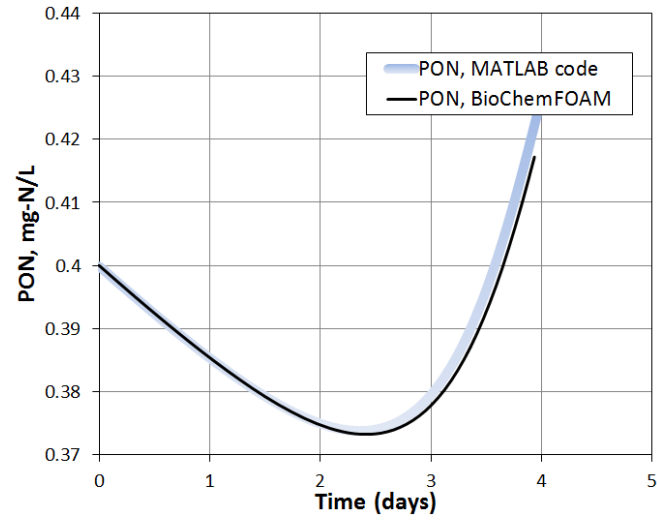
Figure 4-22. Time evolution of particulate organic nitrogen (PON) in BioChemFOAM when the species transport module has the configuration $\mathcal{T} + \mathcal{A} = \mathcal{R}$ and the flow field is zero (velocity is zero). The sample point is located at the center of the cavity. "Batch" reactor ssytem. Light (300 ly/day) and temperature (20°C) are constant

4.4 2D unsteady model of a cavity. Species module with convection and reactions. Hydrodynamic model equations active with a lid velocity. Laminar Flow – Re=100.

The objective of the simulation is to account for the convection of a non zero flow field in the 2-D cavity presented earlier. The main configuration of the species transport module is $\mathcal{T} + \mathcal{A} = \mathcal{R}$.

4.4.1 General configuration- Parameterization, Numerical Mesh, Boundary Conditions (BC), Initial Conditions (IC)

The velocity of the lid is $0.001 m/s$, which corresponds to a Reynolds Number of 100. This flow was selected because the tool will be applied to backwater areas that generally have low velocity (an application is presented in Chapter 6). The only change on BC is impose a constant constant on the moving wall, Figure 4-2.

4.4.2 Results and Comments

The flow field is first compared with a well known result (Ghia et al., 1982) in Figure 4-23. Also, Figure 4-24 shows the velocity comparison between OpenFOAM and (Ghia et al., 1982). Finally, a comparison of the species concentrations of BioChemFOAM and MATLAB over time for two points is presented in Figure 4-8 and Figure 4-9. The figures show that both solutions reproduce the same fate and transport pattern. The first point presented in Figure 4-8 (see bottom right figure of the cavity) was selected to test the model's ability to reproduce the species concentration when flow is comparable to the velocity of the lid. In contrast, the second point, Figure 4-9, was selected to show the model's ability to simulate low flow velocity. This means that even when a small flow is imposed on the solution of the species transport system of equations, the temporal distribution of concentration does not change considerably.
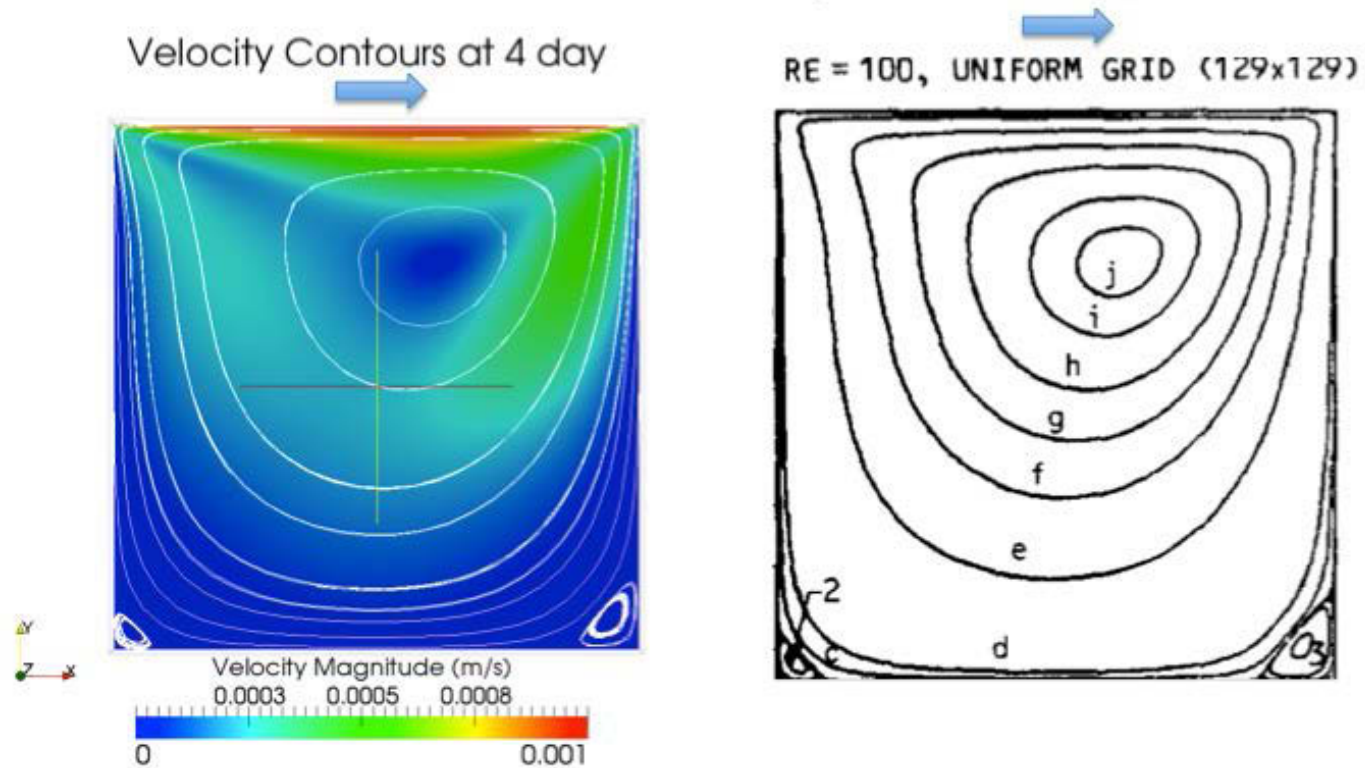
Figure 4-23. Comparison of flow field between BioChemFOAM (left) and published data (Ghia et al., 1982) (right). The blue arrow represent the velocity imposed on the lid of the cavity. The left figure also shows the contours of velocity magnitude for $Re = 100$ calculated with BioChemFOAM and streamlines (in white).
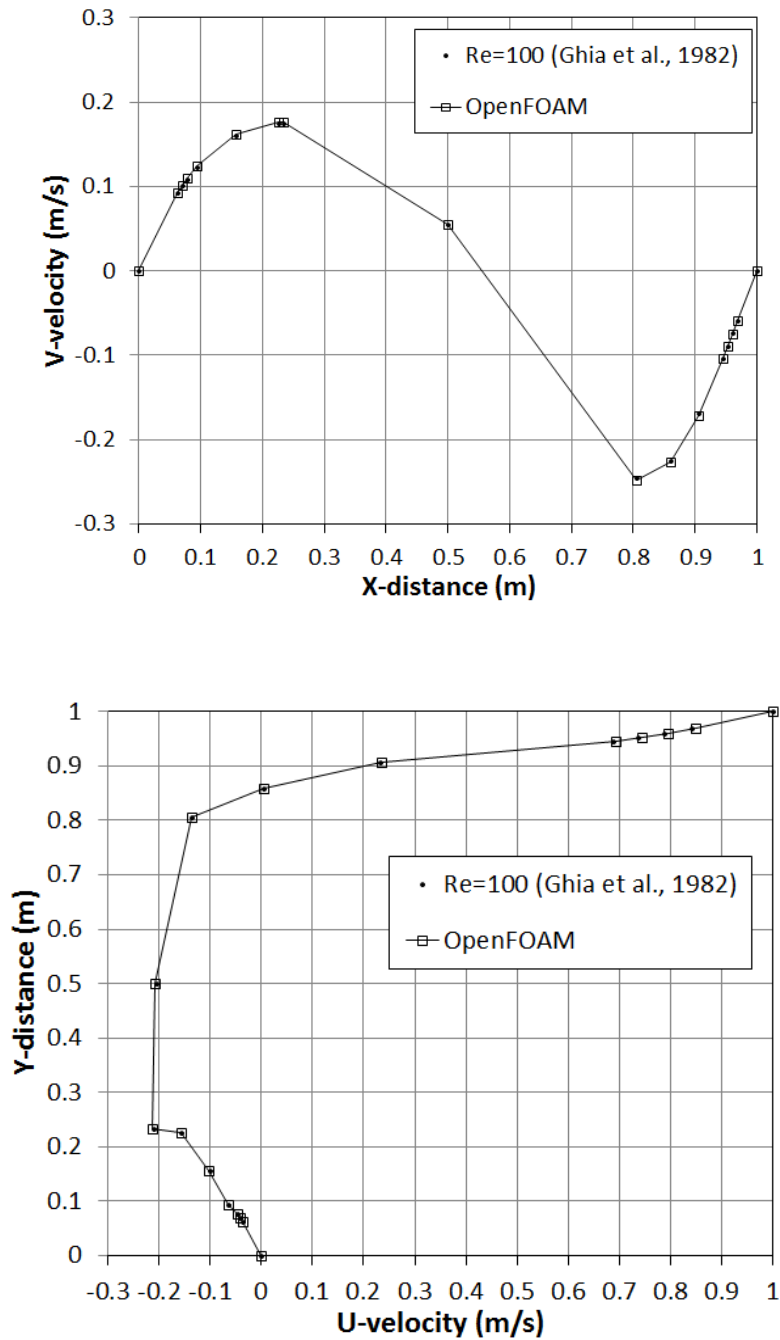
Figure 4-24. Velocity comparison between OpenFOAM and (Ghia et al., 1982) for a line located at the center of the cavity. (top) vertical velocity. (bottom) horizontal velocity.
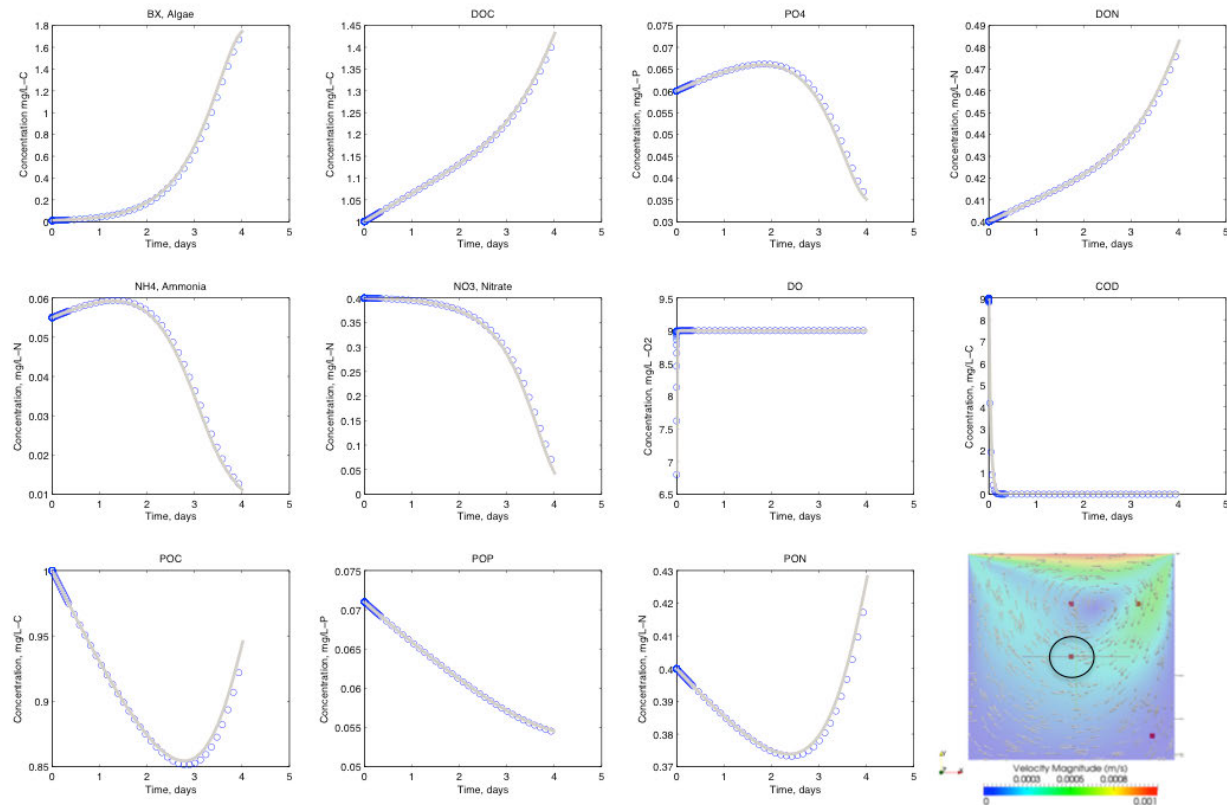
Figure 4-25. Time evolution of species in a point located at the center of the cavity. The BioChemFOAM species transport module has the configuration $\mathcal{T} + \mathcal{A} = \mathcal{R}$, while the flow field is non zero, $Re = 100$. The blue symbols reflects the results from BioChemFOAM, and the gray line represents the results from BioChemMATLAB. The bottom left part of the figure shows the location of the sample point. All other panels show the time evolution of concentration for the 11 species. Bx is algae concentration. DOC is dissolved organic carbon. PO4 is dissolved orthophosphates. DON is dissolved organics nitrogen. NH4 is ammonia. NO3 is nitrate. DO is dissolved oxygen. POC is particulate organic carbon. POP is particulate organic phosphorus. PON is particulate organic nitrogen. COD is chemical oxygen demand.
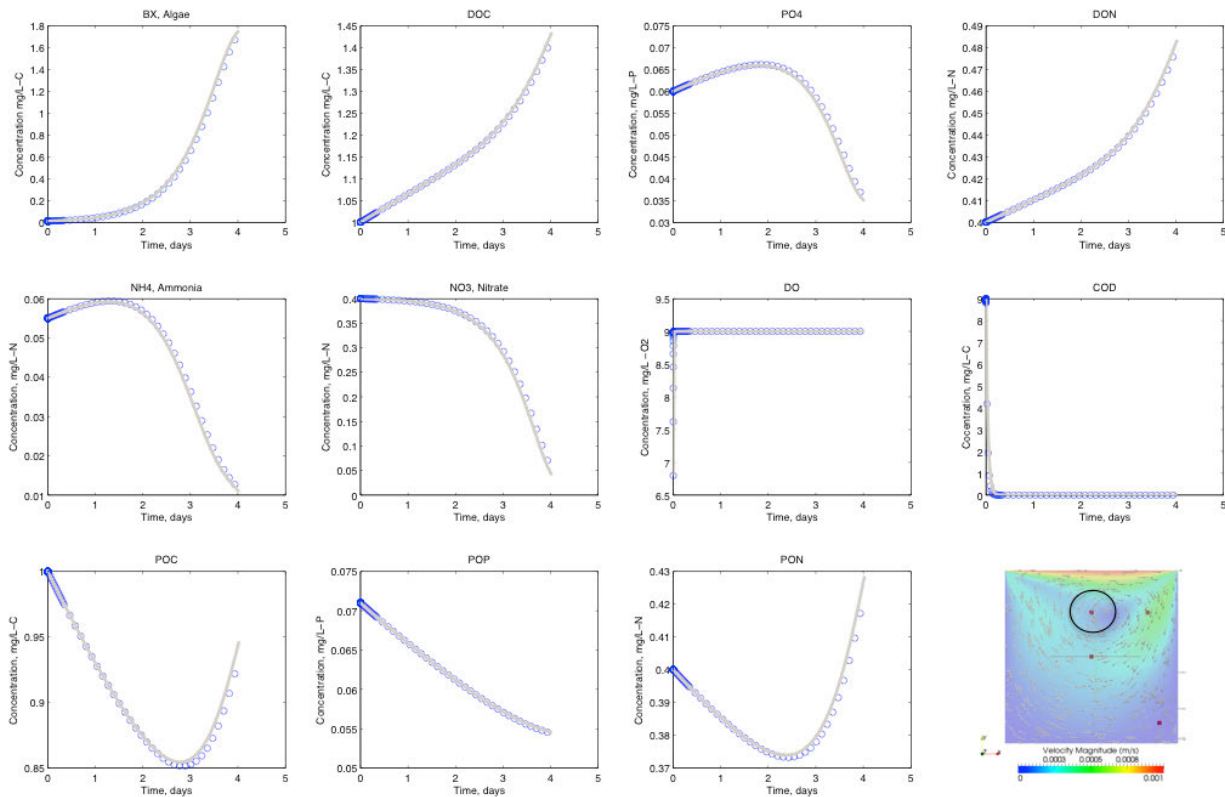
Figure 4-26. Time evolution of species at a point located in a low velocity region. The BioChemFOAM species transport module has the configuration $\mathcal{T} + \mathcal{A} = \mathcal{R}$, and the flow field is non zero, $Re = 100$. The blue symbols are results from BioChemFOAM, and the gray lines show results from BioChemMATLAB. The bottom left part of the figure shows the location of the sample point. All other panels show the time evolution of concentration for the 11 species. Bx is algae concentration. DOC is dissolved organic carbon. PO4 is dissolved orthophosphates. DON is dissolved organic nitrogen. NH4 is ammonia. NO3 is nitrate. DO is dissolved oxygen. POC is particulate organic carbon. POP is particulate organic phosphorus. PON is particulate organic nitrogen. The [point shown in the bottom left corner of the figure has velocity zero.

4.5 2D unsteady model of a cavity. Species module with

convection, diffusion and reactions. Hydrodynamic model

equations active with a lid velocity. Laminar Flow – Re=100.

This case compares and validates the numerical results obtained from BioChemFOAM when the configuration $\mathcal{T} + \mathcal{A} - \mathcal{D} = \mathcal{R}$ is imposed on the species transport module. In general, the concentration distributions for the 11 species are compared with the MATLAB code in points were the velocity is zero or negligible.

4.5.1 General configuration- Parameterization, Numerical Mesh,
Boundary Conditions (BC), Initial Conditions (IC)

The only difference in Boundary Conditions is the imposed constant velocity at the top of the cavity and the definition of a constant diffusion coefficient of $D = 1e - 6 m^2 / s$. This value was selected based on eddy diffusion parameters presented by (Martin & McCutcheon, 1998) .

4.5.2 Results and Comments

The sample concentration for the species in different points of the domain reproduce the same trends as the solution obtained using the MATLAB code. Figure 4-10 the evolution of the concentration over 2 days of simulation for all species. BioChemFOAM was able to reproduce the same fate and transport processes as BioChemMATLAB.
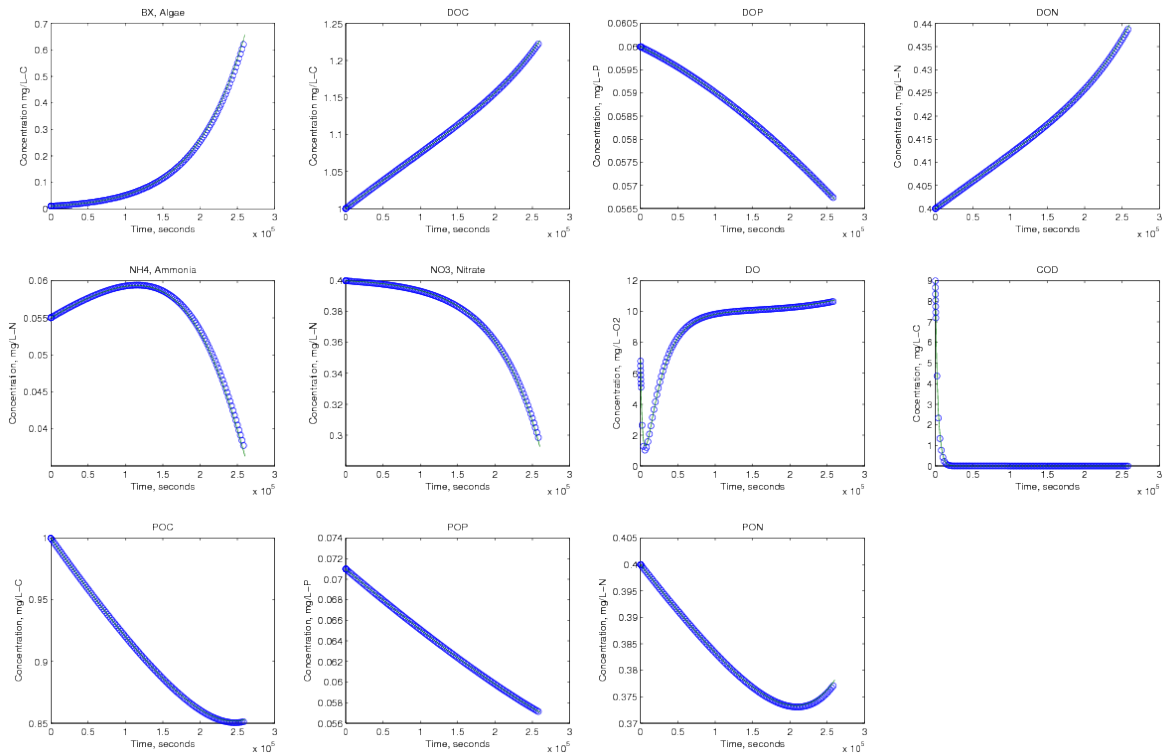
Figure 4-27. Time evolution of species at a point located in a low velocity region. The BioChemFOAM species transport module has the configuration $\mathcal{T} + \mathcal{A} - \mathcal{D} = \mathcal{R}$, and the flow field is non zero, $Re = 100$. Blue symbols are results from BioChemFOAM, and green lines are results from BioChemMATLAB. Bx is algae concentration. DOC is dissolved organic carbon. PO4 is dissolved orthophosphates. DON is dissolved organic nitrogen. NH4 is ammonia. NO3 is nitrate. DO is dissolved oxygen. POC is particulate organic carbon. POP is particulate organic phosphorus. PON is particulate organic nitrogen.

4.6 3D unsteady flow in an ideal canal. Species module with

convection and reactions. Hydrodynamic module with advection.

The following case tests the model in a 3-D hypothetical channel, as shown in Figure 4-11. The idea is to reproduce a plug flow though the system by fixing a constant velocity profile at the entrance of the channel. The velocity (low velocity) of the channel is such that there is enough time for the species to react .

4.6.1 General configuration- Parameterization, Numerical Mesh,

Boundary Conditions (BC), Initial Conditions (IC)

The mesh has 48,696 cells with an average aspect ratio of 12.35 and a maximum orthogonality of 1.91 (values calculated with the "checkMesh" utility of OpenFOAM). The channel has a slope of 0.67% (Figure 4-11). The model was run for 4days, and the results were compared with the 0-D model BioChemMATLAB. Table 4-2 shows the Boundary and Initial conditions. Figure 4-12 shows the procedure followed to compare the solutions from BioChemFOAM(3-D model) with BioChemFOAM(0-D) model.

4.6.2 Results and Comments

The concentration results are sampled along the X-direction of the channel. These values can be converted to time by using the constant velocity at each sample point. The extracted times can be used to sample the solution from MATLAB. In this numerical experiment, the results obtained with BioChemFOAM and MATLAB are the same as shown in Figure 4-12. The values shown in this graph correpond only to 6000 seconds that is approximately 1.7 hours. This means that the fate and transport processes generated in the channel during 4 hours of real time simulation reproduce concentration in the range of 0 to 1.7 hours in the 0-D model.
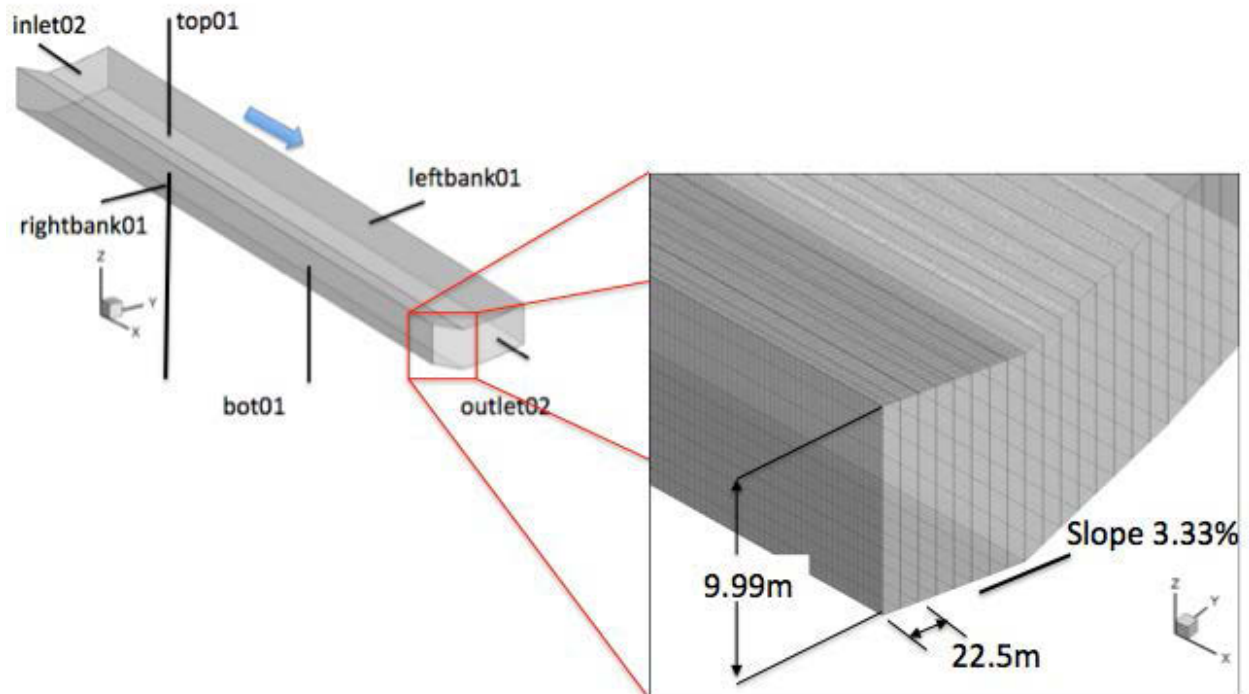
Figure 4-28. General domain of the channel (left). Detail of the mesh (right). The blue arrow indicates flow direction. The surfaces delimiting the domain are : "inlet02", "top01", "rightbank01", "leftbank01", "bot01" and "outlet02".

Table 4-2. Boundary conditions (BC) and Initial Conditions (IC) for the case 3-D ideal channel low velocity, 11 species. fV=fixed value; zG= zero gradient; and NA: non applicable.

	IC value	bot01	inlet02	leftbank01	outlet02	rightbank01	top01
			BC name				
U(m/s)	fV=(0.02,0,0)	zG	fV=(0.02,0,0)	zG	zG	zG	zG
$P/\rho(m^2/s^2)$	0	fV=0	zG	zG	zG	zG	zG
Bx (mg-C/L)	0.01	zG	fV=0.01	zG	zG	zG	zG
DOC (mg-C/L)	1	zG	fV=1	zG	zG	zG	zG
PO4 (mg-P/L)	0.06	zG	fV=0.06	zG	zG	zG	zG
DON (mg-N/L)	0.4	zG	fV=0.4	zG	zG	zG	zG
NH4 (mg-N/L)	0.055	zG	fV=0.055	zG	zG	zG	zG
NO3 (mg-N/L)	0.4	zG	fV=0.4	zG	zG	zG	zG
DO (mg-O$_2$/L)	6.8	zG	fV=6.8	zG	zG	zG	zG
COD (mg-O$_2$/L)	9	zG	fV=9	zG	zG	zG	zG
POC (mg-C/L)	1	zG	fV=1	zG	zG	zG	zG
POP (mg-P/L)	0.071	zG	fV=0.071	zG	zG	zG	zG
PON (mg-N/L)	0.4	zG	fV=0.4	zG	zG	zG	zG
I (ly/day)	300	NA	NA	NA	NA	NA	NA
T (^{o}C)	20	NA	NA	NA	NA	NA	NA
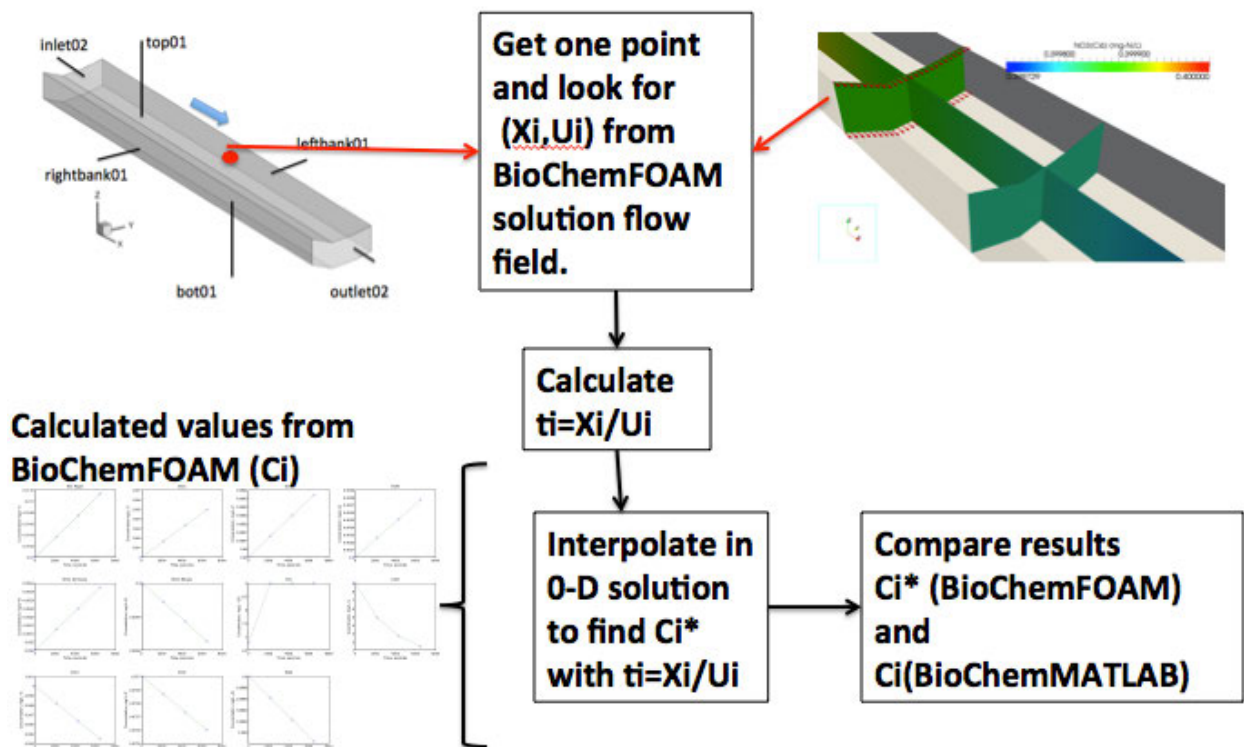
Figure 4-29. Procedure followed to compare 3-D channel species transport mode BioChemFOAM (low velocity $U_x = 0.02 m/s$) with 0-D model BioChemMATLAB. Four steps are shown in the back boxes. Xi is the location along the flow direction represented by the blue arrow at the top left of the figure. Ui is the corresponding velocity at point Xi along the flow direction. Ci* is the concentration of BioChemFOAM interpolated from BioChemMATLAB with ti. Ci is the concentration calculated with BioChemFOAM. Lower left corner Figure can be reviewed from Figure 30.
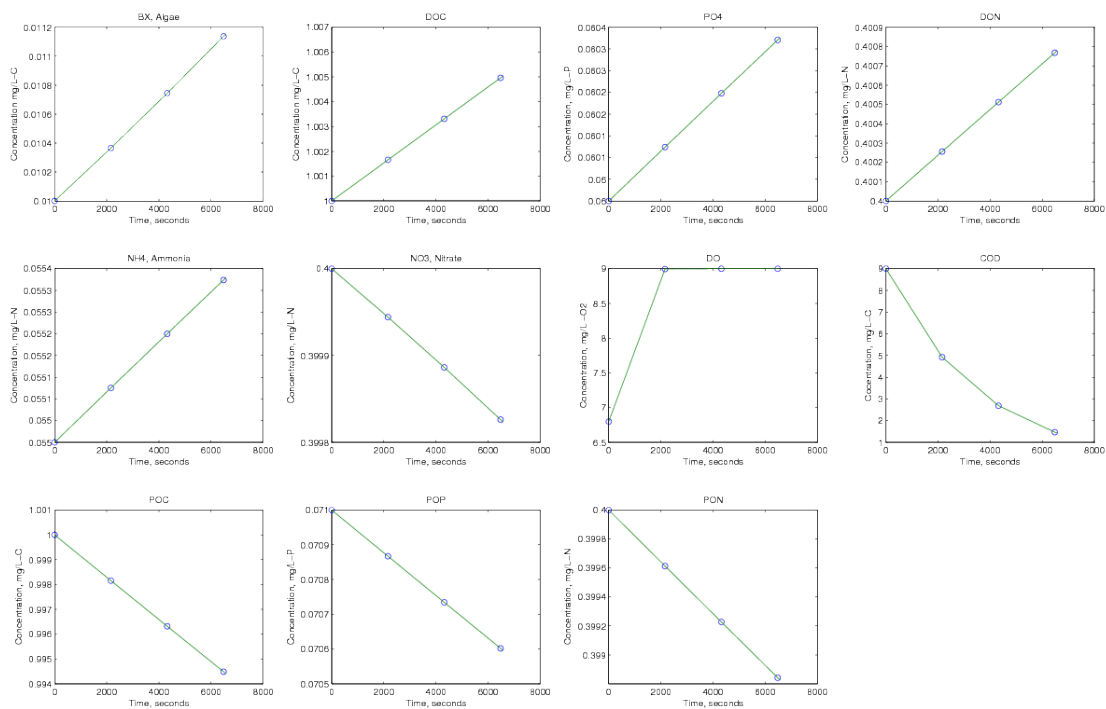
Figure 4-30. Comparison of concentration over time between BioChemFOAM (green line) and BioChemMATLAB (blue dots) following the procedure outlined in Figure 4-12.

4.7 Validation operator splitting method in a 3-D unsteady flow in an ideal canal. Comparison with analytical solution published by (Sun et al., 1999).

This chapter's are based on characteristic values of a backwater area taking from previous studies, see (Cerco & Cole, 1994) and (EPA, 2011). The validation was based on two codes developed in this thesis and shows, in general, that we obtained a precise solution when using the methods presented in Chapter 3. This methodology was followed because the spatial and temporal variation of species were not available at the degree of detail needed to fully calibrate and validate the model in backwater areas (the tool is intended to be used in those zones). We propose our methodology to show that the parameterization in BioChemFOAM implemented through OpenFOAM libraries works when applied to fabricated numerical experiments. In all cases, it was assumed that the method used to solve the set of partial differential equations that describes the fate and transport are correct.

This section presents a further validation of the methods and robustness of the tool to reproduce fate and transport of species. The tool is adapted to simulate a straight channel with imposed: velocity, diffusion coefficient, and reaction coefficients. The case is presented by (Sun et al., 1999) and has an exact mathematical solution for a sequential set of reactions. The model was formulated to prove two points: (1) that the proposed methodworks under different parameterization when compared with an exact mathematical solution and (2) that the tool is flexible enough to include different parameterizations.

4.7.1 General configuration- Parameterization, Numerical Mesh, Boundary Conditions (BC), Initial Conditions (IC)

Figure 4-14 presents the general domain and mesh. It has 10,000 cells distributed in X and Y and one layer in the Z direction. The flow velocity is fix to $0.2cm/h$. The three reactions are $R_1 = -k_1.Ci$, $R_2 = +k_1.Ci - k_2.Ci2$, and $R_3 = +k_2.Ci = k_3.Ci3$ with reaction coefficients

$k_1 = 0.05h^{-1}$, $k_2 = 0.03h^{-1}$ and $k_3 = 0.02h^{-1}$. The diffusion coefficient is $Di = 0.18cm^2/h$. The BioChemFOAM tool was adapted to solve $\mathcal{T} + \mathcal{A} - \mathcal{D} = \mathcal{R}$. The code was modified to solve a system of three coupled species with sequential reaction rates. The initial conditions inside the domain were zero for all species. The boundary conditions at the input section, as shown in Figure4-14 (a), were left fixed and equal to $Ci = 1[M/L^3]$, $Ci2 = 0[M/L^3]$ and $Ci3 = 0[M/L^3]$ (M means mass and L means length) (Sun et al., 1999).

4.7.2 Results and Comments

BioChemFOAM was able to reproduce the same concentrations along the channel as shown in Figures 4-15 and 4-16. Figure 4-15 also shows the distribution of the species over space at the top left. The countours are typical of a plug-flow reactor.
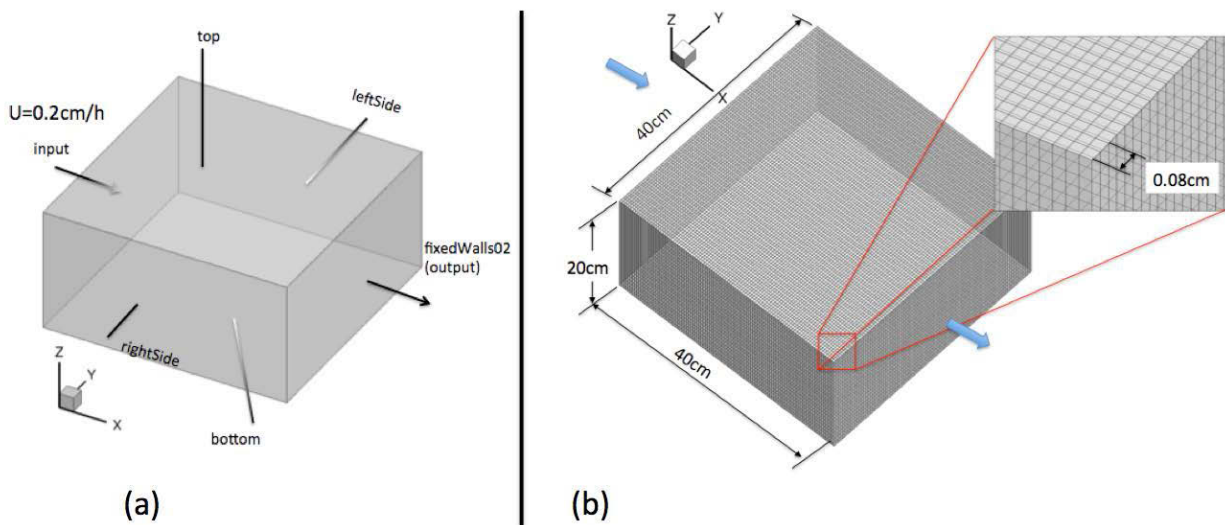
Figure 4-31. Domain configuration using (Sun et al., 1999). (a) Domain with boundary conditions. (b) Detail of the mesh. 100x100x1 (XxYxZ), only one layer in the z-direction (depth). The blue arrow indicates the flow direction.
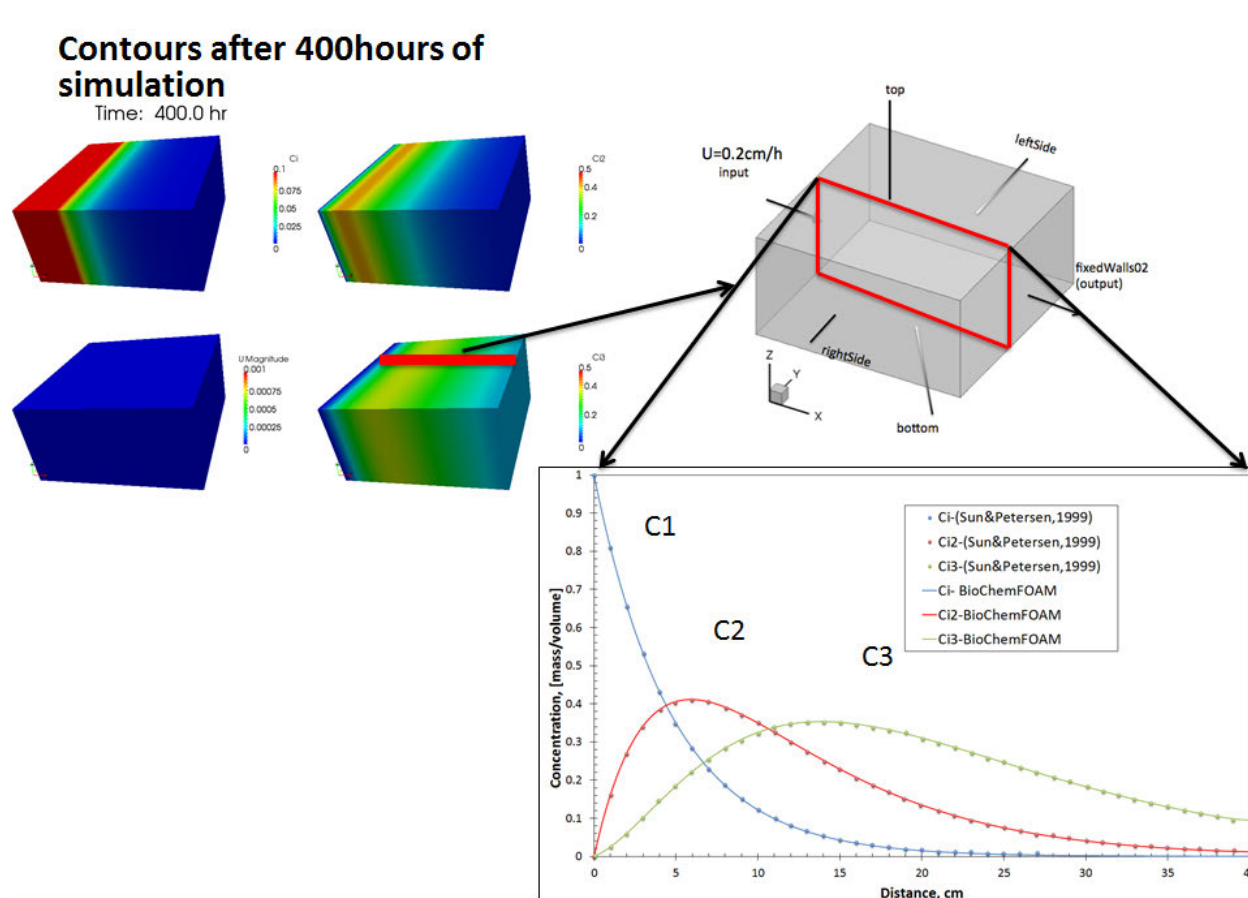
Figure 4-32. Contours for each species concentration and velocity magnitude (top left). Location of cross section to sample concentration after 400hr (top right). Comparison concentration after 400hrs of simulation between BioChemFOAM and (Sun et al., 1999) (dots) (bottom right).
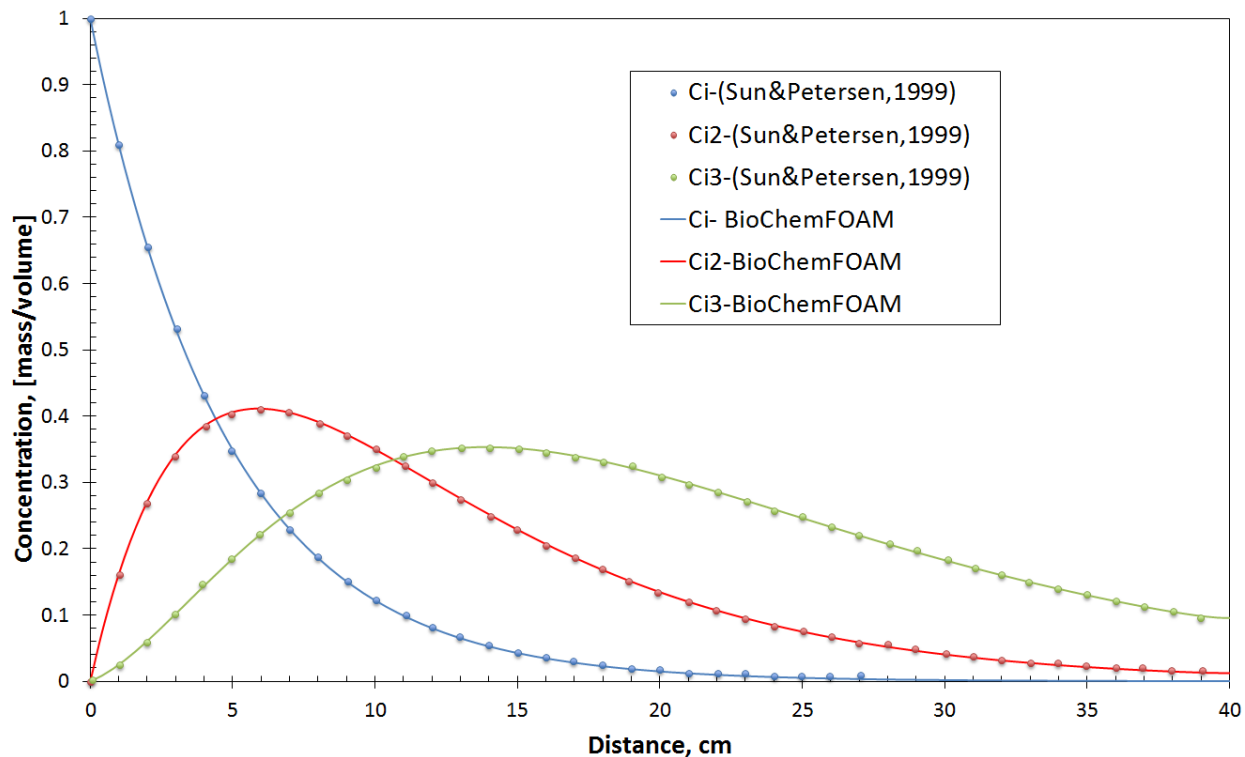
Figure 4-33. The comparison concentration after 400hrs of simulation between (Sun et al., 1999) and BioChemFOAM. Detail of graph comparing concentrations. The vertical axis has units of mass over volume. The three species are hyphothetical and do not have an specific units.

4.8 Summary and Final remarks

The methods and paramterization implemented in BioChemFOAM were able to reproduce characteristic values under different degrees of complexity in a fabricated numerical experiment, as described in Sections 4.2 through 4.7. Comparing results from a 0-D model implemented in MATLAB (BioChemMATLAB) proves to be a valuable tool to check parameterization of processes in BioChemFOAM. Despite both solutions' showing that the results are precise but not accurate, the methodology was used successfully to compare the proposed parameterization in Chapter 3. The implementation in MATLAB helps to understand influence of main processes when formulating an aquatic ecological model for nutrient dynamics. These is highlighted in Figure 4-5, which shows that algae predation, when using characteristic coefficients, is an important process during the fabricated solution.

Additionally, the cases, helped to demostrate the robustness of the tool when only a few physical phenomena are included. For example, in Section 4.5 the species transport model was configured in such a way that advection, diffusion, and reactions are included in a cavity. Further more, Section 4.7 presents a new parameterization in section 4.7 where BioChemFOAM is compared with an exact (Sun et al., 1999).

This chapter showed a series of hyphothetical cases that resembles a tank that is keep at constant temperature and constant light. The cases were useful to test liminig cases when optimal conditions of light are considered for green algae in BioChemFOAM.

CHAPTER 5

VALIDATION BIOCHEMFOAM HYDRODYNAMICS USING DATA FROM
PREVIOUS STUDIES IN A BACKWATER AREA, MISSISSIPPI RIVER

5.1 Introduction

This section introduces a test case done to validate the hydrodynamic components of
BioChemFOAM and to prove that all hydrodynamic component yield reasonable values given
characteristic velocity values from previous studies (Schubert, 2009).

Two scenarios are presented. The first, described in Section 5.2, compares hydrodynamic
patterns from a well know commercial software with previous studies using the hydrodynamic
parameterization presented in Chapter 3. The second scenario, described in Section 5.3, shows an
additional validation of the hydrodynamics obtained by evaluating the Time of Residence when
releasing neutrally buoyant particles. Both scenarios test BioChemFOAM's ability to reproduce
spatial variations that generate hydraulic signature of a Mississippi River backwater area.

5.2 Hydrodynamic comparison BioChemFOAM and previous
results (FLUENT commercial software)

The back water area, Round Lake, is located near La Crosse, Wisconsin (Figure 5-1).
BioChemFOAM was configured to reproduce a summer flow of $6.3 m^/s$ with measured water
surface elevation obtained from previous studies (Schubert, 2009). Round Lake is characterized
by a fast flow zone at the entrance and a slow flow zone in the middle of the pool. This
configuration makes it a challenging case, since different spatial and temporal scales for the
velocity field are present. The model boundary conditions are presented in Figure 5-2. The figure
shows five boundary conditions (surfaces on the domain) where boundary conditions were
defined. The inlet was set as a constant mass flux of $6.3 m^3 / s$ and the the outlet was set to zero
gradient. The measured water surface was set as a symmetry boundary condition. The banks and
bottom of the pool was set to be a wall. Table5-1 presents a review of the boundaries. The mesh

is composed of approximately 325,000 cells with an approximated maximum average size of 10mx10m, Figure 5-3.

The model was run for 7days until reaching a steady flow in the whole domain. Figure 5-4 presents and compares the flow fields. Both solutions reproduce the same flow patterns in the backwater area. The flow is characterized by fast flows in the main entrance channel, red contours in Figure 5-4, and slow flows in the middle part of the pool, which are shown as blue contours in Figure 5-4. Figures 5-5, 5-6, 5-7 and 5-8 show a comparison of velocity magnitudes for the four cross sections in Figure 5-4. The boundary conditions defined in BioChemFOAM influence the solution at the riverbed as shown in Figures5-6, 5-7 and5-8. BioChemFOAM utilizes a no-slip condition with functions for the turbulence field. Despite the differences at the bottom, BioChemFOAM was able to reproduce the characteristic flow patterns calculated with FLUENT.

Finally, Figure 5-9 compares velocity vector between BioChemFOAM and FLUEN.

5.3 Hydrodynamic validation with previous results, Time of Residence

The information from the previous calculations was used as a reference to release particles into the domain and calculate the time of residence. The particles released were neutrally buoyant with one way coupling. The flow was steady. The value reported by (Schubert, 2009) is $11.1hr$ and the values obtained in OpenFOAM after introducing 4868 particles was $10.5hr$ using the Lagrangian tool available in OpenFOAM version 1.7.1. In general, the model is able to reproduce the principal hydraulic features of the study area.

5.4 Summary and Final remarks

This section presented the hydrodynamic validation of BioChemFOAM. In general, the BioChemFOAM model was able to reproduce basic trends in an aquatic environment when compared with previous studies.

The tests validate the code by comparing BioChemFOAM with a well know commercial code reported by (Schubert, 2009). Both cases show a good agreement (RMSE=0.042m/s, for average velocity) in terms of hydrodynamic patterns and time of residence.

The flow field calculated with BioChemFOAM is left constant on the species transport applications presented in Chapters 6 and 7. This is also done when testing the fate and transport module in BioChemFOAM, as presented in Chapter 3. The main reasons to fix the flow are: to reduce the computational time when species are considered in BioChemFOAM and to analyze a characteristic flow condition for summer in Round Lake (backwater area).
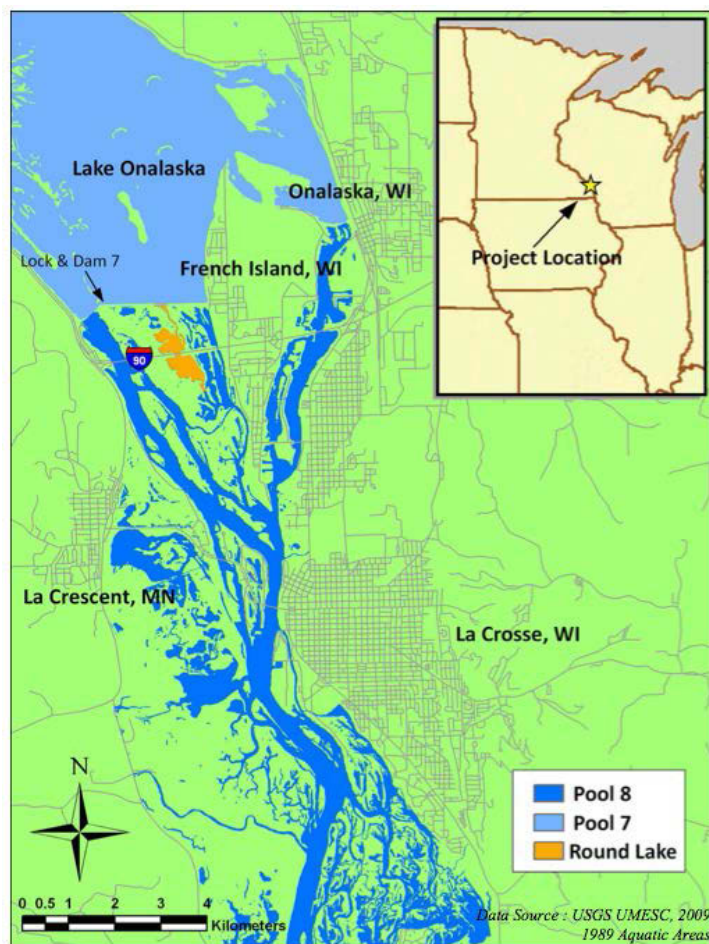
Figure 5-1. Location backwater area: Mississippi River near French Island (Schubert, 2009).

Table 5-1. Boundary conditions (BC) and Initial Conditions (IC) for Round Lake, Backwater area, for a hydrodynamic comparison between BioChemFOAM and FLUENT. Key for boundary conditions on the table: fV= fixed value; nS= no slip; sP= symmetry plane; zG= zero gradient; mF= mass flow rate inlet velocity; eWF= epsilon wall function for dissipation rate; and kWF= turbulent kinetic energy wall function. The location of the BC's (e.g Inlet) is presented in Figure 5-2.

	IC value ↓	BC name				
		Inlet	River Bed	Banks	Water Surface	Outlet
$U(m/s)$	$(0,0,0)$	mF	$fV=(0,0,0)$	$fV=(0,0,0)$	sP	zG
$P/\rho(m^2/s^2)$	0	zG	zG	zG	sP	fV=0
$\mathcal{E}(m^2/s^3)$		fV=1e-6	eWF	eWF	sP	zG
$k(m^2/s^2)$		fV=1e-6	kWF	kWF	sP	zG
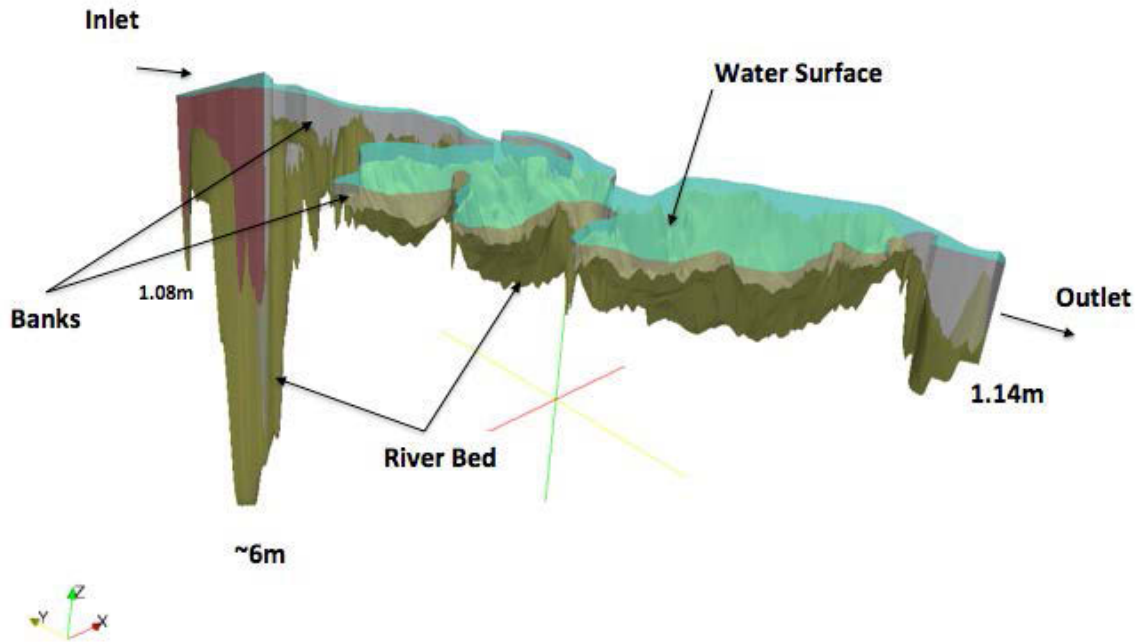
Figure 5-2. Round Lake location of Boundary Conditions(BC). The main flow direction is from left to right. (z direction is not at scale). ~60 indicates the deepest part close to the entrance, and 1.14m shows the depth at the outlet. 1.08 shows the depth at the inlet.
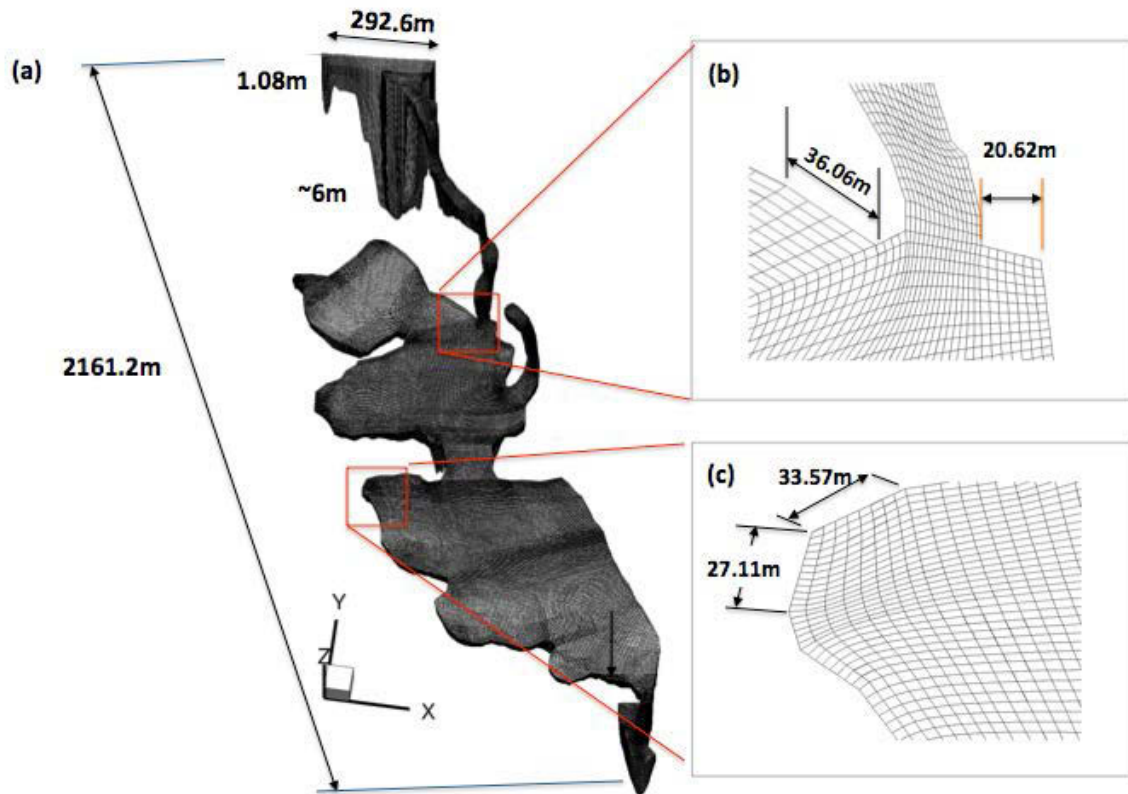
Figure 5-3. Details of mesh generated for Round Lake (z direction is not at scale). Characteristic lengths are shown in the figure. e.g., $6m$ indicates the maximum depth close to the inlet.)
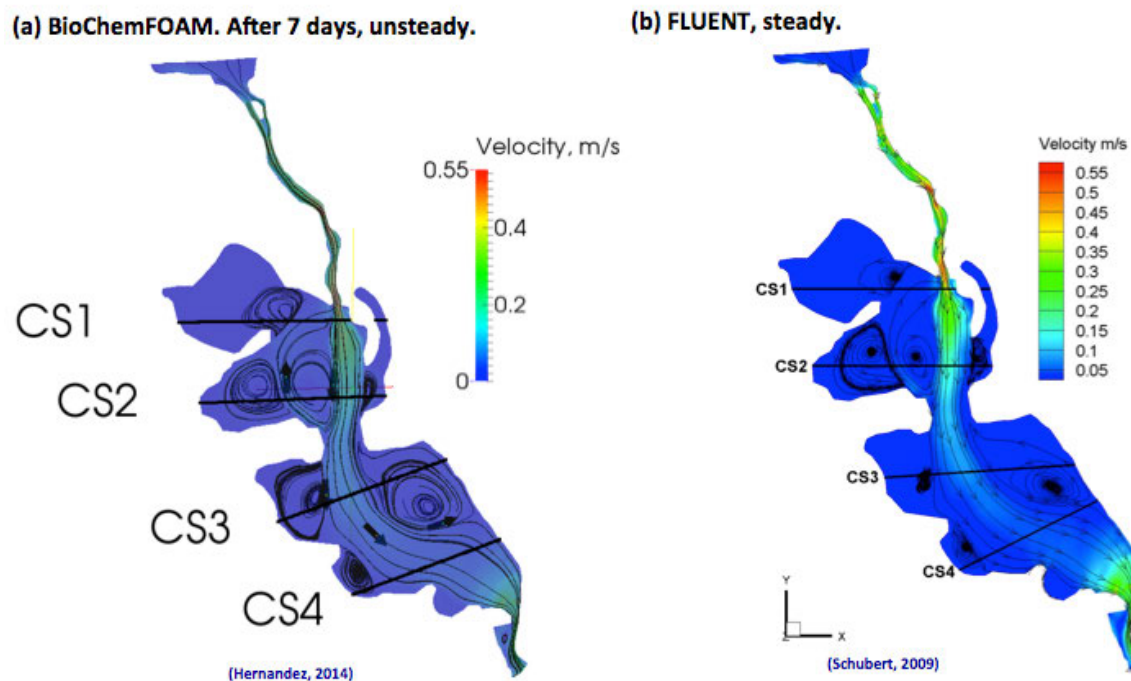
Figure 5-4. Contours of velocity magnitude and characteristic stream lines for BioChemFOAM (left, generated with Paraview software after 7days of simulation) and FLUENT steady solution (right). CS1, CS2, CS3, and CS4 are cross sections.
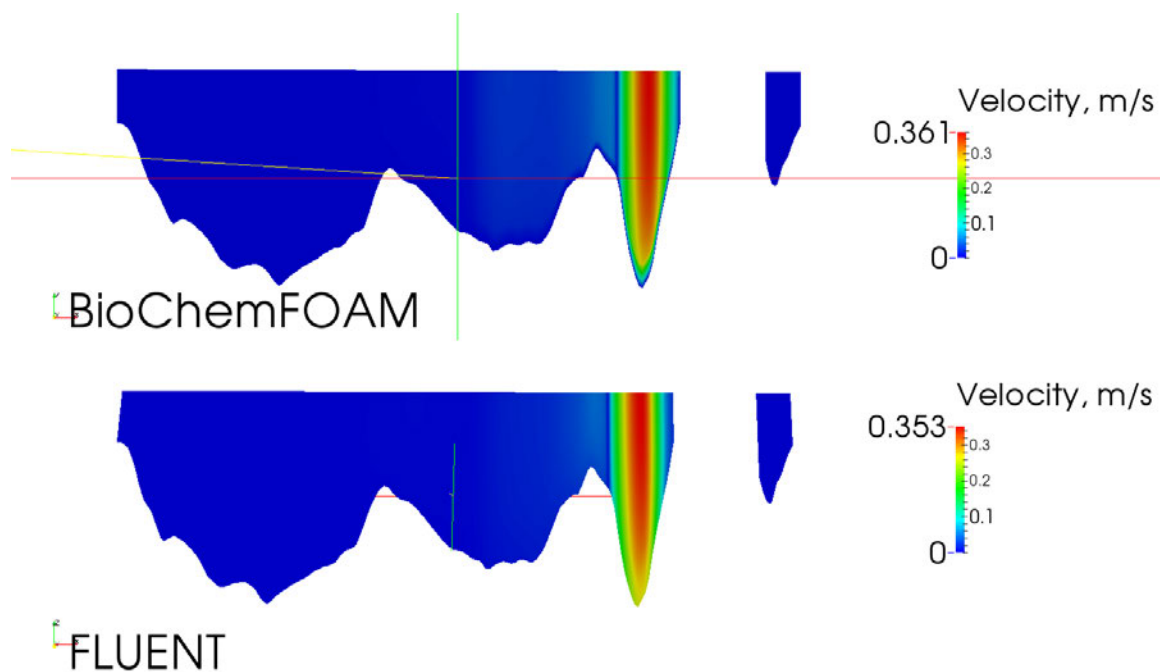
Figure 5-5. Contours of velocity magnitude at Cross Section 1 (CS01, see Figure 5-4 for location on Round Lake.). BioChemFOAM (top) and FLUENT (bottom)
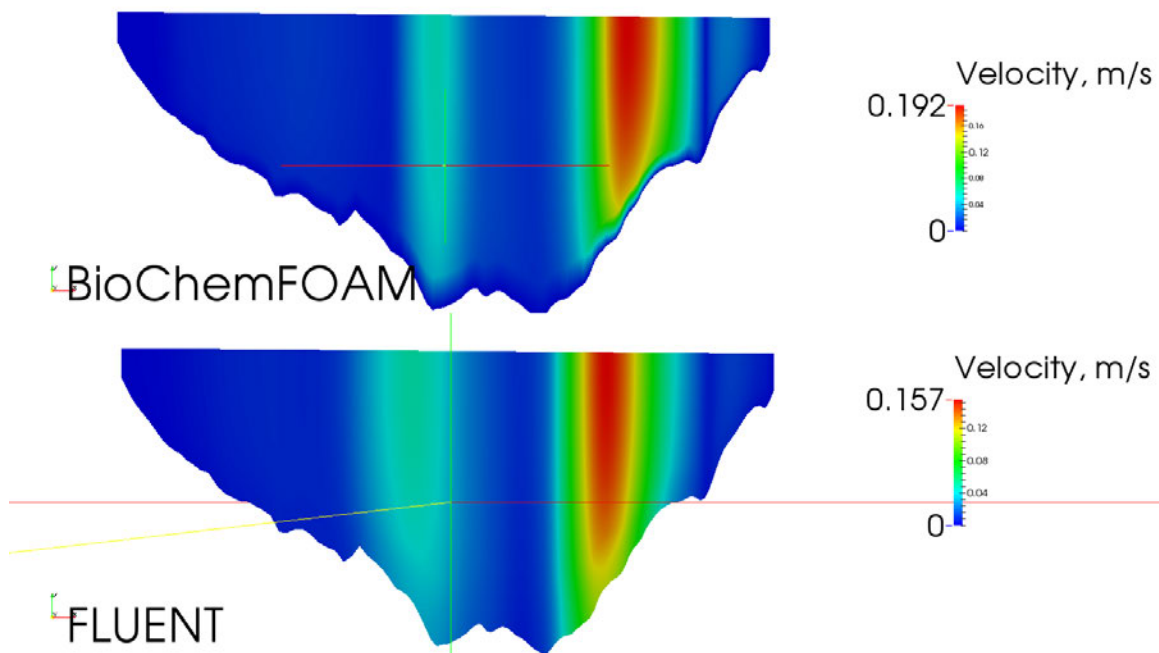
Figure 5-6. Contours of velocity magnitude at Cross Section 2 (CS02, see Figure 5-4 for location on Round Lake.). BioChemFOAM (top) and FLUENT (bottom)
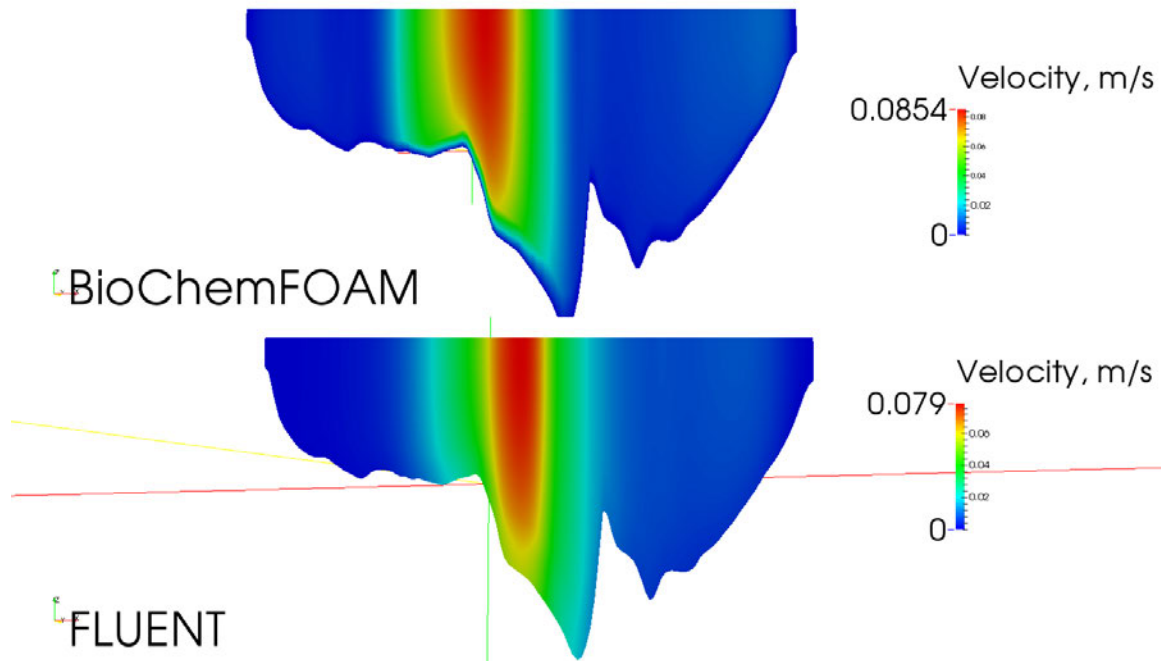
Figure 5-7. Contours of velocity magnitude at Cross Section 3 (CS03, see Figure 5-4 for location on Round Lake.). BioChemFOAM (top) and FLUENT (bottom)
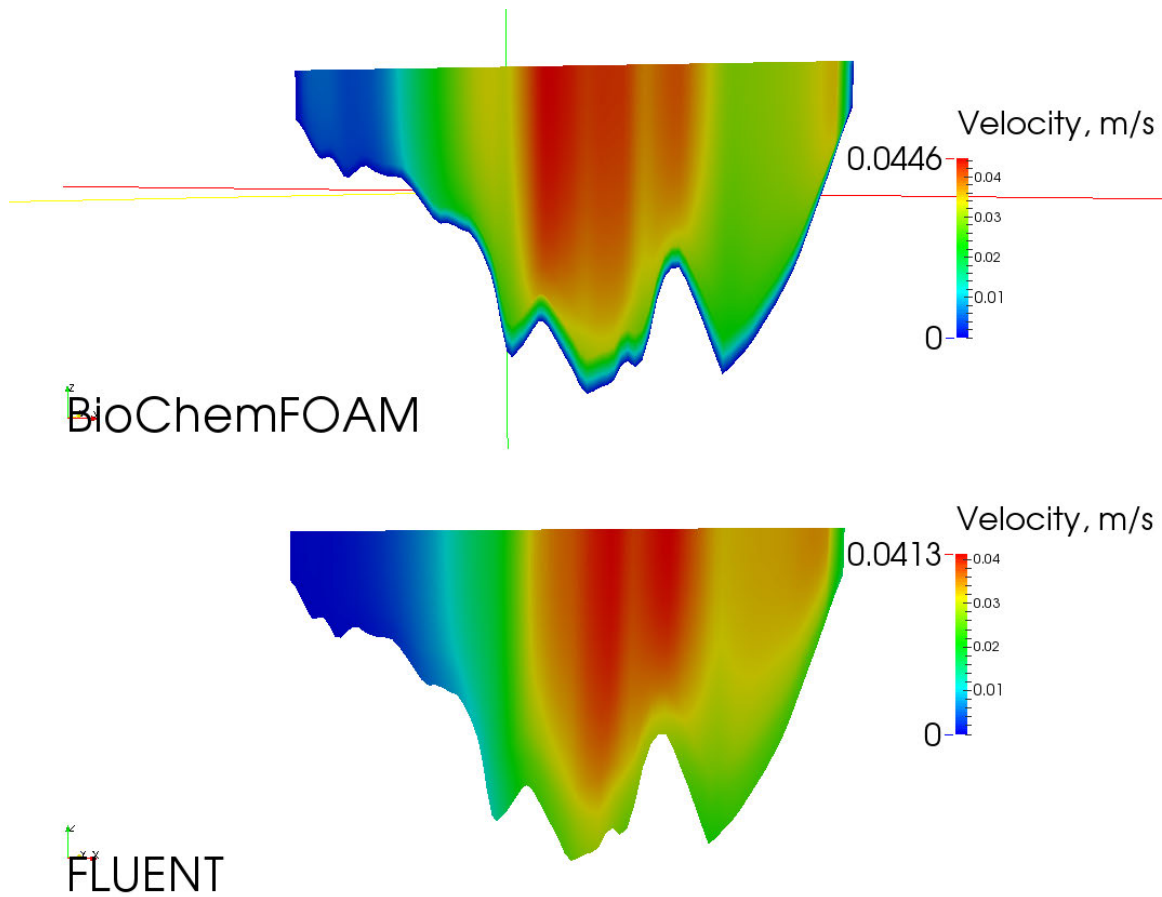
Figure 5-8. Contours of velocity magnitude at Cross Section 4 (CS04, see Figure 5-4 for location on Round Lake.). BioChemFOAM (top) and FLUENT (bottom)
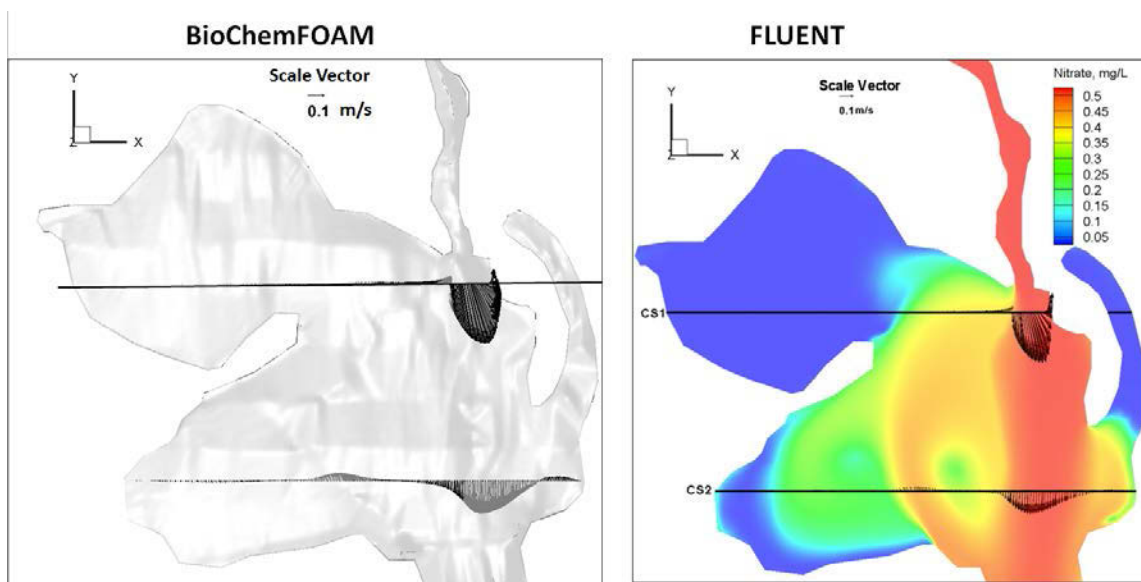
Figure 5-9. Comparison velocity vectors between BioChemFOAM and FLUENT. Cross sections 1 and 2.

CHAPTER 6

VALIDATION OF SPECIES TRANSPORT IN BIOCHEMFOAM USING

SAMPLE DATA FROM A BACKWATER AREA, UPPER MISSISSIPPI

RIVER

6.1 Introduction

This chapter introduces one real case to validate and to study sensitivity in the proposed
model, BioChemFOAM. The goal is to verify that all of the PCBP (Physical, Chemical, and
Biological Processes) included in the model give reasonable values (this is done by comparing
BioChemFOAM with Lake Pepin study) when characteristic sampled values and coefficients are
provided (species calculated are B_x, DOC, DOP, DON, $NH4$, $NO3$, DO, COD, POC,
POP, and PON). The model is applied to a backwater area in the Mississippi River, Round
Lake, based on the measured spatial distribution of nitrate concentration in four cross sections
along the study area. The applications BioChemFOAM's ability to reproduce the spatial
variations of fundamental species along a backwater area when the fluctuations in water are
negligible, flux of temperature changes at the water surface, and light intensity changes at the
water surface. Here, the flow field (velocity, pressure, turbulent kinetic energy and dissipation) is
kept constant in order to speed computations in BioChemFOAM (flow fields defined in Chapter
5) when calculating fate and transport of species. Four cases are introduced to test the model's
ability to reproduce characteristic patterns in an aquatic ecosystem.

The first case, section 6.2, considers only nitrate, $NO3$ (=NO_2^-+NO_3^-), and it is validated
and calibrated with previous studies (Schubert, 2009). Here, we show that a better solution (the
error between measured and calculated values is small) is achieved with the BioChemFOAM
model when using a first order reaction at the wall as a boundary condition.

The second case, section 6.3, considers the full system of partial differential equations
described in Chapter 3 (11 species). This case was set up in order to understand the dynamics of
the system when the full BioChemFOAM parameterization presented in Chapter 3 is used. The

model presents variable temperature (head flux boundary condition) and light at the water-air interface over time to model diurnal variations of species. Also, a comparison of the steady solution is made with characteristic values from (LimnoTech, 2007), which was a water quality study conducted at Lake Pepin, located at Pool 4 in the Mississippi River. Lake Pepin is located upstream of the area of study, Round Lake. This comparison is conducted to prove that the fields distribution calculated with BioChemFOAM are within characteristic concentration range found in similar ecosystems. This is done by generated contours of species and comparing the values with Lake Pepin study. Finally, an explanation of the new boundaries for Dissolved Oxygen (DO) and nitrate (NO3) is presented.

The third case, section 6.4, is similar to the second case with one key difference: the model is tested for nitrate concentration under two different initial conditions in order to show the model's independence from initial conditions when reaching a steady state. The results are compared once the two scenarios reach a steady solution. The steady solution is defined as the point at which the mass loading rate of nitrate at the output reach a constant value for three consecutive days.

Finallly, the fourth case, section 6.5, shows the potential applicability of the model to calculate nitrate removal rates in a backwater area. Different scenarios are defined to evaluate the model's ability to reproduce percentages of nitrate removal (PNR). The scenario that is closer to PNR values reported in the literature is further analyzed by calculating mass loading rates for all species and orders of magnitude of processes affecting nitrate fate and transport.

6.2 Comparison of BioChemFOAM with previous studies - one species model, nitrate

6.2.1 Collected information area of study - sample data

Figure 5-1 illustrates the location of study. Figures 5-2 and 5-3 show the boundary conditions and mesh, respectively. This characteristics are left constant for the remainding cases presented in this research.

BioChemFOAM complexity was reduced to consider only one species, nitrate ($NO3==NO_2^-+NO_3^-$), in order to reproduce the same physical and numerical conditions presented in (Schubert, 2009). Several steps were followed to ensure BioChemFOAM reproduces the conditions as closely as possible.

The first step was to adapt BioChemFOAM to solve the fate and transport of one species. This was done by turning on only the nitrate species in the model. The second step was to define a wall reactive boundary condition that resembled the one defined in FLUENT by (Schubert, 2009). BioChemFOAM was configured to reproduce this condition, as explained in section 6.2.2. Finally, the model's initial condition for nitrate was set to a constant value of 0.55mg-N/L, equal to the one measured at the entrance of the domain in 2009. This value was measured in a previous study by (Schubert, 2009).

6.2.2 Initial conditions (IC) and Boundary conditions (BC)

The value of the initial condition for nitrate (NO3) was set to the value measured in July 2009 by (Schubert, 2009), 0.55mg-N/L. The boundary condition was set in BioChemFOAM with the library Groovy, which is a library of functions that helps to define boundary conditions for a system of partial differential equations in OpenFOAM. The boundary condition defined at the river bed was set using the formulation of a Robin boundary condition or mixed boundary condition available in Groovy library. In the OpenFOAM library Groovy, this can be achieved by using the equation $kd\phi/dn+\alpha(\phi-\phi_0)=0$ (k is species conductivity; α is species convection

of mass; n indicates a normal direction to the river bed; ϕ: is the concentration of the species at the first cell attached to the river bed; ϕ_0 is the concentration at the sediment). The concentration at the sediment side is set to zero ($\phi_0 = 0 mg - N / L$) since it represents a typical value, see (James, Richardson, & Soballe, 2008) for characteristic nitrate and ammonia profiles in sediments in a Mississippi River backwater area. Then, the equation is reformulated as follows: $d\phi / dn + \beta(\phi - 0) = 0$, where only one coefficient is defined $\beta = \alpha / k$. The next step is to discretize the equation to get an expression for the concentration at the face attached to the river bed as follows (details on the derivation are not shown): $\phi_{\text{face}} = (1 - f).\phi_{\text{cellcentre}}$, where $f = (1 / (1 + A)); A = k / (\alpha * \Delta h) = \beta / (\Delta h)$, where Δh is the normal distance from the cell center attached to the sediment of the river bed. The final expression is implemented through the Groovy library and the parameter β is changed until the nitrate concentration resembles the measured values reported by (Schubert, 2009).

6.2.3 Numerical schemes

BioChemFOAM utilizes a splitting-operator technique (Cant & Mastorakos, 2008), to solve the system of partial differential equations. In the process of splitting, two sub-problems need to be solved in one particular time step. One sub-problem that solves time, advection and diffusion (T+A-D=0) components, and th other solves a system of ODEs for the chemical and biological processes (T=R). In the present case, no reactions are considered in the bulk flow. The terms in the T+A-D=0 equation are discretized, with thenumericla schemes shown in Table 6-1. The table also provides the configuration of the solvers.

Finally, BioChemFOAM utilizes only one step of the splitting-operator method, and the boundary conditions are imposed directly on the (T+A-D=0) equation.

Table 6-1. Numerical schemes utilized in BioChemFOAM when implementing nitrate transport. The interpolation of the velocity field is conducted with a linear approximation. PBiCG, the Preconditioned (Bi-) Conjugate Gradient method is utilized to solve the algebraic system of the equation with the DILU, Diagonal incomplete-LU, with assymetry for the preconditioning. The number of iterations is limited to 500, and tolerance is set to 1×10^{-5} with a relative tolerance of zero.

Mathematical expression	Name Numerical scheme
$\underbrace{\dfrac{\partial \left(\phi_i \right)}{\partial t}}_{\text{temporal variation}, \mathcal{T}}$	Euler
$\underbrace{\nabla \cdot \left(\mathbf{u} \phi_i \right)}_{\text{convection}, \mathcal{A}}$	Gauss linear
$\underbrace{\nabla \left(\mu_t \cdot \nabla \phi \right)}_{\text{diffusion}, \mathcal{D}}$	Gauss linear corrected

6.2.4 Results – comparison

BioChemFOAM model was modified successfully, and the fate and transport of nitrate was calculated. The physical time was set to 14 days, and the model reached the solution in 2 hours by using 8 processors. The general spatial distribution of nitrate was optioned and compared with measured data. The parameter β was selected by trial and error until a better solution was optioned. A better solution was defined when the spatial distribution of nitrate with $\beta = 4.0362e-5[1/m]$ in measured points is close to values calculated with BioChemFOAM.

In order to compare the solution optioned with BioChemFOAM, different figures were generated that display the model's performance. First, the spatial distribution of nitrate is compared in Figure 6-1with the values reported by (Schubert, 2009). Here, different cross sections were selected to further compare the results with FLUENT's solution and measured data. Figures 6-2, 6-3, and 6-4 show four cross sections and their comparisons with measured data and a previous study. In all of cases, the model was able to reproduce spatial patterns of

nitrate in the backwater area. In general, all figures show the tendency of assimilate more nitrate in zones of low velocity, such as the red circle shown in Figure 6-2 (left). On the other hand, points located in the main flow path, where velocities are high, i.e., $0.5m/s - 0.01m/s$, present a reduced uptake of nitrate by the river bed (see yellow oval in Figure 6-2, left). This is due to the strong currents that transport parcels of nitrate in a short period of time (e.g. The intense red zones in Figure 6-1 have a velocity that influences the transport of the species). This fast transport presents a time scale smaller than the time scales of the biological and chemical processes. In other words, there is not enough time for a parcel of species in those zones to be totally assimilated by the river bed.

Figure 6-5 shows a comparison of all points measured along the backwater area. The figure shows an improvement when using BioChemFOAM. The figure shows linear regressions for results optioned with BioChemFOAM and FLUENT. The regression line is slightly better with the proposed model. Additionally, a different metric was calculated to define the skill of the models (error). The metrics are calculated as the sum of all the normal distances for each point (e.g., square symbols in Figure 6-5, left) to the 45° line (which represents a perfect match between measured and calculated values). The respective metrics for BioChemFOAM and FLUENT are 1.47 and 1.85 (the smaller the better). The calculated metric shows that BioChemFOAM improves the calculated nitrate distribution in the backwater area.

Finally, a reduction of nitrate is calculated with concentrations and mass loading rates at the inlet and outlet of the backwater area. The calculation is done to further validate the processing of nitrate in the back water area when using a single species, nitrate (NO3). These results were compared with an empirical relation presented by (Seitzinger et al., 2002), where a removed nitrogen value can be calculated with an average depth and a time of travel. The nitrate fate and transport influence the remotion of nitrate in an aquatic ecosystem (see Figure 6-6 for a spatial distribution of nitrate for the present case). This distribution can be used to define a characteristic inlet and outlet mass loading rate. This information can be processed to obtain and estimate the reduction of nitrate in the backwater area. In this case, the reduction rate was 6.5%

(Figure 6-7, right). Additionally, a reduction rate was calculated from mass loading rates entering and exiting the backwater area as shown in Figure 6-7 (left). The figure compares two results BioChemFOAM with a reduction of about 4.2% with results from (Seitzinger et al., 2002) with a reduction of about 6.5%. The calculated reduction rate is of the same order of magnitude as the results in the study presented by (Seitzinger et al., 2002). We can conclude that BioChemFOAM gives a good approximation for the reduction of nitrate in a backwater area when a simple model is utilized to describe the fate and transport of nitrate.
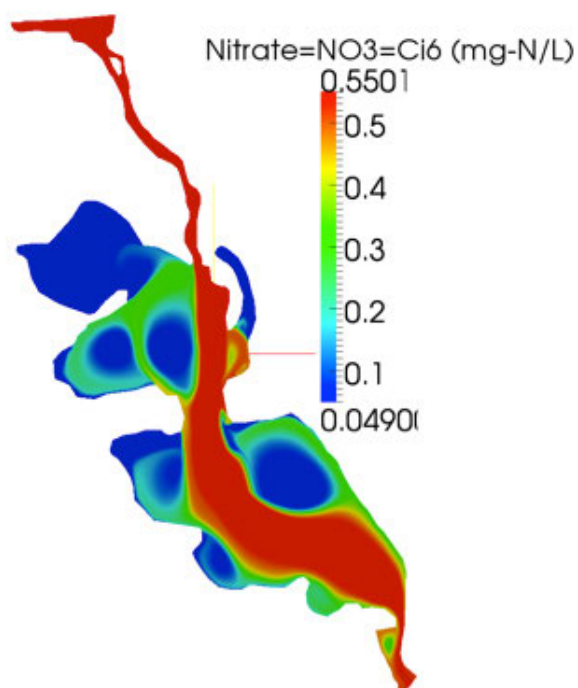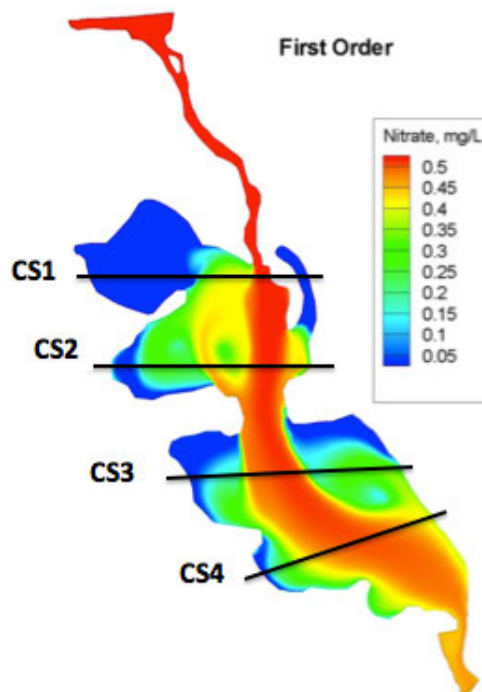
Figure 6-1. Nitrate spatial distribution comparison between BioChemFOAM (left) and FLUENT (right). Also cross section where the mesurements were taken in July 2009 by (Schubert, 2009) are presented, see CS1, CS2, CS3, and CS4. Contours taken at the first layer attached to the water surface.
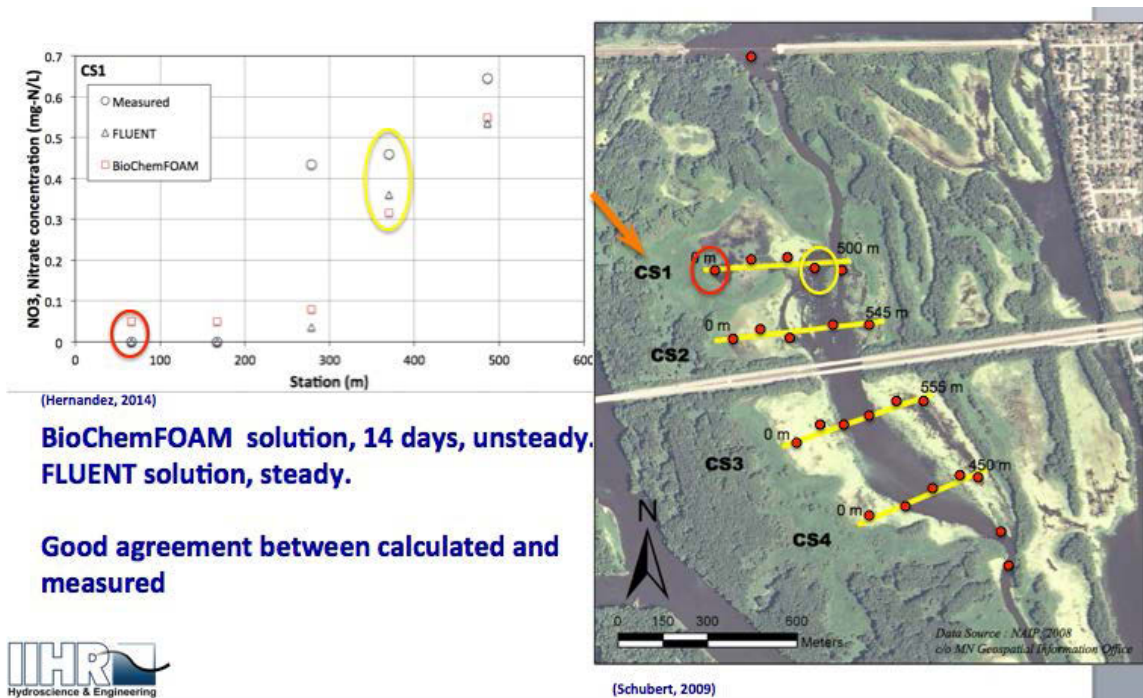
Figure 6-2. Nitrate distribution at Cross Section 1 (CS1). The yellow and red circles indicate a point on the right side of the figure. Comparison between measured data, BioChemFOAM, and FLUENT, cross section detail (left). Location of cross sections and points with concentration in Round Lake (right).
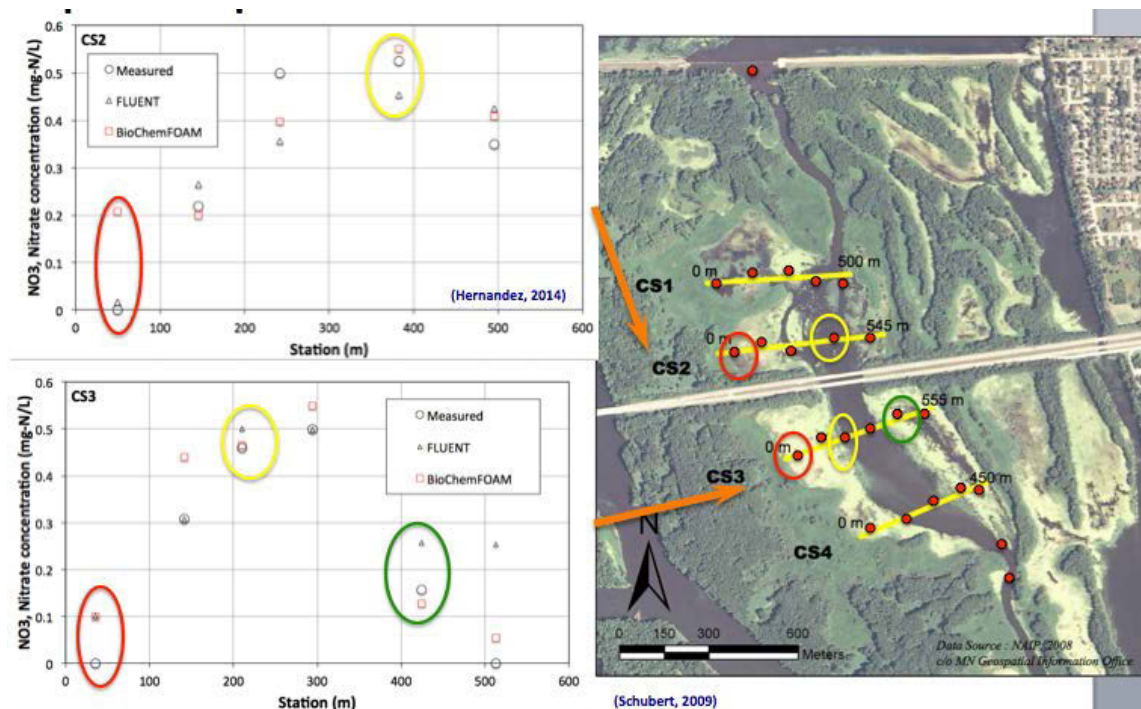
Figure 6-3. Nitrate distribution at Cross Sections 2 (CS2) and 3 (CS3). Yellow, green and red circles indicate a point on the right side of the figure. Comparison between measurements, BioChemFOAM, and FLUENT are located in the left figures. Cross section detail for CS2 (left top). Cross section detail for CS3 (left bottom). Location of cross sections and points with concentration in Round Lake (right).
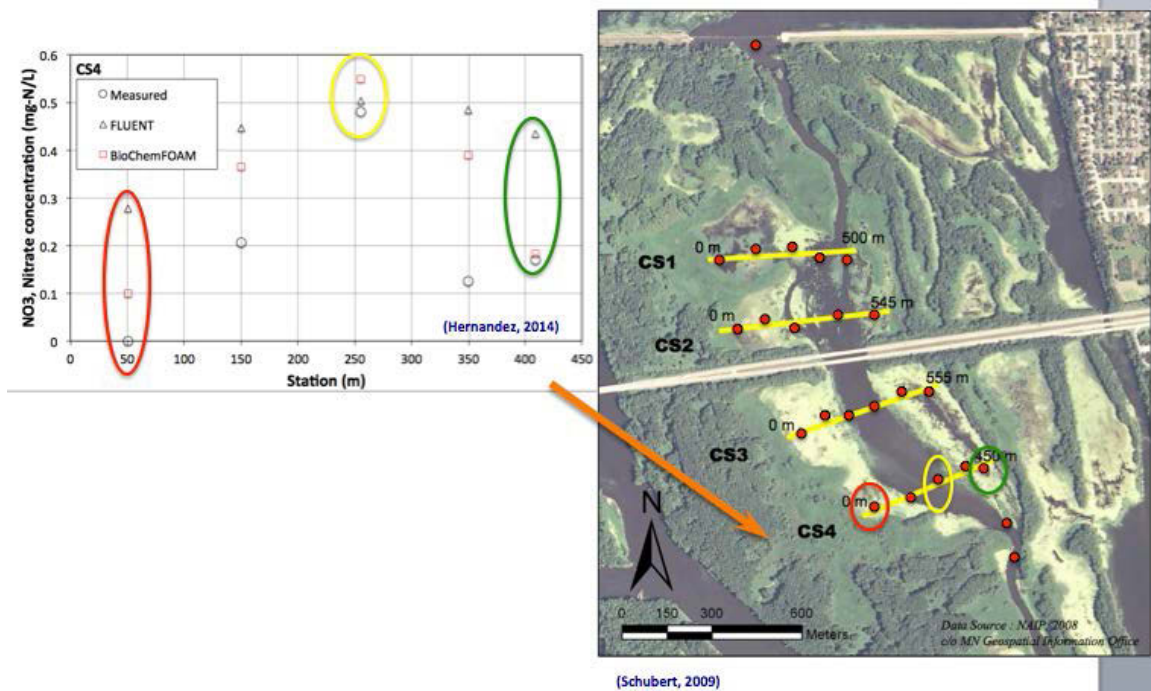
Figure 6-4. Nitrate distribution at Cross Section 4 (CS4). The yellow, green and red circles indicate a point on the right side of the figure. Comparison between measurements, BioChemFOAM, and FLUENT are located in the left figures. Cross section detail for CS4 (left). Location of cross sections and points with concentration in Round Lake (right).
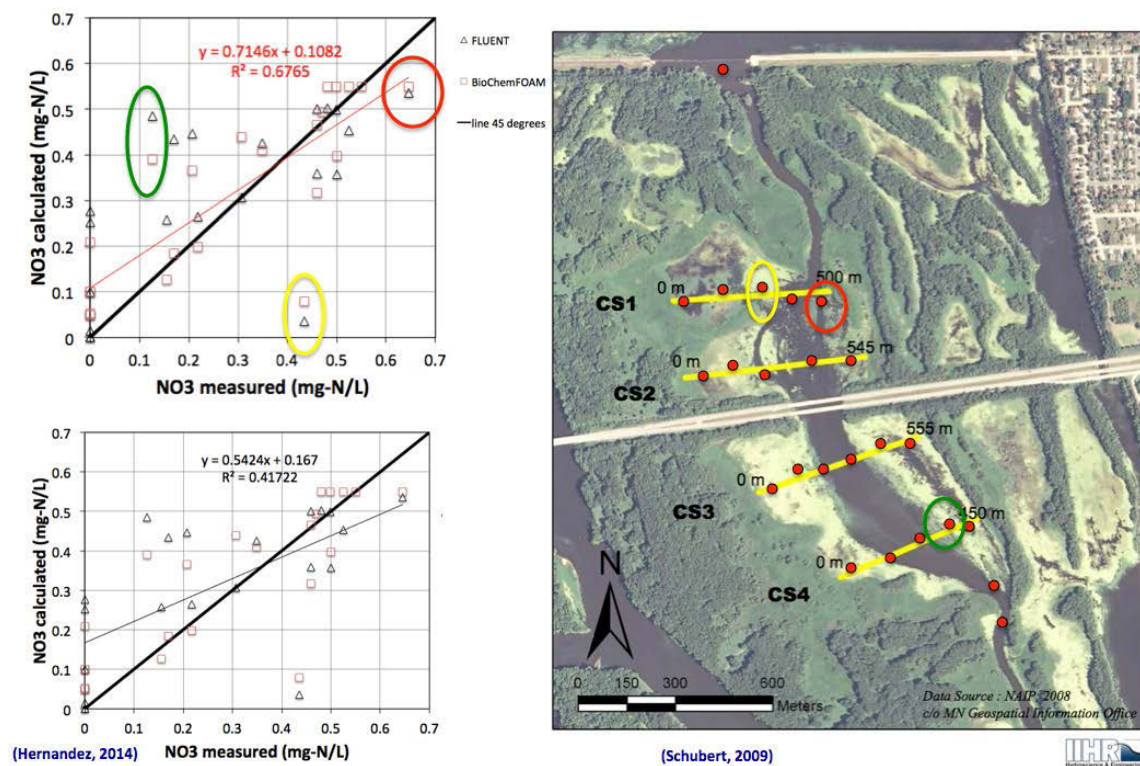
Figure 6-5. Nitrate spatial distribution in the backwater area. Nitrate measured vs. calculated with trend line for BioChemFOAM solution (left top) (red line). Nitrate measured vs. calculated with trend line for FLUENT (left bottom) (thin black line). Location of cross sections and points with concentration in Round Lake (right).
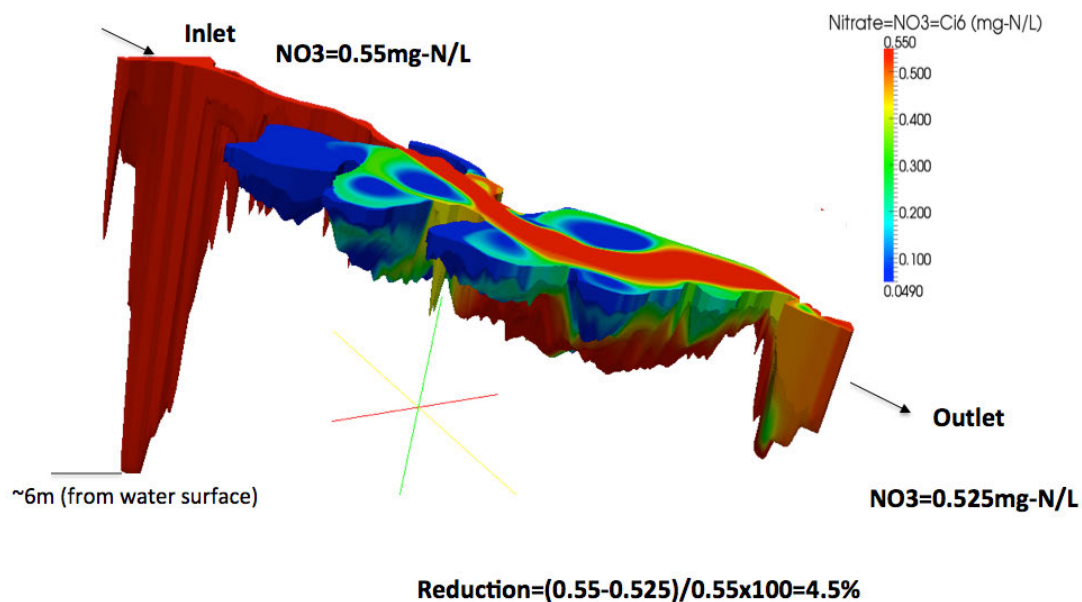
Figure 6-6. Nitrate spatial distribution over the backwater area, Round Lake, Mississippi River. In the figure, the vertical scale is exaggerated by a factor of 250, so the lowest point close to the inlet is about 6m depth from the water surface. The figure also shows the inlet and outlet concentration with a calculated reduction time of nitrate. The black arrows at the inlet and outlet represent the main flow path.
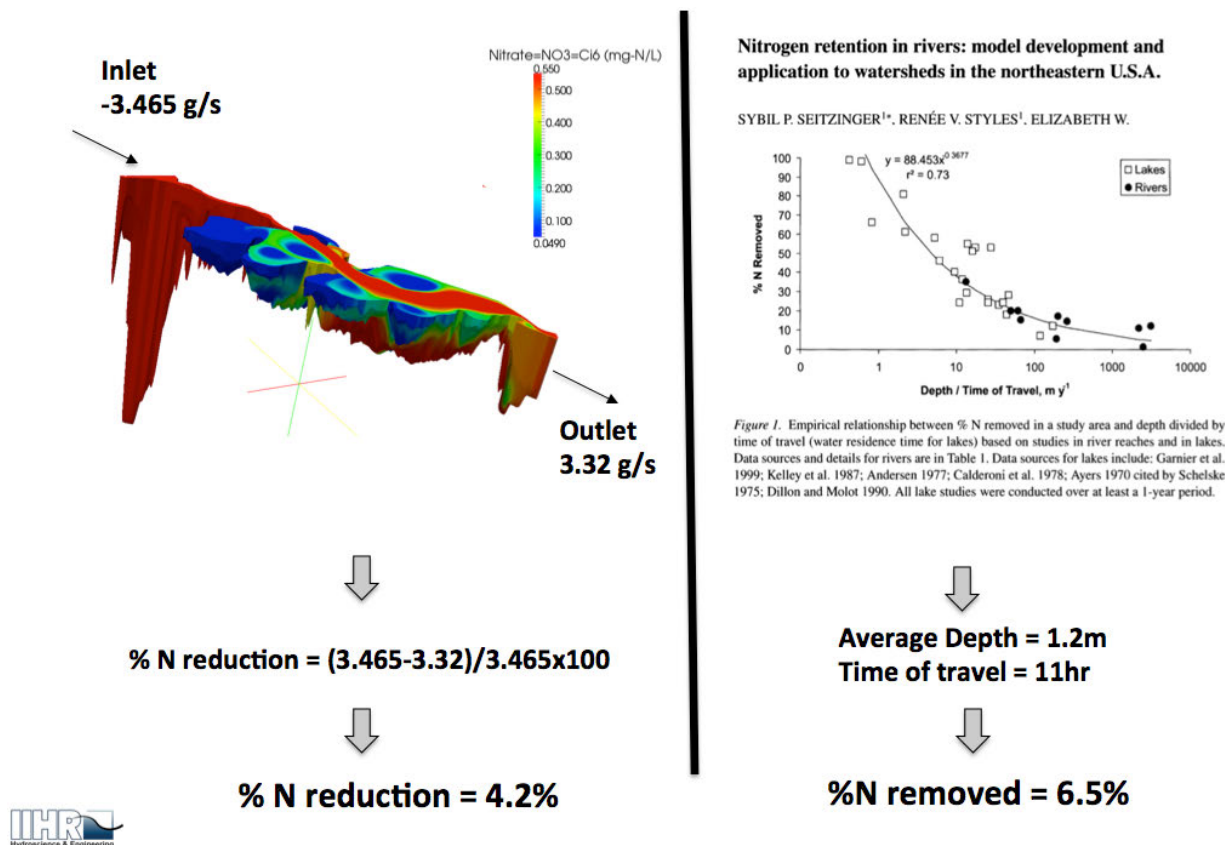
Figure 6-7. The comparison of reduction and removal of nitrate in the backwater area. Spatial distribution of nitrate with mass flow inlet and outlet (left top). Calculation of reduction of nitrate in the backwater area (left bottom). Schematic of reduction calculation with a formula presented by (Seitzinger et al., 2002) based on average depth and time of residence (right). The black arrows at the inlet and outlet represent the main flow path.

<u>6.3 Full BioChemFOAM parameterization for a characteristic</u>

<u>summer flow</u>

6.3.1 Collected information area of study - sample data

The bathymetry and measured concentration and discharge are the same as the ones presented previously. All data is for a typical summer period, July 2009. The mesh and location of boundaries can be seen from previous cases. Additional information regarding the characteristic concentration in Lake Pepin is processed in order to define IC and BC in BioChemFOAM. The values utilized are an approximate average for a summer period presented in (LimnoTech, 2007).

Additionally, temperature of air and light distribution at the water surface were obtained from meteorological data from the National Renewable Energy Laboratory (NREL), http://www.nrel.gov/rredc/.

6.3.2 Initial Conditions (IC) and Boundary Conditions (BC)

This section explains the definitions of initial conditions (IC) and boundary conditions (BC). The coefficients included in the model were previously presented in Chapter 3 when defining the parameterization included in BioChemFOAM.

The IC imposed in this case is constant for all of the species. This means that the spatial distribution of a particular species (e.g. nitrate, NO3) is fixed in all cells. Also the BC at inlet for nitrate was fixed to 0.55mg-N/L, as measured by (Schubert, 2009). The remaining species' concentrations were defined from characteristic values presented in a water-quality modeling study of Lake Pepin, [LimnoTech, 2007]. The report compares the measured concentrations against the concentrations calculated with the EFDC code. The figures presented in the final calibration of the report were utilized to extract the average concentration values for the summer 2009. Figure 6-8 shows an example of the results presented in the report. Characteristic values were obtained from time series from 2001. The characteristic approximated values are:

$Bx = 0.03 - mg - C / L$ (blue green algae defined from figure of time versus percentage of total biomass Figure 3-12 report [LimnoTech, 2007]), $DO = 6.5mg - O2 / L$, $T = 26^{o}C$, $DIP = PO4 = 0.035mg - P / L$, $NO3 = 2.2mg - N / L$ (value for comparison and not set as BC), $NH4 = 0.025mg - N / L$, $TON = 0.8mg - N / L$, $TP = PO4 + POP = 0.1mg - P / L$, $DON = 0.65mg - N / L$, $PON = 0.15mg - N / L$, $DOC = 15mg - C / L$ and $POC = 2.5mg - C / L$ (the values are average over a cross section).

The boundary conditions in BioChemFOAM were presented briefly in Chapter 3 and are discussed in more detail here. The BC values can be sub-divided in BC that influence the PDEs and the BC that influence the ODEs (this doesn't mean that they are not part of the same set of equations; this means that the solution strategy, splitting-operator method, can be adapted to impose boundaries in either of the sub-problems, as explained later in the theis). The inlet for all of the species is set as a fixed value (from characteristic values presented earlier, with one exception, Bx is 0.01mg-C/L. The value was selected since it is expected that algae will growth to values similar to the measurements in Lake Pepin). The remanding boundary conditions are set to a zero gradient with two exemptions; nitrate and dissolved oxygen.

The dissolve oxygen BC is embedded on the system of ODEs and acts only in cells (here, cells denote a volume element defined in the mesh generation, see Figure 5-3) attached to the water-air interface (WAI). This is done to make the code run faster in parallel. The inclusion of the BC in the ODEs implies that equation 3.79 has the reaeration term active only for cells attached to the WAI. The equation implemented at the WAI calculates a reaeration coefficient as follows, from (Chapra, 2008), as follows: $K_r = 0.166U_W^{1.64}(600 / Sc)^{0.5}$ (Kr can be recalled from equation 3.79 and is given in m / s). U_W is the wind speed in m / s, and it is set to $1.3m / s$ (fixed measured value for July 2009 at the area of study and reported in (Schubert, 2009)). Sc is the dimensionless Schmidt number which indicates the ability of the fluid to transport momentum and mass of a particular species, and it's given by $Sc = 0.9*(1953.4 - 128.0*T_k + 3.9918*T_k^2 - 0.05009*T_k^3)$, (Wanninkhof, 1992). T_k is given in degrees celsius (^{o}C). Additionally, the Saturation Dissolved Oxygen is calculated with

$DO_s = 1.42905 * exp(-73.4292 + 249.6339 * (100/T) + 143.3483 * (ln(T/100) - 21.8492 * (T/100)))$ as

presented by the USGS and reported in (Myers, 2011). T is given in degrees kelvin (K).

The nitrate BC is implemented in the ODEs. The value at the boundary is defined as

$k_{NO3} * NO3$, where k_{NO3} is the reaction coefficient with units on $1/s$. The value can be defined

as $K_{NN} * \theta^{(T-20)}$ as in (Schubert, 2009). The calibrated values for Round Lake presented by

[Schubert, 2009] are: $K_{NN} = 74.6 m/yr$, $\theta = 1.09$ and $T = 26.2^o C$. Those values were used to

calculate $K_{NN} * \theta^{(T-20)} = 4.04 \times 10^{-6} m/s$. In order to get a scale for the resistance when mass is

transported from the water to the sediment, a length scale is needed. $K_{NN} * \theta^{(T-20)}$ is divided by

the depth into the sediment where denitrification may occur, and a value of $10 cm$ is defined, as

recommended by (Di Toro, 2001). The final coefficient is given by

$k_{NO3} = K_{NN} * \theta^{(T-20)} * 1/0.1m = 4.04 \times 10^{-5} 1/s$.

Finally two boundary conditions were defined for the temperature and light in the WAI.

Since only one temperature value of $26^o C$ was reported in Round Lake, a meteorological station

in the La Croisse airport was used to adjust the air temperature function (T_a data from the

National Renewable Energy Laboratory). The adjusted sinusoidal function plus measured data

are presented in Figure 6-9. Light intensity at the surface was modeled as typical function e.g.

(Chapra, 2008) see Chapter 30 for solar radiation curves). The trends over time were obtained

from the time series of SUNNY direct normal radiation, which were provided by National

Renewable Energy Laboratory at the La Crosse airport. They typically increases from 5am to

noon and decrease from noon to 7pm. A typical distribution of light in July 2009 is presented in

Figure 6-10 with and adjusted equation implemented in BioChemFOAM. The BC for light was

set as a variable function at the water surface using the Groovy library available in OpenFOAM.

The BC for temperature was set as a heat flux ($q = \alpha(T - Ta)$; where α heat transfer coefficient,

T temperature of water and T_a temperature of air, at the water surface). Taking as a reference

the normal gradient at the water surface an equation of the form $k_1 dT/dn + \alpha_1(T - Ta = 0)$ is

defined with Groovy. The variables and coefficients of the previous equation are:

$k_1 = 1.44e - 7 + v_t$ is the effective thermal conductivity expressed as a function of a molecular

and turbulent contribution (m^2/s). The molecular contribution (1.44e-7m^2/s) is a typical average value optioned from values reported by (Martin & McCutcheon, 1998) (see Figure 16, Chapter 1). The molecular contribution to the thermal conduictivity is between order of magnitude also reported by (Gulliver, 2007) (see Table 3.1, Chapter 3) . The heat transfer coefficients is calculated with

$$\alpha = 4.6394991 = h = C(6.9 + 0.345U_w^2) = 0.62mb/^o C*(6.9 + 0.345*1.3^2)$$ (Ahsan & Blumberg, 1999). C is interpreted as a Bowen coefficient (the ratio between sensible heat and latent heat). U_w is the wind speed in m/s measured in July 2009, Round Lake as $1.3m/s$. The wind speed is assumed constant in the whole water surface.

6.3.3 Numerical schemes and review of solution strategy implemented in BioChemFOAM

The model presented in Chapter 3 is used in the present case. The *COD* equation is included only to test the numerical ability of the model when one species' reaction rate is very slow (time scale of years). This is done because there is no available data for the site of study. The consequences of such an assumption are minor in the DO equation, as mentioned by (Di Toro, 2001). More over, the strategy to solve the system of equations is summarized in Figure 6-11. At the top left corner of Figure 6-11 (a), a typical computational mesh (black boxes) is represented with an imposed velocity field (blue arrows) and species concentration (two species concentrations are represented by a circular and triangular shapes). The species are located in the first cell in the initial time, t_1, and then after a certain period of time the species concentration are advected (solves T+A-D=0) in the First cell, as shown in Figure 6-11 (b). Until this point, the PDEs are solved. Then, a second step is calculated were the species react (solves T=R), as shown in Figure 6-11 (c). This is the end of the second time step, t_2. Assuming that convergence is achieved in this time step, we can proceed to the next time step (gray arrow with caption "Initial

value for next time"), t_3. The cycle starts again and is repeated until the simulation time is reached.

Finally, the numerical schemes used for the other species are the same as the ones presented in Table 24, and no further discussion is presented here.

6.3.4 Results – comparison

BioChemFOAM was executed successfully for 26 days (computer time ~ 3 days with 160 cores at neon high performance computer cluster, The University of Iowa). The simulation starts at night and ends at night on the 26 day. This sections presents a series of figures that shows the ability to reproduce characteristic patterns of the state variables included in the model. The state variables are (see also Chapter 3, Tables 3-2 and 3-3): water temperature (T), light (I), algae concentration Bx, dissolved organic carbon DOC, dissolved orthophosphate $PO4$, dissolved nitrogen DON, ammonia $NH4$, nitrate $NO3$, dissolved oxygen DO, chemical oxygen demand COD, particulate organic carbon POC, particulate organic phosphorus POP, and particulate organic nitrogen PON.

The first set of figures presents the distribution of species when a steady solution is reached. The steady solution is defined as the time it takes for the model to reach a constant mass loading rate (i.e., that is the mass of the species over time that can be defined as $Q.C$, discharge times species concentration.) at the outlet. In this case it was 0.98 g/s (value calculated when integrating $\phi.\vec{V}\cdot\vec{dA}$ over the output surface). The inlet mass loading rate is always fixed to 3.465 g/s since the flow rate is constant and equal to 6.3 m^3/s.

Figure 6-12 shows that dissolved oxygen, temperature, and light remain constant at night at the first cells attached to the WAI. This is possible since BioChemFOAM considers a cyclic boundary condition for ligh and temperature which are the same in all the water surface. On the other hand, algae has an important distribution along the area of study, showing higher values on low velocity zones (see green to red contours in Figure 6-12(a)). Dark blue zones represent low

algae growth, whihch are zones with higher velocities that limit the availability of nutrients. Also, light green zones show a clear growth of algae since the availability of nutrients is not limited by the flow field. This means that the flow is almost stagnant. Therefore, nutrients spend enough time in those zones to be consumed by algae and by the BC at the WSI. In general, the model was able to reproduce characteristic values that were collected from a similar study in Lake Pepin (LimnoTech, 2007).

Figure 6-13 shows the spatial distribution of algae, total organic nitrogen (TON), nitrate (NO3), and total phosphorus (TP). TP remains constant in all of the domains (at first cell attached to the water surface) with except for in a few zones where the concentration is low (see blue zones in Figure 6-13 (d)) and the velocity gradients are located in a slow moving eddy. The TON spatial distribution is heterogeneous along the backwater area. Two zones with higher concentrations are shown in red in Figure 6-13 (b). This is due to the fact that the IC were set at 1.25mg-N/L, which imposed an initial high storage in areas where velocity is low and there is not a direct reaction with the river bed. This condition enhances the reaction of TON in the bulk of the flow.

Figure 6-13 (c) shows the spatial distribution of nitrate concentrated in the main channel (see red to green contours in the figure). Also, Figure 6-13 (c) shows zones where the nitrate was assimilated by the boundary condition defined at the river bed (see dark blue zones). These results were expected since the only important processes affecting the fate of nitrate are the molecular diffusion and the boundary condition uptake. Condition that is imposed by the actual modeling tool, BioChemFOAM.

Figure 6-14 shows the distribution over the study area for dissolved organic nitrogen (DON), particulate organic nitrogen (PON), dissolved organic carbon (DOC), and particulate organic carbon (POC). DON has a low reaction in zones where velocity is high (~0.1-0.58m/s) from the input (see blue zones) until it reaches a zone where the velocity is low (0-0.04m/s) that the concentration starts to react and is accumulated (see zone were blue contour turns green in Figure 6-14 (a)). DON is not distributed uniform illy along the domain. It is possible to see zones

where DON is stored (see red zones in Figure 6-14 (b)). These zones are generated by the flowing water entering and the initial conditions defined in the model. Since the velocity is so low, DON tends to be stored until it is washed out by slow currents or reacts. The DOC distribution is homogeneous in zones where velocity are about 0m/s to 0.05m/s (see blue zones in Figure 6-14 (c)). Finally, POC was deposited in zones with low velocity (see blue and light blue zones in Figure 6-14 (d)) and transported in zones with high velocity (see red to green colors in Figure 6-14 (d)).

Figures 6-15, 6-16, 6-17, and 6-18 show the three-dimensional spatial distribution of the species in the backwater area under study. These figures provide a spatial view of the species considered in BioChemFOAM and characteristic features imposed by the fate and transport of species (see captions on figures).

Figure 6-19 shows a temporal distribution of nitrate (NO3) and illustrates the influence of the boundary condition defined for the removal of nitrate at the bed of the backwater area. The important point is that nitrate is processed near the bed of the backwater area in zones where velocity is low, as shown by Point 2 (blue contours). In contrast, Point 1 (red contours) points to a zone were transport is more important and limits the uptake of nitrate at the boundary. Also, it is possible to red zones in each cross section, that transport more nitrate (located at the center of the cross sections) and green zones that transform more nitrate. In this context, transform means not only that nitrate reacts in the bulk of the flow due to low denitrification (triggered by DOC) but also that it is assimilated by the boundary condition at the bed. Finally, figures (b) through (j) show how nitrate concentration changes over time and how it is processes along the backwater area.

In general the results reproduce an expected distribution of species compared with characteristic values taken from Lake Pepin, (LimnoTech, 2007).
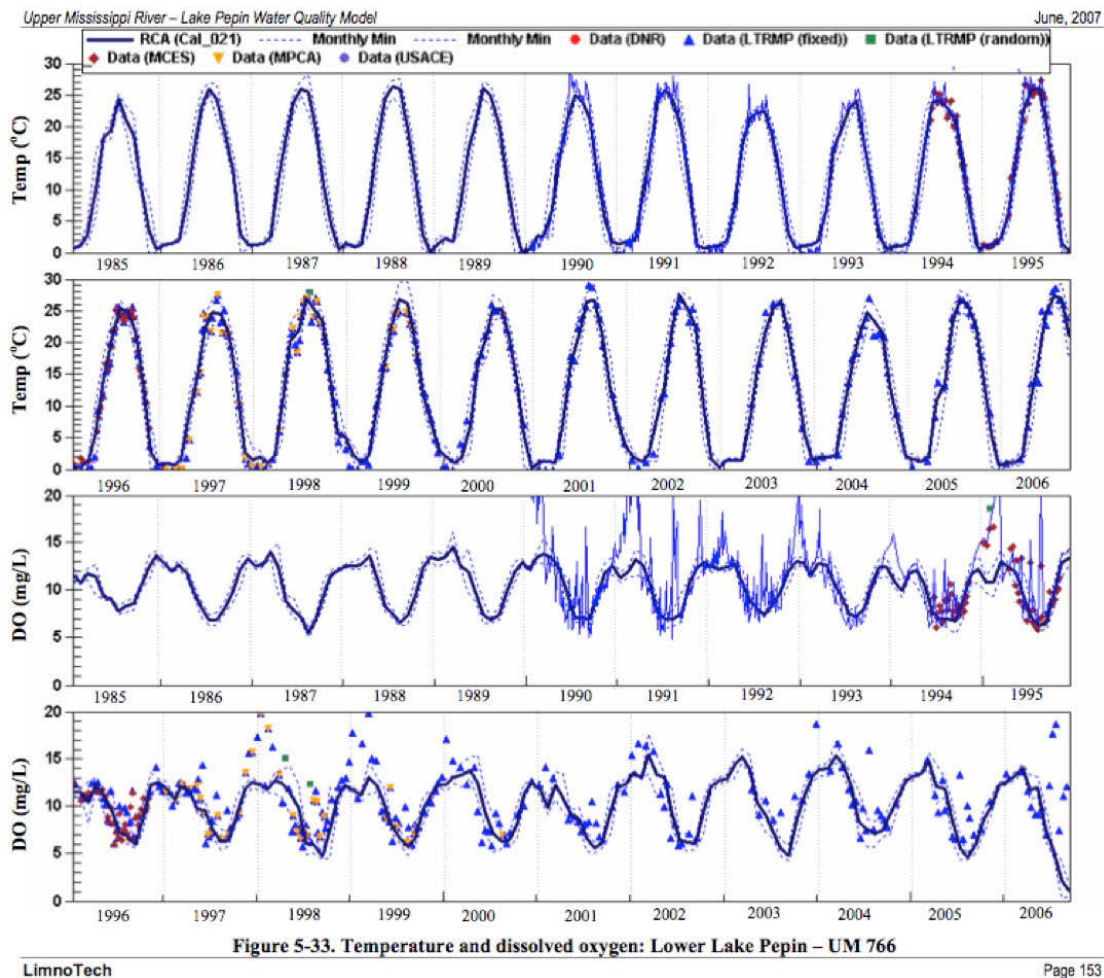
Figure 6-8. Evolution of Temperature and Dissolved Oxygen in Lake Pepin, figure from (LimnoTech, 2007) report.
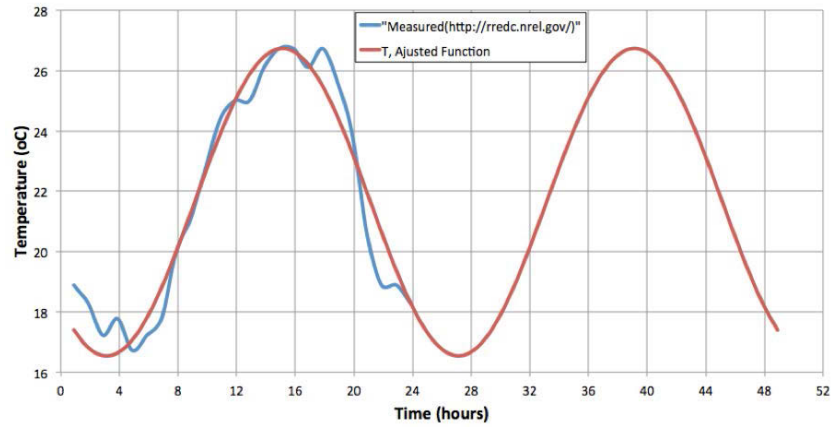
Figure 6-9. Air temperature distribution. Measured and adjusted values. The adjusted function is $T_a = A.\sin^2((\pi/24).t - B)$ with coefficients $A = 10.1897$, $B = -3.14416$, and $C = 16.5435$. t is time in seconds, and T_a is the temperature of air given in $^o C$.
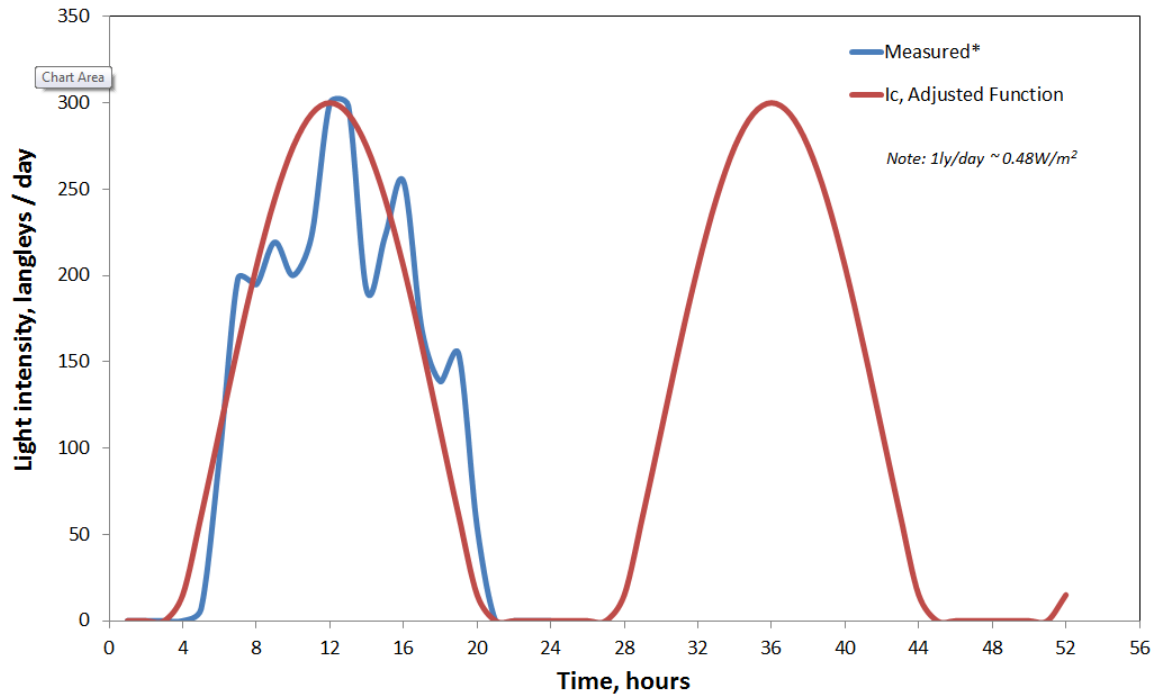
Figure 6-10. Light intensity distribution. Measured and adjusted values. The adjusted function is $I_c = A.\sin^2((\pi/24).t - B)$ with coefficients $A = 380$, $B = 0.0$, and $C = -80$. t is time in seconds, and I_c is the light intensity given in ly/day. *http://rredc.nrel.gov/. The light values are taken as constant regarding of weather conditions. The adjusted values are characteristic for a summer period.
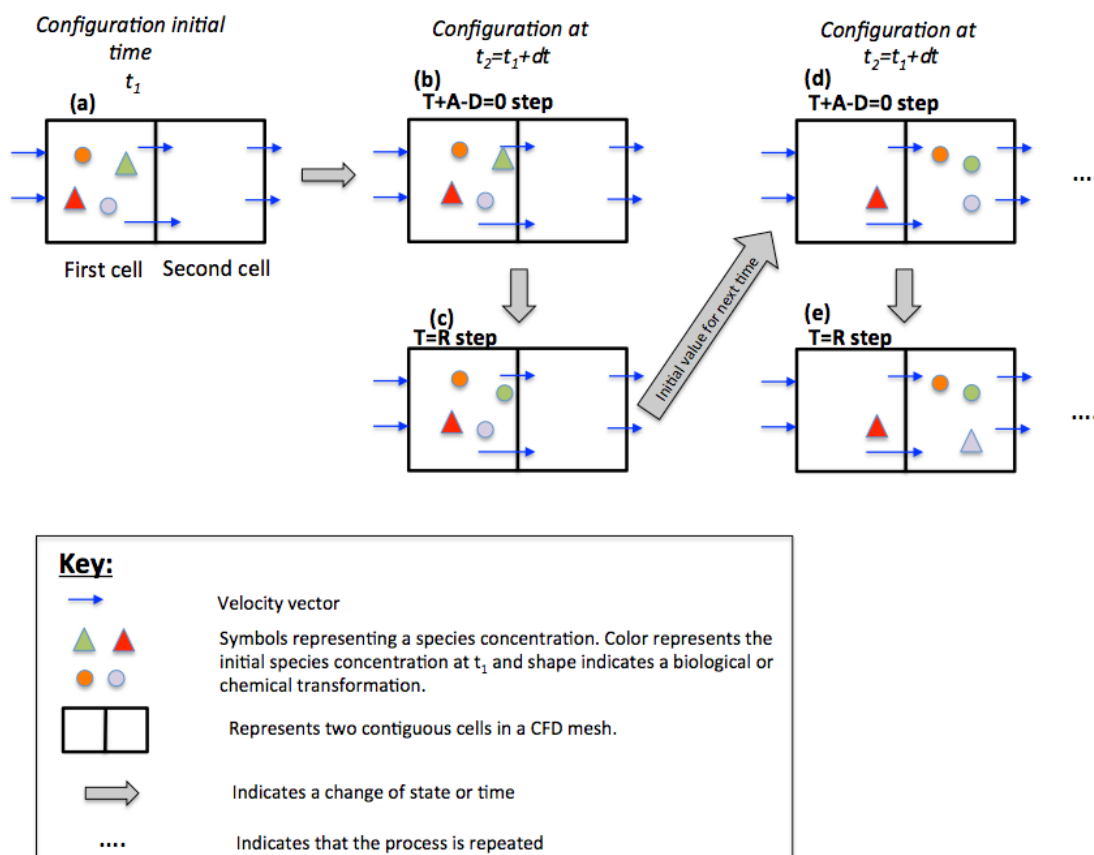
Figure 6-11. Numerical method implemented in BioChemFOAM. The sketch shows a typical iteration procedure when calculating the fate and transport of species. E.g., in interpreting symbols, from figure (b) to (c), a reaction takes place that transforms the green triangle into a green circle. This means that the species is transformed to another one by biological or chemical reactions.
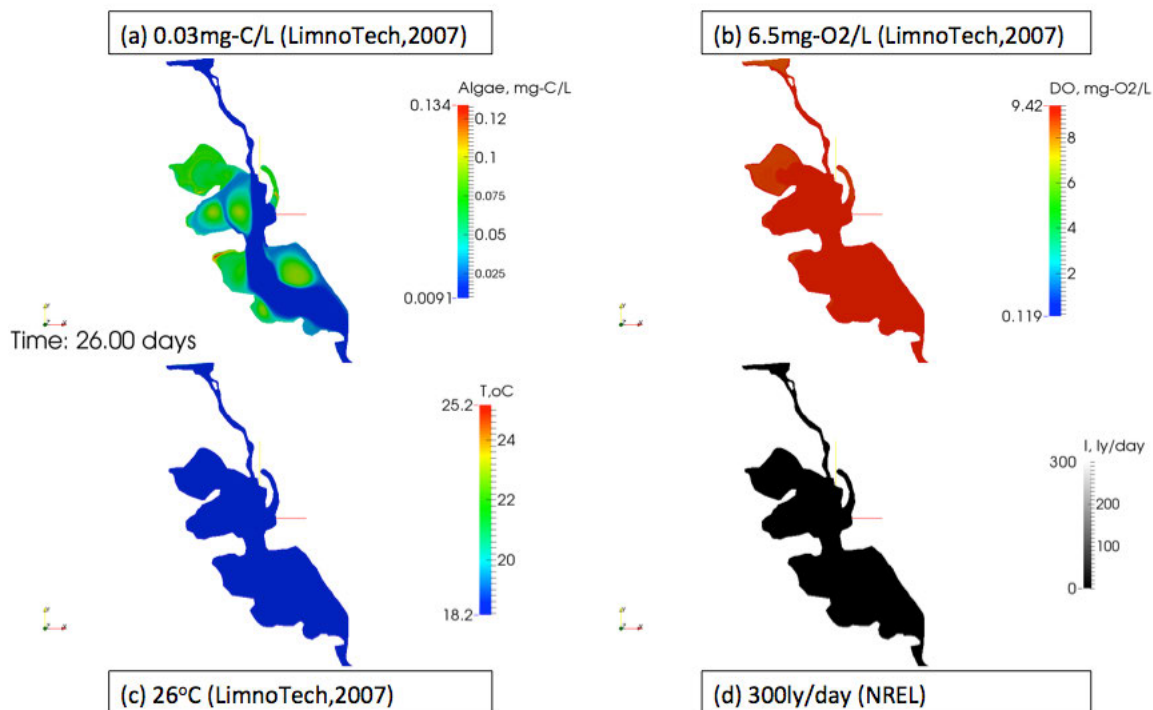
Figure 6-12. BioChemFOAM spatial distribution at 00:00 (night of the 26th day of simulation) of temperature (a), dissolved oxygen (b), temperature (c), and light intensity (d) at the first cell attached to the water surface. The figure also shows a characteristic value for each parameter enclosed in a rectangle. NREL stands for the National Renewable Energy Laboratory, http://www.nrel.gov/rredc/. Contours taken at the first cell attached to the water surface.
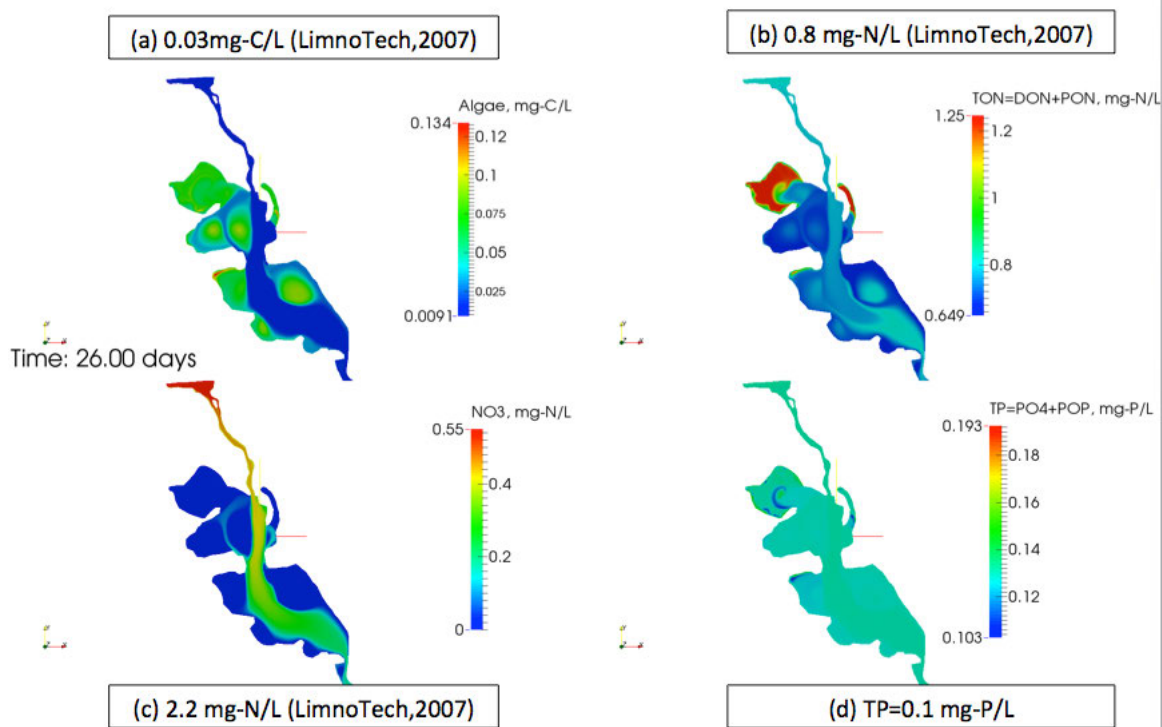
Figure 6-13. BioChemFOAM spatial distribution at 00:00 (night of the 26th day of simulation) of algae (a), total organic nitrogen (b), nitrate (c), and total phosphorus (d); at the first cell attached to the water surface. The figure also shows a characteristic value for each parameter enclosed in a rectangle. NREL stands for the National Renewable Energy Laboratory, http://www.nrel.gov/rredc/. Contours taken at the first cell attached to the water surface.
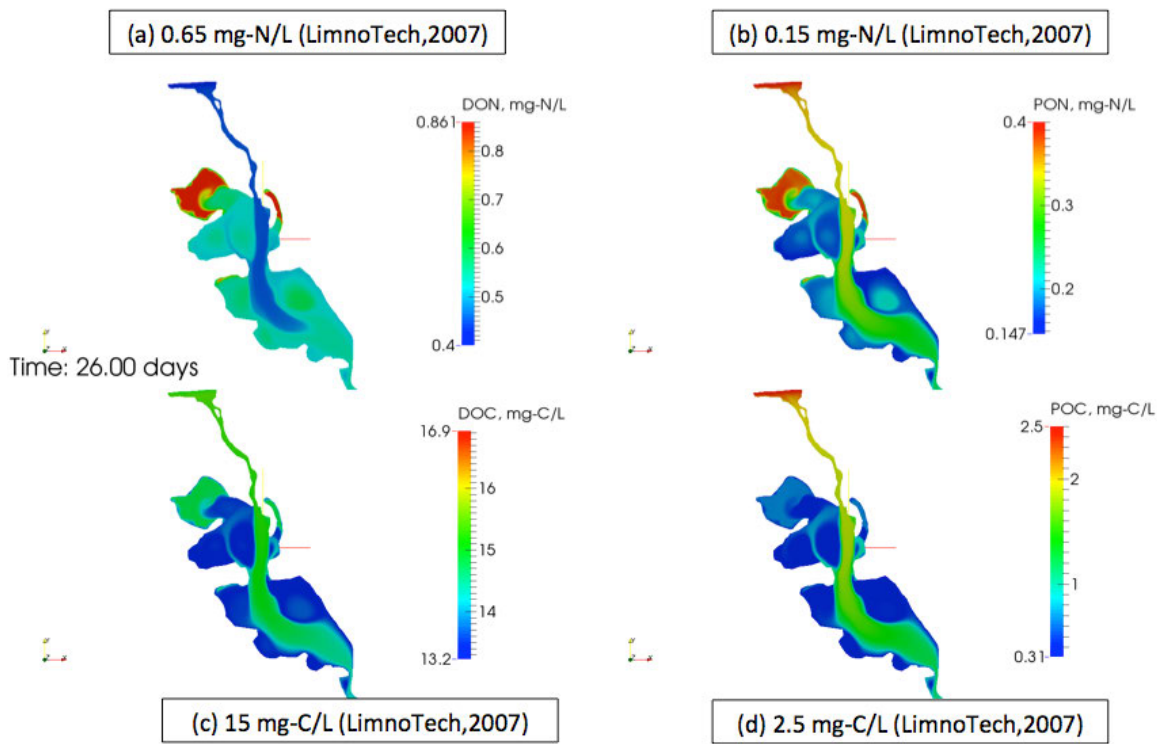
Figure 6-14. BioChemFOAM spatial distribution at 00:00 (night of the 26th day of simulation) of dissolved organic nitrogen (a), particulate organic nitrogen (b), dissolved organic carbon (c) and particulate organic carbon (d); at the first cell attached to the water surface. The figure also shows a characteristic value for each parameter enclosed in a rectangle. NRELstands for the National Renewable Energy Laboratory, http://www.nrel.gov/rredc/. Contours taken at the first cell attached to the water surface.
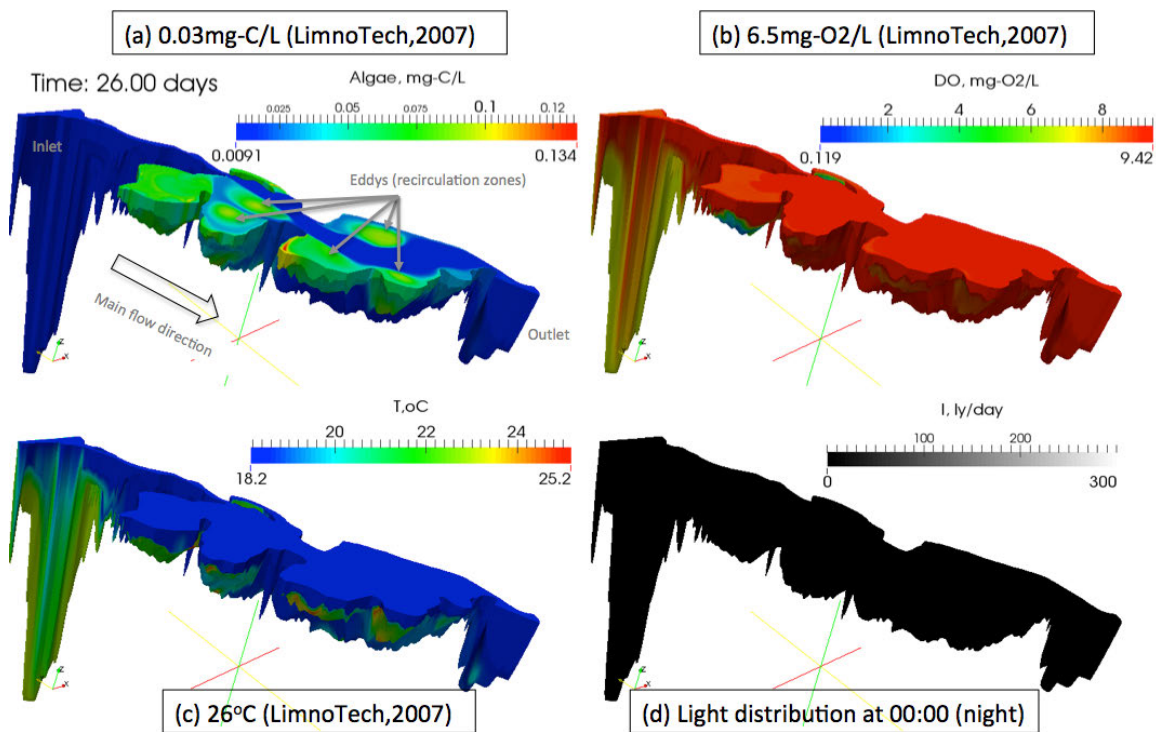
Figure 6-15. BioChemFOAM three-dimensional spatial distribution at 00:00 (night of the 26th day of simulation) of algae (a), dissolved oxygen (DO) (b), temperature (T) (c), and light (I) (d). The figure also shows a characteristic value for each parameter enclosed in a rectangle. Sub-Figure (a) shows the location of the characteristic recirculation zones, inlet, outlet, and main flow direction.
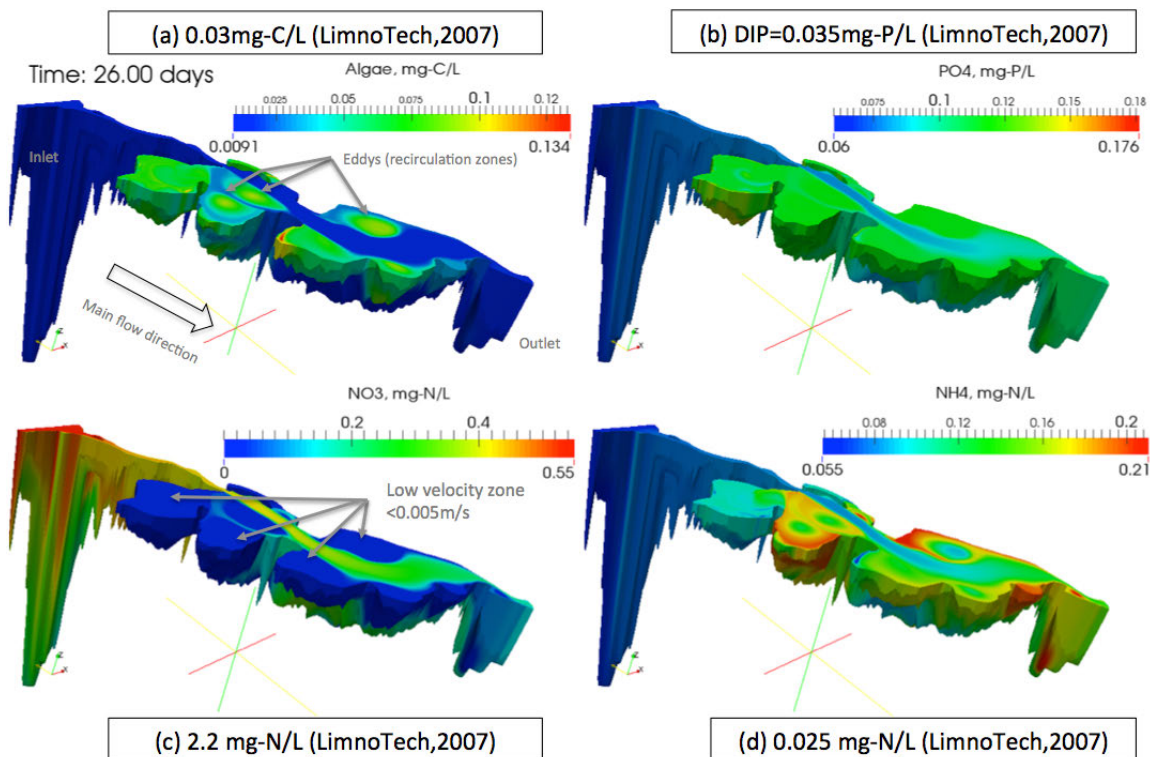
Figure 6-16. BioChemFOAM three-dimensional spatial distribution at 00:00 (night of the 26th day of simulation) of algae (a), dissolved oxygen (DO) (b), temperature (T) (c), and light (I) (d). The figure also shows a characteristic value for each parameter enclosed in a rectangle. Sub-Figure (a) shows the location of the characteristic recirculation zones, inlet, outlet, and main flow direction.
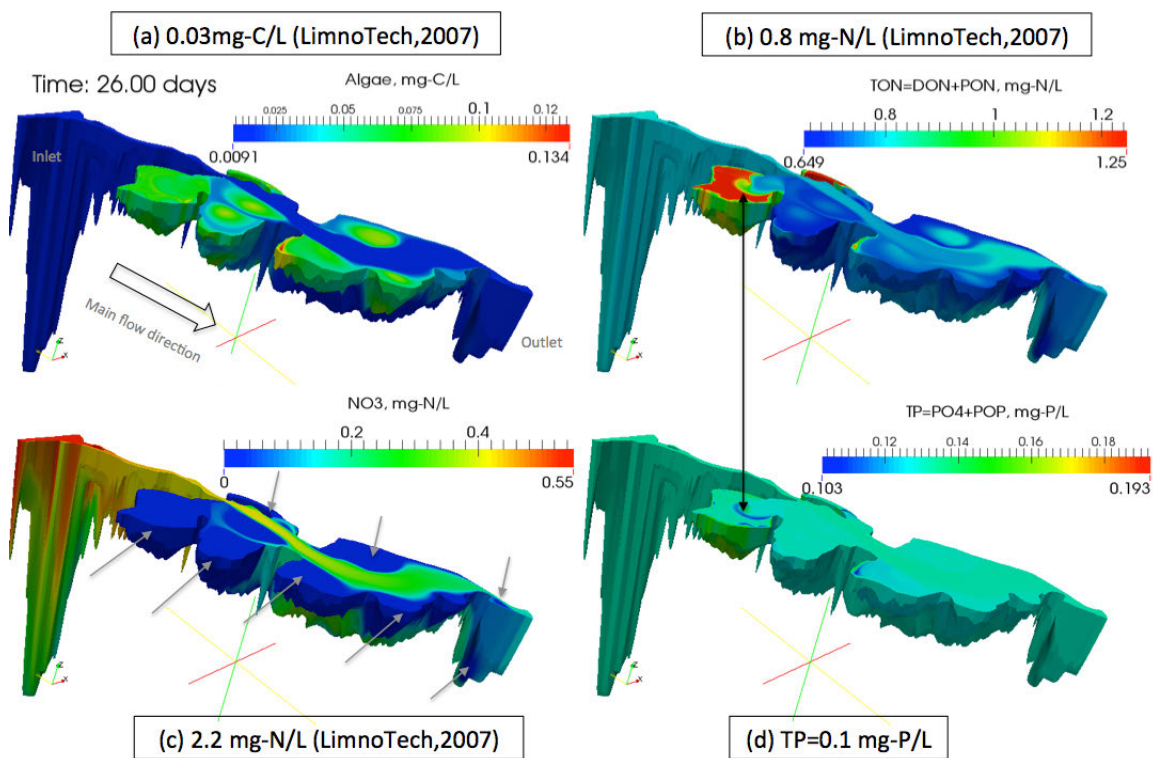
Figure 6-17. BioChemFOAM three-dimensional spatial distribution at 00:00 (night of the 26th day of simulation) of algae (a), dissolved orthophosphate (PO4) (b), nitrate (NO3) (c) and ammonium (NH4) (d). The figure also shows a characteristic value for each parameter enclosed in a rectangle. Sub-Figure (c) demarcates zones with zero nitrate concentration using gray arrows. Sub-Figure (b) and (d) are connected with a black arrow that indicates similar flow patterns due to small eddies.
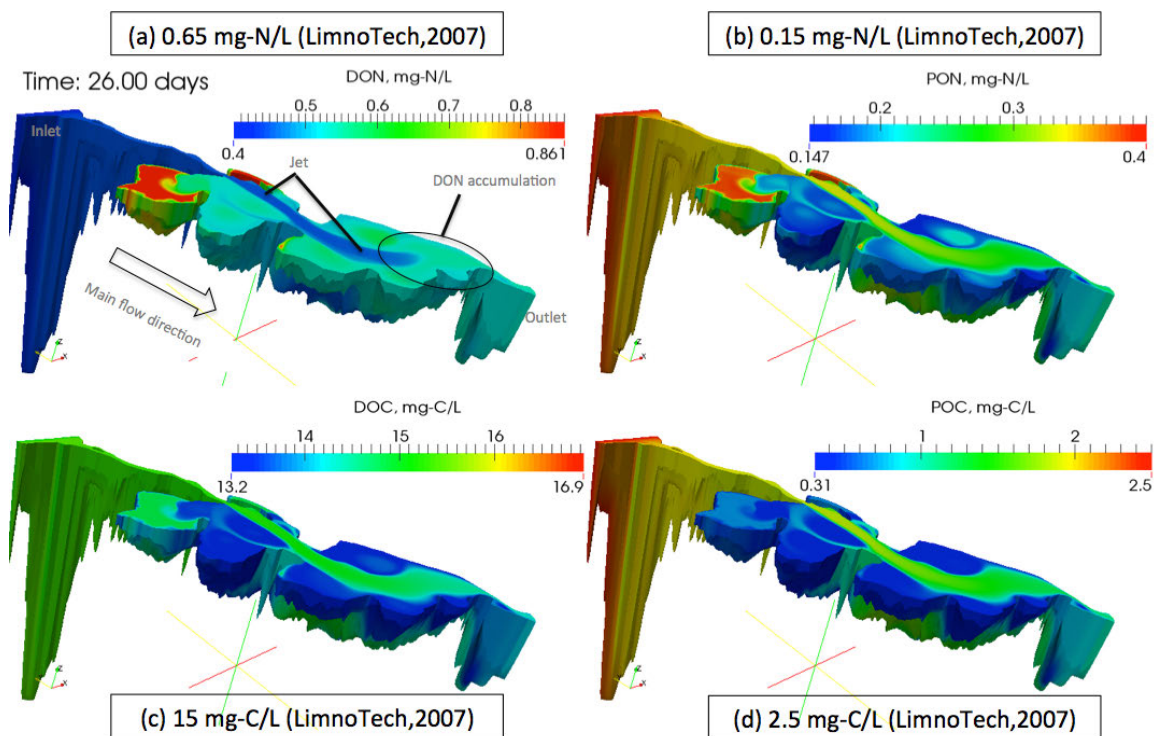
Figure 6-18. BioChemFOAM three-dimensional spatial distribution at 00:00 (night of the 26th day of simulation) of dissolved organic nitrogen (DON) (a), particulate organic nitrogen (PON) (b), dissolved organic carbon (DOC), (c) and particulate organic carbon (POC) (d). The figure also shows a characteristic value for each parameter enclosed in a rectangle. Sub-Figure (a) shows a zone where DON has accumulated and a jet location that influenced the concentration right before it reached the accumulation zone (blue contour 0.4 turns into light green contour ~0.6).
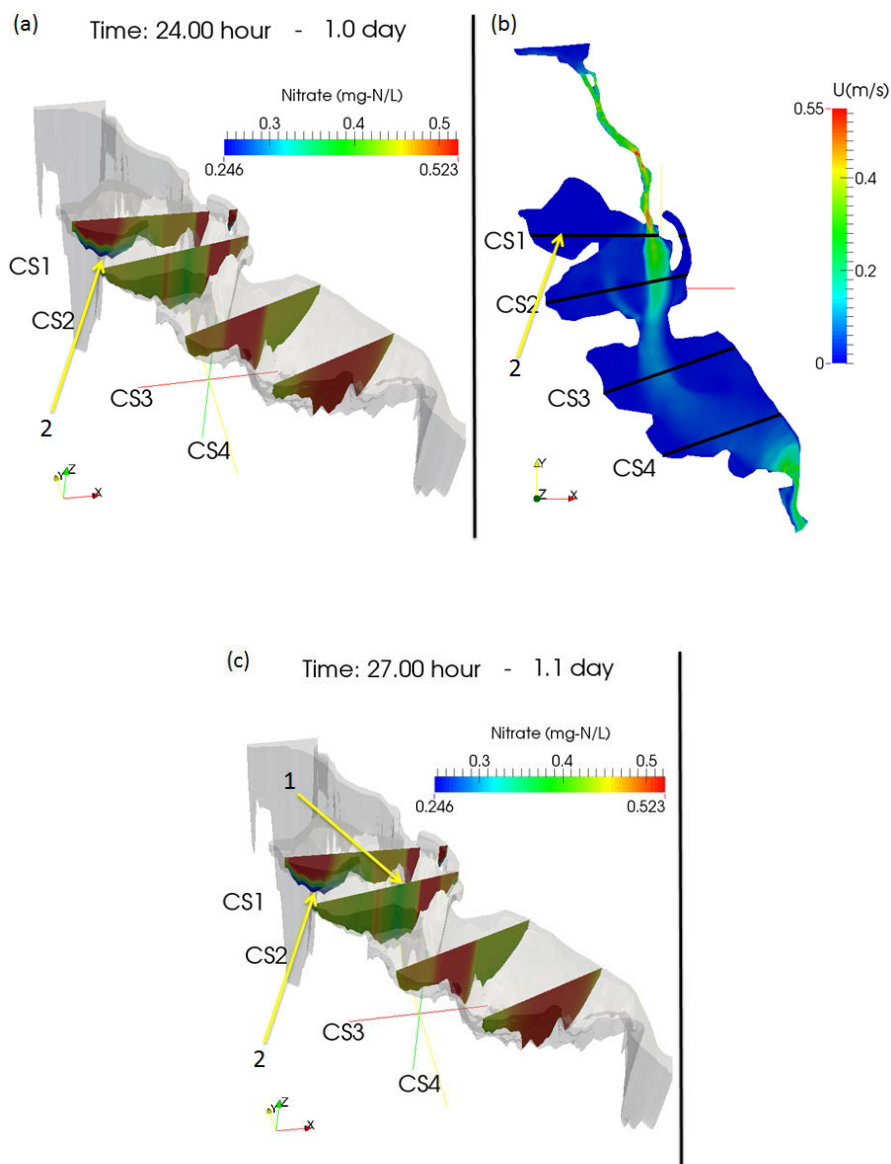
Figure 6-19. BioChemFOAM temporal evolution of nitrate (NO3) in four cross sections indicated by CS1, CS2, CS3, and CS4. (a) Contours of nitrate at the end of the first day of simulation. (b) The distribution of velocity magnitude, location of cross sections and location of points 1 and 2. (c) Contours of nitrate at 17 hours of simulation. Number 1 in (a) indicates a point where nitrate has been removed since it is located at the center of an eddy and has a low velocity. Number 2 in (a) indicates a point at the bottom of CS1 where the reactive boundary condition is acting as a sink to remove nitrate (thin blue contours attached to the bottom of the cross section). Details of contour of nitrate over time can be found in Figures B-9, B-10, B-11, and B-12.

6.4 Response of BioChemFOAM to different IC and nitrate inputs

when a steady physical solution is reached

6.4.1 Case configuration - IC, BC, constant parameters, numerical

schemes

The only difference with previous case, section 6.3, is that the IC for nitrate changes. All other ICs are left constant. Also, the BC values are the same as presented in Section 6.3. The first case (IC_0.01) has an IC for nitrate equal to 0.01 mg-N/L. The second case (IC_0.35) has an IC for nitrate equal to 0.35 mg-N/L. Both cases were calculated until a steady solution was reached for nitrate. This was done by calculating over time the mass loading rate of nitrate at the outlet. Then, both spatial concentrations were compared at cross sections defined in Figure 6-20. Finally, both cases were compared with the results calculated in Section 6.3, which defines an IC of 0.55mg-N/L for nitrate (IC_0.55).

For Case IC_0.01, BioChemFOAM was executed for 14days. At 14 days, the mass loading rate of nitrate at the outlet became constant. The mass loading rate of nitrate at the outlet was utilized in cases IC_0.35 and IC_0.55 to define a steady state. IC_0.35 reaches a steady nitrate mass loading rate at the outlet in 21 days. IC_0.55 reaches a steady nitrate mass loading rate at the outlet in 26 days.

6.4.2 Results showing independence of species distribution when

different initial conditions (IC) are imposed on nitrate

The results showing nitrate distribution are presented in Figures 6-20, 6-21, 6-22, and 6-23. Figure 6-20 shows the spatial distribution of nitrate for 0.01 mg-N/L(left part of the figure) and 0.35 mg-N/L (right part of the figure) nitrate concentrations at the first cell attached to the water surface. The figure shows that both solutions have the same spatial distribution. Furthermore, it shows the values of the mass loading rate that agrees within 0.6% (|0.9857-

0.9914|/09857*100 ~ 0.6%), indicating that a steady solution for nitrate has been achieved (see MFR values on figure).

Figures 6-21 and 6-22 compares the contours of nitrate for four cross sections. Figure 6-21 shows the same nitrate concentration distribution.

Figure 6-22 (a) and (b) shows a Zone A where both cases reproduce the same flow patterns. Additionally, Figure 6-22 (c) and (d) shows a Zone B where the two cases mismatch. Zone B has a low velocity (<0.005m/s). The combination of low velocity and low initial conditions for nitrate enhance the fast assimilation of nitrate at the bottom boundary (Zone A, Figure 6-22 c). The differences in those zones shows that the IC values affect the distribution of nitrate in regions were transport does not plays an important role.

Figures 6-23 and 6-24 show the influence of eddies or recirculation zones in concentrations of nitrate in Cross Section 2 (see orange arrows and box). The influence of the flow field can be seen as a medium concentration of nitrate (see light blue contours in the top left of Figure 6-23, concentration is about ~0.1 mg-N/L). The zone represents a slow moving flow path that transports species. The transport is from CS2 to CS1 (see yellow arrow in Figure 6-23). Regions outside these flow path have a lower concentration, meaning more nitrate is being processed.

The spatial distribution of other species is presented in Appendix B. The main points are:

1. Even though the mass loading rate for nitrate at the outlet is constant and the internal spatial distribution of nitrate is the same for all cases (IC_0.01, IC_0.35 and IC_0.55, see Zone A in Figure B-1), the concentration distribution of the remaining species may be different (see Zone A in Figures B-2, B-3, and B-4). This indicates that the remaining species are actively being transported and transformed, which means that reaching a steady state solution for all species may need more computational time (see next section scenarios for a steady sate solution for all species). This point also explains why the spatial distribution of species is not the same in Zone B indicated in Figure B-1.

2. IC values influence the spatial distribution of species in zones were flow velocity is low, < 0.001 m/s. Lower values defined as IC for nitrate are assimilated faster (see Zone A in Figure B-1) than higher values (see Zone B in Figure B-1).

3. The solution also indicates that not all species reach equilibrium at the same time (see Figures B-2 to B-21).

Figures B-7 and B-8 show a top view of species distribution along the backwater area compared with three different initial conditions: 0.01, 0.35 and 0.55 mg-N/L.

In general, the Figures shown in Appendix B show that modeling of biological and chemical processes is influenced by the selection of initial conditions. This indicates that it takes more time for some of the species to reach a steady state. It was shown that independently of the IC for nitrate the spatial distribution remains the same when imposing different IC for nitrate (see Figures 6-20, 6-21and 6-22).

6.4.3 Closure

This section presented the initial conditions (IC) sensitivity analysis for nitrate and indicated that changing the IC for nitrate does not affect its spatial distribution. Both solutions were compared at a steady state for nitrate based on mass loading rates at the outlet. It also shown that even though a steady solution for nitrate was found, the other species have not reached a steady solution. This implies that more computer time is needed to reach a steady solution. Furthermore, the disparity among reaction rates indicates that the system's dynamics have different time scales, which make it challenging to fully calibrate BioChemFOAM. These time scales dictates the reaction rates of different species included in BioChemFOAM. Unfortunately, no data for other species are available to refine the model calculations.

Two additional remarks can be made. From the calculated solutions, it is possible to state that the farther from a physical solution the longer it takes for the model to reach a steady solution for all of the variables. This was demonstrated by comparing concentration distributions

of nitrate for cases IC_0.01 and IC_0.35. Here, the models run for a limited period of time (IC_0.01 for 14 days, IC_0.35 for 21 days, and IC_0.55 for 26 days). In order to reach a steady solution for all the processes, the model needs to be run for longer periods of time. This may be unfeasible for other ecosystems. The second remark pertains to the spatial distribution of species for cases IC_0.35 and IC_0.55. Although not of all the species reached equilibrium, the figures presented in Appendix B show that both models start to have the same spatial distribution for all the species.

Despite this limitation, BioChemFOAM shows a strong ability to analyze dynamical patterns when multiple species are included in an aquatic ecosystem. The model was also able to reproduce species distributions within expected values in natural systems.

Additionally, this section highlights the need to perform spatial and temporal measurements of species in order to further validate all of the processes included in BioChemFOAM.
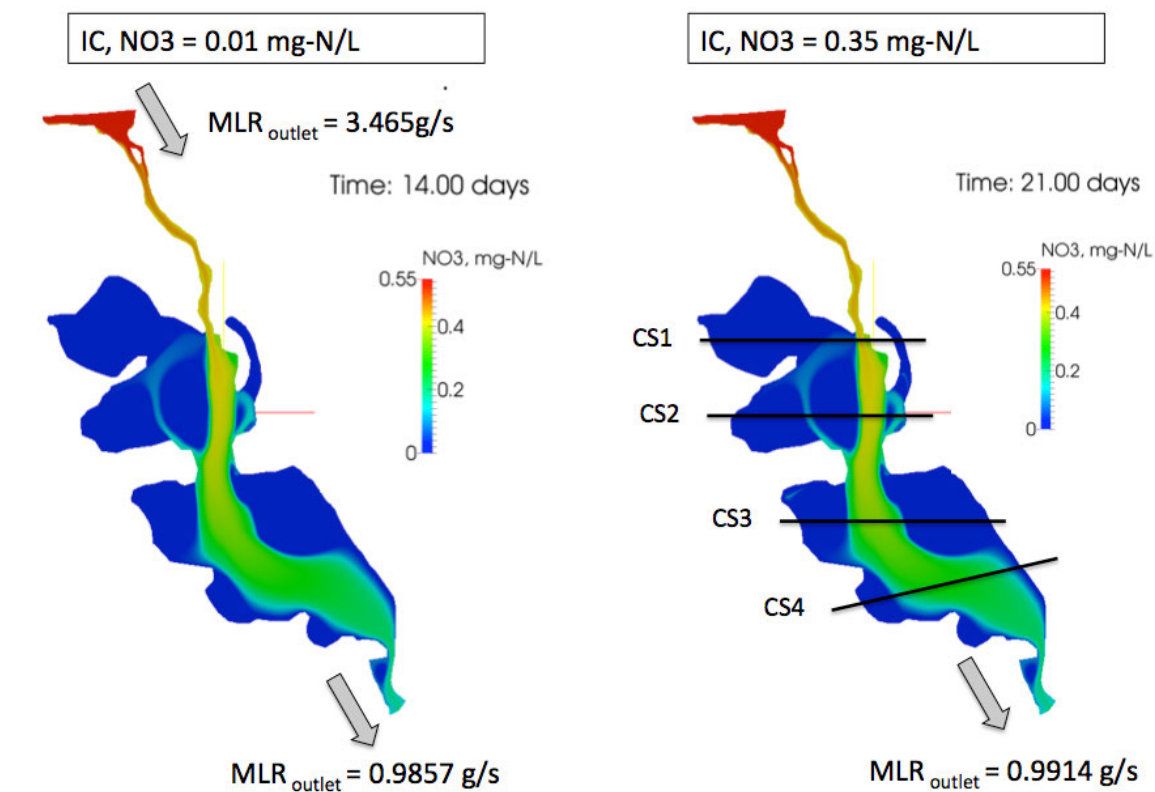
Figure 6-20. Spatial distribution of nitrate for two different initial conditions. IC nitrate = 0.01 mg-N/L (left). Also shown are the mass loading rates at the inlet, 3.465g/s, and outlet, 0.9857 mg-N/L. IC nitrate = 0.35 mg-N/L (right). MLR stands for Mass Loading Rate. Both initial conditions were defined uniformly in the mesh, see Figure 5-3.
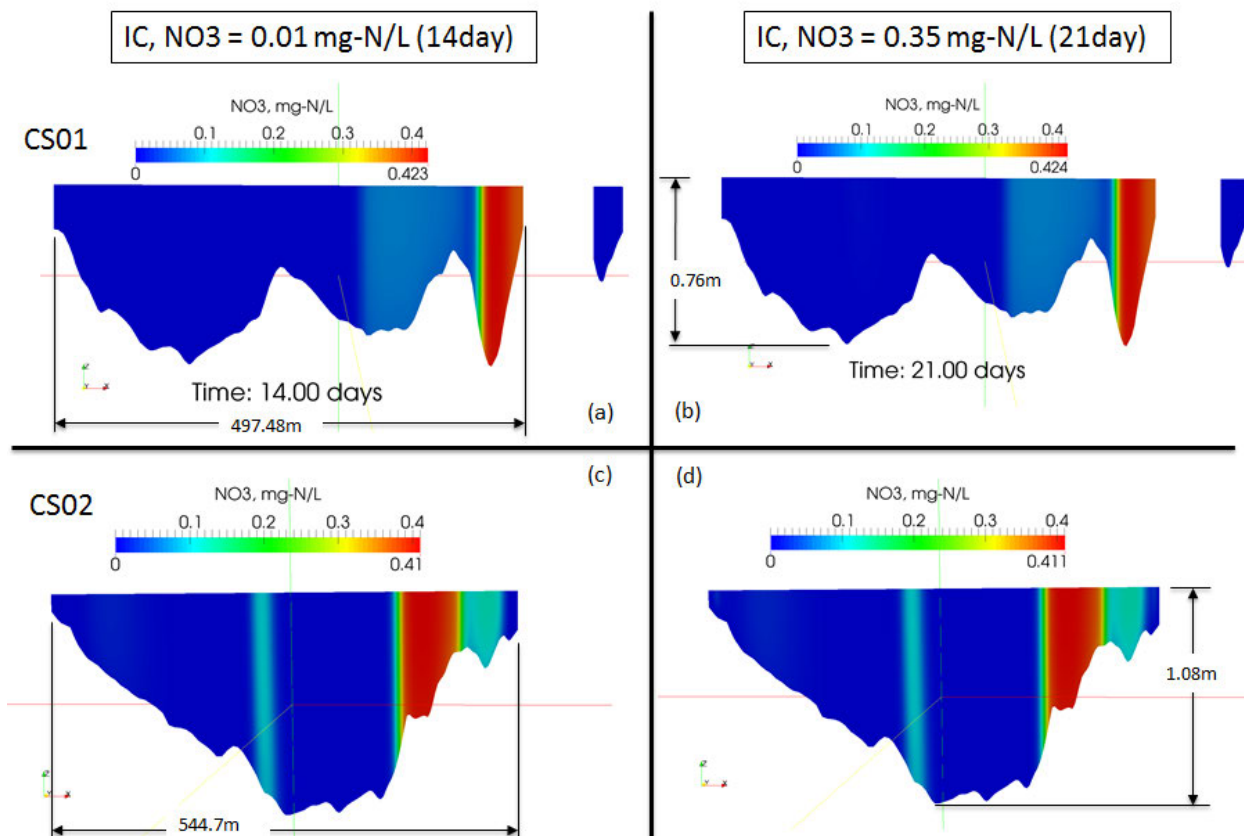
Figure 6-21. Contours of nitrate concentration at Cross Sections 1 and 2 for two ICs. (a) IC = 0.01 mg-N/L, Cross section 1 at 14 day. (b) IC = 0.35, Cross Section 1 at 14 day. (c) IC = 0.01mg-N/L, Cross Section 2 at 21 day. (d) IC = 0.35mg-N/L, Cross Section 2 at 21 day. ICs stands for Initial Conditions. The Cross sections location can be recalled from Figure 6-20. All cross sections are presented looking upstream.
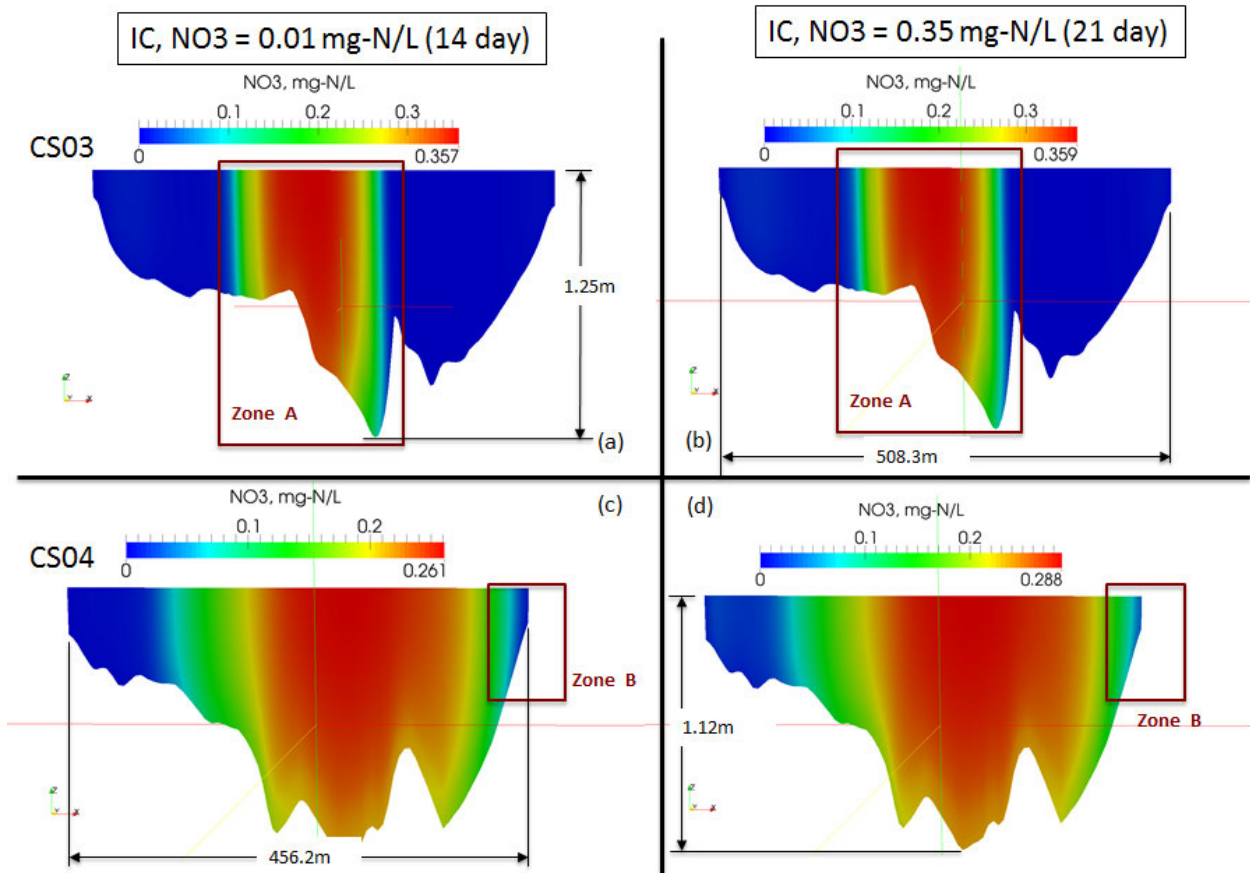
Figure 6-22. Contours of nitrate concentration at Cross Sections 3 and 4 for two ICs. (a) IC = 0.01 mg-N/L, Cross section 1 at 14 day. (b) IC = 0.35, Cross Section 1 at 14 day. (c) IC = 0.01mg-N/L, Cross Section 2 at 21 day. (d) IC = 0.35mg-N/L, Cross Section 2 at 21 day. IC stands for Initial Conditions. Zone A shows a region with similar nitrate distributions. Zone B shows the differences in spatial distribution. The Cross section's location can be recalled from Figure 6-20. All cross sections are presented looking upstream.
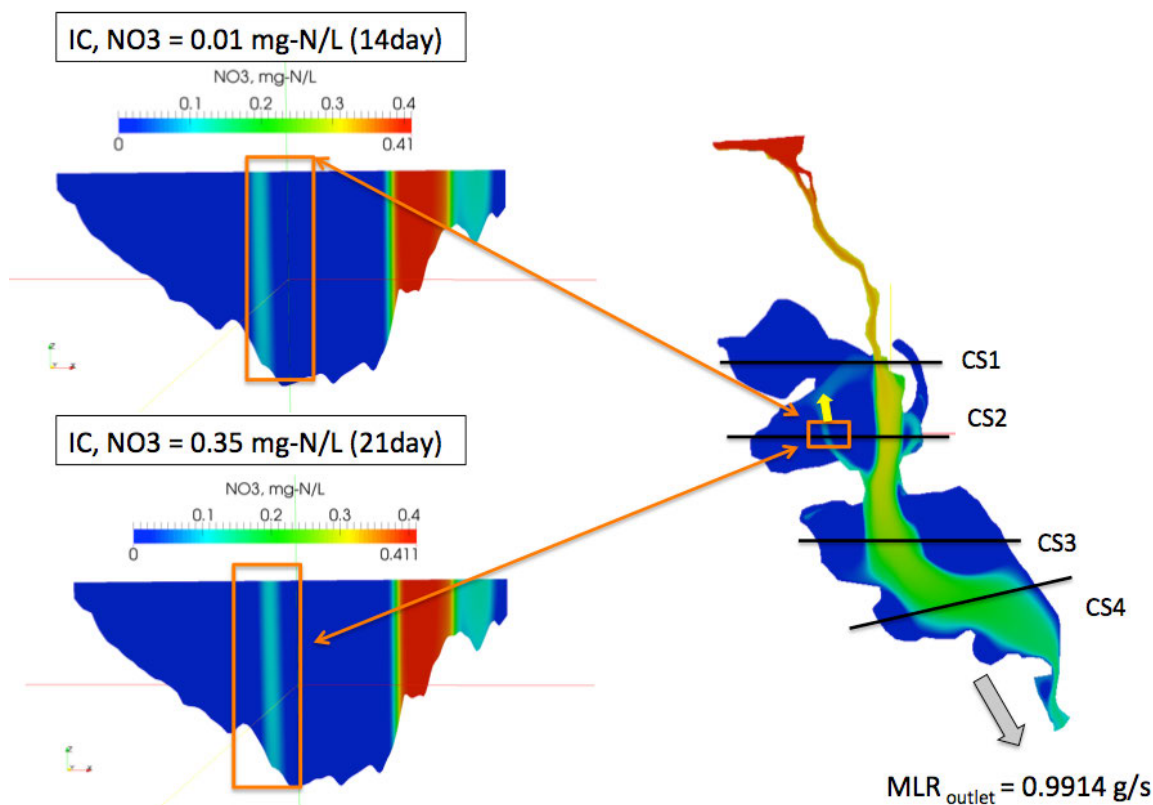
Figure 6-23. The influence of recirculation zones on nitrate distribution. Nitrate concentration contours at Cross Section 2 for ICs = 0.01mg-N/L at 14 days (top left). Nitrate concentration contours at Cross Section 2 for ICs = 0.35mg-N/L at 21 days (bottom left). Spatial distribution of nitrate concentration indicating location of cross sections (right). The orange arrows show a recirculation zone and its effect on the vertical distribution of nitrate (see left figures). The yellow arrow indicates flow direction (see left figure). All cross sections are presented looking upstream.
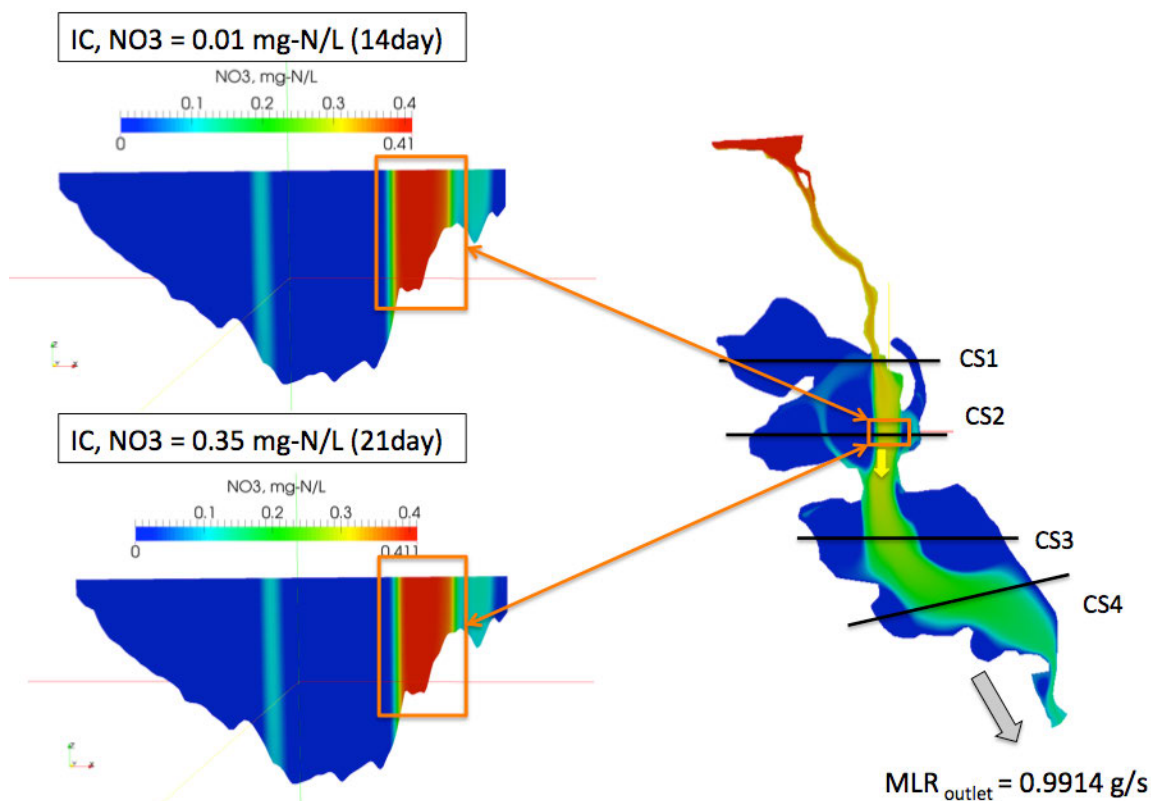
Figure 6-24. The influence of the main channel flow on nitrate distribution. Nitrate concentration contours at Cross Section 2 looking upstream for ICs = 0.01mg-N/L at 14 days (top left). Nitrate concentration contours at Cross Section 2 looking upstream for ICs = 0.35mg-N/L at 21 days (bottom left). The spatial distribution of nitrate concentration indicating the location of cross sections (right). The orange arrows show a main channel flow zone and its effect on the vertical distribution of nitrate (see left figures). Yellow arrow indicates flow direction (see left figure). All cross sections are presented looking upstream.

6.5 Application of BioChemFOAM to calculate nitrate removal percentages in an aquatic ecosystem

6.5.1 Case configuration - IC, BC, constant parameters, numerical schemes

This section presents an application of BioChemFOAM using nitrate spatial distribution in Round Lake, a backwater area located in the Mississippi River. The main objectives are: to show that BioChemFOAM is able to give characteristic spatial distributions of nitrate and percentages of nitrate reduction (PNR) within published data and to test BioChemFOAM parameterization when given limited data. At the moment, there is no data set to fully validate all species. Therefore, the present application is limited to the evaluation of only those processes that influence nitrate dynamics in aquatic ecosystems. The remaining species' concentrations and coefficients are left constant and within characteristic values from Lake Pepin, see Section 6.3 and Chapter 3.

In order to evaluate the ability of BioChemFOAM to give physically valid solutions, a sensitivity analysis is presented by calculating percentages of nitrate reduction (PNR) when varying the following three primary parameters that influence nitrate fate (see Equation 3.68): inlet concentration of algae (Bx), reaction coefficient at the bottom for nitrate (k_{NO3}) and nitrification at the bulk of the flow (Nit_m, see Equation 3.75). All other parameters and coefficients are left constant, as presented in Section 6.3. These parameters were selected since they directly influence the nitrate concentration in the system. Measured values are also available to compare the spatial distribution of nitrate in Round Lake (see section 6.2). All other coefficients affecting the remaining species are left constant and equal to those defined in Chapter 3.

The remainder of this section is organized as follows: 1) first orders of magnitude of denitrification are discussed and calculated from published data; 2) second orders of magnitude

for nitrification are presented; and 3) the strategy to define a physically valid solution is described. The physically valid solution here is defined as a combination of parameters that

- reproduce published PNR values,

- reproduce similar spatial distribution of nitrate concentrations,

- and reproduce a similar order of magnitude for denitrification and nitrification processes affecting nitrate dynamics.

The orders of magnitude to define fate and transport processes at water-sediment interface (WSI) were calculated using published concentration profiles of nitrate at WSI for a backwater area called the Finger Lakes that is located in Pool 5 of the Mississippi river (James et al., 2008). It has a maximum depth of 2.0 m, an average depth of 0.60 m, an area of 11ha and a volume of 67500m^3. The discharge varies from 0 m^3/s to 1.6 m^3/s, and its mean theoretical water residence is about 1.7 days. This work is selected because it may represent conditions as Round Lake's also located in the Mississippi River, and there is not available data in the study area. The work was used to estimate a reaction rate, k_{NO3}, which is implemented as a boundary condition at the bed in BioChemFOAM. The steps followed to get the reaction rate, from concentration profiles of nitrate, were:

- Read concentration of nitrate at the first layer of water attached to the WSI for June, July and August given in (James et al., 2008).

- Make a plot ln(NO3 concentration) vs. time.

- From the previous plot estimate the reaction coefficient, units in 1/seconds [1/s]. This was done by calculating a linear regression to fit the data and retrieving the slope.

- The last three steps were repeated for one more measured station presented in (James et al., 2008), and the final values for mass transport at the WSI are defined as a reaction coefficient. The reaction rates for denitrification for the two locations calculated were 5.54e-8 [1/s] and 6.48e-7 [1/s].

Additionally (Schubert, 2009) calibrated a value of denitrification at the wall of 2.36e-6 m/s or 4.74e-5 [1/s] (assuming 5cm of a layer into the sediment where denitrification take place,

value within suggested ranges by (Di Toro, 2001)). Finally, in the present research in section 6.2, a one species model implemented on BioChemFOAM gives a value of $\beta = 4.0362e-5[1/m]$ or 3.80e-8[1/s] (value calculated by using characteristic diffusion coefficient at WSI of 1.9e-9 m^2/s for nitrate presented by (James et al., 2008) and depth into the sediment of 0.05m as suggested by (Di Toro, 2001)). From the collected data, we determine that the parameter may range in natural systems from 1e-5 up to 1e-8 [1/s].

The nitrification reaction scales were more difficult to define, but the orders of magnitude of the process and reaction rates were derived from: mass balances of nitrate presented by (Richardson et al., 2004), (James et al., 2008), and reaction rates published by (Cerco & Cole, 1994). The work of (Richardson et al., 2004) presents a global mass balance for Pool 8, Mississippi River. The reported mass loading rates for nitrification were comparable to the denitrification rates. They are equal and about 7% of the input mass loading rate, 6939+/- 342 t.year^{-1}. These results suggest that both processes have similar order of magnitude in a backwater area. Moreover, (James et al., 2008) also present a mass balance for a smaller backwater area in a summer period, described earlier, for which the denitrification is about 11% of the input mass loading rate (927mg.m^{-2}.d^{-1}) of nitrate and nitrification is about 3% of the input mass loading rate of nitrate. These two works presented by (Richardson et al., 2004) and (James et al., 2008) give an idea of the order of magnitude of the coupling action of denitrification and nitrification processes in a backwater area. These results are used later since they provide an order of magnitude for the coupling processes, denitrification and nitrification, included in BioChemFOAM. Furthermore, an additional information from coefficients presented in Table 3-11 for Nit$_m$ (Maximum denitrification rate at TNit where TNit is the optimum temperature for nitrification)from Chesapeake Bay model, (Cerco & Cole, 1994), suggests values for different ecosystems between 0.006 to 0.446 mg-N/L.day or in units of [1/s] 6.9e-8 to 5.16e-6 (values calculated with and average ammonia concentration of 0.055mg-N/L, defined from (LimnoTech, 2007)). Additionally, the limits were calculated with the ammonia concentration for July from (James et al., 2008) and the Nit$_m$ is given between 1e-5 to 1.67e-4 [1/s]. The rate coefficient

provided (Cerco & Cole, 1994) gives the typical reaction rate coefficients for nitrification. The information collected suggests a rate coefficient for nitrification of between 1e-5 to 1-6 [1/s].

Finally, the strategy to find the response of BioChemFOAM to different combinations of BC for algae at the input, the reaction rate of denitrification at the bed, and nitrification is defined based on the results calculated in Section 6.3.

The process used to define a physically valid solution can be summarized as follows:

- Calculate the curve of the percentage of nitrate reduction (PNR) for the base scenario presented in Section 6.3. Calculate the maximum PNR rate when a steady state has been reached. Take the curve presenting the percentage of reduction of nitrate based on input and output mass loading rates (Figure 6-25). The maximum removal rate when reaching a steady state is 71% at 26 day of the simulation. The value is high compared with published data from (Seitzinger et al., 2002) (~6.5% empirical relation, see Section 6.2 Figure 6-7), (James et al., 2008) (total nitrate uptake 44.9%, Net Nitrate uptake=41.3% and Lake wide denitrification=27%), (Schubert, 2009) (16.4%, based on measured concentrations and 20.5% based on a first order reaction analysis), and (Richardson et al., 2004) (20%, denitrification + uptake + other losses). The published data ranges from 6% to 50%, approximately. Also, the spatial distribution of nitrate (Schubert, 2009) shows that a f PNR value of 71% indicates an over processing of nitrate compared with measured data in the system (see Figure C-1). The coefficients utilized in the base scenario, [0] (Table 6-2), are the same as the ones presented in Section6.3 and case scenario IC_0.55 discussed in case scenario IC_0.55 discussed in Section 6.4.

- The previous step shows a steady solution for nitrate, but PNR is too high compared with published data. The parameters defined previously were adjusted in order to improve the PNR and spatial distribution of nitrate. A series of scenarios were defined that cover ranges of algae concentrations, nitrification and denitrification rates discussed previously. The scenarios are defined in Table 6-2.

- Then BioChemFOAM was executed for each scenario (see Table 6-2).

- A curve for PNR based on mass loading rate of nitrate input and output were calculated for each scenario (Figure 6-26).

- PNRs were calculated from the curves and compared with published data.

- For the scenarios selected based on PNR, the nitrate spatial concentration distribution were compared with measured data. The scenario that best fit the data was selected to further validate denitrification and nitrification processes.

- The final scenario selected was utilized to calculate a mass balance for nitrate. The magnitude of nitrification and denitrification was compared with the published data discussed earlier. This is the last step used to define a physically valid solution.

Table 6-2. Scenarios defined to validate BioChemFOAM when the spatial nitrate concentrations and reduction rates of nitrate are available from the literature.

ID	Name scenario	BC at inlet for algae, Bx	k_{NO3}, reaction rate at river bed boundary	Nit_m, nitrification reaction rate
[0] (t25_8_4)	Base scenario	0.01	1e-5	3.125e-7
[1] (Bx0.0001)	Low algae at inlet	0.0001	1e-5	3.125e-7
[2] (kno3_1e-10)	Slow reaction at bed	0.01	1e-10	3.125e-7
[3] (kno3_5e-6)	Mild reaction at bed	0.01	5e-6	3.125e-7
[4] (Nit_01)	Fast reaction at bed and slow nitrification reaction	0.01	2.37e-5	5.16e-6
[5] (Nit_02)	Fast reaction at bed and mild nitrification reaction	0.01	2.37e-5	5.16e-5
[6] (Nit_03)	Fast reaction at bed (Denitrification) and nitrification rate, same order of magnitude	0.01	2.37e-5	2.37e-5
[7] (Nit_04)	Slow reaction at bed (Denitrification) and nitrification rate, same order of magnitude.	0.01	5.5e-8	5.5e-8

6.5.2 Results – comparison

The scenarios were successfully calculated and PNR figures were generated for all cases. The PNR lines are presented in Figure 6-26. In general, all curves present an initial period, first two days, where the PNR curve has abrupt changes (e.g. see Figure 6-25 first two days). This is due to the Initial Conditions that are imposed on the system. In other words, it takes some time for the system to experience all of the processes included and to adjust the concentrations to get a physical value defined by the model parameterization.

Each scenario was evaluated based on PNR and spatial distribution of nitrate extracted at the water surface, see Appendix C.

Scenario [0], base scenario, removes 71% of nitrate, and spatial distribution is far from measurements (Figures C-1). This scenario helps provide an upper limit for PNR, as shown in Figure 6-25s and 6-26 (red line).

Scenario [1], low algae at inlet, shows that changing the green algae concentration does not improve the PNR, see figure 6-26. The PNR have the same trend as scenario [0]. The simulation was stopped before reaching a steady state since the PNR is out of the defined bounds (6-50%).

Scenario [2], slow reaction at bed, gives a smoother PNR curve, but the rate of denitrification, k_{NO3}, value is two orders of magnitude smaller than the published data. This means that the uptake of nitrate at the bed is reduced over time. Since nitrate uptake is slow, the PNR slope is small (see Figure 6-26). The scenario was discarded since the denitrification rate is out of reported data.

Scenario [3], mild reaction at bed, in Figure 6-26 shows PNR values that are out of the limits imposed by the references, even though the reaction parameter for denitrification is closer to published data. The scenario was only executed for 21 days since the graph shows that it overestimates PNR (see value at 21 days Figure 6-26). The scenario was discarded since the PNR is out of imposed limits.

Scenarios [4] (fast reaction at bed and slow nitrification) and [5] (fast reaction at bed and mild denitrification reaction) were defined to find patterns imposed by a slow and fast nitrification rate.

Scenario [4] (see Figure 6-26 line [4]), defines a slow nitrification process (5.16e-7 s^{-1}) and a fast denitrification processing (2.37e-5 s^{-1}). Also, the rate of reaction is about one order of magnitude higher than the rate of denitrification. On the other hand, Scenario [5] defines a fast nitrification rate (2.37e-5 s^{-1}) and a fast denitrification rate (5.16e-5 s^{-1}). However, in the case of scenario [5], the rate of reaction has a slightly higher nitrification rate. The higher nitrification rate implies that BioChemFOAM is going to produce more NO_3^- that will increase nitrate concentrations (NO3) in the model (see Figure 6-26 line [5]).

Scenario [5] serves as a lower limit to define nitrification rates (see Figure 6-26). The figure shows a gain of nitrate in the system, e.g., negative PNR values in Figure 6-26 (pink line). This situation is not feasible according to the measured values of nitrate at the outlet (Schubert, 2009). This scenario was discarded but utilized to define a lower limit for PNR curves.

Scenario [6] shows a PNR curve within published data (see Figure 6-26 line [6]). The PNR curve increases from 1 day to 17 days until it reaches a steady state for nitrate mass loading rates. The PNR value at steady state is about 39%. Additionally, Figure 6-27 shows the PNR in conjunction with inlet and outlet mass loading rate for the scenario. This scenario was selected to further study its spatial distribution of nitrate.

Scenario [7] shows a PNR value that is within the published data. It shows a quasi-steady state from 6 to 8 days, and then it increases steadily from day 8 to day 33. This indicates that the model is removing more nitrate after the day 8. Despite the model did not reach a steady solution, the scenario was keep to compare its spatial distribution of nitrate.

In general, Figure 6-26 gives an idea of which combination of parameters produces a PNR within the published data range. Scenarios [6] and [7] were selected as best alternatives based on PNR agreement with published data.

Scenario [7] did not reach a steady state during the period of simulation of 33 days (see Figure 6-28). Its nitrate distribution did not match measured values by (Schubert, 2009) (see Figure C-10). For this reason, the model was discarded and not studied further.

Scenario [6] has a better agreement of PNR (value of ~39% for steady state) (see Figure 6-27). In addition, the spatial distribution of nitrate concentration is closer to values measured by (Schubert, 2009), as shown in Figures 6-29, 6-30, and 6-31.

Figure 6-29 shows all measured points compared with BioChemFOAM calculations. In general, the BioChemFOAM estimates lower concentrations than measured values (see red square symbols below 45 degrees line in black). Furthermore, a trend line for previous models (FLUENT in figure) and BioChemFOAM shows a better performance of the model. An additional parameter was calculated to estimate the deviation from measured data. The parameter, which is called normal error distance metrics, adds the normal distances from each point on the figure to the 45° line to give a single value. This gives a measure of how close all the values are to the ideal line at 45° (perfect match between measured and calculated value). The metrics value, called normal error distance metrics (NEDM), gives values greater than zero, and the smaller the values are, the better (e.g. zero value means a perfect agreement between model and measurements). The BioChemFOAM value for the normal error distance metrics is NEDM=1.46, and in previous works NEDM=1.85 ((Schubert, 2009)). The proposed model is better than previous studies despite the lack of information for other species.

Figures 6-30 and 6-31 show a comparison between previous works' and BioChemFOAM at different cross sections. The model was able to reproduce characteristic patterns of nitrate concentrations.

In addition to nitrate concentration, total nitrogen spatial values were available for the same locations presented in Figure 6-29 (Schubert, 2009). The values were compared with BioChemFOAM results and presented in Figure 6-32. The total nitrogen values are also lower than the measured values, as shown in the figure. The mains errors between the model and measured values are points located outside the main flow path (the main flow path can be seen

by following the gray and yellow arrows on the figure). Additionally, Figures 6-31 and 6-32 present a comparison along cross sections. The figures show good agreement between BioChemFOAM and measured values. The NDM value for total nitrate was 2.0.

In order to further understand the dynamics presented in Scenario [6], an analysis of mass loading rates for all the species and processes affecting nitrate fate and transport is presented. Figure 6-35 shows mass loading rates for all species at the outlet of the backwater area. The mass inlet loading rates (MILR) for each species (not shown in the figure) are: MILR(Bx) = 0.063 g-C/s, MILR(DOC) = 94.5 g-C/s, MILR(PO4) = 0.378 g-C/s, MILR(DON) = 2.52 g-N/s, MILR(NH4) = 0.35 g-N/s, MILR(DO) = 42.84 g-O2/s, MILR(COD) = 56.7 g-O2/s, MILR(POC) = 15.75 g-C/s, MILR(POP) = 0.45 g-P/s, MILR(PON) = 2.52 g-N/s, and MILR(NO3) = 3.465 g-N/s. All of the mass outlet loading rate (MOLR) curves show a typical shape when a constant inlet mass loading rate is defined (e.g., for a plug-flow system, the response of the outlet to a continuous inlet is a decaying curve at the outlet, see page 81 (Schnoor, 1996)). Furthermore, the MOLR reaches a steady patter for the 33 days of simulation with three exceptions: DO, NH4, and Bx. Dissolve oxygen (DO), ammonia (NH4), and algae (green algae, Bx) show a fluctuating pattern mainly due to the boundary condition imposed for DO at the water-air interface. This pattern reflects the daily changes of species concentrations.

Figure 6-35 also shows the influence of the fast rate of reaction imposed at the bed for nitrate and the fast rate of reaction imposed for the nitrification process. NO3 decreased for the first 12 days and then reached an steady state. On the other hand, NH4 decreased the first 3 days and then started to fluctuate. The values of NH4 oscillate between 0.013 at noon and 0.17 g-N/s at night. Also, green algae is being produced at noon (0.09 g-C/s) and consumed at night (0.07 g-C/s). The explanation of this oscillatory pattern is due to the dependence of nitrification on oxygen. This means that the amount of bacteria nitrosomonas and nitrabacter enhances the process of nitrification, (see stoichiometric reactions in Chapter 3).

The mass loading rates of scenario [6] (fast nitrification and denitrification at bed) and [7] (slow nitrification and denitrification at bed) were compared. The outlet mass loading rate for scenario

[7] is presented in Figure 6-36. This shows the influence of the reaction rates of nitrification and denitrification on the outlet mass loading rate (MOLR) curves. When the rate coefficients for denitrification and nitrification are fast (high reaction rate), MOLR for NH4 fluctuate each day, as shown in Figure 6.35 (right). On the other hand, when the rate coefficients for denitrification and nitrification are slow, MOLR for the NH4 response change to weeks (see Figure 6-36 right). In conclusion, BioChemFOAM was not only able to reproduce the spatial variation of nitrate concentration and the total nitrogen but it was also able to reproduce the temporal responses of processes affecting nitrate fate and transport.

Finally, a global mass balance is presented to show the influence of each process affecting the chemical and biological processing of nitrate in Scenarios [6] and [7].

Figure 6-37(a, c and e) shows the detailed contribution of processes affecting chemical and biological processing in Scenario [6], the physically valid solution. These discussed in Chapter 3, equation 3.68, and the details of the calculated values in the figure are provided in Appendix C-2. Figure 6-37 (a) shows all of the processes affecting NO3's biological and chemical processing. Nit = second term in equation 3.68. Alg = first term in equation 3.68. DenWater = third term in equation 3.68. DenBed=boundary condition imposed in BioCHemFOAM at the water-sediment interface, defined as a reaction rate constant multiplied by the nitrate water concentration. The figure shows the influence of each process over time. The nitrification process (Nit in figure) is about 7.7% of the nitrate mass inlet, which is within the rage of published data. The denitrification processing at the bed (DenBed in figure) is about 6.7%, the value within the published data discussed earlier. BioChemFOAM was able to reproduce typical nitrification and denitrification rates in an aquatic ecosystems. A global mass balance for nitrate shows that ΔS(storage)=Input-Outputs=58.74kg = (Nitrification +Mass at Inlet)-(Algae uptake+Denitrification at Bulk of the flow+denitrification at bed+Mass at Outlet)=(11.54+149.69)-(0.20+0.79+10.03+91.47)=(151.23)-(102.49).

Figure 6-37(b, d, and f) shows the detailed contribution of the processes affecting chemical and biological processing in scenario [7]. The processes are discussed in Chapter 3,

equation 3.68. This part of the figure shows the influence of changing the rate reaction parameters affecting nitrification and denitrification. Figure 6-36 (c) and (d) shows that slower nitrification and denitrification rates increase the algae concentration at day 12 of the simulation. Also, the slower reaction rates slow the processing due to denitrification at the bed (see Figure 6-37 d). In general, the figure shows the sensitivity of the model when choosing a different rate of reaction for denitrification and denitrification.

6.5.3 Closure

This section shows that even though only nitrate measurements are available and characteristic coefficients are defined from the literature, BioChemFOAM was able to reproduce the spatial patterns of nitrate and characteristic removal rates reported in the literature.

The physically valid solution was Scenario [6], with a fast denitrification and nitrification reaction rates.

BioChemFOAM was able to reproduce spatial distributions of nitrate and characteristic percentages of the reduction of nitrate in a backwater area. In general, it was shown that the inlet algae concentration has a minor influence on adjusting the nitrate concentrations as shown in Figure 6-29, for the current conditions. Moreover, the coupling between denitrification and nitrification was fundamental to finding a better spatial distribution of nitrate, as presented in Figures 6-27 (time vs. mass loading vs. removal) and 6-30 and 6-31(cross section comparison). Furthermore, a comparison of mass loading rates was performed for all species to ensure that the model reaches a steady concentration for all of the species. Finally, a mass balance analysis for nitrification was presented and compared with typical percentages of nitrification and denitrification (see Figure 6-35 and 6-36).

In summary, BioChemFOAM parameterization was able to reproduce not only spatial patterns of nitrification and total nitrogen but also characteristic parameters (PNR, mass loading rates and mass balances) that are important in order to improve best management practices in

aquatic ecosystems and to enhance understanding of fundamental processes affecting nutrient dynamics.

Figure 6-25. Percentage of Nitrate Reduction (PNR) curves (red line with circle symbols) for base scenario [0]. The inlet (square symbols) and outlet (triangle symbols) mass loading rates are also shown.
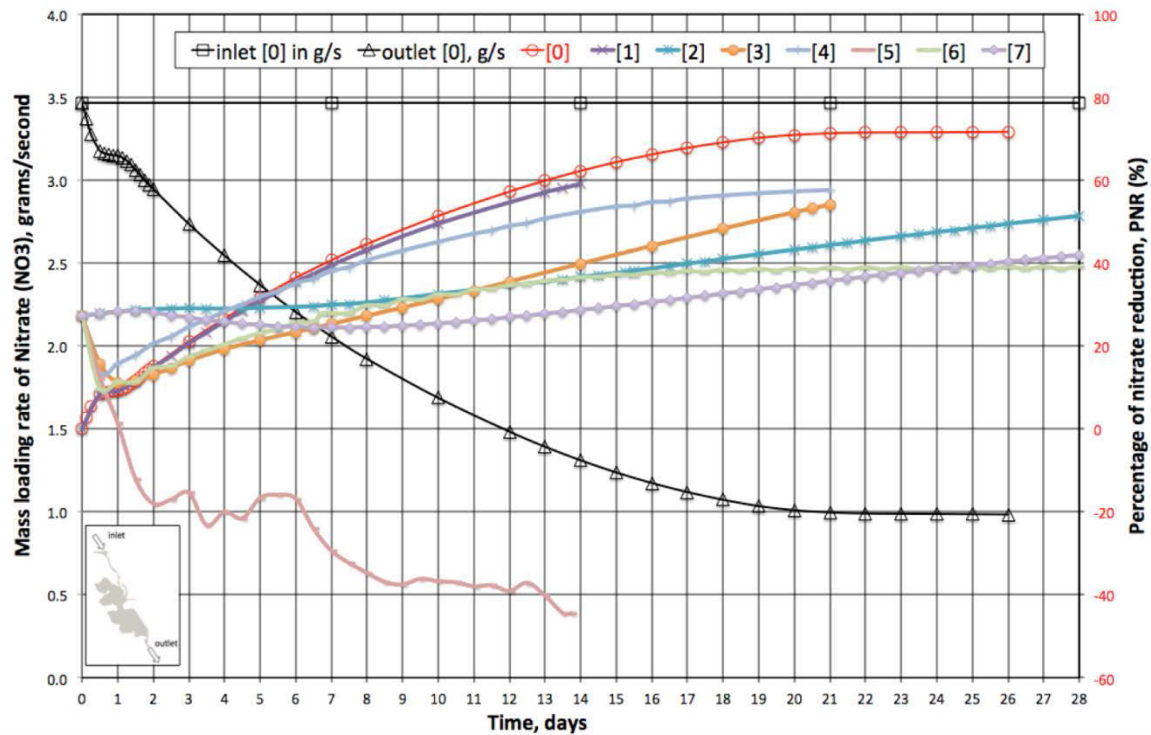
Figure 6-26. Percentage of Nitrate Reduction (PNR) curves all scenarios. The inlet (square symbols) and outlet (triangle symbols) for scenario [0] mass loading rates are also shown.
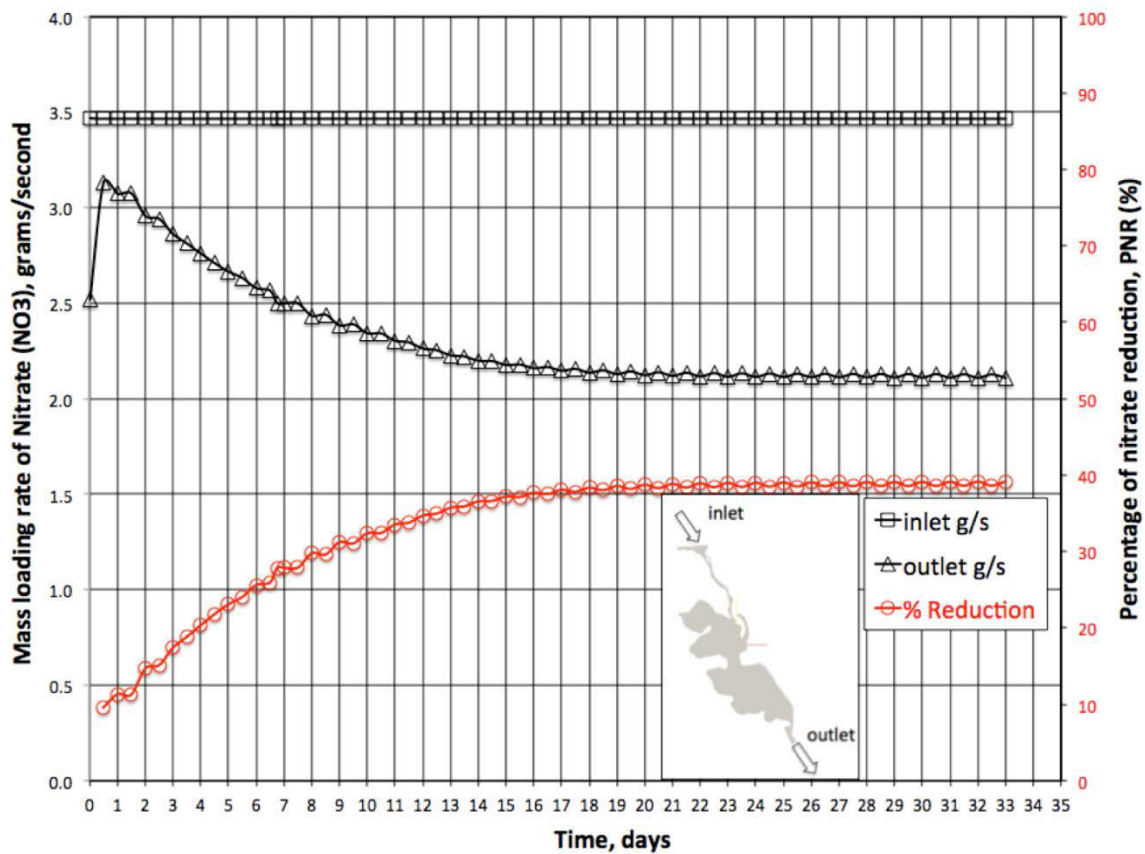
Figure 6-27. Percentage of Nitrate Reduction (PNR) curves (red line with circle symbols) for base scenario [6]. The inlet (square symbols) and outlet (triangle symbols) nitrate mass loading rates are also shown.
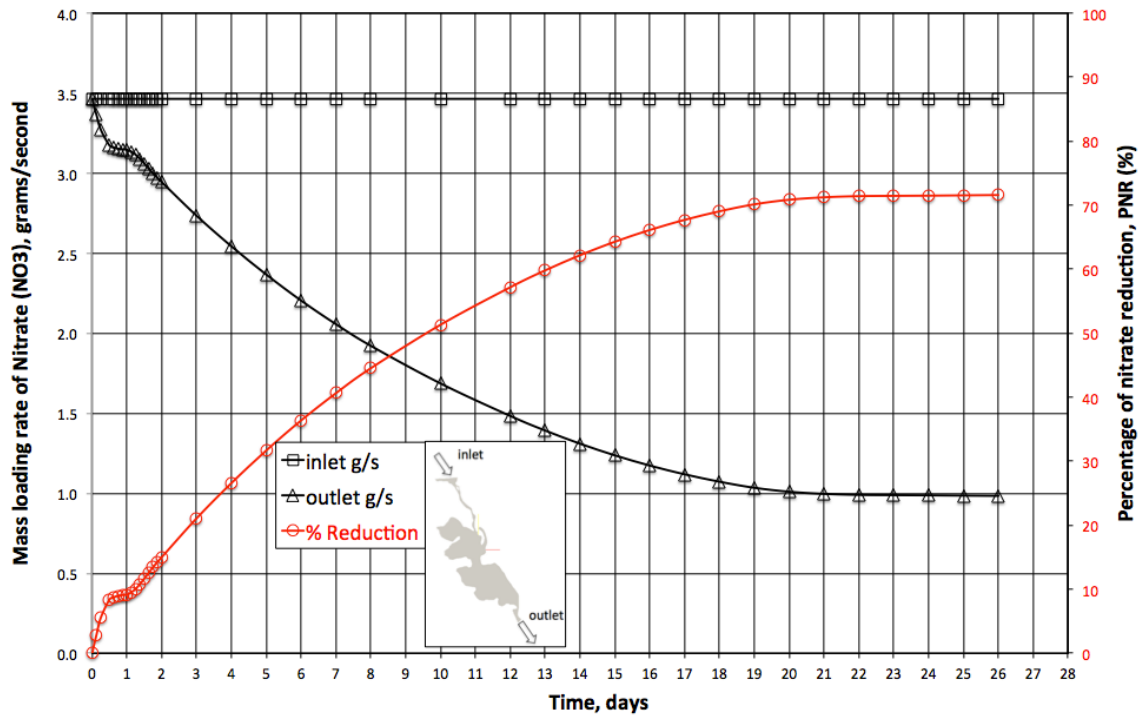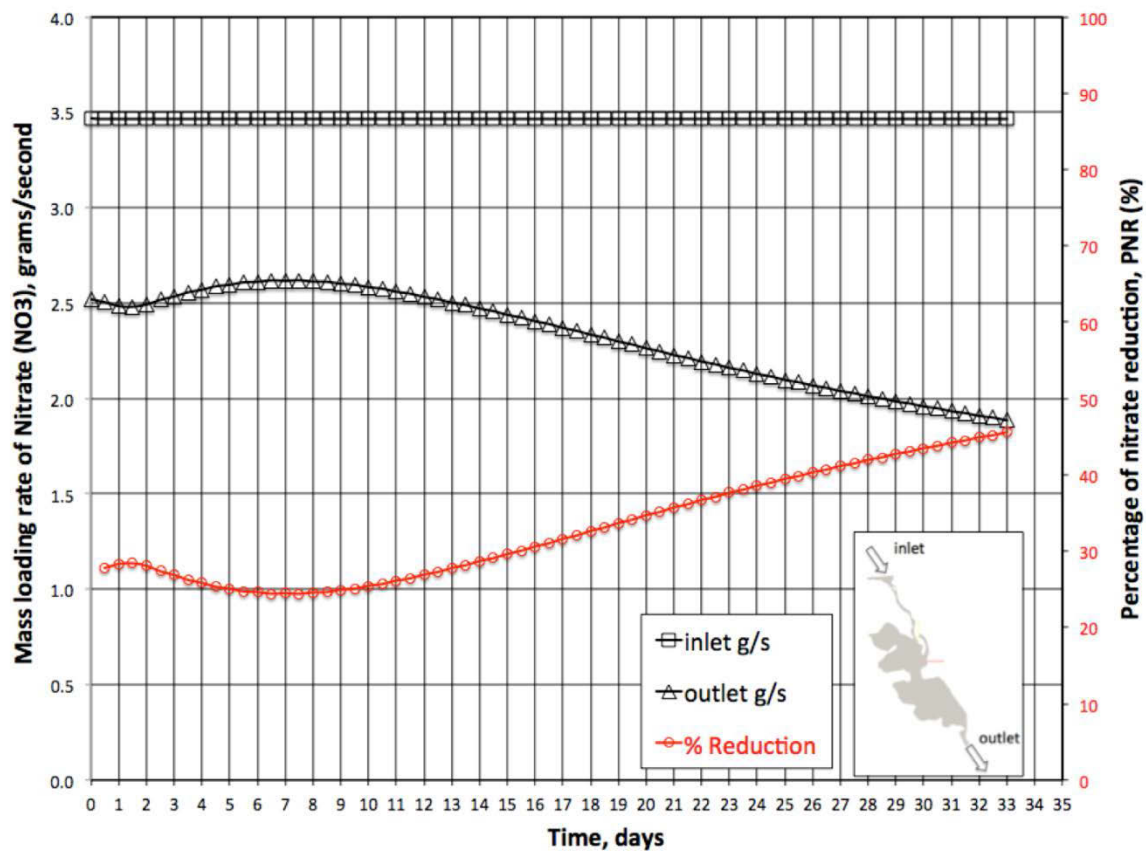
Figure 6-28. Percentage of Nitrate Reduction (PNR) curves (red line with circle symbols) for base scenario [7]. The inlet (square symbols) and outlet (triangle symbols) nitrate mass loading rates are also shown.
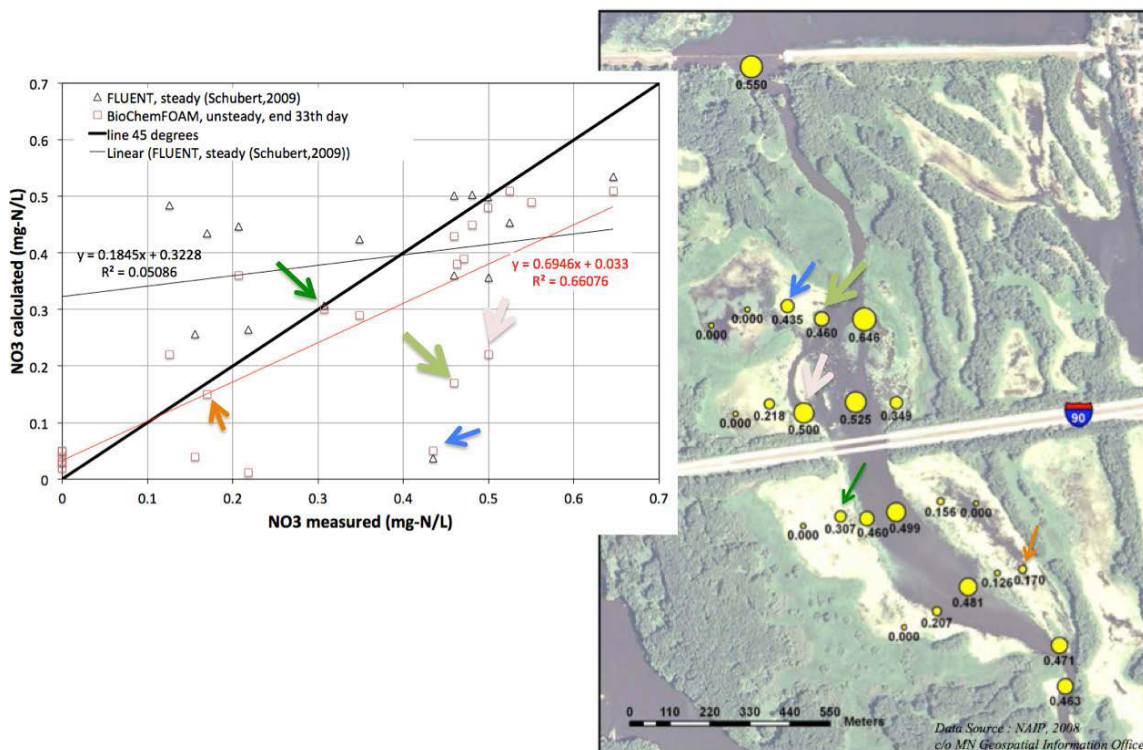
Figure 6-29. Nitrate measured vs. calculated with trend line for BioChemFOAM solution (red line) and with trend line for FLUENT solution (black line) (left figure). Location of sample data (righ map). Arrows in both figures show the location of points in the back water area.

Figure 6-30. Nitrate distribution at Cross Section 1 (top, CS1) and 2 (bottom, CS2), looking upstream. The colored arows indicate a point on the back water area, see Figure 6-29.
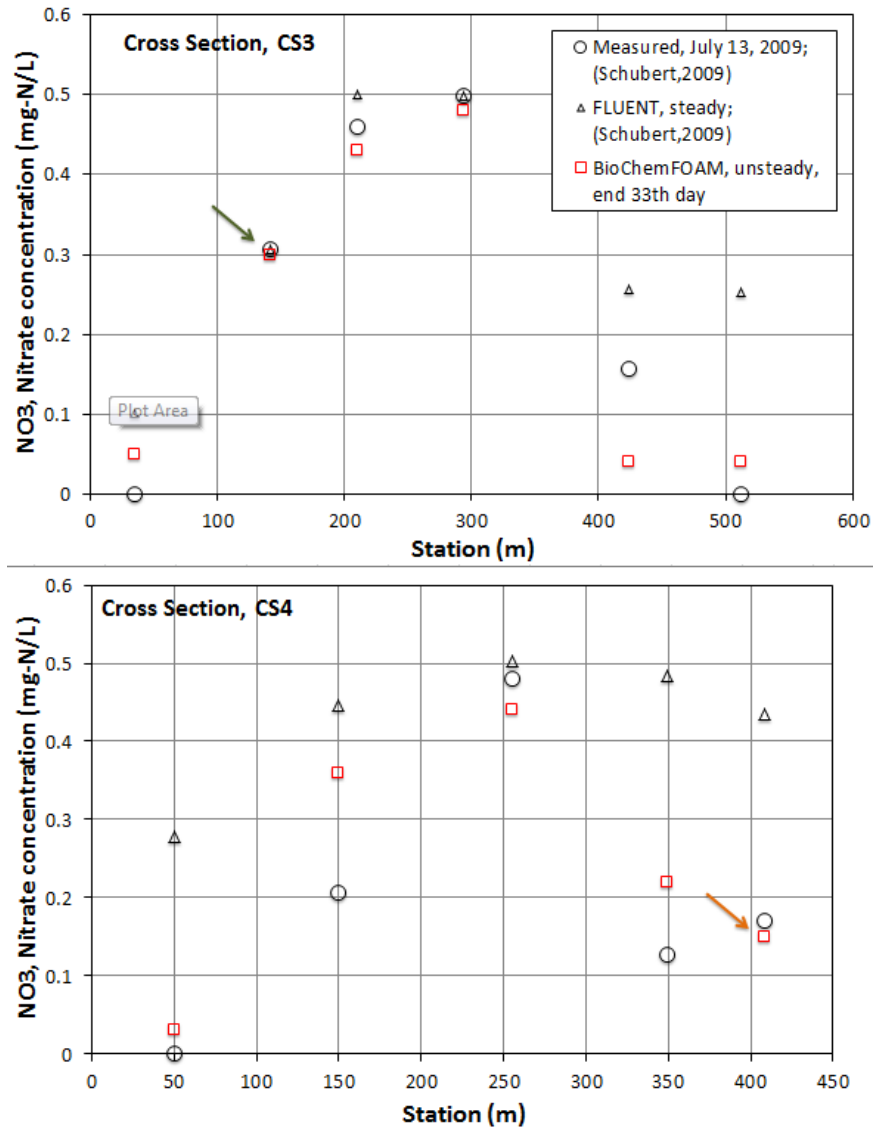
Figure 6-31. Nitrate distribution at Cross Section 3 (top, CS3) and 4 (bottom, CS4), looking upstreams. The colored arrows indicate a point on the back water area, see Figure 6-29.
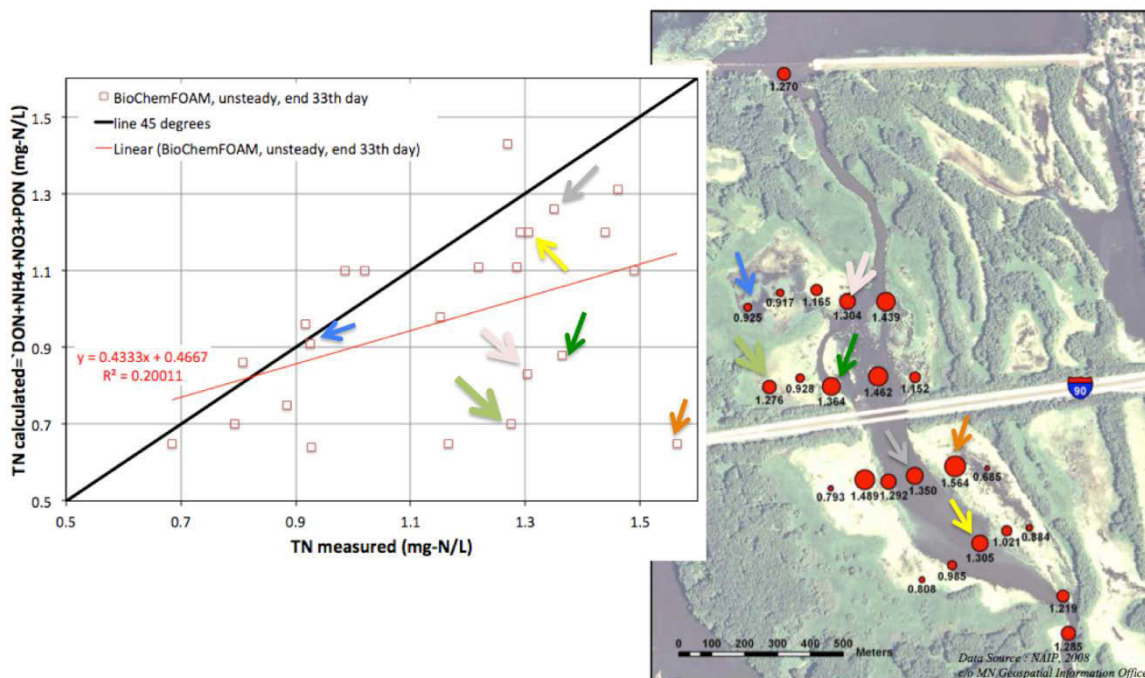
Figure 6-32. Total nitrate measured vs. calculated with trend line for BioChemFOAM solution (red line) (left figure). Location of sample data (righ map). The arrows in both figures show the location of points in the back water area.
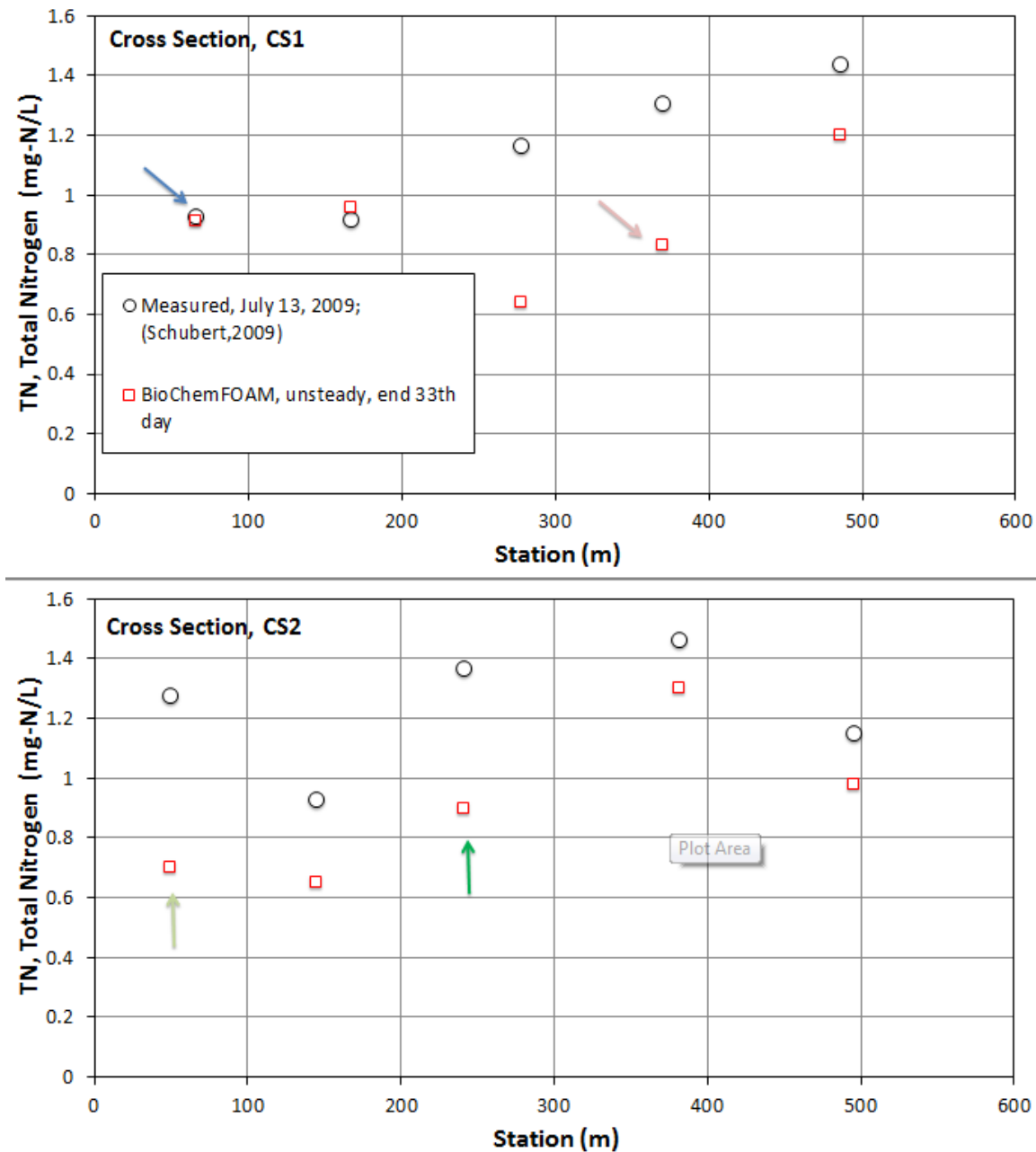
Figure 6-33. Total Nitrogen distribution at Cross Section 1 (top, CS1) and 2 (bottom, CS2), looking upstream. The colored arrows indicate a point on the back water area, see Figure 6-32.

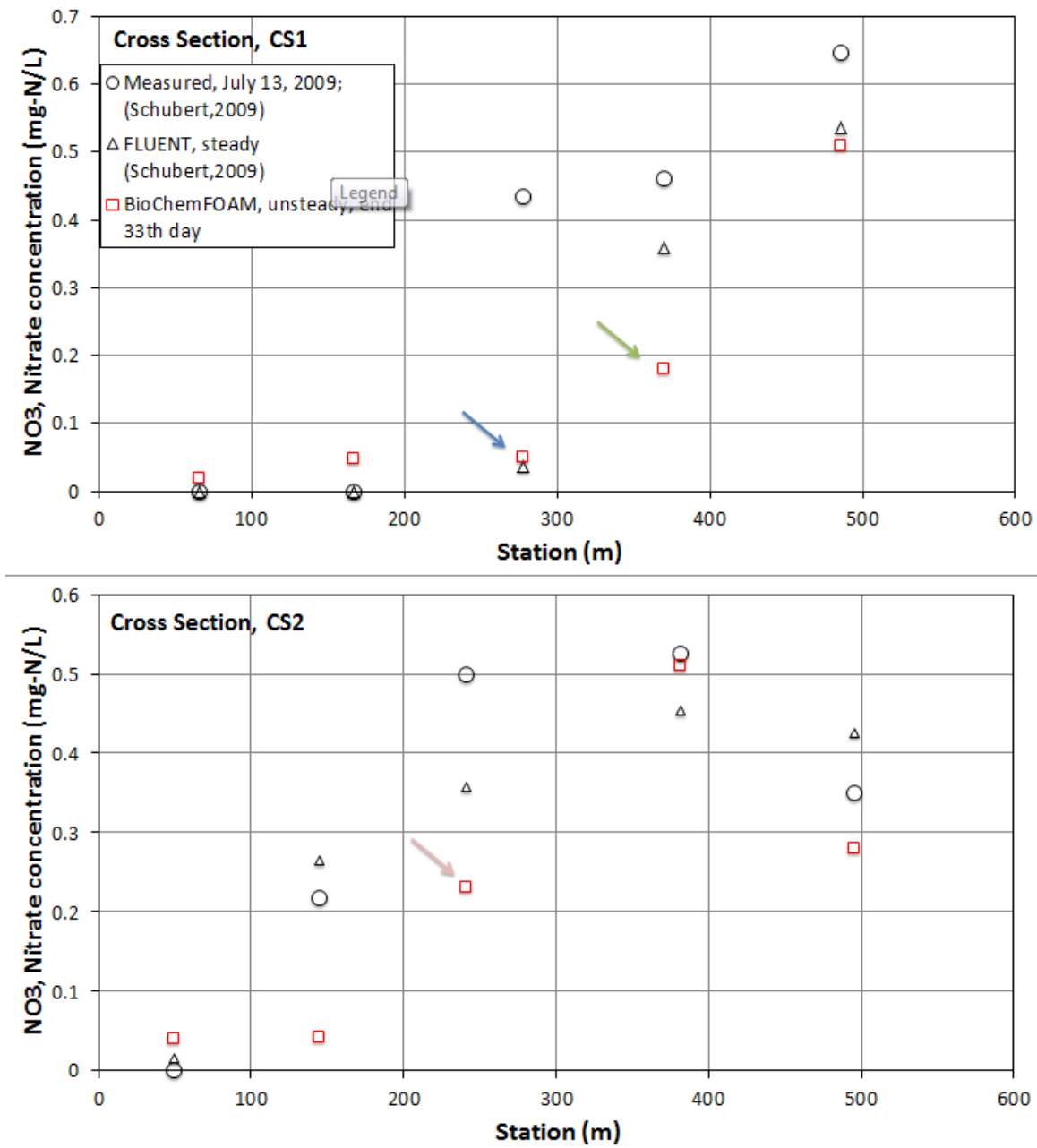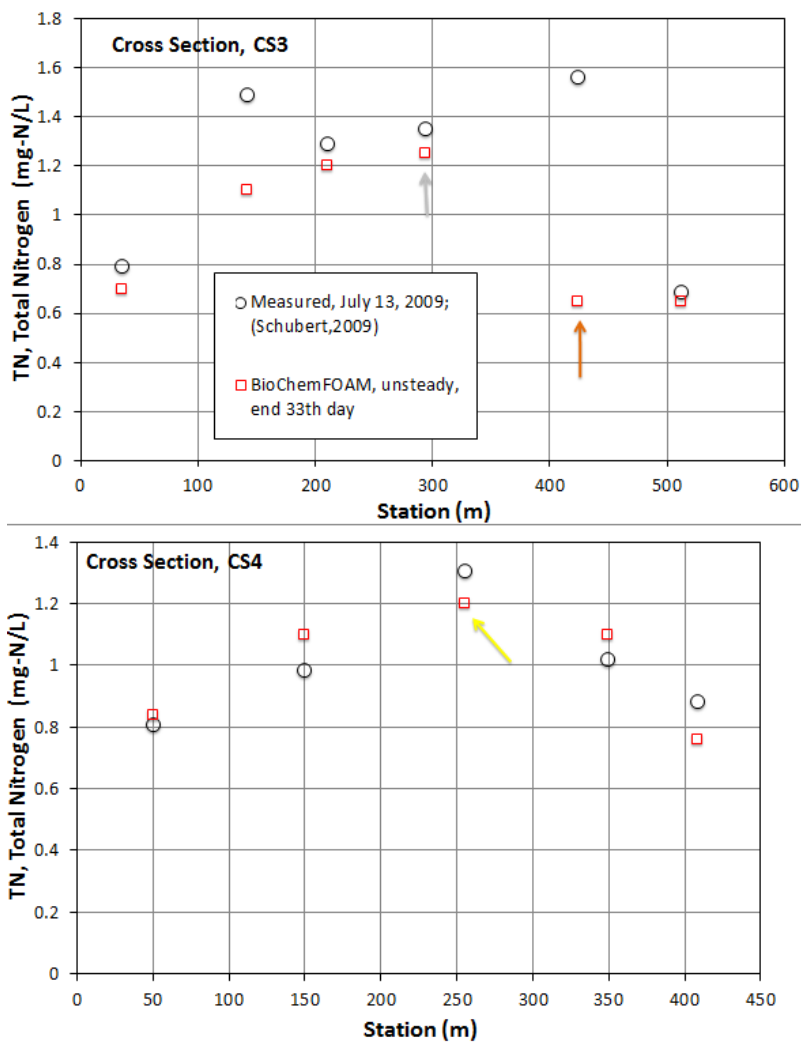Figure 6-34. Total Nitrogen distribution at Cross Section 3 (top, CS3) and 4 (bottom, CS4), looking upstream. The colored arrows indicate a point on the back water area, see Figure 6-32.
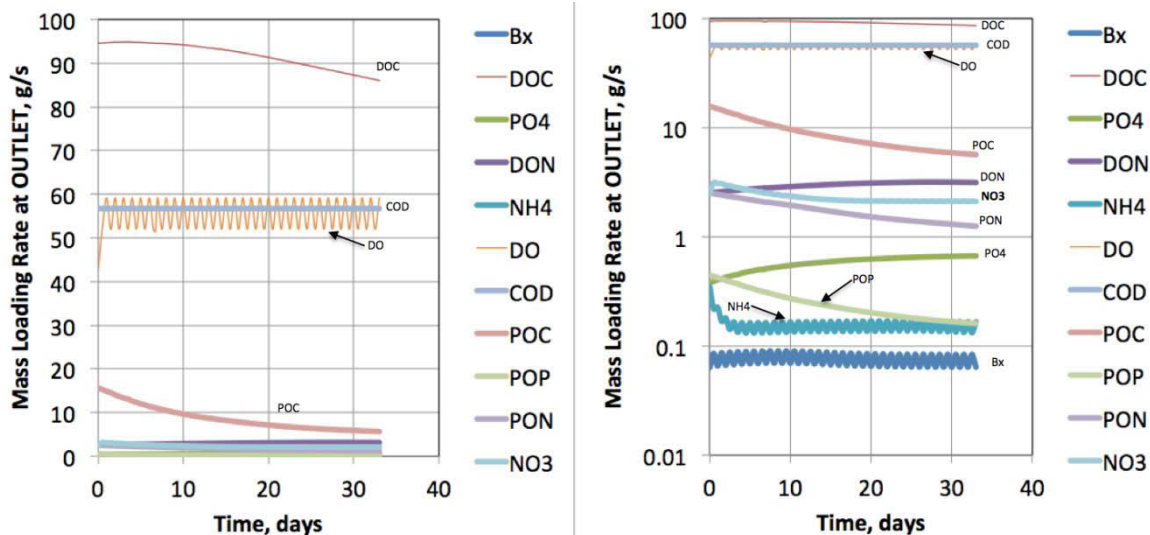
Figure 6-35. BioChemFOAM computed mass loading rate at the outlet vs. time for all species for Fast reaction at bed and fast nitrification rate, same order of magnitude (see Scenario [6], Table 6-2). The vertical axes in normal scale (left). The vertical axes in log scale (right). Bx is algae. DOC is dissolved organic carbon. PO4 is dissolved orthophosphate. DON is dissolved organic nitrogen. NH4 is ammonia. DO is dissolved oxygen. COD is chemical oxygen demand. POC is particulate organic carbon. POP is particulate organic phosphorus. PON is particulate organic nitrogen. NO3 is nitrate.
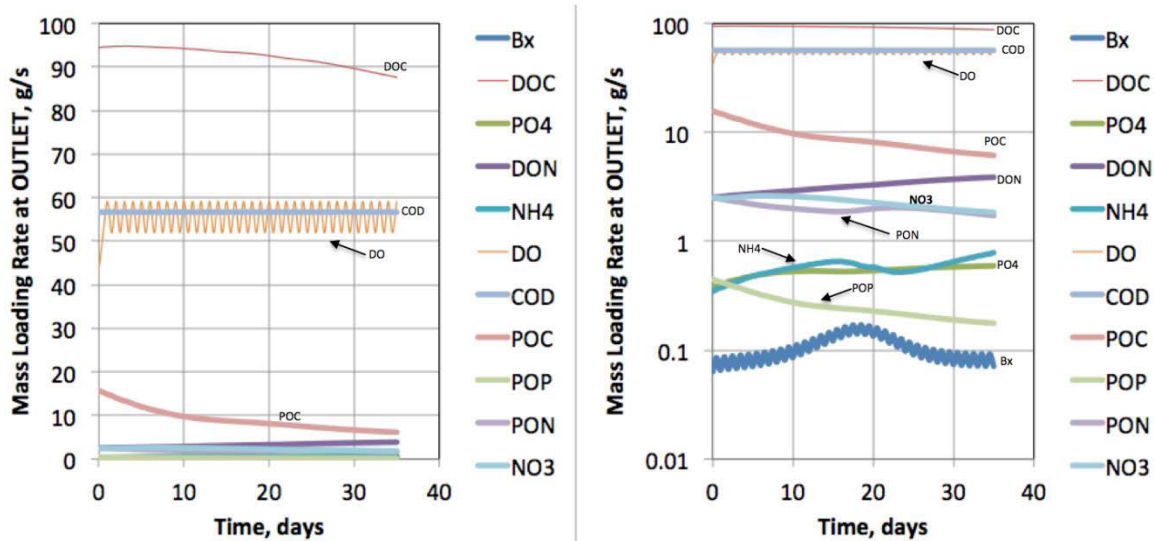
Figure 6-36. BioChemFOAM computed mass loading rate at outlet vs. time for all species for slow reaction at bed and slow nitrification rate, same order of magnitude (see Scenario [7], Table 6-2). The vertical axes in normal scale (left). The vertical axes in log scale (right).
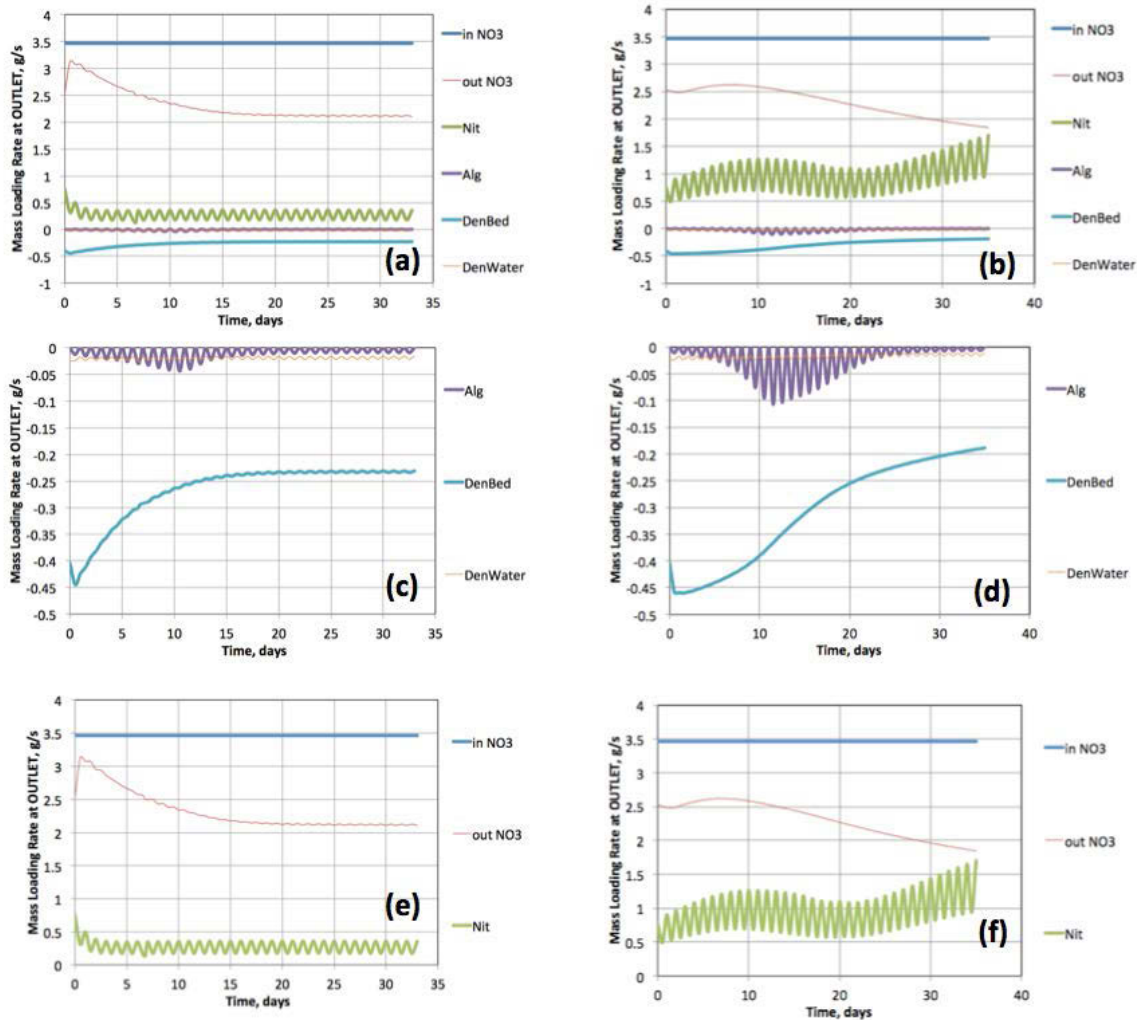
- Figure 6-37. BioChemFOAM chemical and biological processes affecting nitrate concentrations over time for Scenarios [6] (left figures: a, c, and e) and [7] (right figures: b, d, and f). Each point is the value of the process as expressed in equation 3.68. e.g., Nitrification is calculated with term $Nit(DO, NH4, T).NH4$ were $Nit(DO, NH4, T)$ is a function defined in equation 3.75.

CHAPTER 7

CONCLUSIONS AND FUTURE WORK

7.1 Conclusions

A robust model linking chemistry and flow, called BioChemFOAM was developed to simulate nutrient dynamics for aquatic ecosystems. The computational fluid dynamic model is based on parameterization of several key chemical and biological processes using 11 state variables is able to simulate different degrees of complexity. BioChemFOAM was validated with numerical test solutions and available spatial nitrate and total nitrogen concentration data collected in the field. The model was primarily developed using the numerical libraries available in OpenFOAM, an open source computational fluid dynamics platform. BioChemFOAM showed good agreement between numerical experiments and real world applications.

In addition, this thesis documents the development of a comprehensive analysis to validate BioChemFOAM which integrates hydrodynamics, chemical and biological processes as complexity is varied. BioChemFOAM implements both a hydrodynamic and a species transport module on a robust platform that can run all modules in parallel on high performance computers. Since BioChemFOAM can represent different degrees of complexity, the base implementation considers both a hydrodynamic and a species transport module. The hydrodynamic component solves the Reynolds Average Navier-Stokes equations RANS with a k-epsilon turbulence model. The primary variables solved in the hydrodynamic module are velocity, pressure, turbulent kinetic energy and dissipation rate. The species transport module solves a system of coupled passive scalar equations in conjunction with a light intensity equation and temperature equation (energy). The passive scalar equations solves spatial and temporal concentrations of algae (green algae), dissolved organic carbon, dissolved orthophosphate, dissolved organic nitrogen, ammonia, nitrate, dissolved oxygen, chemical oxygen demand, particulate organic carbon, particulate organic phosphorus and particulate nitrogen. The light intensity is solved with a

simple diffusion process that depends on algae concentration. In this research, the concentration of Green algae was low, so there was not an attenuation of the incident radiation. The light equation utilizes a flux boundary conditions to simulate diurnal changes sue to solar radiation. Moreover, the temperature equation solves a scalar equation with advection and diffusion.

BioChemFOAM solves hydrodynamic equations with a PISO algorithm. In addition, the spatial distribution of species and its interaction with the flow field can be found by solving a system of coupled passive scalar equations. A novel splitting-operator numerical method was implemented in OpenFOAM to accurately solve the system of partial differential equations over time. The unsteady solver that was implemented was successfully validated against published data by (Sun et al., 1999), numerical fabricated solutions, and a real application to a backwater area in the Mississippi River.

Numerical experiments were formulated to test BioChemFOAM for constant light and temperature. Different degrees of complexity were defined to validate BioChemFOAM, since the availability of bench mark cases and data to fully corroborate the tool's full parameterization in real aquatic ecosystems is scarce. It was found that the use of an additional model, BioChemMATLAB, helped to validate the parameterizations of chemical and biological processes. Specifically, BioChemFOAM's advection and diffusion were defined as close to zero in 0-D, 2-D and 3-D zero in order to compare solutions between the two codes. This procedure verified that this was the correct approach to use when solving the system of equations that encapsulate the biological and chemical processes since there isn't a benchmark case to validate all the chemical and biological processes. Therefore the thesis contribution includes both the model and the methodology used to systematically validate the processes included in BioChemFOAM.

BioChemFOAM hydrodynamic module was successfully validated with numerical experiments and data from the Round Lake backwater area located in the Mississippi River. In particular, a comparison of velocity contours with data reported by (Schubert, 2009) shows good

agreement. The model was able to reproduce similar patterns of nitrate and total nitrogen as documented by (Schubert, 2009).

The earlier work in Pool 8 presented by (Schubert, 2009) illustrated a computer simulation of nitrate using the CFD model FLUENT and a measured spatial distribution of nitrate and total nitrogen for a summer flow, July 2009. As an added check the present research applied BioChemFOAM to reproduce spatial concentrations of nitrate and total nitrate using this data set. Therefore, two models with different degrees of complexity for the species transport module were compared using the spatial distribution of nitrate and total nitrogen. The first model implemented only nitrate fate and transport with a reactive boundary condition. The second was much more complex implementing eleven species with changing boundary conditions for dissolved oxygen, light and temperature at the water-air interface. Errors based on a normal error distance metrics (NEDM) were determined for both models, with the smaller and closer to zero the NEDM, the better. The first model that was implemented shows an improvement of nitrate spatial distribution that went from NEDM=1.84 to NEDM=1.64. The second model implemented shows an acceptable agreement, with a nitrate spatial concentration distribution of NEDM=1.85 and with a total nitrogen spatial concentration distribution of NEDM=2.0.

A sensitivity study of parameters influencing nitrate fate and transport was performed for the eleven species model in order to find a better physically valid solution. A physically valid solution was defined as a solution that fulfills three criteria, e.g., PNR, nitrate and total nitrogen spatial concentration distribution, and mass balance analysis for nitrate was defined to identify a physically valid solution. The solution was defined as physically valid if the criteria are within published measured data on similar ecosystems. The parameters that were changed in the sensitivity analysis were the input algae concentration, the reaction rate of denitrification at the bed, and nitrification rate reaction at the bulk of the flow. The sensitivity analysis shows that the appropriate definition of reactions rates for nitrification at the bulk of the flow and denitrification at the bed greatly influences the spatial distribution of nitrate and total nitrogen. Figures of PNR were generated to define limits of possible physically valid solutions in a

backwater area. The limits calculated ranges that extended from 71% to 39%. The sensitivity analysis showed that the coupled interaction of denitrification at the bed and nitrification was a crucial factor when defining a PNR that falls within the published data, ranging from 6-50%.

Additionally, it was shown, with the current parameterization, that green algae did not have a great influence when trying to refine PNR and spatial distributions of nitrate; its changes in PNR were less than 5%, see Figure 6-26 scenarios [0] and [1].

A physically valid solution was defined with the proposed sensitivity analysis. The physically valid solution was obtained with a low inlet concentration of green algae of 0.01mg-C/L, a fast reaction at the bed (denitrification) of $2.37e-5s^{-1}$, and a fast denitrification rate of $2.37e-5s^{-1}$. The physically valid solution presents a PNR of 39%. The nitrate and total nitrogen concentration obtained from BioChemFOAM were compared with the available measured data and showed a NDM for nitrate of about 1.46 and 2.0 for total nitrogen. The model shows that the most sensitive parameter was the nitrification rate.

A study of the mass loading rates and mass balances for nitrate fate and transport was conducted for the physically valid solution. The average time to reach a steady solution for all species was about 33 days. The mass balance for the physically valid case shows an oscillatory pattern produced by diurnal oxygen variation. The values of NH4 oscillate between 0.013 at noon and 0.17 g-N/s at night. Also, the algae data shows that more green algae is being produced at noon (0.09 g-C/s) than at night (0.07 g-C/s). A comparison of mass balances between slow and fast reaction rates showed ammonia fluctuations on a daily basis when a process has a fast reaction rate, whereas, fluctuates on a weekly basis when a process has a slow reaction rate.

The application to a backwater area improved our understanding of the complex interactions among hydrodynamic, chemical and biological processes. The quantitative validation with available data for nitrate and total nitrogen proves the tool's potential as a predictive tool for different complexity levels in different aquatic ecosystems. Despite the lack of information, the present work shows the potential application of the tool to simplify models that could be used to understand nutrient dynamics in aquatic ecosystems.

BiochemFOAM at the moment solves unsteady hydrodynamic and species transport models until reaching an steady state.

7.2 Future work

The present work introduced a tool called BioChemFOAM to study hydrodynamic and species transport processes in an aquatic ecosystem. Its ability to incorporate different complexity levels makes it a viable alternative to implement different parameterizations.

Chapter 3 introduced the modeled equations currently available in BioChemFOAM and a series of improvements that could be made in the future are listed below:

- The light module implements a diffusion model were the coefficients change based on algae concentration. It may be possible to improve the model by adding a radiation model like a P-1 model to simulate light attenuation in water.

- It would be beneficial to consider cyanobacteria on the calculations in conjunction with macrophytes. These processes affect directly the nutrient dynamics in an aquatic ecosystem.

- The boundary condition at the water-sediment interface only includes a reaction term that encapsulates many processes. It has been mentioned by (Haag, Schmid, & Westrich, 2006)and (Di Toro, 2001) than the mass transport at the WSI is a complex process that is mainly influenced by turbulence, bioturbation, diffusion and tortuosity. It may be possible to improve this by implementing the coupling between ammonia and nitrate at the water-sediment interface.

- Diatoms could be added to the model in future work.

- Additional validation with more flow measurements in conjunction with species concentration would be helpful, if the full parameterization presented in Chapter 3 is utilized.

The model also shows the need of experimental data to further validate each process influencing chemical and biological processing of aquatic ecosystems.

- Finally, a simplified version of the 11 species model presented in this thesis could improve the predictive capabilities of the tool. The important variables that such model should include are: nitrate, ammonia, dissolved oxygen, temperature, algae or chlorophyll-a, light and bacteria. Bacteria could be modeled as $dX/dt=(k_g-k_d)X$, where X is the concentration of bacteria (cells.L^{-1}), k_g is the bacterial growth rate (hr^{-1}) and k_d (hr^{-1}) is the bacteria death rate. The relation between the growth rate and the concentration of substrate can be describes by the following empirical formulation ((Chapra, 2008)): $k_g=k_{g,max} (S/(k_s+S))$, where $k_{g,max}$ is the maximum growth rate when food is abundant (hr^{-1}), S is the substrate concentration (mg.L^{-1}), and k_s is the half-saturation constant (mg.L^{-1}).

BioChemFOAM as introduced in this research, could be couple with a 2-D Saint-Venant solver to study changes in nutreint dynamics at bigger scales. E.g., chatchments.

REFERENCES

Ahsan, A. Q., & Blumberg, A. F. (1999). Three-dimensional hydrothermal model of Onondaga Lake, New York. *Journal of Hydraulic Engineering, 125*(9), 912-923.

Ambrose, R. B., Wool, T. A., & Martin, J. L. (1993). The water quality analysis simulation program, WASP5, Part A: Model documentation. *Environmental Research Laboratory, US Environmental Protection Agency, Athens, GA*.

Andersson, B. (2012). *Computational fluid dynamics for engineers*: Cambridge University Press.

Aulenbach, B. T., Buxton, H. T., Battaglin, W. A., & Coupe, R. H. (2007). Streamflow and nutrient fluxes of the Mississippi-Atchafalaya River basin and subbasins for the period of record through 2005: U. S. Geological Survey.

Bermúdez, A., García, L. G., Quintela, P., & Delgado, J. (2008). Water Quality Simulation of a Future Pit Lake *Progress in Industrial Mathematics at ECMI 2006* (pp. 790-794): Springer.

Bowie, G. L., & Tech, T. (1985). Rates, constants, and kinetics formulations in surface water quality modeling.

Brown, S. D. (2011). *Integrated Toolset for Water Quality Modeling in the Great Lakes*: State University of New York at Buffalo.

Cant, R., & Mastorakos, E. (2008). *An introduction to turbulent reacting flows*: World Scientific.

Cerco, C. F., & Cole, T. (1995). *User's Guide to the CE-QUAL-ICM Three-dimensional Eutrophication Model: Release Version 1.0*: US Army Engineer Waterways Experiment Station.

Cerco, C. F., & Cole, T. M. (1994). Three-Dimensional Eutrophication Model of Chesapeake Bay. Volume 1: Main Report: DTIC Document.

CFDOnline. (2014). CFD Online - OpenFOAM. from http://www.cfd-online.com/Forums/openfoam/

Chao, X., Jia, Y., Cooper, C. M., Shields Jr, F. D., & Wang, S. S. (2006). Development and application of a phosphorus model for a shallow oxbow lake. *Journal of Environmental Engineering, 132*(11), 1498-1507.

Chapra, S. C. (2008). *Surface water-quality modeling*: Waveland Press.

Chippada, S., Dawson, C., Parr, V. J., Wheeler, M. F., Cerco, C., Bunch, B., & Noel, M. (1998). PCE-QUAL-ICM: A parallel water quality model based on CE-QUAL-ICM. Center for research on parallel computation: Rice University.

Cho, J. H., & Ha, S. R. (2010). Parameter optimization of the QUAL2K model for a multiple-reach river using an influence coefficient algorithm. *Science of the total environment, 408*(8), 1985-1991.

Chock, D. P., & Carmichael, G. R. (2002). *Atmospheric Modeling* (Vol. 130): Springer.

Clair, N. S., Perry, L., & Gene, F. P. (2003). Chemistry for environmental engineering and science. *Mcgraw-Hill, New York*.

Conley, D. J., Carstensen, J., Vaquer-Sunyer, R., & Duarte, C. M. (2009). Ecosystem thresholds with hypoxia *Eutrophication in Coastal Ecosystems* (pp. 21-29): Springer.

Craig, J. K., & Crowder, L. B. (2005). Hypoxia-induced habitat shifts and energetic consequences in Atlantic croaker and brown shrimp on the Gulf of Mexico shelf. *Marine Ecology Progress Series, 294*, 79-94.

DELTARES. (2009). Deltares Software. 2012, from http://www.deltares.nl/

DHI, M. (2004). MIKE 21 - MIKE 3 FLOW MODEL FM Mike 21 - Mike 3 Flow Model FM, Hydrodynamic Module. MIKEbyDHI.

DHI, M. (2011). ECO Lab - ecological modelling made easy. 2012, from http://www.mikebydhi.com/Products/ECOLab.aspx

Di Toro, D. M. (2001). *Sediment flux modeling* (Vol. 116): Wiley-Interscience New York.

Diaz, R. J. (2001). Overview of hypoxia around the world. *Journal of Environmental Quality, 30*(2), 275-281.

Dortch, M., Schneider, T., Martin, J., Zimmerman, M., & Griffin, D. (1990). CE-QUAL-RIV1: A Dynamic, One-Dimensional (Longitudinal) Water Quality Model for Streams. User's Manual: DTIC Document.

Dortch, M. S., Tillman, D. H., & Bunch, B. W. (1992). Modeling water quality of reservoir tailwaters: DTIC Document.

EPA. (2011). River and Stream Water Quality Model (QUAL2K). 2011, from http://www.epa.gov/athens/wwqtsc/html/qual2k.html

EPA. (2012). Water Quality Models. from http://water.epa.gov/scitech/datait/models/index.cfm

Ernst, M., Frossard, W., & Mancini, J. (1994). Two eutrophication models make the grade. *Water Environment and Technology, November*, 15-16.

ESI. (2014). OpenFOAM web page. from http://www.openfoam.org/

Ferziger, J. H., & Perić, M. (1996). *Computational methods for fluid dynamics* (Vol. 3): Springer Berlin.

Galloway, J. N., Dentener, F. J., Capone, D. G., Boyer, E. W., Howarth, R. W., Seitzinger, S. P., . . . Holland, E. (2004). Nitrogen cycles: past, present, and future. *Biogeochemistry, 70*(2), 153-226.

Ghia, U., Ghia, K. N., & Shin, C. (1982). High-Re solutions for incompressible flow using the Navier-Stokes equations and a multigrid method. *Journal of computational physics, 48*(3), 387-411.

Goolsby, D. A., Battaglin, W. A., Aulenbach, B. T., & Hooper, R. P. (2001). Nitrogen input to the Gulf of Mexico. *Journal of Environmental Quality, 30*(2), 329-336.

Goolsby, D. A., Battaglin, W. A., Lawrence, G. B., Artz, R. S., Aulenbach, B. T., Hooper, R. P., . . . Stensland, G. J. (1999). Flux and sources of nutrients in the Mississippi-Atchafalaya River Basin. *White House Office of Science and Technology Policy Committee on Environmental and Natural Resources Hypoxia Work Group*.

Gulliver, J. S. (2007). *Introduction to chemical transport in the environment*: Cambridge University Press.

Haag, I., Schmid, G., & Westrich, B. (2006). Dissolved Oxygen and Nutrient Fluxes Across the Sediment–Water Interface of the Neckar River, Germany: In Situ Measurements and Simulations. *Water, Air, & Soil Pollution: Focus, 6*(5-6), 413-422.

Hodges, B. R., Imberger, J., Saggio, A., & Winters, K. B. (2000). Modeling basin-scale internal waves in a stratified lake. *Limnology and Oceanography, 45*(7), 1603-1620.

James, W. F., Richardson, W. B., & Soballe, D. M. (2008). Contribution of sediment fluxes and transformations to the summer nitrogen budget of an Upper Mississippi River backwater system. *Hydrobiologia, 598*(1), 95-107.

Jasak, H. (1996). *Error analysis and estimation for the finite volume method with applications to fluid flows*. Imperial College London (University of London).

Ji, Z.-G. (2008). *Hydrodynamics and water quality: modeling rivers, lakes, and estuaries*: John Wiley & Sons.

Kadlec, R. H., & Wallace, S. (2008). *Treatment wetlands*: CRC press.

Kee, R. J., Coltrin, M. E., & Glarborg, P. (2005). *Chemically reacting flow: theory and practice*: John Wiley & Sons.

Kennedy, R. H. (1995). Application of the BATHTUB Model to Selected Southeastern Reservoirs: DTIC Document.

Kitware-ParaView. (2014). ParaView. from http://www.paraview.org/

LimnoTech. (2007). Upper Mississippi River - Lake Pepin Water Quality Model; Development, Provisional Calibration and Preliminary Application: Minnesota Pollution Control Agency.

Martin, J. L., & McCutcheon, S. C. (1998). *Hydrodynamics and transport for water quality modeling*: CRC Press.

Mitsch, W. J., & Day Jr, J. W. (2006). Restoration of wetlands in the Mississippi–Ohio–Missouri (MOM) River basin: experience and needed research. *Ecological Engineering, 26*(1), 55-69.

Mitsch, W. J., Day, J. W., Gilliam, J. W., Groffman, P. M., Hey, D. L., Randall, G. W., & Wang, N. (2001). Reducing Nitrogen Loading to the Gulf of Mexico from the Mississippi River Basin: Strategies to Counter a Persistent Ecological Problem Ecotechnology—the use of natural ecosystems to solve environmental problems—should be a part of efforts to shrink the zone of hypoxia in the Gulf of Mexico. *Bioscience, 51*(5), 373-388.

Mitsch, W. J., & Gosselink, J. G. (2008). *Wetlands*.

Mitsch, W. J., Zhang, L., Stefanik, K. C., Nahlik, A. M., Anderson, C. J., Bernal, B., . . . Song, K. (2012). Creating wetlands: primary succession, water quality changes, and self-design over 15 years. *Bioscience, 62*(3), 237-250.

Monod, J. (1949). The growth of bacterial cultures. *Annual Reviews in Microbiology, 3*(1), 371-394.

Mooij, W. M., Trolle, D., Jeppesen, E., Arhonditsis, G., Belolipetsky, P. V., Chitamwebwa, D. B., . . . Downing, A. S. (2010). Challenges and opportunities for integrating lake ecosystem modelling approaches. *Aquatic Ecology, 44*(3), 633-667.

Myers, D. N. (2011). *Change to Solubility Equations for Oxygen in Water*. USGS- Office of Water Quality Thecnical Memorandum 2001.03. USGS. USGS.

NCCHE. (2012). CCHE3D model, The University of Mississippi.   Retrieved 2014, 2014, from http://www.ncche.olemiss.edu/cche3d

NESP. (2006). Upper Mississippi River System Navigation and Ecosystem Sustainability Program, Environmental Science Panel Report: Implementing Adaptive Management, U.S. Army Corps of Engineers, Rock Island, NESP ENV Report 2 (pp. 137).

Olsen, N. R. B. (2011). A three-dimensional numerical model for simulation of sediment movements in water intakes with multiblock option. *User's manual*.

OpenFOAM. (2012). SnappyHexMesh, mesh genration OpenFOAM. from http://www.openfoam.org/docs/user/snappyHexMesh.php

OpenFOAMWiki. (2014). Unofficial OpenFOAM Wiki. from http://openfoamwiki.net/index.php/Main_Page

Oveisy, A., Boegman, L., & Imberger, J. (2012). Three-dimensional simulation of lake and ice dynamics during winter. *Limnology and Oceanography, 57*(1), 43.

Park, K., Jung, H.-S., Kim, H.-S., & Ahn, S.-M. (2005). Three-dimensional hydrodynamic-eutrophication model (HEM-3D): application to Kwang-Yang Bay, Korea. *Marine Environmental Research, 60*(2), 171-193.

POINTWISE. (2012). POINTWISE meshing software. from http://www.pointwise.com/gridgen/

PSU, W. Q. R. G. (2012). CE-QUAL-W2, model. 2012, from http://www.cee.pdx.edu/w2/

Rabalais, N. N., Turner, R. E., & Scavia, D. (2002). Beyond Science into Policy: Gulf of Mexico Hypoxia and the Mississippi River Nutrient policy development for the Mississippi River watershed reflects the accumulated scientific evidence that the increase in nitrogen loading is the primary factor in the worsening of hypoxia in the northern Gulf of Mexico. *Bioscience, 52*(2), 129-142.

Richardson, W. B., Strauss, E. A., Bartsch, L. A., Monroe, E. M., Cavanaugh, J. C., Vingum, L., & Soballe, D. M. (2004). Denitrification in the Upper Mississippi River: rates, controls, and contribution to nitrate flux. *Canadian Journal of Fisheries and Aquatic Sciences, 61*(7), 1102-1112.

Rusche, H. (2003). *Computational fluid dynamics of dispersed two-phase flows at high phase fractions.* Imperial College London (University of London).

Schnoor, J. L. (1996). *Environmental modeling: fate and transport of pollutants in water, air, and soil*: John Wiley and Sons.

Schubert, M. A. (2009). Computational fluid dynamics applications for nitrate removal in an Upper Mississippi River backwater.

Seitzinger, S. P., Styles, R. V., Boyer, E. W., Alexander, R. B., Billen, G., Howarth, R. W., . . . Van Breemen, N. (2002). Nitrogen retention in rivers: model development and application to watersheds in the northeastern USA *The Nitrogen Cycle at Regional to Global Scales* (pp. 199-237): Springer.

Singer, M., Pope, S., & Najm, H. (2006). Operator-splitting with ISAT to model reacting flow with detailed chemistry. *Combustion Theory and Modelling, 10*(2), 199-217.

Spieles, D. J., & Mitsch, W. J. (1999). The effects of season and hydrologic and chemical loading on nitrate retention in constructed wetlands: a comparison of low-and high-nutrient riverine systems. *Ecological Engineering, 14*(1), 77-91.

Stern, F., Xing, T., Yarbrough, D. B., Rothmayer, A., Rajagopalan, G., Prakashotta, S., . . . Hutchings, B. (2006). Hands-On CFD Educational Interface for Engineering Courses and Laboratories. *Journal of Engineering Education, 95*(1), 63-83.

Stumm, W., & Morgan, J. J. (1981). *Aquatic chemistry: an introduction emphasizing chemical equilibria in natural waters*: John Wiley.

Sucsy, P., & Hendrickson, J. (2004). Calculation of nutrient reduction goals for the Lower St. Johns River by application of CE-QUAL-ICM, a mechanistic water quality model. *Water Resources Department Technical Memorandum, St. Johns River Water Management District, Palatka, Florida.*

Sun, Y., Petersen, J., & Clement, T. (1999). Analytical solutions for multiple species reactive transport in multiple dimensions. *Journal of contaminant hydrology, 35*(4), 429-440.

TECPLOT. (2014). TECPLOT. from http://www.tecplot.com/

TheOpenFOAMExtendedProject. (2014). The OpenFOAM Extended Project. from http://www.extend-project.de/

Tilman, D., Fargione, J., Wolff, B., D'Antonio, C., Dobson, A., Howarth, R., . . . Swackhamer, D. (2001). Forecasting agriculturally driven global environmental change. *Science, 292*(5515), 281-284.

Tufford, D. L., & McKellar, H. N. (1999). Spatial and temporal hydrodynamic and water quality modeling analysis of a large reservoir on the South Carolina (USA) coastal plain. *Ecological modelling, 114*(2), 137-173.

USACE. (2012). Environmental Laboratory Website. from http://el.erdc.usace.army.mil
Versteeg, H. K., & Malalasekera, W. (2007). *An introduction to computational fluid dynamics: the finite volume method*: Pearson Education.

Wanninkhof, R. (1992). Relationship between wind speed and gas exchange over the ocean. *Journal of Geophysical Research: Oceans (1978–2012), 97*(C5), 7373-7382.

Weller, H. G., Tabor, G., Jasak, H., & Fureby, C. (1998). A tensorial approach to computational continuum mechanics using object-oriented techniques. *Computers in physics, 12*(6), 620-631.

Wetzel, R. (2001). *Limnology, Lake and River Ecosystems* (3 ed.): Elseiver.

WEZERNAK, C. T., & GANNON, J. J. (1968). Evaluation of nitrification in streams.

Wlosinski, J. H., & Collins, C. D. (1985). Evaluation of a water quality model (CE-QUAL-R1) using data from a small Wisconsin reservoir. *Ecological modelling, 29*(1), 303-313.

Wlosinski, J. H., Lessem, A. S., Dortch, M. S., Schneider, M., & Martin, J. L. (1995). CE-QUAL-R1: A Numerical One-Dimensional Model of Reservoir Water Quality; User's Manual: DTIC Document.

Yoshida, T., Jones, L. E., Ellner, S. P., Fussmann, G. F., & Hairston, N. G. (2003). Rapid evolution drives ecological dynamics in a predator–prey system. *Nature, 424*(6946), 303-306.

-

APPENDIX A

DESCRIPTION OF BIOCHEMMATLAB

Since all the equations were formulated in Chapter 3 of the thesis here a general description is presented regarding the model implementation in MATLAB.

The code was developed to test the solutions of BioChemFOAM under characteristic conditions. The characteristic conditions are defined by data of concentration and parameter collected in the literature. It is proveed that if both models have the same parameterization but different numericla methods to solve the sytem of equations both models should reproduce the same PCBP (Physical, chemical and biological processes).

The numerical implementation utilizes an Euler scheme to driscretize the time terms and an implicit iterative method to discretize terms describing the PCBP affecting the aqutic ecosystem. The general idea followed to solve the equations were to star by solving algae equations first and then the others as follows: DOC. PO4, DON, NH4, NO3, DO, COD, POC, POP and PON. The sequential solution of those equations utilizes the latest value calculated for each species. E.g. After the concentration for ammonia is calculated, then this new value is utilized in the calculation of nitrate, see Figure A-1 for an example of the code and procedure. This process is followed when calculated each dsicretized equation for the eleven species.

```
%NH4+
       %f1N1=(c0(6,1))/(KHNx+c0(5,1)+c0(6,1));
       %Px1=PMx*f1N1*f2_I(I,Ik)*f3_T(T,KTG1x,KTG2x,TM1x,TM2x);%not· needed
       PNx=(c0(6,1)/((KHNx+c0(5,1))*(KHNx+c0(6,1)))+KHNx/((c0(6,1)+c0(5,1))*(KHNx+c0(6,1))));
       a11=(FNIx*(BMx))*ANCx*c1(1,1);
       a12=(FNIP*(PRx))*ANCx*c1(1,1);
       a13=KDON*c1(4,1);
       a1=a11+a12+a13;
       %f1N2=c0(5,1)/(KHNx+c0(5,1)+c0(6,1));
       Px2=PMx*f1N2*f2_I(I,Ik)*f3_T(T,KTG1x,KTG2x,TM1x,TM2x);%not· needed
       Nit=(c0(7,1)/(KHNitDO+c0(7,1)))*(c0(5,1)/(KHNitN+c0(5,1)))*Nitm*fNit_T(T,TNit,KNit1,KNit2);%add· c0(5,1)
       a21=(PNx)*(Px)*ANCx*c1(1,1);%Px1+Px2· NO·->·Px·
       a2=-a21-Nit;
       c1(5,1)=(cI2(5,1)/dt+a1)/(1/dt-(a2));
       cR_proc_NH4(1,kk+1)=a11;°       °.%Metabolism
       cR_proc_NH4(2,kk+1)=a12;°       °°.%Predation
       cR_proc_NH4(3,kk+1)=-a21;°       ° .%Uptake
       cR_proc_NH4(4,kk+1)=a13;°       °°°.%DON·mineralizati
       cR_proc_NH4(5,kk+1)=-Nit*c1(5,1);°  °°°.%Nitrification
```

A

```
       %NO3
       gamma=ANCx*c1(1,1);
       f1N1=(1/(KHNx+c1(5,1)+c0(6,1)))*(c1(3,1)/(KHPx+c1(3,1)));%(NH4+NO3)/(KHNx+NH4+NO3);· add·Ci3·(DOP)
       Px1=PMx*f1N1*f2_I(I,Ik)*f3_T(T,KTG1x,KTG2x,TM1x,TM2x);
       PNx1=(c0(6,1)/((KHNx+c1(5,1))*(KHNx+c0(6,1)))+KHNx/((c0(6,1)+c1(5,1))*(KHNx+c0(6,1))))*c1(5,1);
       Nit=(c0(7,1)/(KHNitDO+c0(7,1)))*(c1(5,1)/(KHNitN+c1(5,1)))*Nitm*fNit_T(T,TNit,KNit1,KNit2);%OK·
       fNit_T(T,TNit,KNit1,KNit2)
       f1N2=(c1(5,1)/(KHNx+c1(5,1)+c0(6,1)))*(c1(3,1)/(KHPx+c1(3,1)));
       Px2=PMx*f1N2*f2_I(I,Ik)*f3_T(T,KTG1x,KTG2x,TM1x,TM2x);
       %PNx2=((c1(5,1)*KHNx)/((c0(6,1)+c1(5,1))*(KHNx+c0(6,1))));
       Denit=(KHORDO/(KHORDO+c0(7,1)))*(1/(KHDNN+c0(6,1)))*AANOX*(KDC+KDCalg*c1(1,1))*KDOC;
       a1=-(1-PNx1)*Px2*gamma+Nit*c1(5,1);°°·
       %f1N3=1/(KHNx+c1(5,1)+c0(6,1));
       %Px1_3=PMx*f1N3*f2_I(I,Ik)*f3_T(T,KTG1x,KTG2x,TM1x,TM2x);
       a11=(1-PNx1)*Px1*gamma
       a12=ANDC*Denit*c1(2,1);
       a2=-a11-a12;
       c1(6,1)=(cI2(6,1)/dt+a1)/(1/dt-a2);
       cR_proc_NO3(1,kk+1)=-a11;°       °°.%Algal·uptake
       cR_proc_NO3(2,kk+1)=Nit*c1(5,1);°  °°°.%Nitrification
       cR_proc_NO3(3,kk+1)=-a12;°       °°°.%Denitrification¶
```

Figure A-1 Example code BioChemMATLAB. Section where ammonia (NH4) and nitrate (NO3) reaction equations are discretized. The red arrow indicates were the latest value of ammonia is utilized to define the new value for nitrate. Numerical Discretization of ammonia equation 3.66, Chapter 3 (top left). Numerical discretization of nitrate equation 3.68, Chapter 3 (Bottom right)

APPENDIX B

ADDITIONAL FIGURES CASE SECTION 6.3 AND 6.4

B.1. Additional Figures section 6.4

The following figures complements the results analyzed in section 6.4. This section presents an analysis of the influence of initial conditions on the nitrate distribution when a constant mass loading rate is reached at the outlet.
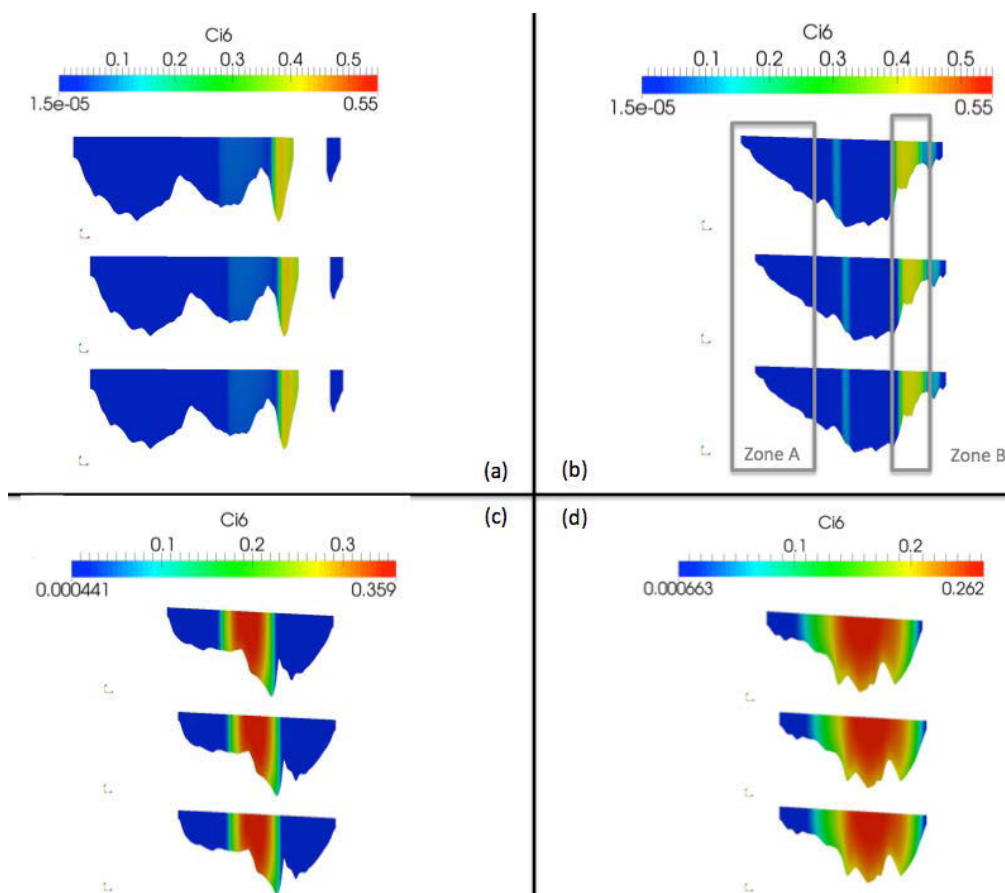
Figure B-1 . Spatial distribution of nitrate concentration at 4 cross sections. CS1 (a). CS2 (b). CS3 (c). and CS4 (d). All cross section presented looking upstream. The main flow (e.g., see yellow contours in figure a) is from CS1 to CS4.
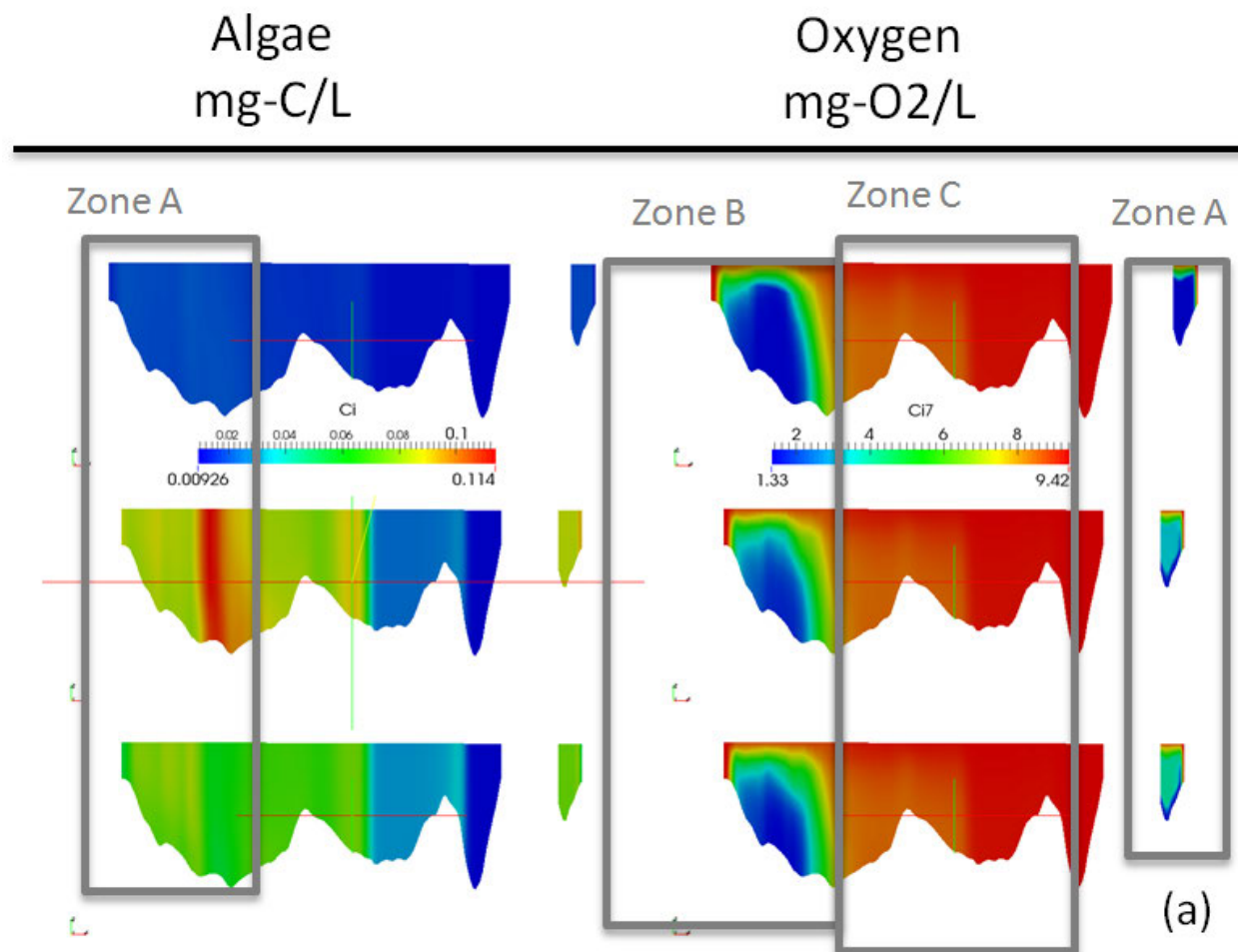
Figure B-2. Algae and dissolved oxygen concentration contours at CS1 (a). Figures show results for IC nitrate 0.01mg-N/L (top), IC nitra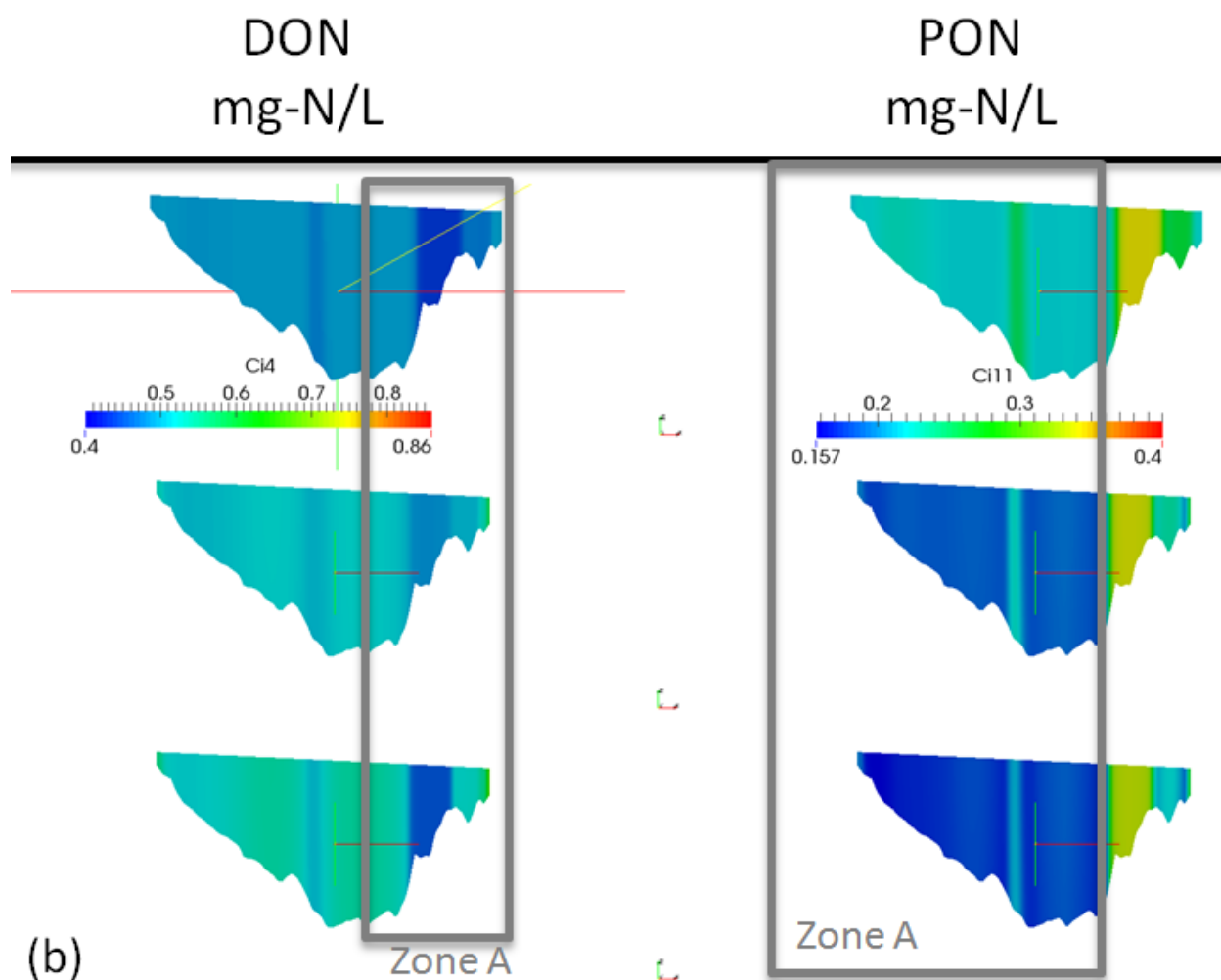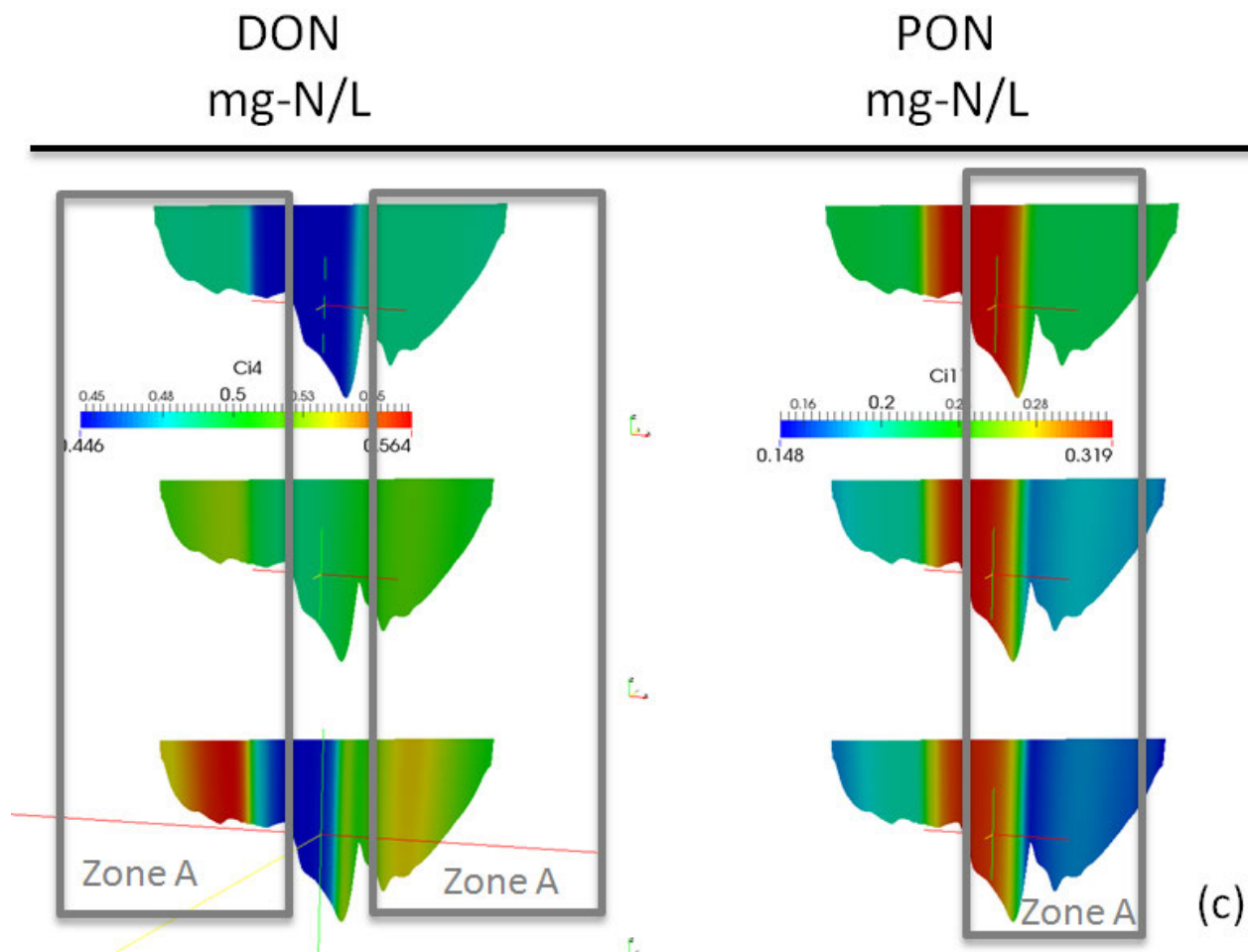te 0.35 mg-N/L (middle) and IC nitrate 0.55 mg-N/L (bottom). Zone A showing different distribution of species. Zone B and C showing same distribution of the species.
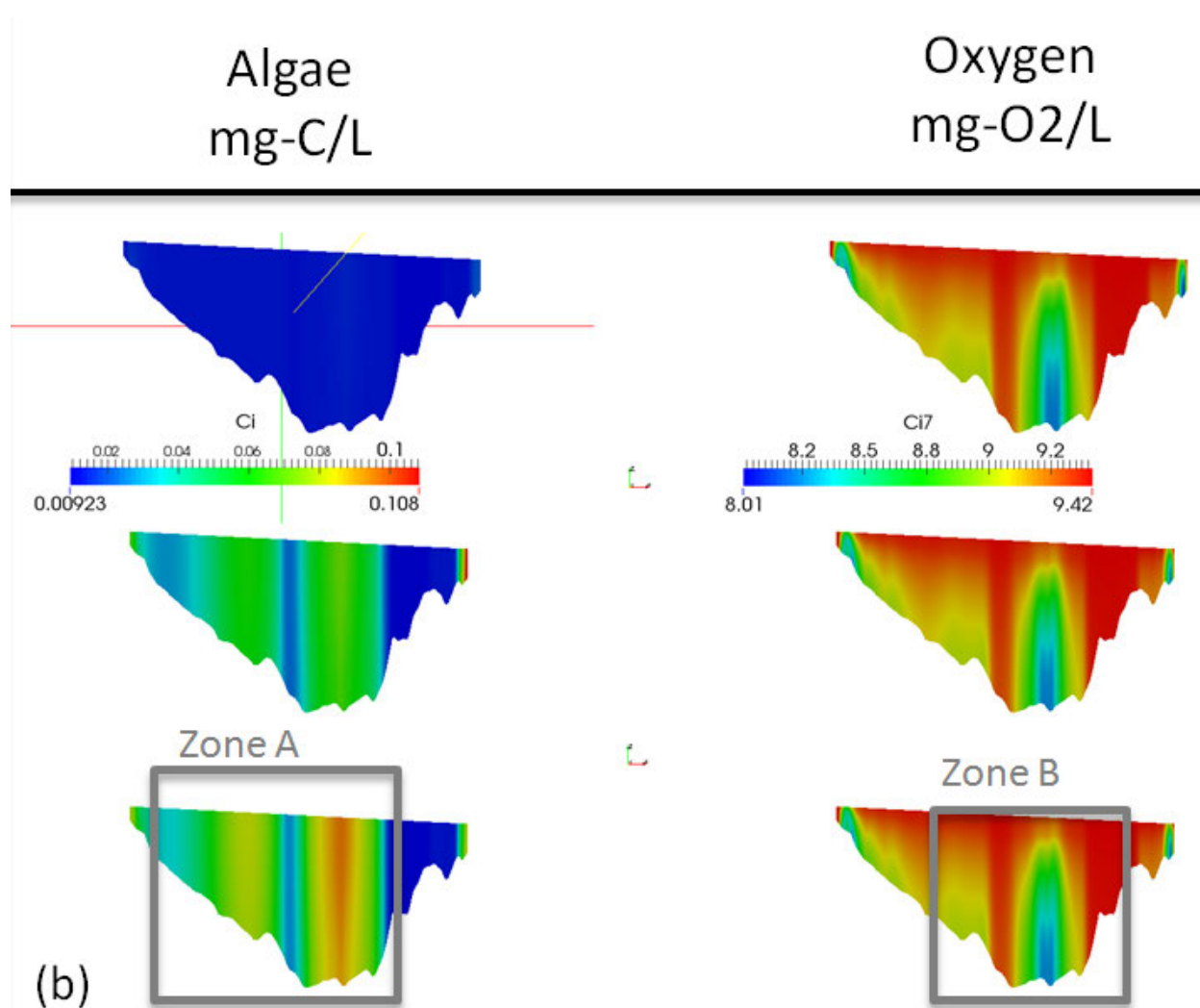
Figure B-3. Algae and oxygen concentration contours at CS2 (b). Figures show results for IC nitrate 0.01mg-N/L (top), IC nitra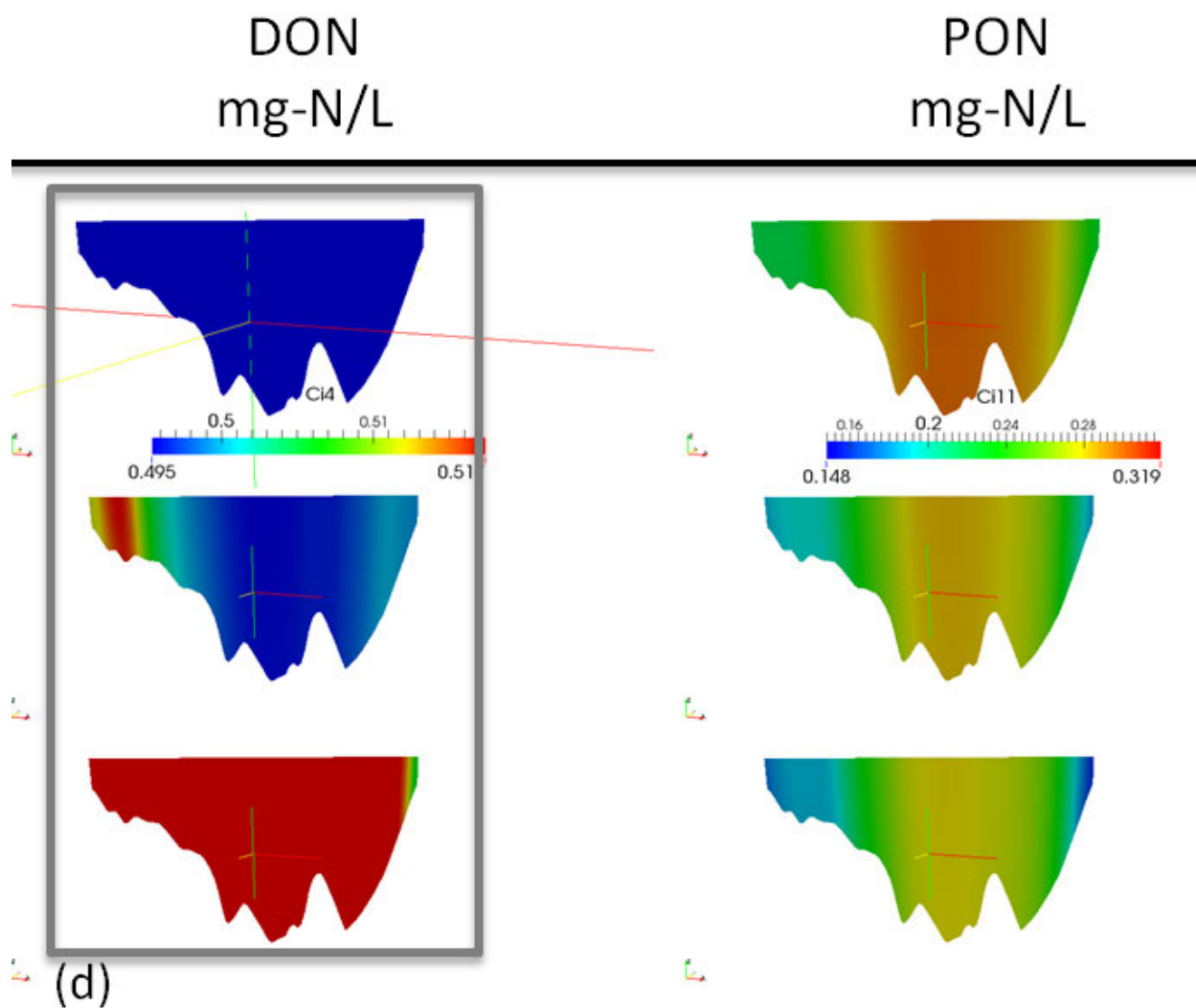te 0.35 mg-N/L (middle) and IC nitrate 0.55 mg-N/L (bottom). Zone A different distributions. Zone B and C same distribution of the species.
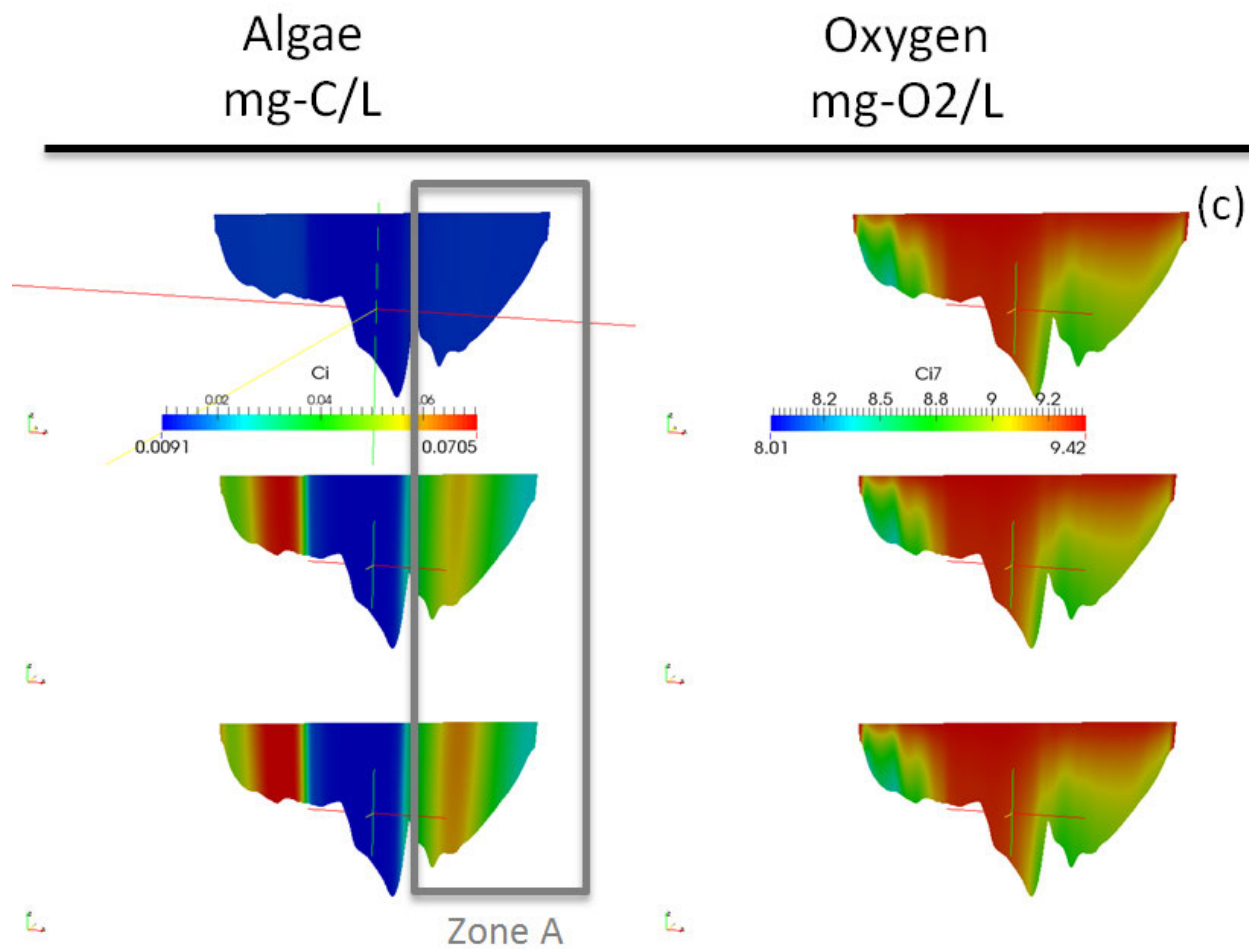
Figure B-4. Algae and oxygen concentration contours at CS3 (c). Figures show results for IC nitrate 0.01mg-N/L (top), IC nitra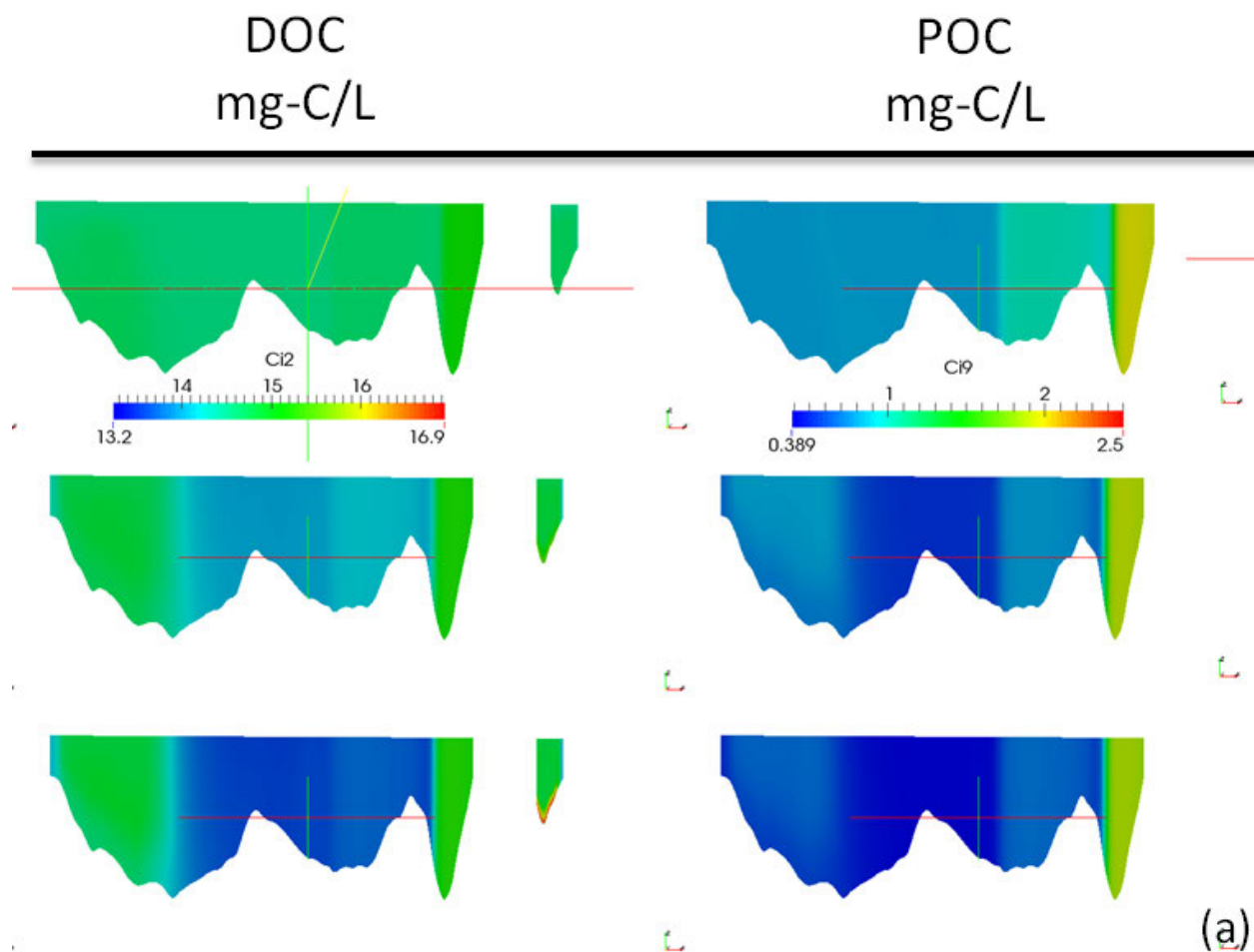te 0.35 mg-N/L (middle) and IC nitrate 0.55 mg-N/L (bottom). Zone A different distributions. Zone B and C same distribution of the species.
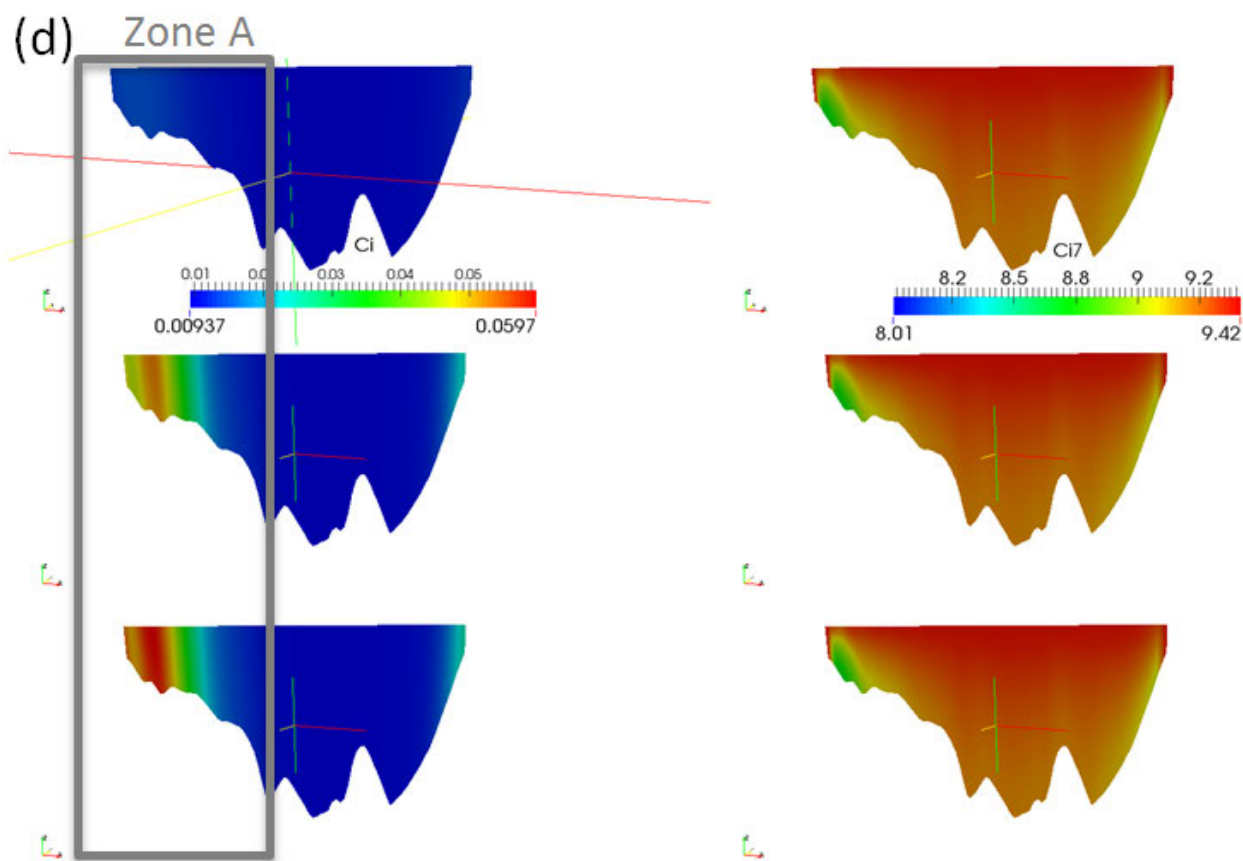
Figure B-5. Algae and oxygen concentration contours at CS4 (d). Figures show results for IC nitrate 0.01mg-N/L (top), IC nitra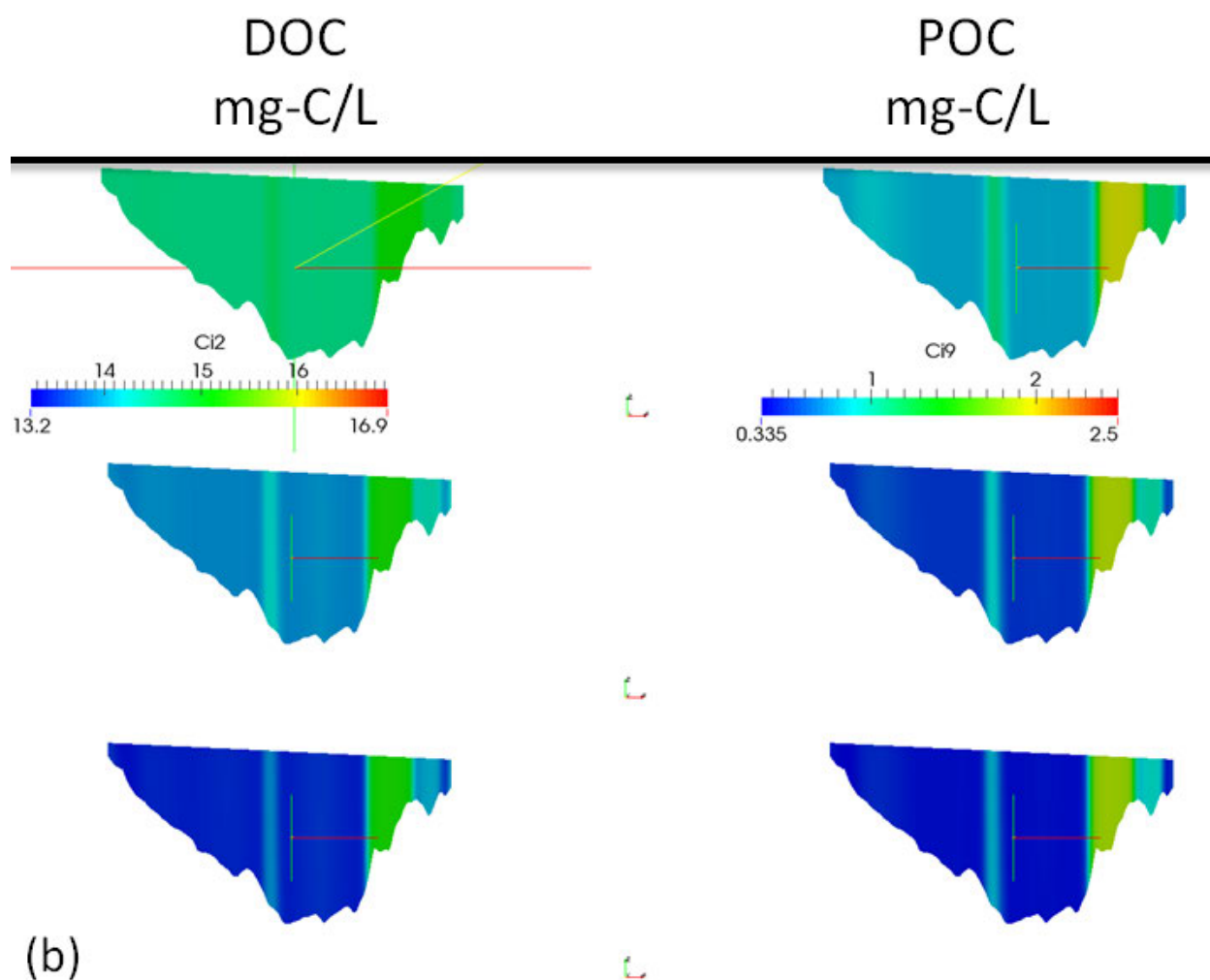te 0.35 mg-N/L (middle) and IC nitrate 0.55 mg-N/L (bottom). Zone A different distributions. Zone B and C same distribution of the species.
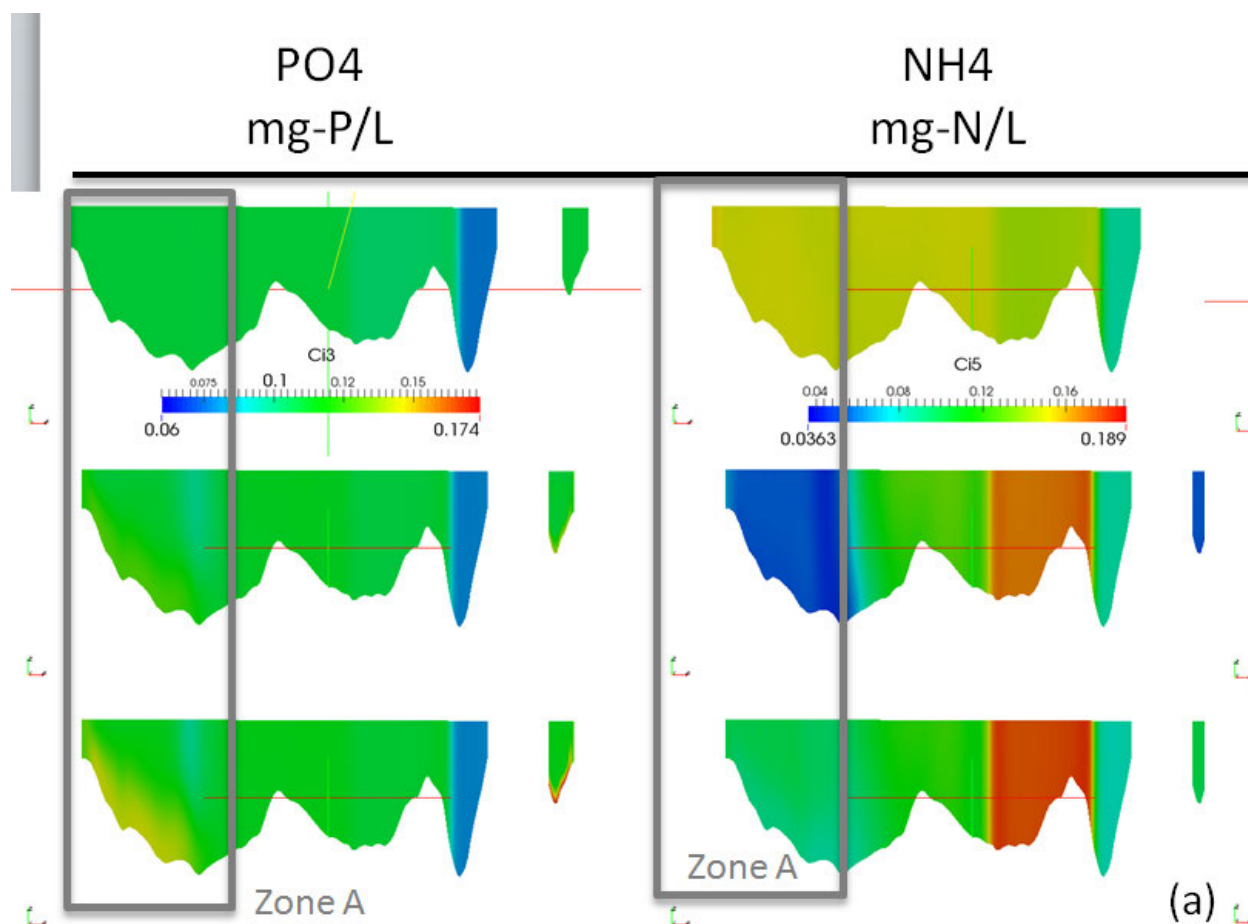
Figure B-6. Algae and dissolved oxygen concentration contours at CS1 (a). Figures show results for IC nitrate 0.01mg-N/L (top), IC nitrate 0.35 mg-N/L (middle) and IC nitrate 0.55 mg-N/L (bottom). Zone A showing different distribution of species
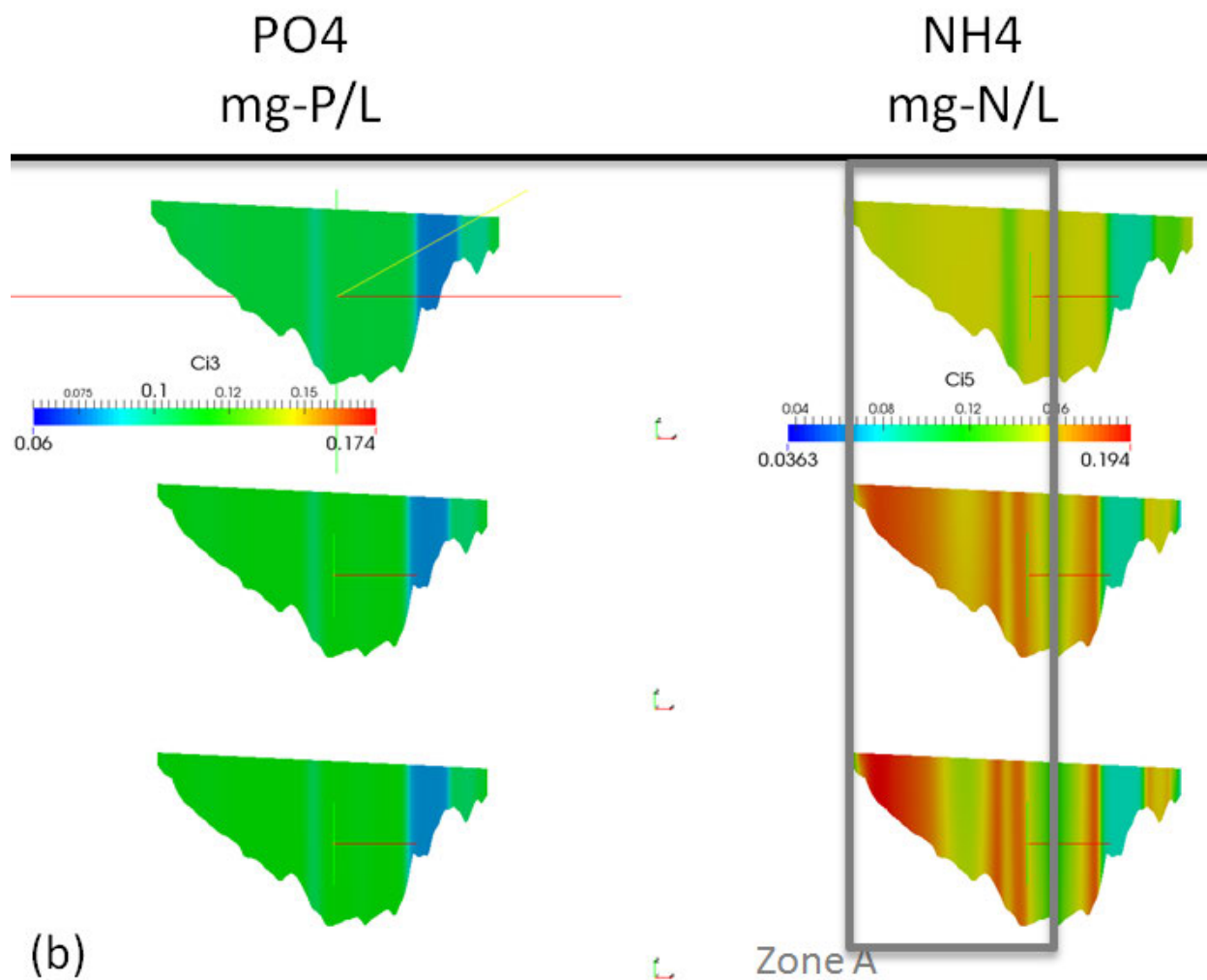
Figure B-7. Algae and dissolved oxygen concentration contours at CS2 (b). Figures show results for IC nitrate 0.01mg-N/L (top), IC nitrate 0.35 mg-N/L (middle) and IC nitrate 0.55 mg-N/L (bottom). Zone A showing different distribution of species.
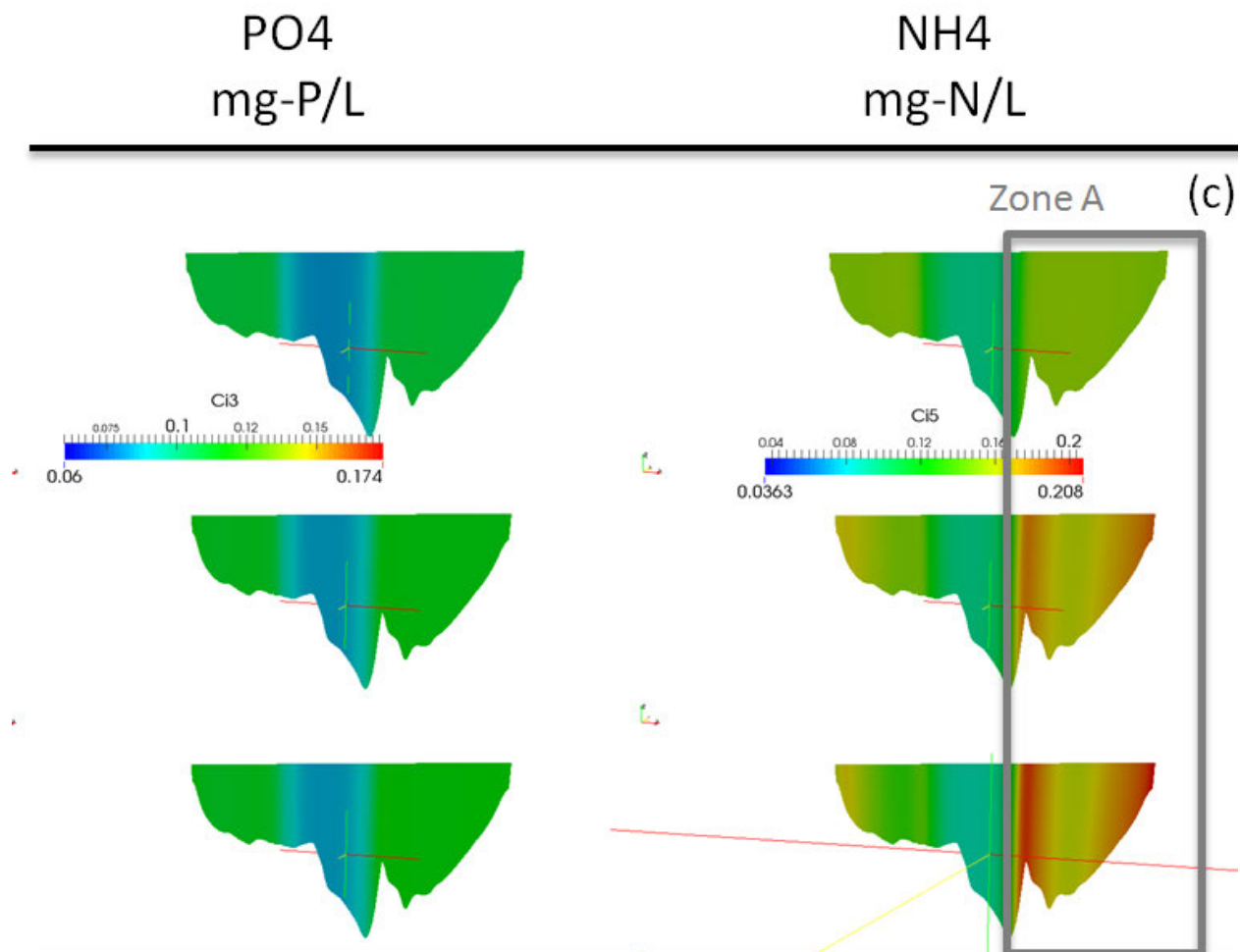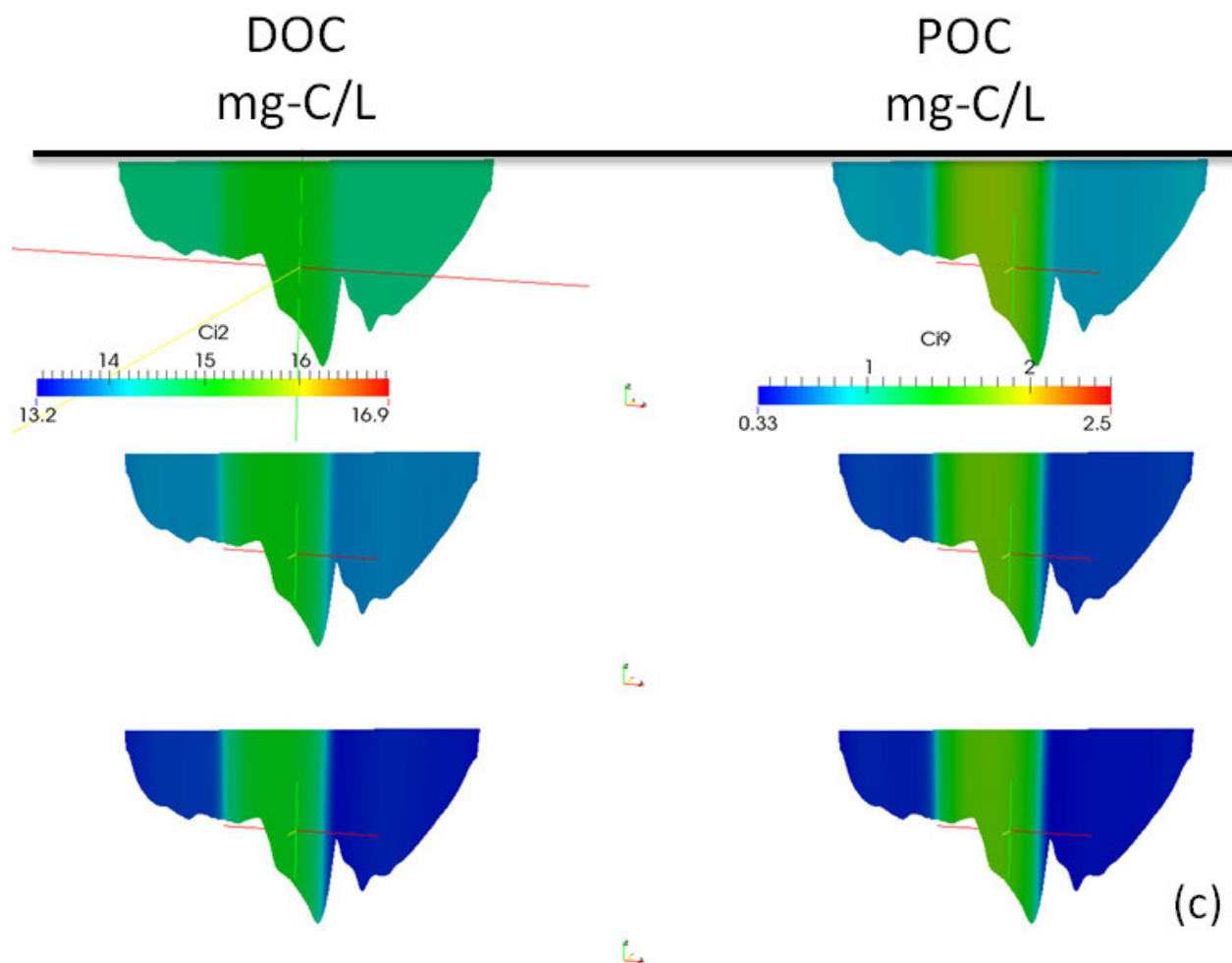
Figure B-8. Algae and dissolved oxygen concentration contours at CS3 (c). Figures show results for IC nitrate 0.01mg-N/L (top), IC nitrate 0.35 mg-N/L (middle) and IC nitrate 0.55 mg-N/L (bottom). Zone A showing different distribution of species.
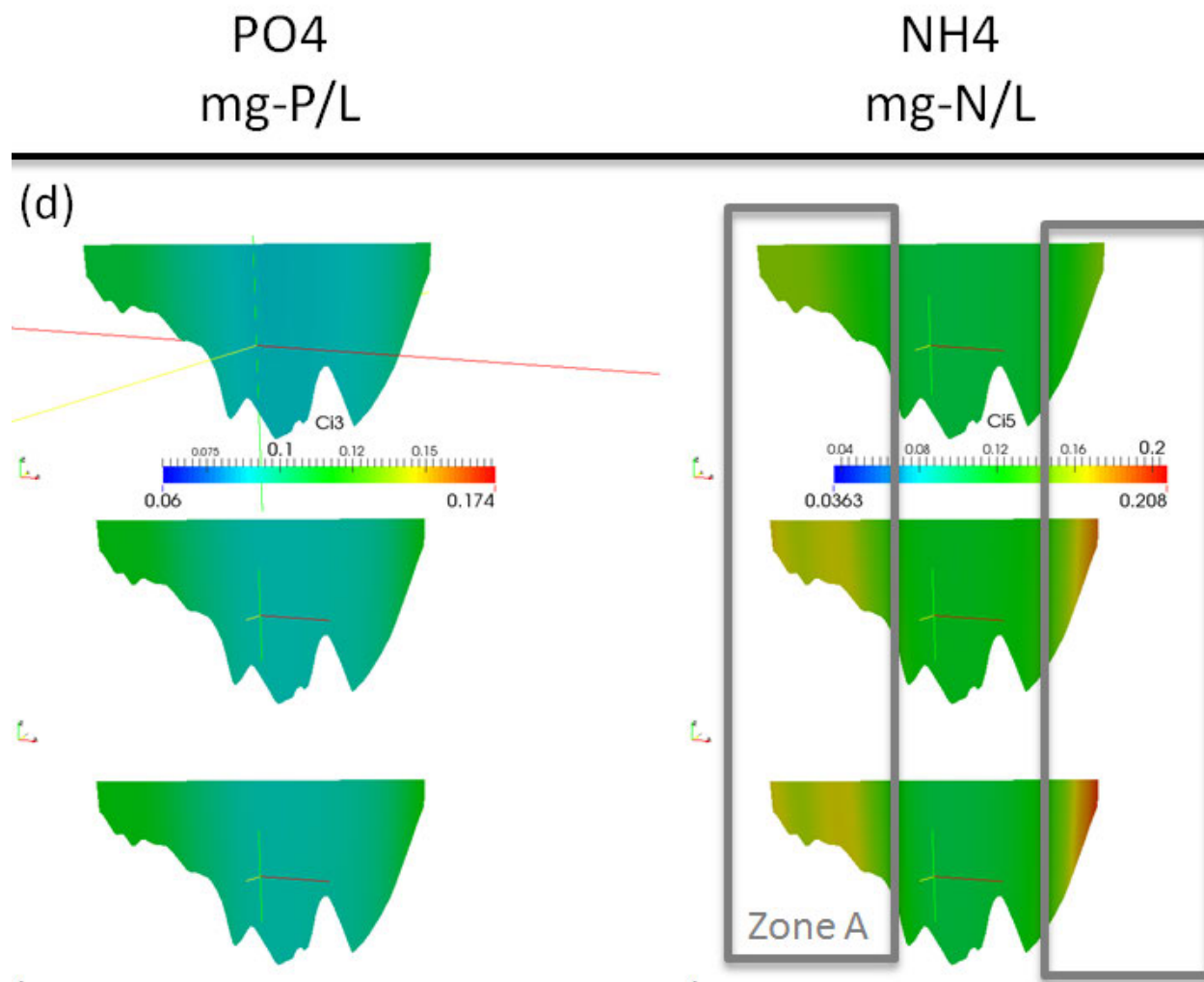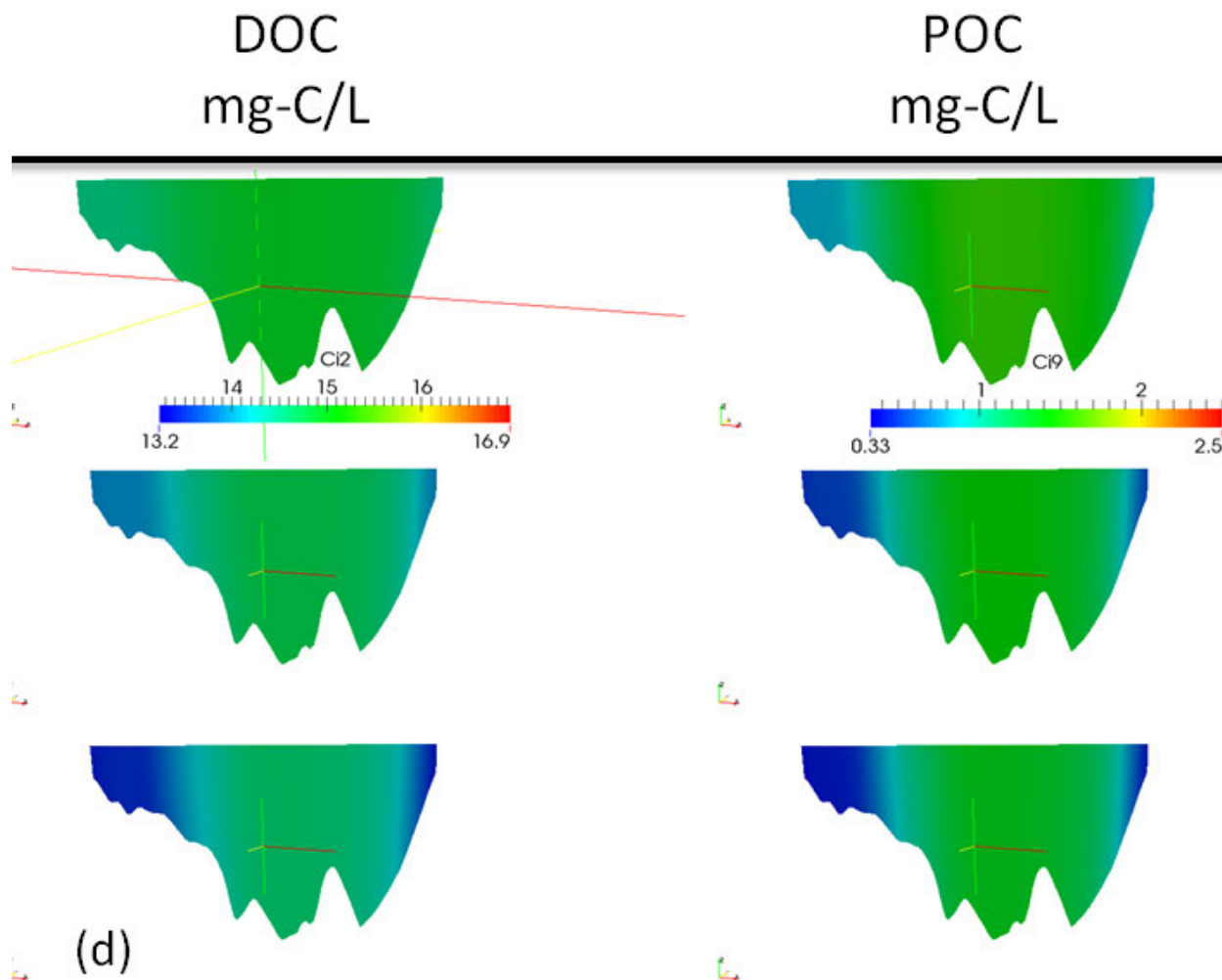
Figure B-9. Algae and dissolved oxygen concentration contours at CS4 (d). Figures show results for IC nitrate 0.01mg-N/L (top), IC nitrate 0.35 mg-N/L (middle) and IC nitrate 0.55 mg-N/L (bottom). Zone A showing different distribution of species
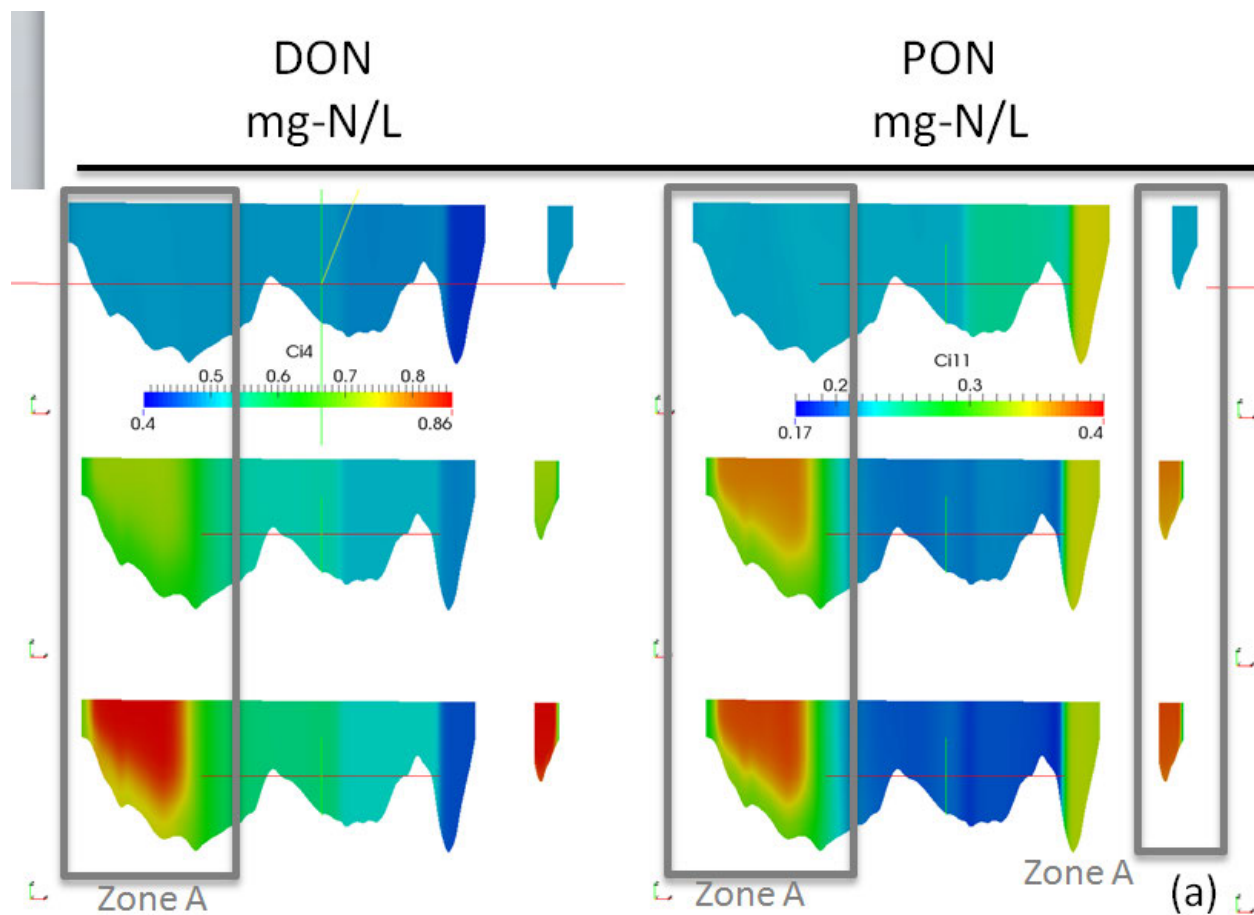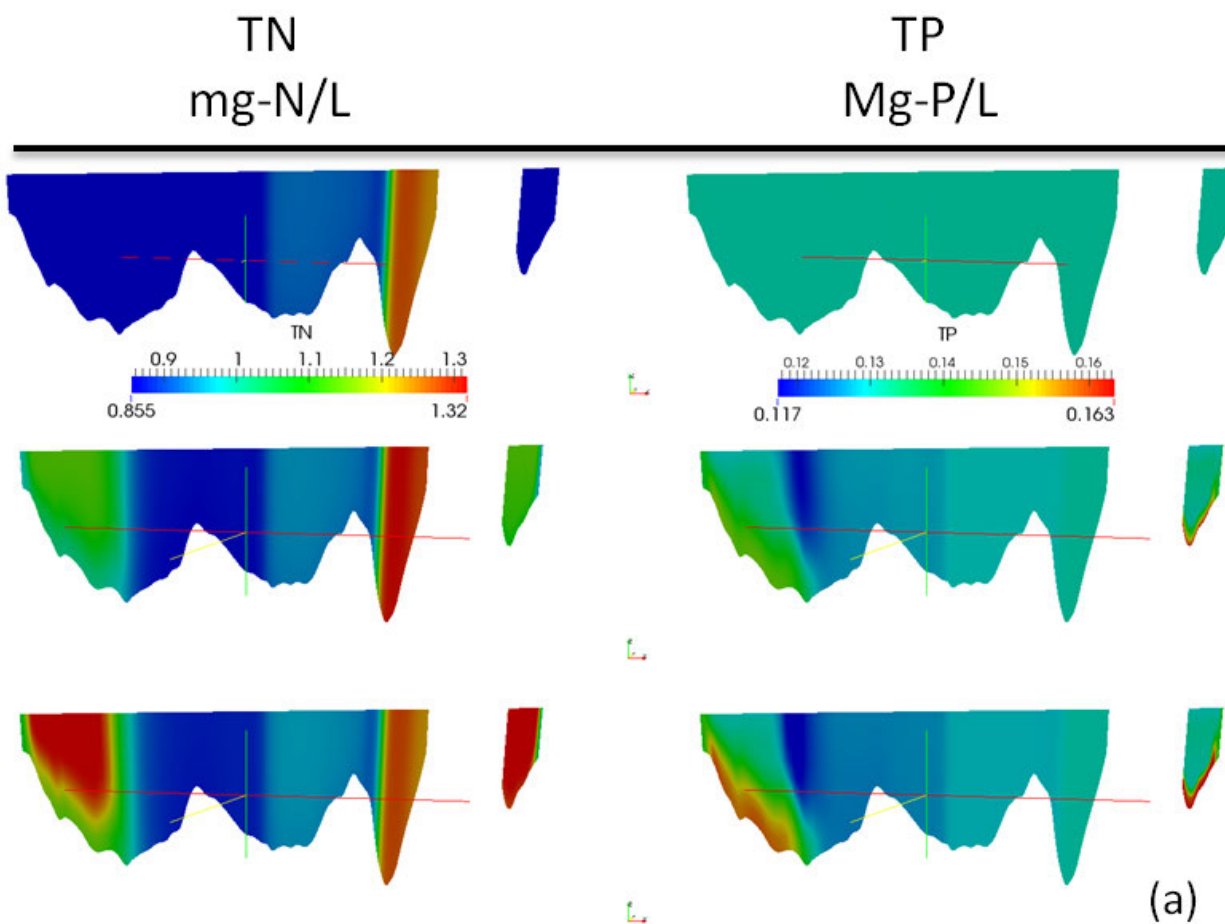
Figure B-10. Dissolved organic nitrogen (DON) and particulate organic nitrogen (PON) concentration contours at CS1 (a). Figures show results for IC nitrate 0.01 mg-N/L (top), IC nitrate 0.35 mg-N/L (middle) and IC nitrate 0.55 mg-N/L (bottom).

Figure B-11. Dissolved organic nitrogen (DON) and particulate organic nitrogen (PON) concentration contours at CS2 (b). Figures show results for IC nitrate 0.01 mg-N/L (top), IC nitrate 0.35 mg-N/L (middle) and IC nitrate 0.55 mg-N/L (bottom).
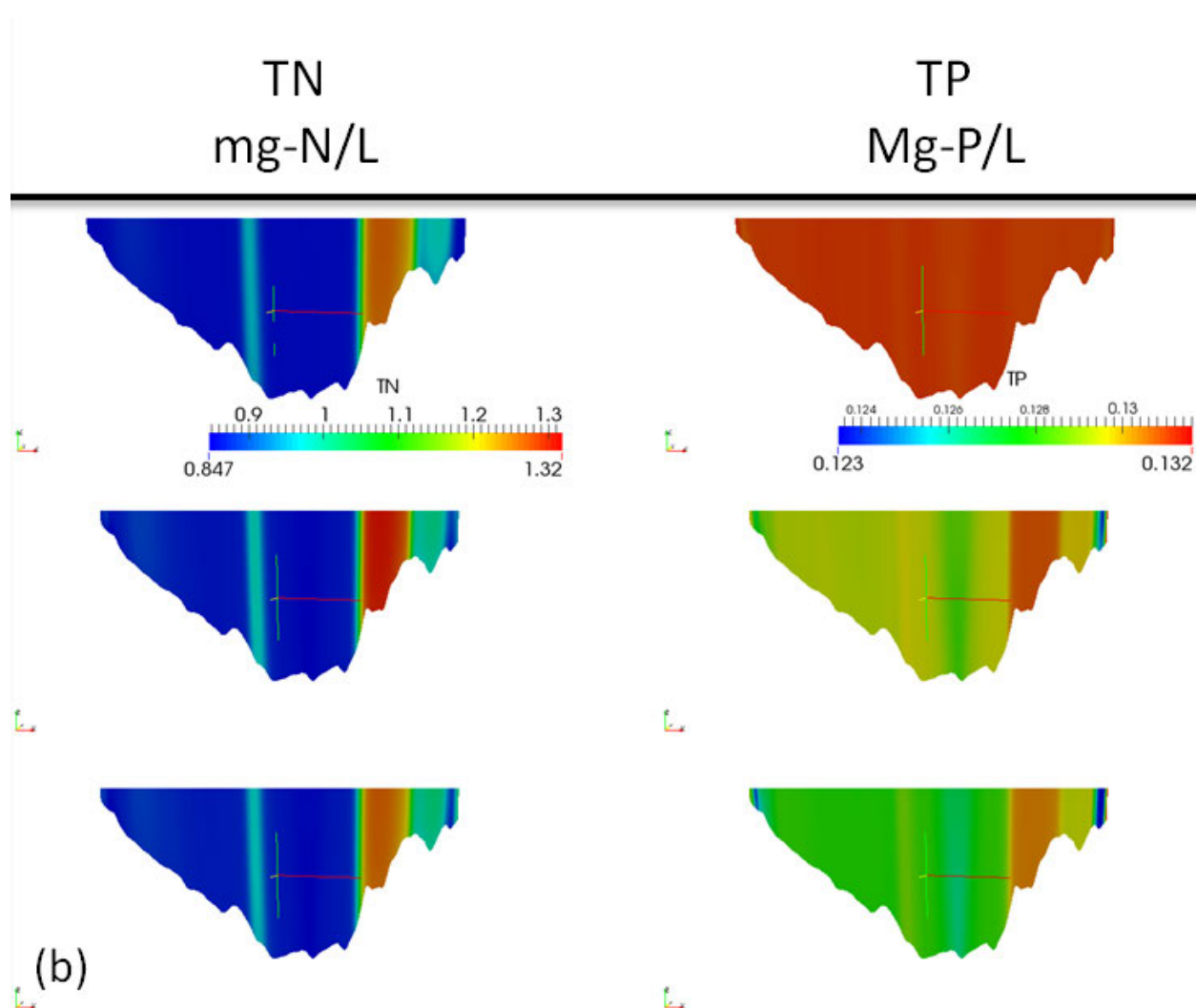
Figure B-12. Dissolved organic nitrogen (DON) and particulate organic nitrogen (PON) concentration contours at CS3 (c). Figures show results for IC nitrate 0.01 mg-N/L (top), IC nitrate 0.35 mg-N/L (middle) and IC nitrate 0.55 mg-N/L (bottom).
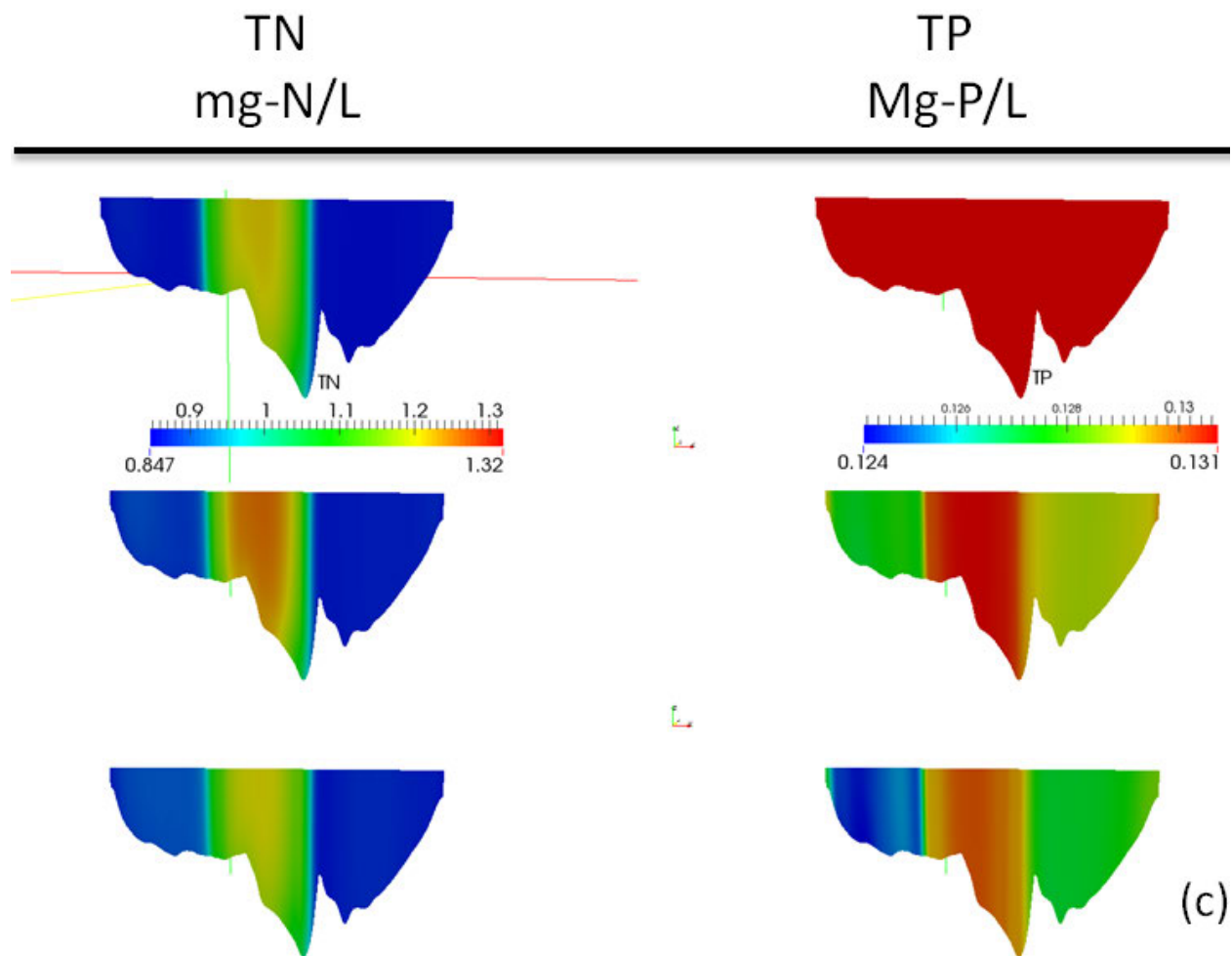
Figure B-13. Dissolved organic nitrogen (DON) and particulate organic nitrogen (PON) concentration contours at CS4 (d). Figures show results for IC nitrate 0.01 mg-N/L (top), IC nitrate 0.35 mg-N/L (middle) and IC nitrate 0.55 mg-N/L (bottom).
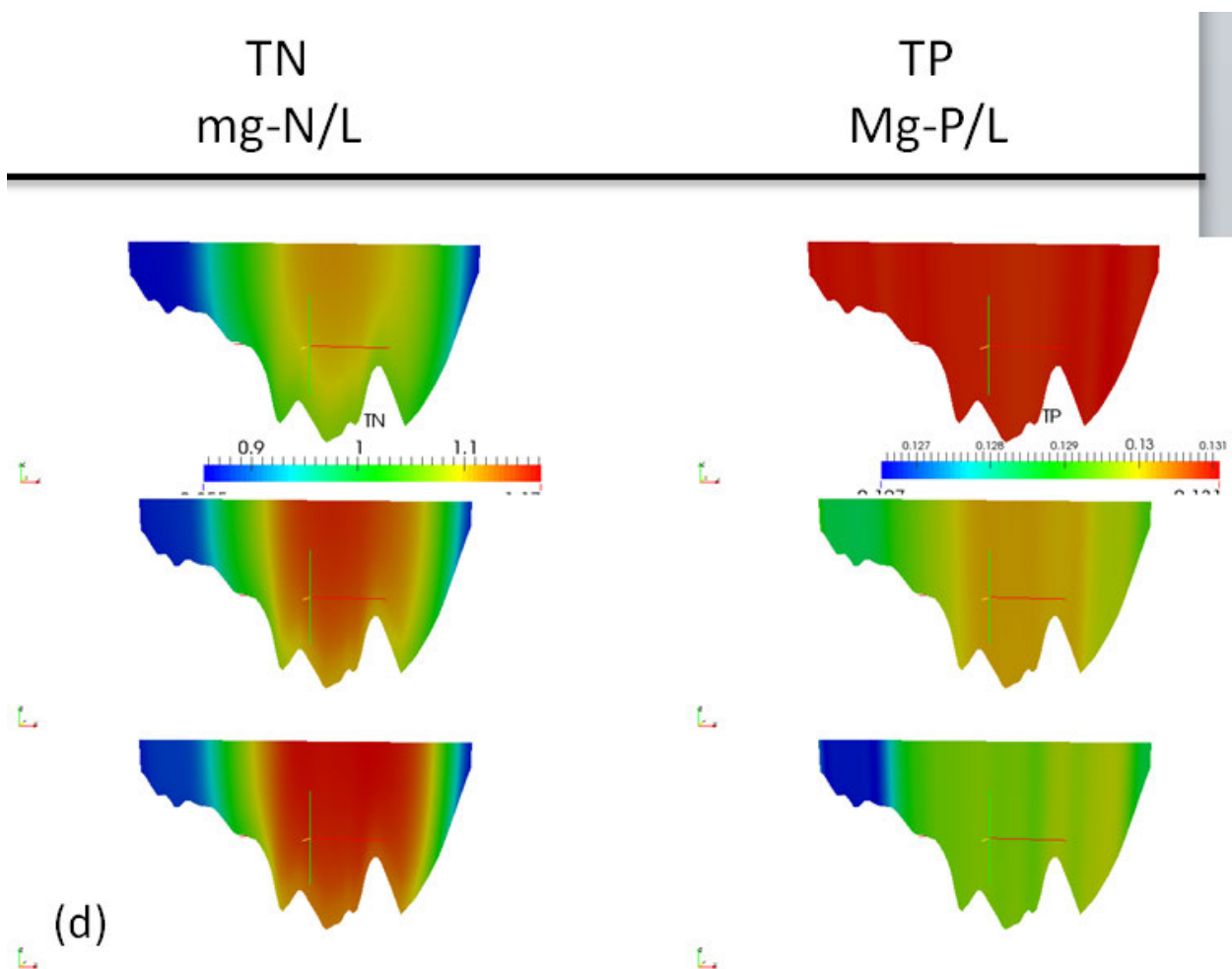
Figure B-14. Dissolved organic carbon (DOC) and particulate organic carbon (POC) concentration contours at CS1 (a). Figures show results for IC nitrate 0.01 mg-N/L (top), IC nitrate 0.35 mg-N/L (middle) and IC nitrate 0.55 mg-N/L (bottom).
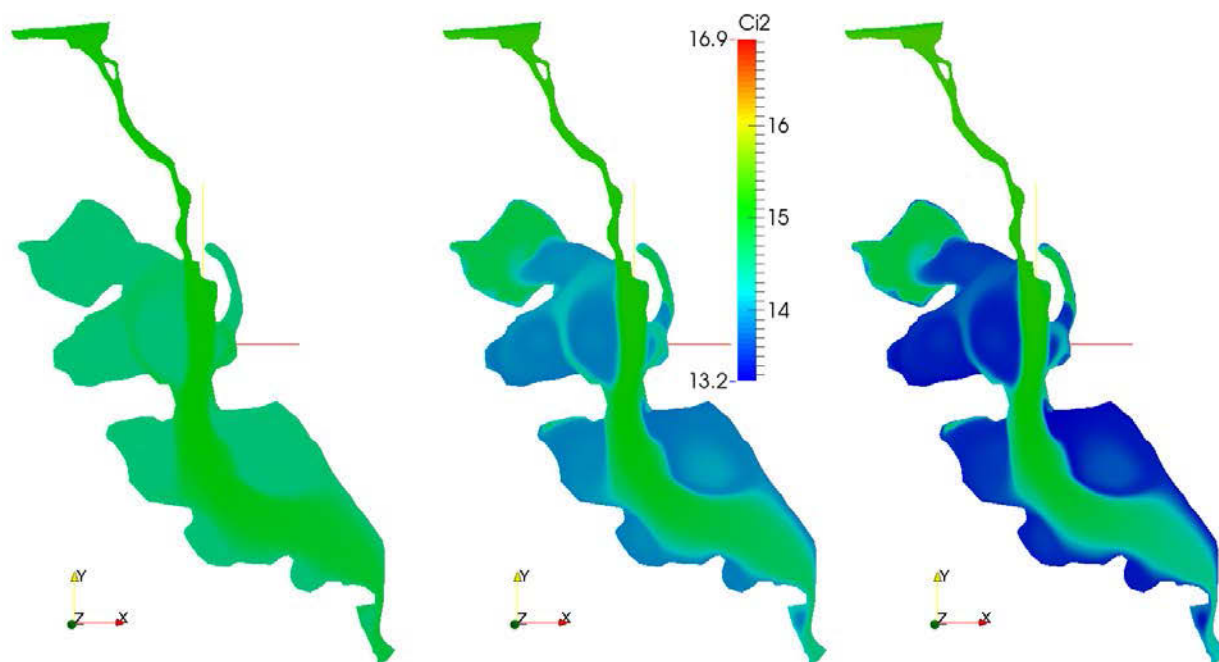
Figure B-15. Dissolved organic carbon (DOC) and particulate organic carbon (POC) concentration contours at CS2 (b). Figures in panel (b) show results for IC nitrate 0.01 mg-N/L (top), IC nitrate 0.35 mg-N/L (middle) and IC nitrate 0.55 mg-N/L (bottom).

Figure B-16. Dissolved organic carbon (DOC) and particulate organic carbon (POC) concentration contours at CS3 (c). Figures in panel (b) show results for IC nitrate 0.01 mg-N/L (top), IC nitrate 0.35 mg-N/L (middle) and IC nitrate 0.55 mg-N/L (bottom).

Figure B-17. Dissolved organic carbon (DOC) and particulate organic carbon (POC) concentration contours at CS4 (d). Figures in panel (b) show results for IC nitrate 0.01 mg-N/L (top), IC nitrate 0.35 mg-N/L (middle) and IC nitrate 0.55 mg-N/L (bottom).

Figure B-18. Total Nitrogen and Total Phosphorus concentration contours at CS1 (a). Figures show results for IC nitrate 0.01 mg-N/L (top), IC nitrate 0.35 mg-N/L (middle) and IC nitrate 0.55 mg-N/L (bottom).

Figure B-19. Total Nitrogen and Total Phosphorus concentration contours at CS2 (b). Figures show results for IC nitrate 0.01 mg-N/L (top), IC nitrate 0.35 mg-N/L (middle) and IC nitrate 0.55 mg-N/L (bottom).

Figure B-20. Total Nitrogen and Total Phosphorus concentration contours at CS3 (c). Figures show results for IC nitrate 0.01 mg-N/L (top), IC nitrate 0.35 mg-N/L (middle) and IC nitrate 0.55 mg-N/L (bottom).

Figure B-21. Total Nitrogen and Total Phosphorus concentration contours at CS4 (d). Figures show results for IC nitrate 0.01 mg-N/L (top), IC nitrate 0.35 mg-N/L (middle) and IC nitrate 0.55 mg-N/L (bottom).

Figure B-22. Spatial distribution of Dissolved Organic Carbon (DOC) at the first layer of the mesh attached to the water surface. (Left) IC nitrate 0.01 mg-N/L. (Middle) IC nitrate 0.35 mg-N/L. (Right) IC nitrate 0.55 mg-N/L.
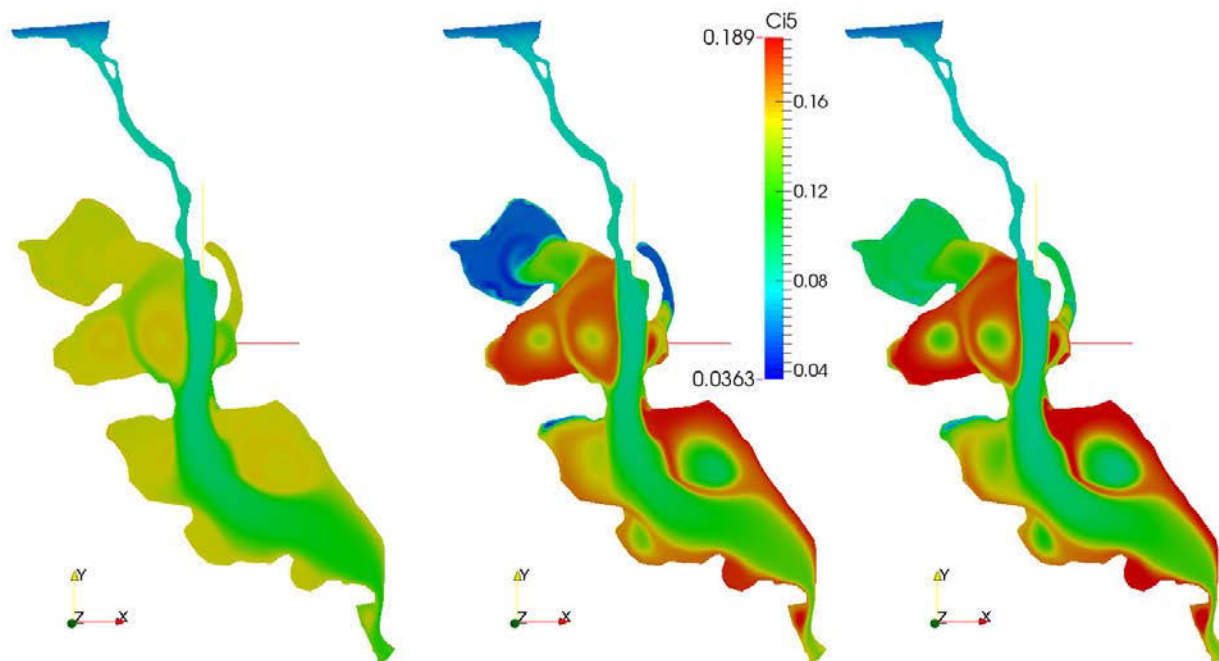
Figure B-23. Spatial distribution of ammonia (NH4) at the first layer of the mesh attached to the water surface. (Left) IC nitrate 0.01 mg-N/L. (Middle) IC nitrate 0.35 mg-N/L. (Right) IC nitrate 0.55 mg-N/L.

B.2. Additional Figures section 6.3
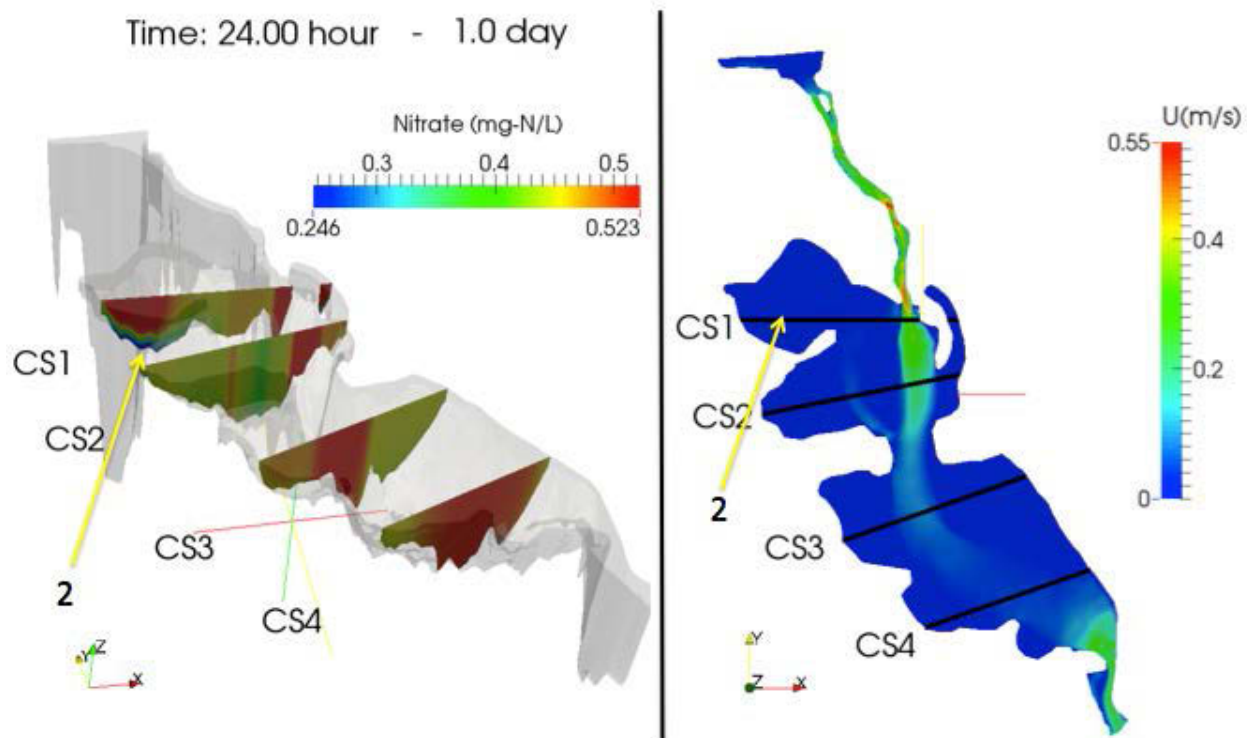
Figure B-24. Detail Figure 6-19 (b).
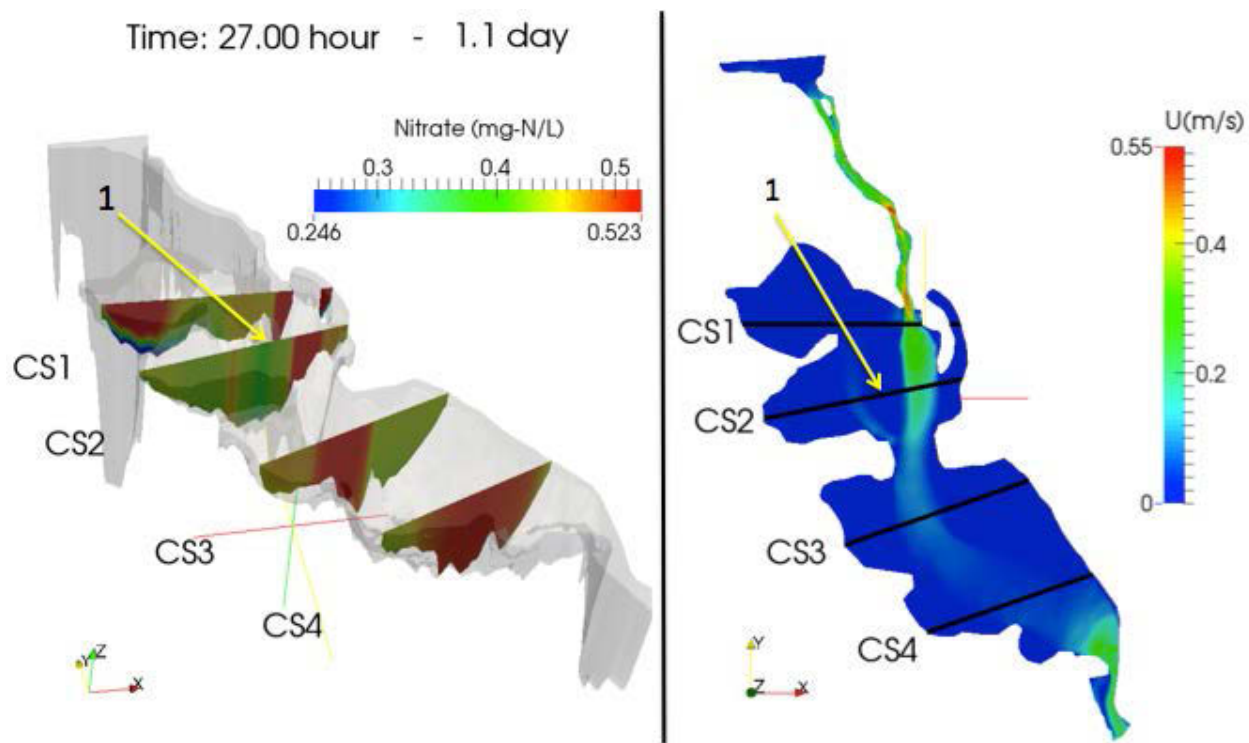
Figure B-25. Detail Figure 6-19 (c).
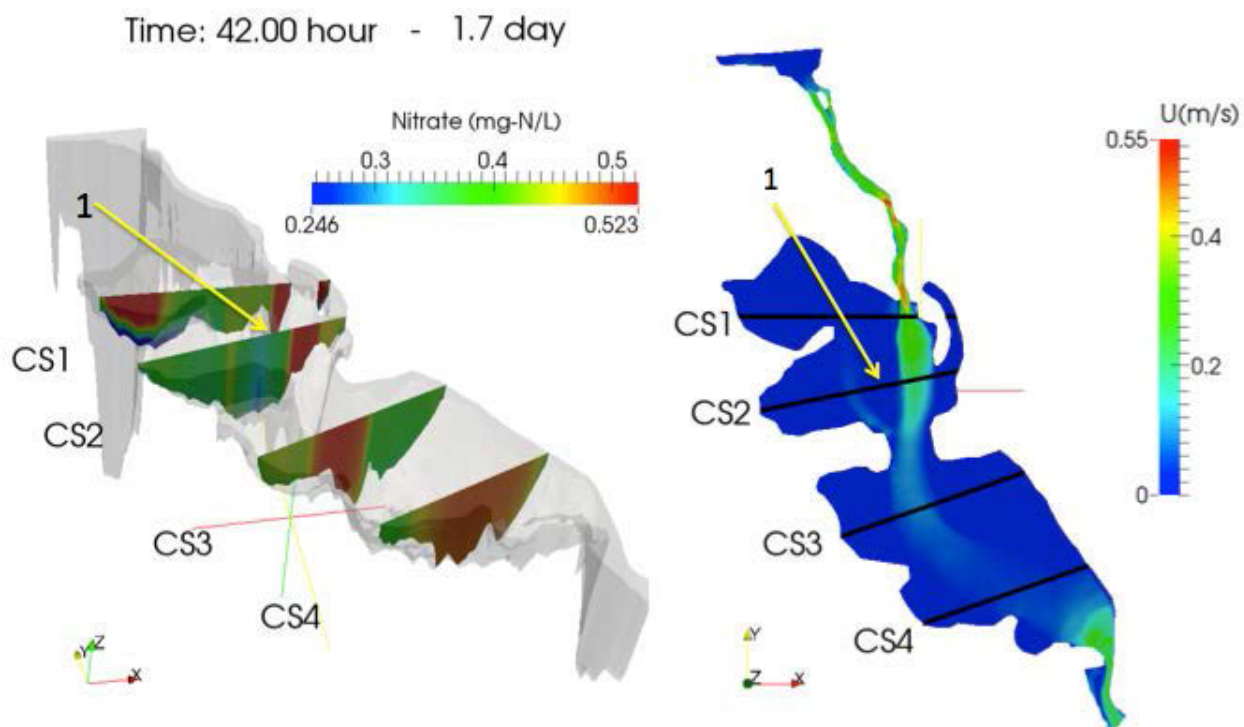
Figure B-26. Detail Figure 6-19(h).
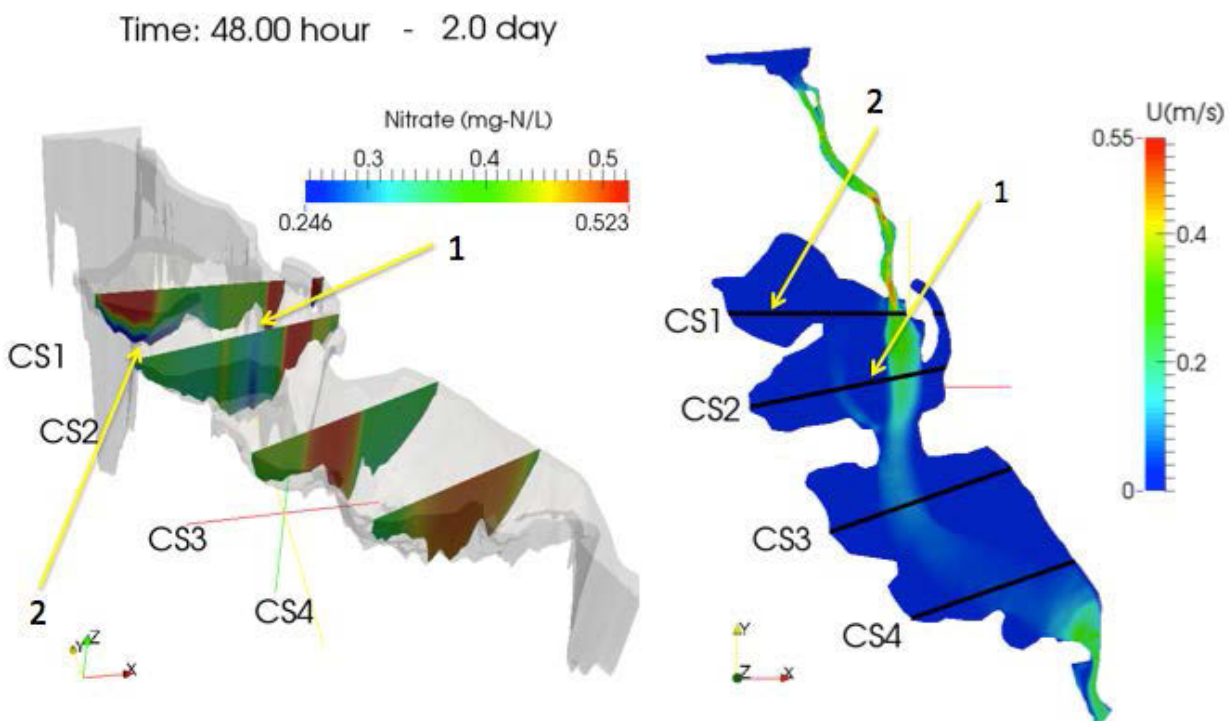
Figure B-27. Detail Figure 6-19 (j).

-

APPENDIX C

ADDITIONAL FIGURES AND ANALYSIS CASE SECTION 6.5

C-1 Additional Figures

The following figures complements the results analyzed in section 6.5.
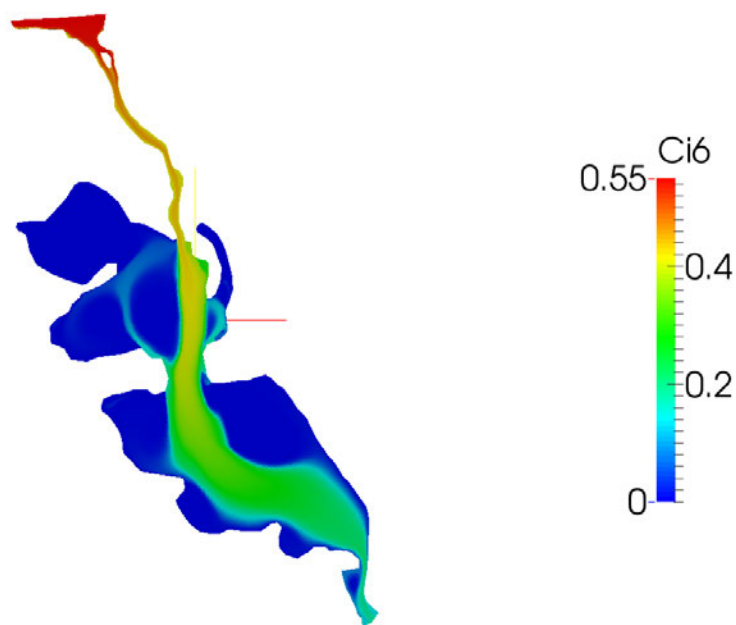
Figure C-1. Contours of nitrate concentration for scenario [0] presented in Table 6-2 at 26 day of simulation, midnight. Contours located at the water surface, first cell.
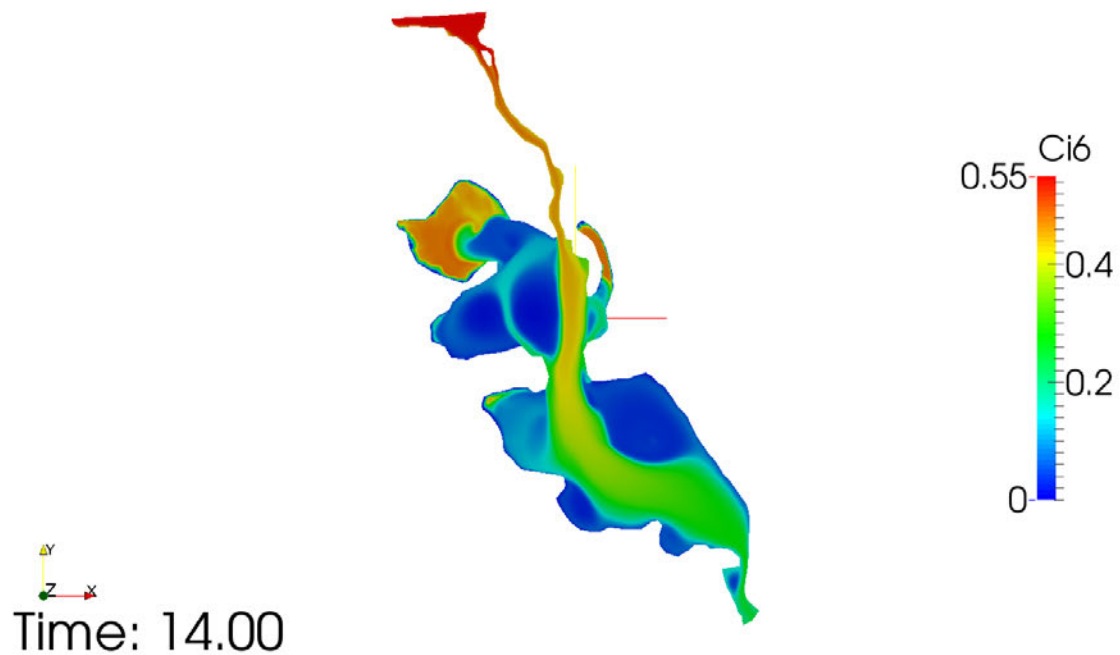
Figure C-2. Contours of nitrate concentration for scenario [1] presented in Table 6-2 at 14 day of simulation, midnight. Contours located at the water surface, first cell.
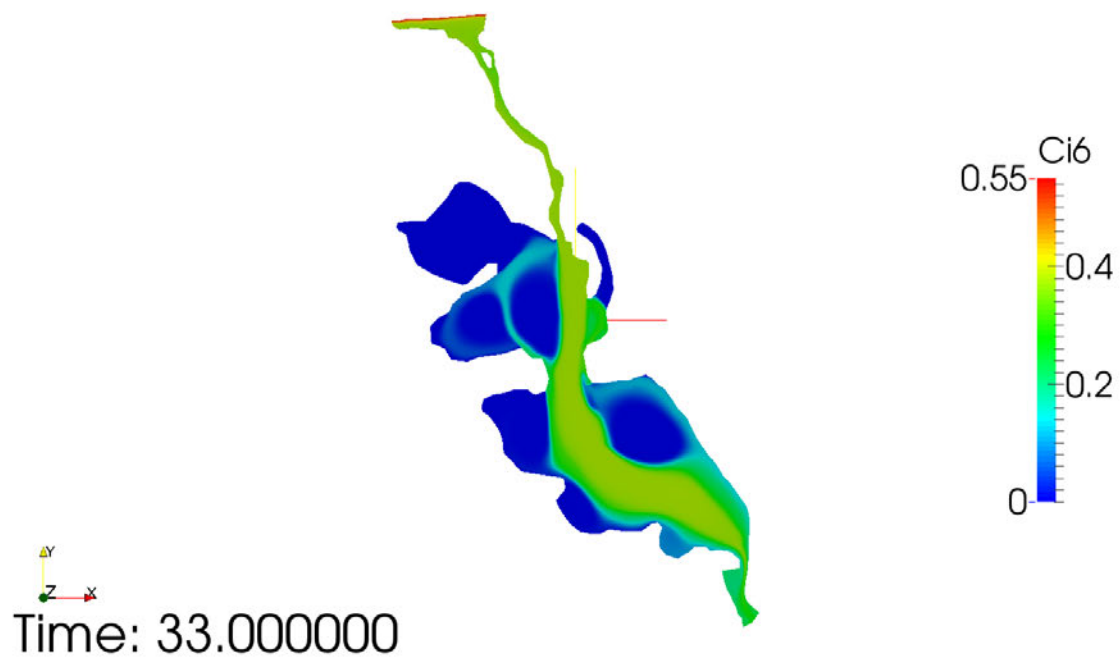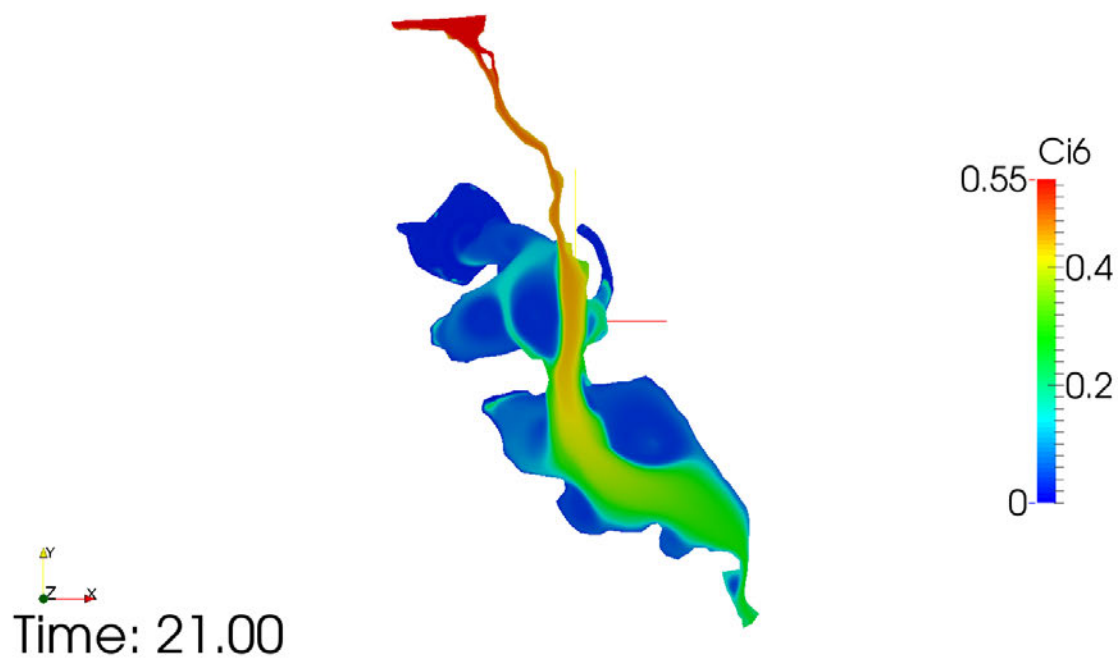
Figure C-3. Contours of nitrate concentration for scenario [2] presented in Table 6-2 at 33 day of simulation, midnight. Contours located at the water surface, first cell.
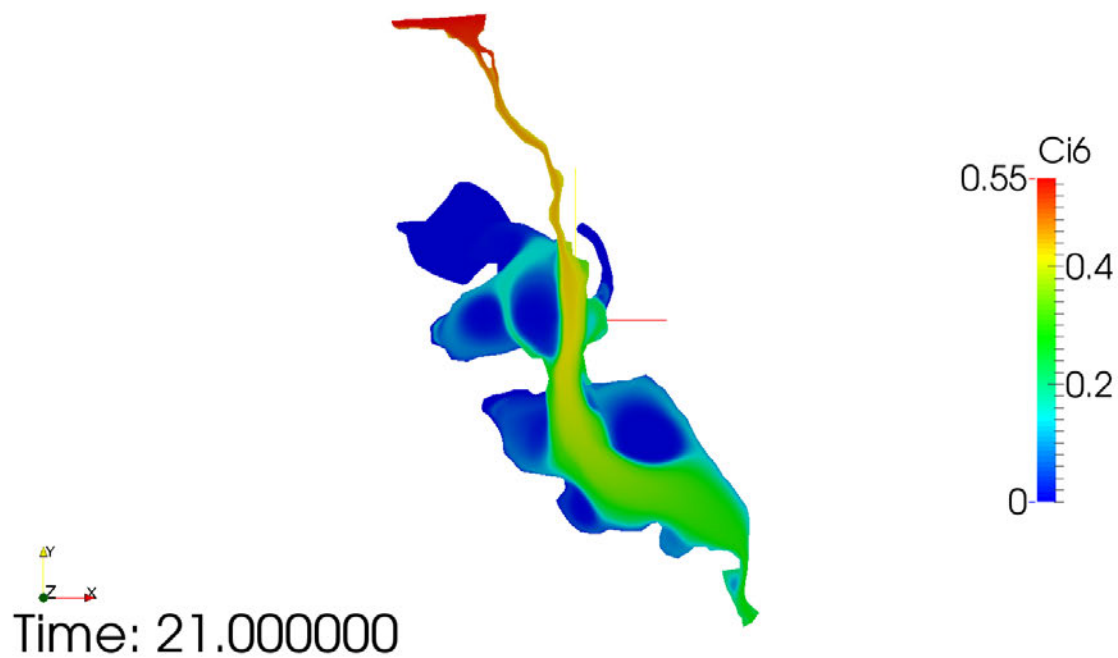
Figure C-4. Contours of nitrate concentration for scenario [3] presented in Table 6-2 at 21 day of simulation, midnight. Contours located at the water surface, first cell.

Figure C-5. Contours of nitrate concentration for scenario [4] presented in Table 6-2 at 21 day of simulation, midnight. Contours located at the water surface, first cell.
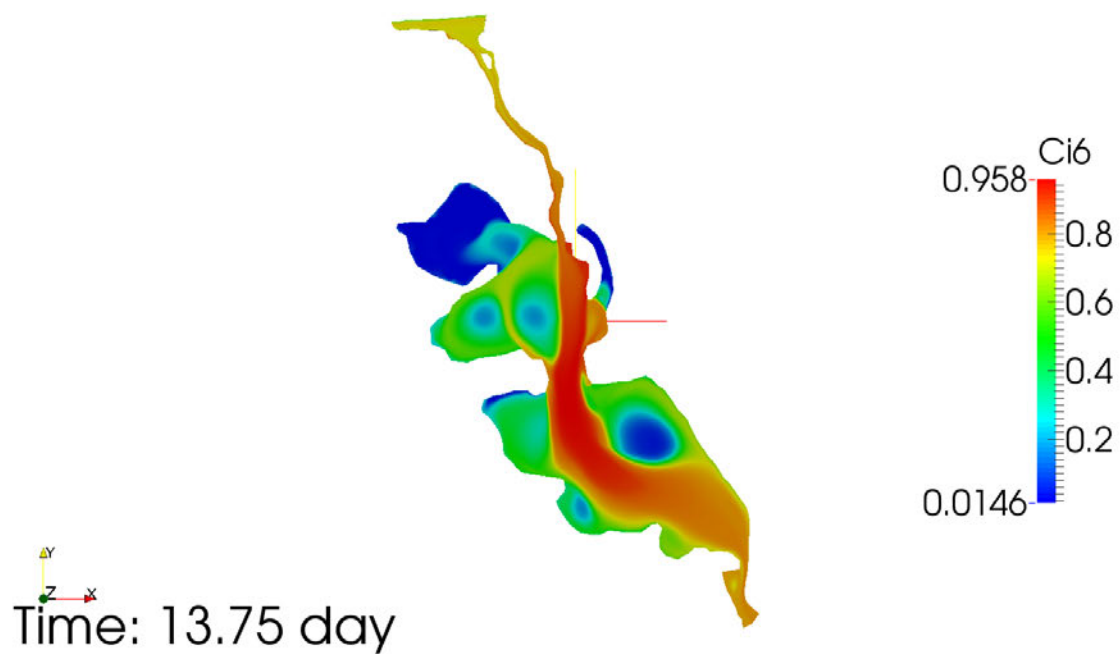
Figure C-6. Contours of nitrate concentration for scenario [5] presented in Table 6-2 at end of 13 day of simulation, 6pm. Contours located at the water surface, first cell.
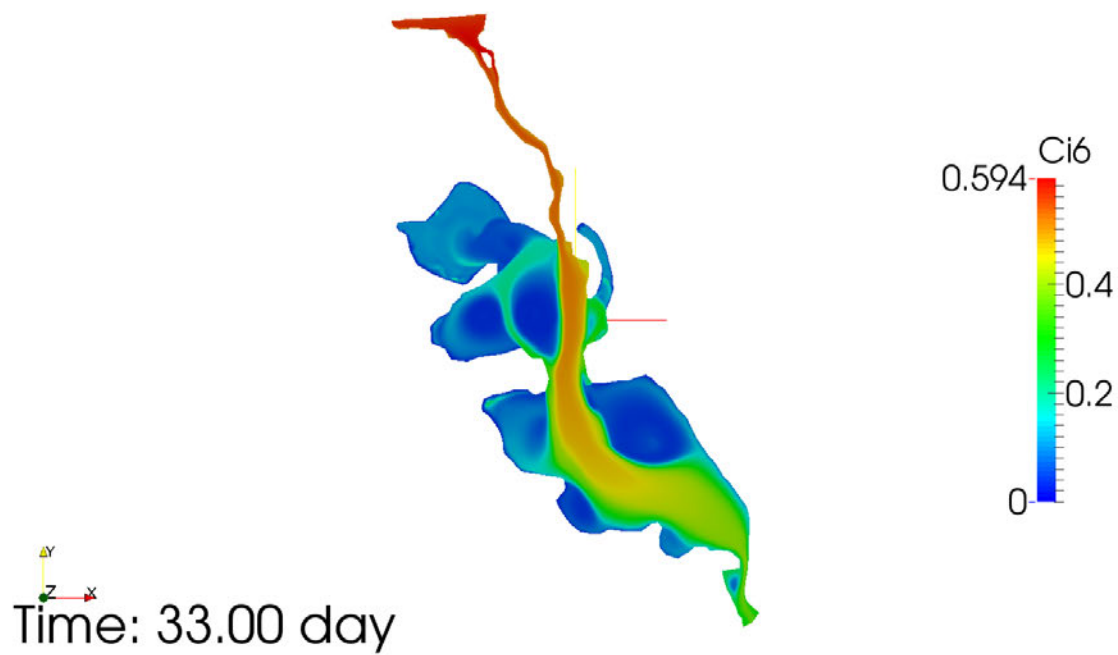
Figure C-7. Contours of nitrate concentration for scenario [6] presented in Table 6-2 at end of 33 day of simulation, midnight. Contours located at the water surface, first cell.
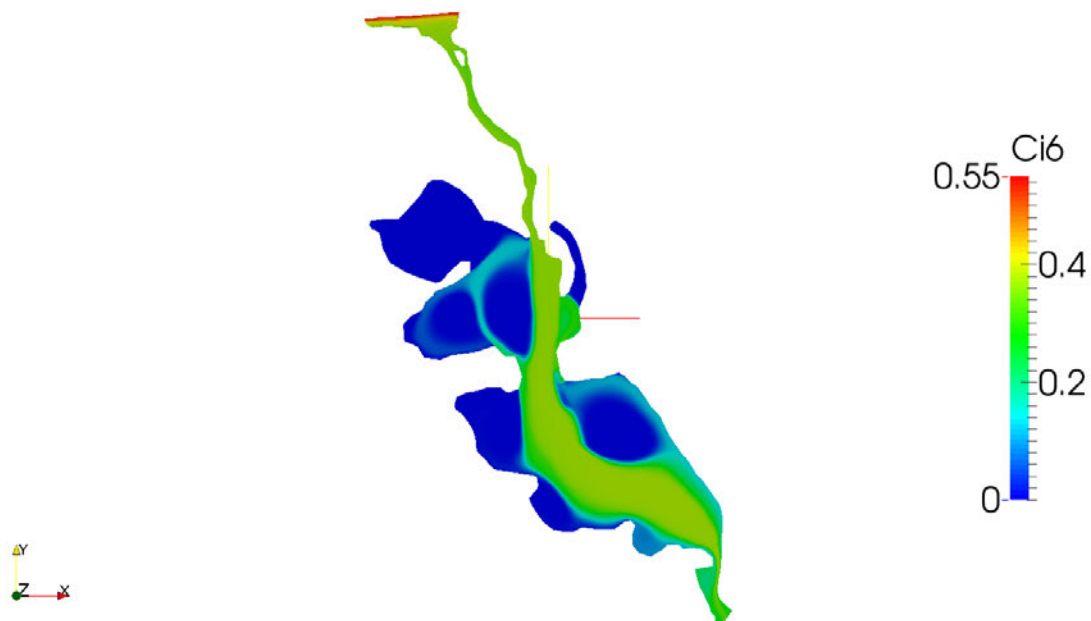
Figure C-8. Contours of nitrate concentration for scenario [7] presented in Table 6-2 at end of 33 day of simulation, midnight. Contours located at the water surface, first cell.
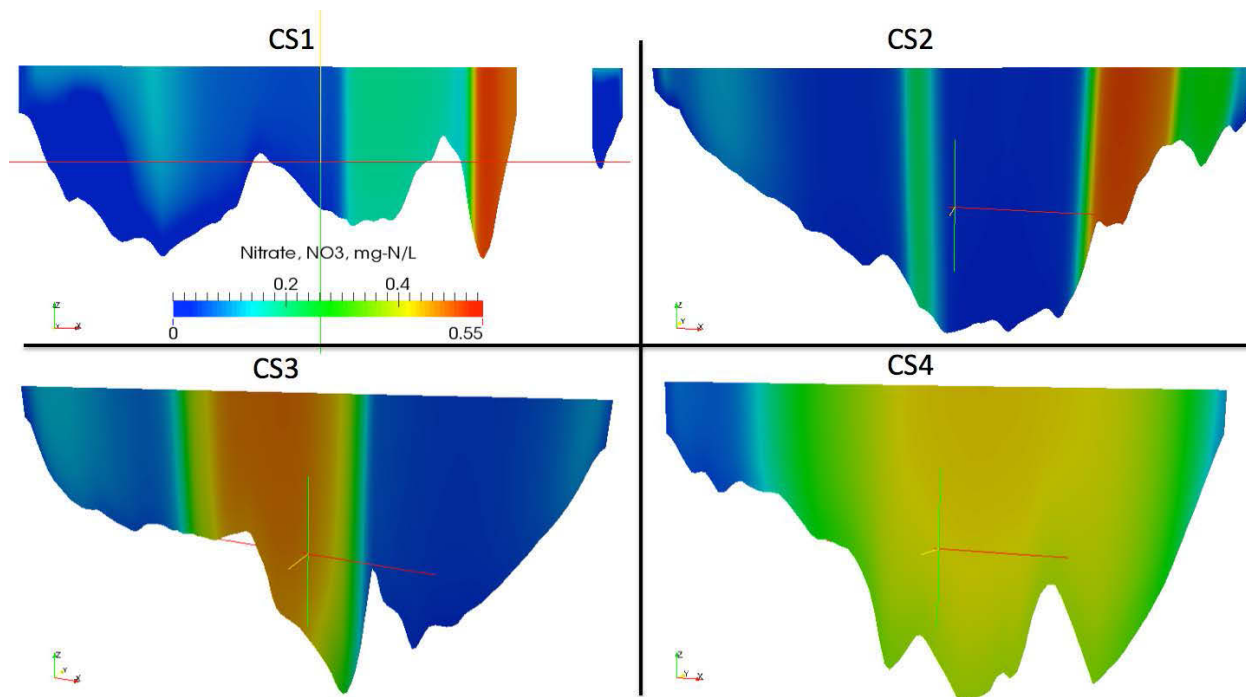
Figure C-9. Contours of nitrate concentration at fourth cross sections shown in Figure 6-29 for scenario [6], Fast reaction at bed and nitrification rate, same order of magnitude defined in Table 6-2.
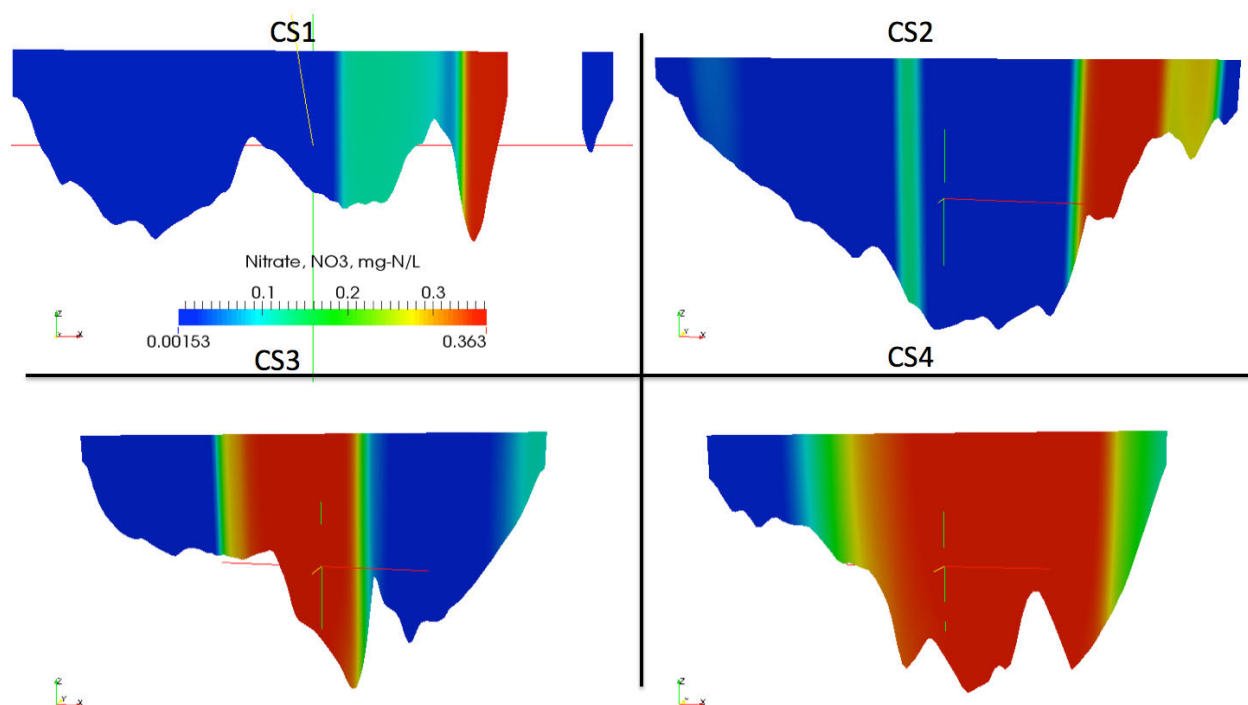
Figure C-10. Contours of nitrate concentration at fourth cross sections shown in Figure 6-29 for scenario [7], Fast reaction at bed and nitrification rate, same order of magnitude defined in Table 6-2.

C-2 Additional explanation of calculations

Global mass balances presented in Figure 6-37in Chapter 6 calculations are present next.

Each process was calculated as a sum of process contribution for all cells presented in the

domain. The idea is to generate an instantaneous value for each term in the following equation

(recalled from Chapter 3)

$$R_9 = \underbrace{\sum_x^1 \left[[1 - PN_x(NH4, NO3)].P_x\right].ANC_x.B_x}_{\text{algaluptake}}$$

$$+ \underbrace{Nit(DO, NH4, T).NH4}_{\text{nitrification}}$$

$$- \underbrace{ANDC.Denit(DO, NO3, Bx, T).DOC}_{\text{denitrification}} \qquad (3.68)$$

E.g. for a particular time the term Nit*NH4*volume cell (second term in last equation) is

calculated for all cells and then all values are added. The final value is one point on Figure 6-37.

This procedure is followed for all terms and for all time steps.

- The tool funkyDoCalc available in OpenFOAM was utilized to derive the final value in

  conjunction with a linux shell script developed in this research (details are not shown).